Quantification of isoprenoids in brain tissue - Cerebral regulation of FPP and GGPP in Alzheimer's Disease and aging

Dissertation

zur Erlangung des Doktorgrades

der Naturwissenschaften

vorgelegt beim Fachbereich Biochemie, Chemie und Pharmazie
der Johann Wolfgang Goethe-Universität
in Frankfurt am Main

von
Gero Peter Hooff
aus Kempten

Frankfurt am Main (2010)
(D30)

vom Fachbereich 14 der

Johann Wolfgang Goethe – Universität als Dissertation angenommen.

Dekan:	Prof. Dr. D. Steinhilber
Gutachter:	Prof. Dr. W.E. Müller
	Prof. Dr. M. Karas
Datum der Disputation:	14.04.2011

ABBREVIATIONS

Abbreviation	Full term
AA	Amino acid
AB	Antibody
APCI	Atmospheric pressure chemical ionization
APP	Amyloid precursor protein
a.u.	Arbitrary units
B	Blank (matrix sample processed without IS)
BBB	Blood brain barrier
BCA	Bicinchoninic acid (protein determination reagent)
Bq	Becquerel
BSA	Bovine serum albumine
CC	Calibration (Curve) sample
CE	Collision energy
CERAD	Consortium to Establish a Registry for Alzheimer's Disease
Ci	Curie
cpm	Counts per minute
CUR	Curtain gas
CV	Variation coefficient
CXP	Collision cell exit potential
D*GCVLL	Dansyl-GCVLL (amino acid single letter code)
D*GCVLS	Dansyl-GCVLS (amino acid single letter code)
DAD	Diode array detector
DMEM	Dulbecco's Modified Eagle Medium
DMPP	Dimethylallyl pyrophosphate
DMSO	Dimethyl sulfoxide
DNP	Dansyl-para-nonylphenol
DOXP	1-deoxy-D-xylulose 5-phosphate
DP	Declustering potential
DP	N-(5-dimethylamino-1-naphthalenesulfonyl)-1, 2-dioleoyl-sn-glycero-3-phosphoethanol-amine
DTT	Dithiothreitol
E. coli	Escherichia coli
em	Emission wavelength (on fluorescence detector)
EP	Entrance potential
ER	Endoplasmic reticulum
ESI	Electrospray ionization
EtOH	Ethanol
ex	Excitation wavelength (on fluorescence detector)
FA	Formic acid
FCS	Fetal Calf Serum
FDA	Food and Drug Administration
FPP	Farnesylpyrophosphate
FPP*	Dansyl labeled FPP

FPPS	Farnesylpyrophosphate synthase
FTase	Farnesyltransferase
FT-ICR MS	Fourier-transform ion cyclotron resonance mass spectrometer
FWHM	full width at half maximum
GBM	Glioblastoma multiforme
GC	Gas Chromatography
GDP	Guanosin triphosphate
GDS	Global deterioration scale
GGPP	Geranylgeranylpyrophosphate
GGPP*	Dansyl labeled GGPP
GGPPS	Geranylgeranylpyrophosphate synthase
GGTase	Geranylgeranyltransferase
GPP	Geranyl pyrophosphate
GS1	Ion source gas 1
GS2	Ion source gas 2
GTP	Guanosin triphosphate
HBS	Hank´s Balanced Salts
HBSFRC	Human Brain and Spinal Fluid Resource Centre
HCl	Hydrochloric acid
HLB	Hydrophilic lipophilic balance
HMG-CoA	3-hydroxy-3 methyl-glutaryl-Coenzyme A
HMGR	3-hydroxy-3 methyl-glutaryl-Coenzyme A reductase (gene name)
HPLC	High performance liquid chromatography
HPTLC	High performance thin layer chromatography
HRP	Horse radish peroxidase
ICH	International Conference on Harmonisation of Technical Requirements for Registration of Pharmaceuticals for Human Use
ihe	Interface heater
IPP	Inositol pyrophosphate
IS	Internal standard
LLOQ	Lower limit of quantification
LOD	Limit of detection
LTM	Long term potentiation
MEP	2-C-methyl-D-erythritol 4-phosphate
MK	Mevalonate kinase
MMSE	Mini-mental status examination
MRM	Multiple reaction monitoring
MS	Mass spectrometry
NC	Nitro cellulose
ne	Non-essential (amino acids)
NINCDS-ADRDA	The National Institute of Neurological and Communicative Disorders and Stroke, and the Alzheimer's Disease and Related Disorders Association
NMR	Nuclear magnetic resonance
P/S	Penicillin, streptomycin
PBS	Phosphate buffered saline

ppm	Parts per million
PPT	Protein precipitation
PT(E- / Z-)	Prenyltransferse (E- / Z-)
PTM	Post-translational modification
PVDF	Polyvinylidene fluoride
QC	Quality control sample
REP	Ras escort protein
ROCK	Rho associated coiled-coil forming protein kinase
ROS	Reactive oxygen species
RP	Reverse phase
RSD	Relative standard deviation
rt	Retention time
RT	Room temperature
SAD	Sporadic Alzheimer´s Disease
SAM	S-adenosyl methionine
SCAP	SREBP cleavage-activating protein
SD	Standard diviation
SDS	Sodium dodecyl sulfate
SEM	Standard error of the mean
SPE	Solid phase extraction
SPM	Synaptosomal plasma membrane
SREBP	Sterol regulatory element-binding protein
SZ	Zero sample (matrix sample processed with IS)
TBS	Tris buffered saline
TGN	Trans Golgi network
THF	Tetrahydrofuran
TLC	Thin layer chromatography
TMS	Tetramethylsilane
Tris	Tris(hydroxymethyl)aminomethane
UHPLC	Ultra high performance (pressure) liquid chromatography
UV	Ultra violet
V	Volt
WHO	World Health Organization
ww	Wet weight

1. INTRODUCTION

The mevalonate- (MVA-) pathway is a crucial metabolic pathway for nearly all eukaryotic cells, of which the most recognized product is cholesterol (Figure 1).[1] This pathway also provides cells with indispensable lipids including isoprenoids. The long-chain isoprenoids dolichol and ubiquinone participate in membrane organization and mitochondrial oxygen consumption, respectively. The short-chain isoprenoids farnesylpyrophosphate (FPP) and geranylgeranylpyrophosphate (GGPP) covalently attach to small GTPases, which act as molecular switches in various biochemical pathways.[2] This essential attachment enables these proteins to be inserted into membranes, resulting in the activation of pathways involved in inflammation, oxidative stress, and cell proliferation etc.[3,4,5,6,7] The Rho family of GTPases are one of the major regulators in synaptic plasticity, both in dendrite morphogenesis and stability as well as in growth cone motility.[8,9,10,11] Another vitally important role of FPP is that it is the key branch point for cholesterol and GGPP (Figure 1). There is keen interest in the role of FPP and GGPP in post-translational modification (PTM) of proteins and cell function in Alzheimer's Disease (AD).[3,12,13] FPP and GGPP like cholesterol are derived from mevalonate (Figure 1) but unlike cholesterol, there is little if any information on their regulation and abundance in the brain. The absence of such data is in stark contrast to the aforementioned interest in the role of those isoprenoids in protein prenylation and cell function. The following sections build on a comprehensive review by Cole et al.[3] and summarize the current knowledge on isoprenoids, recent findings regarding their regulation and targeted proteins with special focus on AD.

1.1. Cholesterol

1.1.1. Biosynthesis

The mevalonate- (MVA-) pathway is a crucial metabolic pathway in all eukaryotic cells, with the exception of mature red blood cells.[14] It converts mevalonate via a complex biosynthesis, including more than 30 intermediates, into cholesterol. It is most recognized for the biosynthesis of cholesterol, while it provides cells with further indispensable substrates, such as squalene and the isoprenoids FPP and GGPP.

Initial steps of the MVA-isoprenoid pathway involve the synthesis of 3-hydroxy-3-methylglutaryl- coenzyme A (HMG-CoA) from acetyl-CoA via acetoacetyl-CoA (Figure 1).

HMG-CoA reductase, the rate limiting step of the entire pathway then forms mevalonate.[1] Biosynthesis mainly occurs in the endoplasmic reticulum (ER) but also in peroxisomes.[15] After mevalonate production mevalonate kinase (MK) catalyzes the phosphorylation of mevalonic acid to phosphomevalonate. Phosphomevalonate kinase catalyzes the reaction of mevalonate 5-phosphate and adenosine triphosphate (ATP) to mevalonate 5-diphosphate where the latter is subjected to decarboxylation and forms isopentenyl pyrophosphate (IPP), which equilibrates with its isomer dimethylallyl pyrophosphate (DMAPP), catalyzed by the isopentenyl pyrophosphate isomerase. IPP or DMAPP then undergo subsequent condensation reactions to produce a 10-carbon lipid geranylpyrophosphate (GPP), the 15-carbon FPP and the 20-carbon GGPP. The synthesis of GPP and FPP is catalyzed by farnesylpyrophosphate synthase (FPPS) while GGPP is synthesized by geranylgeranylpyrophosphate synthase (GGPPS).[16,17] FPP is a key branch point of the pathway leading to GGPP synthesis and to squalene, which is catalyzed by farnesyldiphosphate farnesyltransferase (FDFT), also known as squalene synthase. From squalene two subsequent enzymatic reactions result in the production of lanosterol, this represents the basic chemical structure of all steroids. Subsequent reactions lead to the production of desmosterol and 7-dehydrocholesterol and finally to cholesterol. See Figure 1 for a summary of the MVA-pathway.

1.1.2. Cholesterol homeostasis in the brain

Cholesterol is an essential compound for the structure and functionality of cells. The mevalonate pathway, as described in the previous paragraph, underlies very complex regulatory mechanisms due to its immensely important role in cell and tissue physiology. Fundamental research, focusing on cholesterol biosynthesis was conducted by Clayton and Bloch in 1956 [18] and Goodman et al. in 1962 [19], and even today after more than roughly 50 years of research, there are still ambiguities concerning feedback mechanisms, transcription, translation and the regulation of the activity of enzymes within the MVA-pathway.

The role of cholesterol in the brain becomes obvious when looking at the sterols enormous abundance compared to any other tissue in the human body. Approximately, 25% of all the cholesterol found in the body is located in the central nervous system (CNS), while the total weight of the organ only accounts for about 2% of the body weight.[20,21] Within the brain cholesterol makes up 20-30% of all existing lipids[20] it has become generally accepted that most

of it is derived from *de novo* synthesis and brain levels are generally independent from plasma cholesterol levels, due to the function of the blood brain barrier (BBB).[22] Investigations on age-related brain cholesterol synthesis in different species ruled out possibilities that the synthesis rate is high in the fetus and newborn but declines considerably in later life.[23] Consequently, the levels of human brain cholesterol increases in average from ~ 6 mg/g in a newborn to a maximum of 23 mg/g in the young adult brain [23] with an estimated half-life of approximately 5 years for the sterol. Furthermore, the cholesterol half-life in rodent brain was estimated to be only 2-6 month.[24]
Many of the studies regarding cholesterol turnover are based on the measurement of its major metabolite, the 24*S*-hydroxycholesterol, for two reasons: it is the major oxysterol in the brain and it is also the main cholesterol metabolite crossing the BBB and therefore traceable in plasma.[25] Björkhem et al. [24] approximated the transfer of 24*S*-hydroxycholesterol from the CNS into the periphery to be ca. 4 mg/day where it can be subsequently excreted via the bile in a sulphated or glucuronidated form.[24,26] The cytochrome P450 isozyme CYP46A1 is located in neurons spread out in different regions in the brain and is responsible for the conversion in the brain.[27] A recently published review by Farooqui et al.[28] also emphasized two further oxysterols, 25- and 27-hydroxycholesterol to be important for brain cholesterol homeostasis.[28]
For the most part the transport of cholesterol and its metabolites in the opposite direction, from the circulation into the CNS is prevented under physiological conditions by the BBB. However, a flux of 27-hydroxycholesterol into the brain compartment was shown by Heverin et al.[29] and in the same context a novel elimination route via 7α-hydroxy-3-oxo-4-cholestenoic acid was recently described.[30] In general 27-hydroxycholesterol levels in the plasma are low, leading to a 27-hydroxycholesterol/24-hydroxycholesterol ratio of ~ 2 and ~ 0.4, in the periphery and in the brain, respectively.[31] Moreover, the absolute concentration or the ratio is discussed by several groups to be changed under pathological conditions, which affect the brain (e.g. neurodegeneration).[25,31,32]

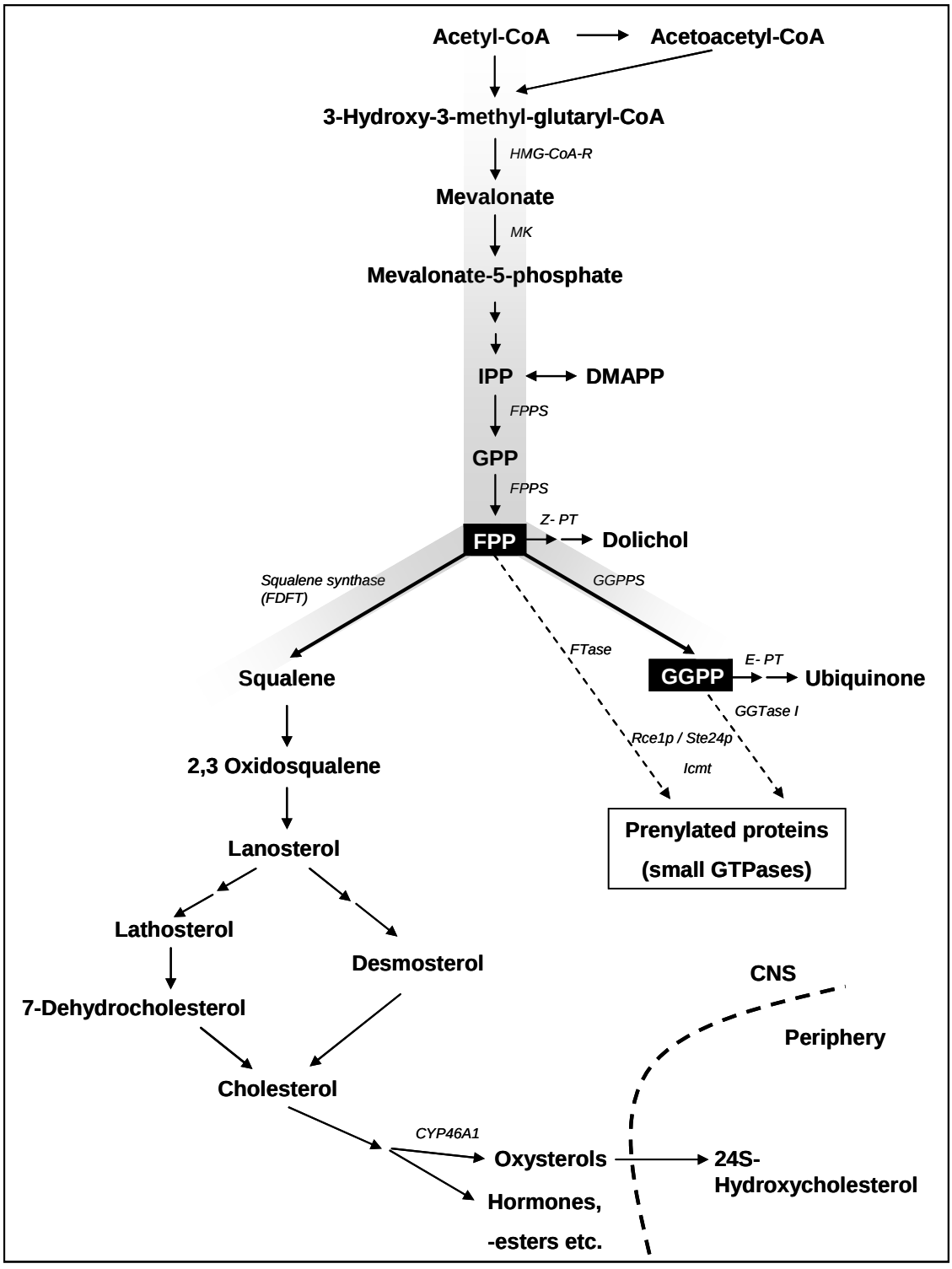

Fig. 1. Outline of the mevalonate/isoprenoid/cholesterol pathway. The overview depicts the major intermediates and enzymes involved in the biosynthesis of the isoprenoids and cholesterol. Single arrows (→) depict a one step conversion, while double arrows (→ →) omit one or several intermediates. - - - - symbolizes the blood brain barrier (BBB). A detailed description with all abbreviations can be found in section 1.1.1. and section 1.1.2. of the introduction. E- and Z-PT depict the prenyltransferases leading to the E- or Z-stereoisomers.

1.1.3. The role and function of brain cholesterol

As briefly mentioned earlier cholesterol plays a fundamental role in brain development and maintenance of function. It contributes to protein functionality and is an indispensable compound of neuronal membranes where it strongly influences their fluidity and stability in general. Besides being a component of plasma membranes of neurons and astrocytes, the major part of brain cholesterol is associated with the myelin sheath, leading to especially high cholesterol content within the white matter.[20] Differences in cholesterol distribution between the white and the grey matter but also a difference in synthesis rate and abundance are apparent in various other regions of the brain.[33,34] Furthermore, neurons and astrocytes vary in cholesterol synthesis, e.g. astrocytes feature a higher rate. In the developed brain there is a possibility for the transport of cholesterol from astrocytes to neurons, when there is an excessive requirement for the sterol.[35,36] For the lipid transport, the brain is equipped like the periphery, with apolipoproteins (Apo). The proteins present in the brain are Apo-I, A-IV, D, E and J[37], while ApoE has the most dominant role and is widely discussed in the context of AD.[38,39,40] The role of ApoE after brain damage and for maintenance of neuronal function has also been discussed and the involvement of ApoE in synaptic plasma membrane formation was indicated in studies with ApoE deficient mice.[41]

1.2. The physiology of the cell membrane

Today's fundamental conception of the assembly of biological cell membranes is based on the fluid mosaic model described in 1972[42], which was revisited in 1995[43] and is now regarded as a more complex entity consisting of caveolae, lipid rafts and other lipid sub-domains.[44] Depicted by the primary model the cell membrane can be considered as a two-dimensional oriented liquid, consistent of a lipid bilayer divided into a cytofacial and an exofacial (inner and outer) leaflet. The main constituent of this structure are the phospholipids thus building a hydrophilic surface layer with their phosphate groups while the fatty acids paralleling to each other form the lipophilic interlayer. The hydrophobic ´tails` of each layer oppose each other and fulfill two basic requirements: on the one hand the lipid bilayer provides the structural properties required for membrane bound proteins (integral or peripheral) such as ion channels, receptors and enzymes and on the other hand it provides a natural barrier especially for polar solutes or ions to diffuse freely through the membrane and therefore allows the cell to establish certain essential concentration gradients.

Besides the aforementioned phospholipids and proteins, the cell membrane also consists of other lipids like cholesterol, sphingomyelin and glycolipids and other carbohydrates. The composition of the bilayer is very heterogeneous and can vary in a wide range depending on the function of the cell and in accordance to changes originating from age-dependant processes or pathological conditions.[45] For example, higher cholesterol content or elevated levels of saturated fatty acids can lead to decreased membrane fluidity, influencing cell activities associated with the membrane. It was shown that cholesterol is the main regulator of membrane fluidity as it intercalates between the fatty acids of the membrane and sterically hampers their movements, overall leading to a more rigid behavior of the bilayer.[46]

The cholesterol distribution between the two leaflets of the cell membrane is asymmetric and undergoes substantial changes during aging. In young mice (3-4 months) approximately 15% of synaptosomal plasma membrane (SPM) cholesterol was found in the exofacial leaflet and roughly doubled in aged mice (24-25 month).[47] Furthermore, this age-dependant distribution shift also affects lipid rafts, distinct island like domains in which a main proportion of membrane associated cholesterol is found.[48] Besides these lipid rafts, also called detergent resistant membranes (DRMs) caveolae harbor high concentrations of cholesterol. Both are cell surface micro-domains and rich in cholesterol and sphingolipids. Caveolae are primarily characterized by the abundance of caveolin, a membrane bound protein not present in lipid rafts and by its flask-shape appearance.[49] They are involved in signal transduction, vesicle transport via endocytosis and in various disease pathologies like for example during interactions with the human immunodeficiency virus (HIV).[50,51,52]

Lipid rafts are planar micro-domains creating a tightly packed lipid aggregation containing flotillin and alkaline phosphatase as marker proteins. They are plasma membrane reaction centers especially for protein-protein interactions, cell signaling and trafficking.[53,54] Besides being involved in several diseases[55] they are also discussed for their role in synapse formation and function[56] and are therefore studied with interest in the field of neurodegenerative diseases including AD.

In contrast to caveolae it is difficult to visualize these planar structures in the membrane by common techniques like electron microscopy.[57] Recent advances were able to clearly demonstrate the existence of lipid rafts[58,59] devitalizing inconsistent argumentations on rafts being artifacts of detergent extractions[60,61] and emphasizing the impact of the isolation technique.[58]

To widen the knowledge on raft associated proteins several groups addressed the issue by proteomic approaches, most notably the work by Mann in 2006.[62] The advancements in this relatively new field have been summarized by Zheng et al.[63]

The integrity of proteins and their functionality are highly dependant on the overall composition of the surrounding membrane and especially on the abundance of cholesterol, sphingo- and ganglioside lipids. Based on the impact of lipid rafts on multiple biochemical pathways, modulation of lipid raft composition is used to study related disease pathways and potentially offers a target for pharmacological intervention.[64]

1.3. Isoprenoids – Chemistry and Structure

Isoprenoids are a large heterogeneous class of biologically active lipids. There is an estimated 55.000 natural products, which virtually all derive from the C_5-unit IPP or its isomer DMAPP.[65] Two metabolic pathways are assumed to be responsible for the synthesis of higher isoprenoids (also known as terpenes) and their secondary products. The MVA-pathway which is the only source of isoprenoids in archaebacteria, fungi, animals and humans, and the 1-deoxy-D-xylulose 5-phosphate/2-C-methyl-D-erythritol 4-phosphate (DOXP/MEP) pathway, which is only present in higher plants, most eubacteria and for example in the malaria parasite *plasmodium falciparum*. Moreover, plants are the only organisms using both pathways for isoprenoid biosynthesis, though in different compartments.[17,66]

Regarding the nomenclature, terpenes are generally classified with a prefix characterizing the number of isoprene units present. Compounds consisting of a single (C_5-) isoprene unit are called hemiterpenes, followed by monoterpenes (C_{10}-), sesquiterpenes (C_{15}-) like for example FPP, diterpenes (C_{20}-) like GGPP and further polyterpenes.

In mammals the initially mentioned structural isomers IPP and DMAPP form GPP catalyzed by the FPPS, 80 kDa homodimer[67], via a “head-to-tail” condensation. Following this step the identical enzyme catalyzes the condensation of GPP and IPP to form the C_{15} FPP. While the subsequent “head-to-tail” reaction of an additional 5-carbon lipid via the GGPPS, a 195 kDa homo-oligomer[67], leads to the C_{20} GGPP. The “head-to-head” reaction of two FPP molecules results in the production of squalene (C_{30} unit) (see Figure 1).[17] These two mechanisms are the basic reactions for chain elongation concerning non-cyclic or cyclic isoprenoids.

1.3.1. Longer chain isoprenoids – dolichol and ubiquinone

In mammals FPP is the precursor of dolichol and ubiquinone. Ubiquinone (coenzyme Q) as part of the electron transfer between complex I, II and III of the respiratory chain[68,69] is mainly localized in the inner mitochondrial membrane. Its synthesis proceeds upon conversion of GGPP, leading to chain elongation and predominately takes place in the ER–Golgi system.[70] The enzyme trans-prenyltransferase (also known as E-prenyltransferase or E-PT) is involved in the biosynthesis of ubiquinone (see Figure 1).[17,71] The number of incorporated isoprene units and therefore the chain length varies among different organisms and is commonly indicated by the following number e.g. coenzyme Q_{10}.[17,71] Ubiquinone is essential for normal cell function and misdirected biosynthesis results in pathological respiratory chain deficiencies.[72,73,74]

Dolichol biosynthesis involves the only cis-prenyltransferase (also known as Z-prenyltransferase or Z-PT) known in humans (see Figure 1).[17,71] This longer chain isoprenoid is widely distributed in all tissues and membranes and besides carrying a terminal free hydroxyl group it exists in a phosphorylated, dephosphorylated or in an esterfied form.[17,75,76] Although knowledge on dolichol function is limited, it has been proposed as a biomarker for aging.[76,77] Numerous *in vitro* and *in vivo* experiments reported on interactions of dolichol with cellular membranes. The unesterfied dolichol was shown to modify the organization and packing of phospholipids in model membranes.[78] The free and the phosphorylated forms were found to be mediators of protein glycosylation or as sugar carriers.[17,71] The lipophilic molecule dolichol intercalates into the bilayer of cell membranes and interacts with the phospholipids.[76] A study by Wood et al.[79] showed that dolichol increased membrane fluidity of SPMs isolated from brains of young and old mice. The same study revealed higher endogenous dolichol levels in isolated SPMs of aged mice and it was concluded that dolichol might act as a regulator of membrane fluidity.[79] Several studies have reported higher dolichol levels with increasing age in peripheral tissue and in the brain.[80,81,82] Besides dolichol potentially regulating membrane fluidity, another hypothesis is that membrane localization of free dolichol may act as an antioxidant to counteract cell toxicity.[81] It remains to be elucidated whether elevated dolichol levels with aging are a consequence of a loss of enzymatic regulation in the MVA-pathway, as proposed by Pallottini et al.[83]

1.3.2. Analytical approaches for the quantification of longer chain isoprenoids

The following describes several methods, which have been employed to better understand the role of dolichol and ubiquinone in cell physiology. Early experiments for the quantification of

dolichol and the synthesis rate of distinct enzymes were carried out with radioactive ($^{14}C/^{3}H$ ratios) labeled acetate. Incorporation into the MVA-pathway derived products (e.g. dolichol, sterols) was monitored by scintillation counters following sample preparation and high performance liquid chromatography (HPLC) and thin layer chromatography (TLC) separation.[84,85] Later on, researchers used ultra violet light (UV) HPLC detectors for non-radioactive quantifications.[86] Such analytical enhancements made the applications available to a broader group of researchers based on the usual equipment of laboratories, where HPLC systems are far more common and manageable than radioactive facilities. Another enhancement was achieved by the incorporation of an internal standard (IS) in the analysis of dolichol, thereby strengthening the application in respect to robustness and reliability of the data.[87] In the field of quantitative analytics the most state of the art detection and quantification of the whole spectrum of analytes is via mass based detectors. Often used in combination with HPLC mass spectrometers (MS) allow a very sensitive and selective form of detection. The two most conventional and convenient ways to couple a liquid chromatography system to a MS is via electro spray (ESI) or atmospheric chemical ionization (APCI). Consequently, a recent publication detailed the technically advanced quantification of dolichol via LC ESI-MS.[88] At this point it is also worth mentioning that an isolation technique with subsequent HPLC-MS quantification is described in the literature for the determination of human brain dolichol levels.[89] Similar analytical techniques can be found for the quantification of ubiquinone in tissue or plasma.[88,90,91] Interestingly, this MVA-pathway end-product drew growing attention in the last decade due to the developing sector of life science research and the possible beneficial effects of Q_{10} supplementation.

1.3.3. Farnesyl- and geranylgeranylpyrophosphate

1.3.3.1. Role and function of FPP and GGPP

As described in the previous sections FPP and GGPP play a decisive role within the MVA-pathway and for the synthesis of essential compounds involved in cellular processes. Notably, FPP plays a significant role as it is the branching point of the whole pathway and serves as a substrate for several enzymes. Figure 1 depicts the utilization of both isoprenoids for various downstream products. Aside from the well-known and previously described conversion of FPP into GGPP, cholesterol, Heme A and dolichol it also serves as a substrate for the FTase for the

prenylation of various members of the superfamily of small GTPases (see section 1.6.). GGPP however, undergoes conversion to form ubiquinone and is further utilized by two different prenyltransferases, namely geranylgeranyltransferase I and II (GGTase I and II), described in further detail in section 1.6.1.

1.3.3.2. Analytical approaches for the quantification of FPP and GGPP

Despite the large interest in the two MVA-pathway intermediates, FPP and GGPP, with regards to cell physiological and pathological regulation, there is a lack of valid quantitative data on endogenous levels, especially for human tissue. As described in the following, early publications focused on FPP determination, while more recent studies attempted to simultaneously quantify both isoprenoids.

One of the earliest publications describing the quantification of FPP alone uses the enzymatic conversion into the free alcohol via an alkaline phosphatase followed by petroleum ether extraction. The quantification was conducted on a HPLC-UV system.[85] The quite common determination with radioactive labeled substrates for enzymatic conversion in the 1980s was also applied for the quantitative analysis of FPP via comparative TLC and subsequent measurements in a scintillation counter. Within the same study IPP was determined via the same methodological setup.[92] The general term for this sort of experimental design is called double-radio-isotope dilution method. An improvement for the detection in plasma utilized the enzymatic dephosphorylation into farnesol and further enhanced the detection by subsequent chemical coupling to 9-anthroylcyanide. The resulting labeled C_{15} chain was separated and analyzed via a sensitive HPLC fluorescence detection (FLD) system.[93] The most relevant studies in regard to the current work were conducted by Tong et al., who simultaneously measured FPP and GGPP in cells.[94] After a liquid/liquid extraction the two diphosphates were enzymatically converted into two different dansyl-labeled pentapeptides, whereas the pre-column derivatization took advantage of the physiology of the isoprenoids (for a more detailed description see section 3.1.1.). The two enzymes which were employed were FTase and GGTase I and as coupling reagents two distinct artificial dansyl-labeled pentapeptides, containing the respective CaaX-motives were used. The same group improved upon their own method during the development of the current work and published their developed technique for the quantification in different mouse tissues, including brain tissue.[95]

Last but not least it should be noted that two further studies determined FPP alone and simultaneously FPP and GGPP after conversion to their respective alcohols via gas chromatography mass spectrometry (GC-MS) in yeast and *Escherichia coli* (*E.coli*).[96,97] Furthermore, it is also worth mentioning that two recent publications addressed the quantification of the precursors for FPP. One publication shows the HPLC-FLD analysis of GPP[98] and a different study used a HPLC-MS approach to simultaneously quantify mevalonate, IPP, DMAPP and GPP in cells.[99] The analytical approaches prior the onset of the current work are summarized in Table 1.

Analyte	**Applied biomaterial**	**Isolation conditions**	**Conversion / Derivatization**	**Separation & Detection**	**Reference**
FPP	rat liver	petroleum ether	FOH (by AP)	HPLC-UV	Keller et al. 1979 [85]
FPP	rat / mouse liver	ammoniac 1-butanol	FOH (by AP)	TLC – double isotope dilution	Bruenger et al. 1988 [92]
FPP	human / dog plasma	n-hexane / ethanol	FOH (by AP) / 9-anthroylcyanide	HPLC-FLD	Saisho et al. 1997 [93]
FPP	E. coli	anion exchanger suspension	FOH (by AP)	GC-MS	Song et al. 2003 [96]
FPP GGPP	cultured cells	ammoniac ethanol / 1-butanol	dansyl-labeled peptides	HPLC-FLD	Tong et al. 2005 [94]
FPP GGPP	E. coli	ammoniac ethanol / 1-butanol	FOH, GGOH (by AP)	GC-MS	Vallon et al. 2008 [97]
FPP GGPP	cultured cells	NH_4CO_3 / 2-propanol		HPLC-MS/MS	Henneman et al. 2008 [99]
FPP GGPP	cultured cells; mouse brain, liver kidney, heart	ammoniac ethanol / 1-butanol; SPE	dansyl-labeled peptides	HPLC-FLD	Tong et al. 2008 [95]

Tab. 1. Summary of the published analytical methods for the determination of FPP and GGPP. The conversion by AP stands for an enzymatic conversion of the diphosphate to the free alcohol via alkaline phosphatase under basic conditions. Additional information about the methods is given in section 1.3.3.2. of the introduction.

1.4. Regulation of the mevalonate/isoprenoid/cholesterol pathway by sterols

Mainly three processes determine the functionality of the HMG-CoA reductase:

(1) Decreased cell cholesterol levels lead to an up-regulation of HMG-CoA reductase gene transcription, triggered by sterol regulatory element-binding proteins (SREBPs). Evidence implicates that not only HMG-CoA reductase transcription is regulated by SREBPs but also the transcription of other, if not all downstream enzymes of the MVA-pathway.[100]

(2) De-phosphorylation by lysosomal phosphatases activates the HMG-CoA reductase. Under physiological conditions 25-30% of the total enzyme are activated.[83,101]

(3) Further, the degradation of the HMG-CoA reductase is modulated by the cellular demand for cholesterol and isoprenoid compounds.[16]

The predominant regulation of isoprenoid and cholesterol synthesis is achieved by the modulation of the HMG-CoA reductase protein abundance and activity as it constitutes the rate limiting step of the entire MVA-pathway. The families of membrane-bound sterol regulatory element binding proteins (SREBPs) represent one major regulator of HMG-CoA reductase. However, SREBPs also affect most enzymes involved in cholesterol biosynthesis.[100] These transcription factors regulate the transcription of over 30 genes participating in cholesterol and fatty acid biosynthesis.[102,103] Upon synthesis of the three known isoforms of the protein (SREBP-1a, - 1c and -2), in the ER, the precursor protein forms a complex with the insulin-induced gene 1 protein (INSIG-1) and the SREBP cleavage-activating protein (SCAP), which serves as a sterol sensor and escort protein.[104] Following intracellular sterol depletion INSIG-1remains bound to the ER and the SREBP-SCAP complex migrates to the Golgi apparatus. Consequently two distinctive proteases cleave off SREBP in a process called regulated intermembrane proteolysis (RIP). The released SREBP migrates to the nucleus where it leads to an upregulation of the transcription of a number of genes involved in cholesterol biosynthesis, uptake and transport, by binding to the sterol element binding site (SRE).[105,106]

Cholesterol homeostasis is further regulated by oxidized cholesterol metabolites 24*S*- and 25*S*-hydroxycholesterol. The oxysterol 24*S*-hydroxycholesterol was hypothesized to interact with the liver-X receptor (LXR). The LXR is a member of the nuclear receptors and two isoforms, LXR-α and LXR-β have been identified and both are expressed in the brain.[107] Neurons treated with the oxysterol showed an up-regulation of Apo E. Apo E and SREBP-1c expression are under transcriptional regulation of the LXR[108,109] and it was concluded that 24*S*-hydroxycholesterol is a

LXR ligand.[110] 25*S*-hydroxycholesterol was shown to bind to INSIG, thus inhibiting the detachment of the SREBP-SCAP complex.[111]

As stated earlier the SREBP pathway influences a whole range of enzymes involved in cholesterol biosynthesis.[100] It is worth mentioning that 24*S*-hydroxycholesterol treatment in neurons led to a direct down-regulation of FPPS expression.[110] Additionally to regulation of gene expression, enzymes involved in the MVA-pathway are modulated by protein degradation, demonstrated by *in vitro* cell studies.[112,113]

1.5. Regulation of the mevalonate/isoprenoid/cholesterol pathway by non-sterols

Activity of the FPPS (i.e., production of FPP) was reported to be several fold higher than activity of GGPPS (i.e., production of GGPP) in bovine brain cytosol.[114] Even though FPP is a substrate for GGPPS, there are data suggesting that synthesis of GGPP may be dependant on its distribution in the cytosol versus the membrane and it was reported that abundance of certain small GTPases might stimulate GGPP production.[115] In contrast to FPP, GGPP inhibited its own synthesis in rabbit reticulocytes.[116] Another study found similar results and it was also observed that GGPP could inhibit GGPPS activity.[117]

It was concluded from structural studies that GGPP does bind in an inhibitory manner to GGPPS and may be a means of regulating GGPP levels.[67] Another potentially novel regulatory role of GPPP is stimulation of the ubiquitination and degradation of HMG-CoA reductase.[113] FPP did not have a similar effect and it was suggested that GGPP might be prenylating a protein that is responsible for regulation of HMG-CoA reductase.[113] There is evidence that SREBP-2 may activate FPP synthase gene expression. The promoter region of FPP synthase contains a binding site for SREBP-2, which is also present in other genes associated with cholesterol synthesis. What is not well-understood is if changes in FPP levels alone, where cholesterol levels are unaffected alter SREBP function. The idea that SREBP-2 activation may not be responsive to FPP levels is that depletion of mevalonate in Caco-2 cells stimulated SREBP-2 activation but adding FPP did not reduce activation[118], which would be expected if FPP was acting in a similar manner as cholesterol. There is limited information on the transcriptional regulation of FPP synthase. FPP synthase gene expression was directly stimulated by the transcription factor LXR.[119] Activation of FPP synthase gene expression was stimulated by the LXR agonist, hypocholamide, in immortalized brain cell lines.[119] On the other hand, FPP synthase gene expression was significantly reduced in brain tissue of LXR-null mice.[107]

Taken together, the regulation of the HMG-CoA reductase expression and its degradation involves a multivalent feedback mechanism by sterol and non-sterol products of the MVA pathway. The degradation of HMG-CoA reductase itself is assumed to be carried out by the 26 S proteasome.[120,121]

1.6. Protein prenylation – small GTPases

Over 100 proteins in the human proteome are potential substrates to undergo prenylation.[3,13,122,123] Many of those proteins belong to the super family of small GTPases, with molecular masses ranging from 20 – 40 kDa.[124] Small GTPases are integral components of complex signalling networks and control diverse cellular activities including intracellular vesicle transport, cell adhesion, endocytosis, cytoskeletal organization, receptor signalling, vesicle trafficking, cell cycle progression and gene expression.[124,125,126]

1.6.1. Prenylation – a post-translational modification

Prenylated proteins include Ras and related small GTP-binding proteins such as Rho, Rab and Rac, the subunits of trimeric G-proteins, nuclear lamins and other proteins.[13] Prenylation of proteins by FPP and GGPP is critical for enabling those proteins to be inserted into membranes, thus determining their localization and function.[13] Prenylation is a lipid based PTM involving the covalent attachment of either FPP catalyzed by FTase or GGPP catalyzed by GGTase I or II to the cysteine residue in defined consensus motives.[4,127,128,129,130] This motive is the so called CaaX-box, where ‘C’ is a cystein, ‘a’ an aliphatic amino acid and ‘X’ the terminal amino acid mainly determining which isoprenoid will be attached.[131] Both, the Ftase and GGTase are heterodimers sharing a common α subunit.[132] For the prenylation reactions the prenyltransferases require a zinc ion in the active centre of the binding site of the CaaX containing protein, allowing for enhanced affinity to the transferase.[128,133,134] Upon attachment to the protein substrate, the cysteine residue of the CaaX-motive is believed to coordinate with the Zn^{2+}. This has been verified through biochemical studies, which have demonstrated the need for Zn^{2+} for catalytic activity as well as its coordination with the cysteine thiol of the CaaX-motive.[135] Mg^{2+} is also required in millimolar concentrations for optimal enzymatic activity of the transferases, though it may not be strictly necessary for catalysis.[134]

It is generally accepted that Ftase substrates contain a CaaX-motive with a terminal 'X' amino acid, which is either serine, alanine, methionine or glutamine, and for the GGTase I the terminal amino acid must be a leucine.[4,127,128,130,136] A list of some of the most common prenylated proteins with their respective C-terminal CaaX-motive can be seen in Table 2.

Subfamily	**Exemplified protein**	**CaaX-motive***	**Predominant isoprenoid modification****
Ras GTPases	H-Ras K-Ras N-Ras	-CVLS -CVIM -CVVM	farnesylation
Rho GTPases	Rac1 Rac2 Cdc42 RhoA	-LLL -SLL -VLL -LVL	geranylgeranylation
Rab GTPases	Rab1a Rab5a	-GGCC -CCSN	double geranylgeranylation
	Rab8a H Rab11	-CVLL -CQNI	geranylgeranylation
Ran GTPases	Ran	-	-
Sar1/Arf GTPases	Sar1a Arl6	-	-

Tab. 2. Brief overview over the 5 main subfamilies of the small GTPases (see also section 1.6.2.) with exemplified protein members and their respective CaaX-motives (- no CaaX-motive and consequently no C-terminal prenlyation). * For some members of the small GTPases different isoforms with partly varying CaaX-motives were identified (not shown in table). ** Depending on the small GTPases and the physiology/pathology of the cell prenylation by the respective prenyltransferase is either stringent or the proteins partly undergo cross-prenylation (examples are given in section 1.6.1.).

Nevertheless, these requirements do not seem to be ultimatively stringent as shown for example by kinetic studies with artificial CaaX-substrates.[137] Moreover, it was reasoned that the peptide sequence upstream of the CaaX-motive might also play a role in the substrate specificity of the two prenyltransferases.[138,139]

These studies also revealed that the binding of either isoprenoid to the prenyltransferases is not imperative and that variation of the 'aa' amino acids in the small GTPase can impact its affinity to the respective prenyltransferase; this was illustrated by means of crystallographic analysis.[140]

Furthermore, reports on cross-prenylation substantiate the notion that prenylation is flexible to a certain degree. One representative example is the cross prenylation of K-Ras occurring when Ftase is inhibited or when FPP is in limited supply. The GTPase contains a classical CaaX-motive (cystein-valine-isoleucine-methionine = CVIM) for farnesylation, but becomes a substrate

for GGTase I under the aforementioned conditions.[141] Another example indicates that GGTase I is capable of transferring the farnesyl moiety to RhoB, which possesses the GTPases CaaX-motive CKVL (cystein-lysine-valine-leucine). Accordingly, farnesylated and geranylgeranylated versions of this protein are evident in cells, both reactions being catalyzed by GGTase I.[142] It is worth mentioning that such cross-prenylation reactions might partly explain failures of prenylation inhibitors as anti-cancer treatments.[143]

Besides the CaaX GTPases other family members, which contain a CC-, CXC- or CCXX-motive undergo di-geranylgeranylation where two GGPP lipids attach to the two cysteine residues of the motive.[130,144] These motives are found exclusively amongst the Rab subfamily of GTPases. Although the majority of Rab proteins possess such a di-cysteine motive, there is a select number of proteins such as Rab8, Rab11 and Rab13, which possess the CaaX-motive.[144] The process of di-geranylgeranylation is catalyzed by GGTase II, also known as Rab geranylgeranyltransferase. This enzyme specifically modifies Rab family members of the GTPases but only when they are associated with the Rab escort protein (REP), which is capable of binding to both prenylated and unprenylated Rab proteins. In the unprenylated form, REP presents a Rab GTPase to the GGTase II, allowing the sequential addition of two GGPP molecules to its two C-terminal cysteine residues. Upon binding to the prenylated form of the GTPase, REP facilitates the incorporation of the protein within the intracellular membrane.[130,145]

Following prenylation, the prenylation motive containing proteins undergo two further processing steps. The diphosphate is cleaved off by the Ras converting enzyme (Rce1p) and the Ste24p endogenous proteases remove the terminal three amino acids (-aaX).[146,147,148] Upon cleavage of the terminal tripepetide, the remaining prenylated cysteine residue undergoes carboxymethylation by a methyl group, delivered from S-adenosyl methionine (SAM) (Figure 2). This conversion is catalyzed by isoprenylcysteine carboxyl methyltransferase (Icmt). Icmt is located in the Golgi apparatus, ER and nuclear membranes.[149] Under physiological conditions, the carboxymethylation is reversible.[150] It is assumed that the intermediates during these subsequent enzymatic reactions exist only transiently and are rapidly converted into the mature prenylated protein.[127] Overall, prenylation enhances lipophilicity and favours lipid-lipid interactions of small GTPases with cellular membranes.[151] Its physiological importance is further underscored by affinity studies of the enzymes utilizing FPP as a substrate. As summarized by Winter-Vann and Casey for the squalene synthase a K_m value of 2 µM was found and the K_m values of the GGPPS was calculated to be about 1 µM and of the Ftase about 5 nM for FPP.[123] These studies highlight

the importance of the prenylation reactions for cell physiology and support the notion of a higher affinity of the isoprenoid pathway enzymes for FPP than those of the cholesterol pathway.[1,152] Following prenylation some proteins like for example N-Ras, H-Ras or RhoB are also palmitolayted. This modification entails a thioester linkage of the palmitoleic acid chain to the sulphur group of a cysteine residue, which is in close proximity to the prenylated cysteine.[4] Similar to the previously described processes of protein prenylation and carboxylmethylation, protein palmitoylation allows membrane binding and intracellular localization by increasing lipophilicity of certain proteins.[153,154]

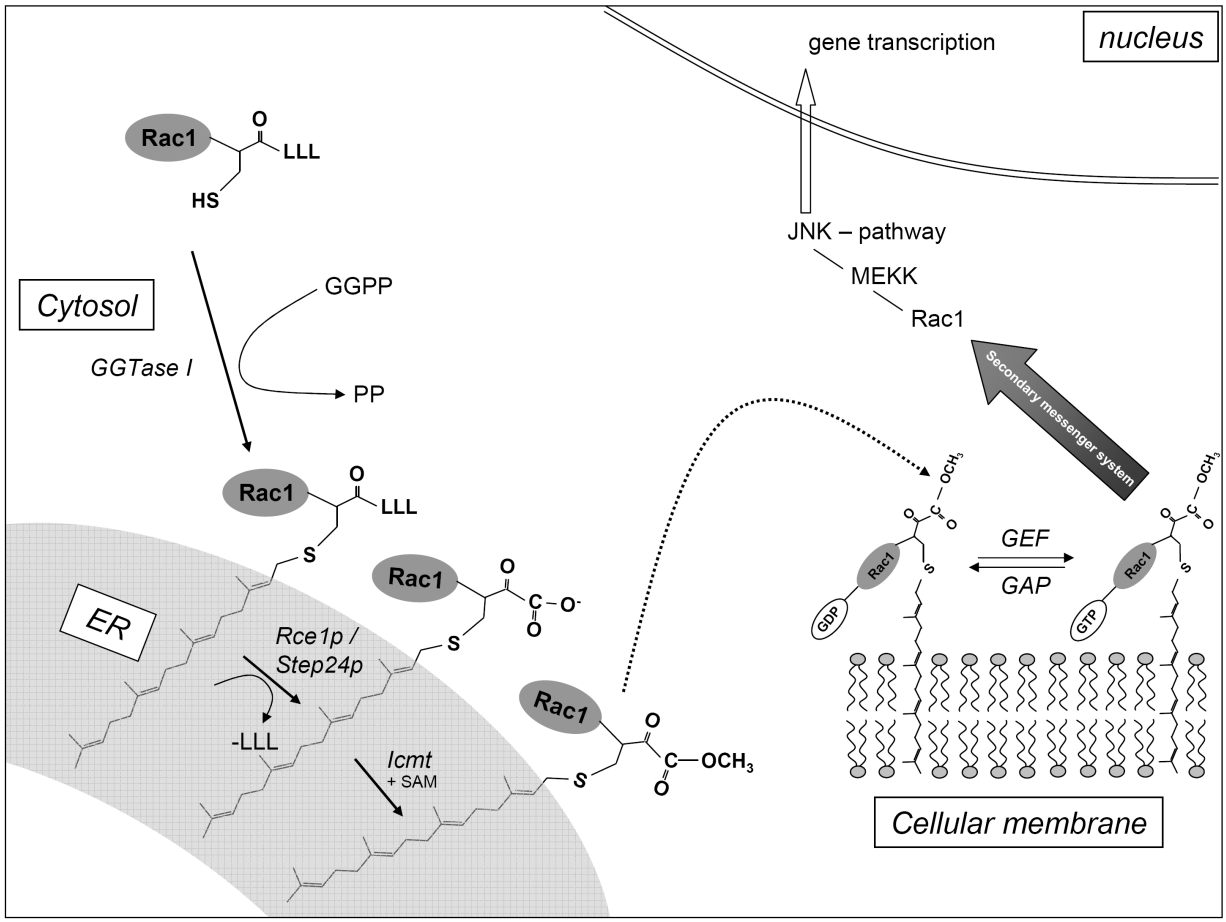

Fig. 2. Exemplified overview describing the chronological post-translational modification (PTM) of Rac1. The newly translated protein becomes geranylgeranylated and subsequently modified by Rce1p or Step24p, two endopeptidases cleaving off the terminal three amino acids (-LLL) of the CaaX-motive. The last step describes the modification by the isoprenylcysteine carboxyl methyltransferase (Icmt), using S-adenosyl methionine (SAM). The latter two reactions are mainly taking place in the endoplasmatic reticulum (ER) and in the Golgi apparatus (not shown in the figure). The final products (activated GTPases) possibly undergo further PTMs before being inserted into the target membrane. Final activation and deactivation depend on the GDP/GTP status governed by GEFs/GAPs and partially by the GDIs (refer to section 1.6.2. for further details). The activated, GTP loaded enzyme activates downstream, secondary messengers, finally leading to modulated gene transcription of distinct genes. Depicted in the current figure is the Rac1-MEKK-JNK pathway.[155]

1.6.2. Prenylated proteins – the small GTPases

Small GTPases are guanine nucleotide-binding molecules (G-proteins). Small GTPases play a fundamental role in a multitude of intracellular signal transduction pathways involving vesicle trafficking, cell growth, differentiation and cytoskeletal function. The small GTPases bind guanosine triphosphate (GTP) when activated and guanosine diphosphate (GDP) when inactivated. In response to an upstream signal as for example proposed for amyloid beta (Aβ)[155], GDP dissociates from the GTPase and then binds a GTP molecule. Two types of regulatory proteins mainly execute the GDP/GTP exchange of all small GTPases. The guaninenucleotide-exchange factors (GEFs) promote the GTP bound and therefore active form of the G-protein[156], while the GTPase activating proteins (GAPs) lead to the GDP bound inactive form by stimulating the weak intrinsic GTP hydrolysis capacity of the GTPases.[157] RhoA, Rac1, Cdc42 and Rab proteins possess the same GEFs and GAPs regulatory mechanisms while additionally regulated by a third class of proteins, the guanine nucleotide dissociation inhibitors (GDIs).[124,158] After complex formation of a GDI with a GTPase, GEF stimulated dissociation of GDP from its GTPase is inhibited and these GTPases cycle between membrane and cytosol.[124] Binding of GTP leads to a conformational change in the downstream effector associated region and to activation of secondary effector pathways, such as the MEKK-JNK/p38 – pathway (Figure 2).[156]

A classification of the small GTPase superfamily into at least five different families is generally accepted and briefly described below. The differentiation was based on sequence and functional similarities between the members of each branch.[3,124,159]

The Ras family. The family name of this group of small GTPases originates from Ras sarcoma (Ras) and these GTPases have been the most extensively studied proteins due to their well-known role in oncogenesis.[160] Signaling pathways including Ras GTPases are commonly activated in various tumors, including glioblastoma multiforme (GBM).[161] Additionally, about 30% of all human cancers have been associated with mutations in the Ras proto-oncogen.[162] H-Ras, K-Ras and N-Ras are the most renowned members of this family and they are constantly activated as a consequence of the mutation in the proto-oncogen.[161] Furthermore, the majority of the Ras subfamily members are known to be farnesylated and interestingly K- and N-Ras but not H-Ras can be geranylgeranylated when physiological farnesylation is inhibited .[161,163] Despite the fact that Ras proteins are associated with carcinogenesis, it is worth mentioning that other Ras family members, such as RhoB seem to act as tumor suppressors.[162]

The Rho family. Extracellular stimuli activate Ras homologous (Rho) proteins, which are involved in proliferation, apoptosis, actin formation, adhesion, and motility.[159,162] RhoA, Rac1 and Cdc42 belong to the Rho GTPases[164], which effect on more than 30 secondary effector proteins, such as ROKα/β or MEKK1,4.[165] While the classical members RhoA, Rac1 and Cdc42 are known to be geranylgeranylated other Rho subfamily members were found to be farnesylated (Table 2).[166]

The Rab family. The 60 Ras-like proteins in the brain (Rab) represent the largest group within the superfamily of small GTPases.[167] These proteins and their effectors, such as Rabex-5 or Coronin 3 are mainly involved in intracellular vesicular transport, including vesicle formation, organelle motility and directing vesicles between different compartments.[168,169,170,171] As mentioned earlier Rab proteins, with the non-CaaX-motive undergo di-geranylgeranylation by the GGTase II.[129,172]

The Ran family. The Ras-like nuclear proteins (Ran) function in nucleo-cytoplasmic transport, mitotic spindle and nuclear envelope assembly and DNA replication.[173,174] The transport mechanism relies on a unique gradient of Ran-GTP between the nucleus and the cytosol.[159]

The Sar1/Arf family. The ADP-ribosylation factor (Arf) and secretion-associated and Ras-related (Sar) proteins are mainly involved in vesicle formation and intracellular trafficking.[124,175] For example, Arf1 regulates the formation of vesicle coats at different steps in the exocytic and endocytic pathways. Beside others, Arf1 controls the formation of coat protein I (COPI)-coated vesicles involved in retrograde transport between the Golgi and ER, of clathrin/adapter protein 1 (AP1)-complex-associated vesicles at the trans-Golgi network (TGN) and on immature secretory vesicles, and of AP3-containing endosomes.[159] In addition to prenylation, some members of the Arf family are post-translationally modified with a myristate fatty acid at their N-terminus.[159]

1.6.3. Analytical approaches for the quantification of farnesylated proteins

A review by James P. in 1997 is titled as "*Protein identification in the post-genome era: the rapid rise of proteomics*" and shows the emerging role of the new field of proteomics in the 90s.[84] Over 10 years later there is an enormous amount of publications available on this still relatively young topic and the numbers are growing by the month. Many of these advancements

would have been possible without mass spectrometry. Many of these studies also included the identification of various small GTPases whereby one study should be highlighted herein due to its involvement of the farnesyl moiety.

Appels et al. quantified farnesylated proteins in isolated cells by LC-MS/MS measurements. The idea behind their approach was the detection of the farnesylated methylcystein (Fmc) C-terminus, which is cleaved of by endogenous proteases upon cell lysis.[127] This fragment was further used for multiple reaction monitoring (MRM) analysis in a triple quadrupole mass spectrometer (QqQ). In these measurements the first quadrupole selects the parent ion while the second one serves as a collision cell for this specifically selected ion, filled with an inert gas (e.g.: nitrogen) to induce fragmentation. The third quadrupole is set for a certain fragment ion mass deriving from the impact of the parent ion with the gas molecules. Such measurements are more selective and are used for quantification purposes.

1.7. The aging brain and pathological implications of the MVA-pathway

Aging is the major risk factor for the development of the most common neurodegenerative diseases like AD, Parkinson Disease, Cerebrovascular Disease or Amyotrophic Lateral Sclerosis. In the developed industrial countries a clear link between the constantly aging population and the rising prevalence of these diseases can be identified. Aging is recognized as physiological process, which leads to specific structural, physiological and functional changes in the body, including the brain and affecting mental activity, social behavior and memory function.[176,177,178]

1.7.1. Cholesterol and aging

As previously described MVA-pathway products massively impact a wide range of cellular processes. Cholesterol as the best-established end-product of the pathway has been the focus of research for over 40 years. One of the very first publications in this area dates back to 1965 and investigated white and grey matter cholesterol content of human brains, between 19 months and 55 years.[179] Since then a lot of research has circled around brain cholesterol alterations as a function of aging, some of which was summarized in comprehensive reviews.[23,180,181] The overall findings indicate that cholesterol *de novo* synthesis declines as we grow older while total cholesterol levels steadily increase but with a different magnitude depending on the brain region and the developmental phase of the brain. For example, a significant change of cholesterol levels

can be observed in distinct areas in mice brains or as mentioned earlier, in isolated SPMs from different aged mice (see section 1.2.). The cerebral cortex of 3, 6 and 25 month old mice showed a steady and statistically significant increase in cholesterol with aging[182], while another study reported unchanged levels of cholesterol in isolated SPMs of young, middle-aged and aged mice.[47] However, more than twice the cholesterol content in the exofacial leaflet of the aged mice from the same study, revealed a drastically altered leaflet distribution of the cholesterol in the SPMs. Since cholesterol is known as an important component of the plasma membrane and additionally a potent modulator of membrane fluidity the same study found a decreased fluidity of the outer leaflet, as a consequence of the age-dependant cholesterol increase. Furthermore, studies on isolated lipid rafts from aged mice brains also showed increased cholesterol levels when compared to lipid rafts isolated from young animal brains.[48] The importance of theses findings lies in the fact, that a change in cholesterol itself and consequently in membrane composition and membrane characteristics possibly affects a large facet of membrane associated intra- and intercellular physiological processes. Several studies were able to either show a link of an altered cholesterol abundance impacting on membrane fluidity or on lipid raft associated proteins which consequently leads to an aberrant activity of distinct physiological processes.[183,184,185,186]

The most prominent genetically caused disorders linked to a defective cholesterol homeostasis are the Smith-Lemli-Opitz syndrome, Huntington´s Disease and Niemann-Pick Disease, type C. Further details concerning causes, diagnosis, symptoms and treatments of these three diseases can be viewed in the following recently published reviews.[187,188,189,190]

1.7.2. Cholesterol-precursors and -metabolites in aging

As described in the previous paragraph cholesterol *de novo* synthesis of the human brain is lower in older subjects as compared to younger ones, but the overall cholesterol abundance increases with age.[23,181,182] Furthermore Thelen and colleagues were able to demonstrate a declined synthesis rate of cholesterol accompanied by significantly lower lanosterol and lathosterol concentrations in the aged human hippocampus.[191] These two lipids are precursors of cholesterol (Figure 1). The same study revealed lower 24*S*-hydroxycholesterol levels in older subjects.[191] A study in rat brain further substantiated these findings by demonstrating a significantly reduced squalene synthase activity when comparing aged rats to young animals.[192] Taken together there is

a consensus that downstream of squalene synthase synthesis rates and concentrations of intermediates and metabolites of cholesterol decline in the aging brain.

1.7.3. Isoprenoids in aging and neurodegeneration

Normal cell function requires prenylated proteins and there is evidence that GGPP is required for long-term potentiation (LTP) in mouse hippocampal slices.[193] However, it is becoming increasingly recognized that prenylated proteins are involved in certain diseases both within and outside of the central nervous system (CNS). Diseases largely outside the CNS in which FPP and GGPP potentially play a significant role are certain types of cancer, osteoporosis, Paget disease, and atherosclerosis.[4,194,195,196] Moreover, recent evidence suggested that inhibition of FPP-induced protein prenylation using a farnesyltransferase inhibitor significantly improved motor function and survival in a mouse model of Hutchinson-Gilford progeria syndrome or what has been referred to by some as premature aging.[197,198] Diseases of the CNS in which isoprenoids and protein prenylation are drawing increasing attention are Parkinson disease, multiple sclerosis, and ischemic stroke.[198,199,200] Recent experimental evidence indicates that isoprenylated small GTPases are involved in AD pathogenesis.[3,201,202,203]

1.7.3.1. Isoprenoids and aging

Aging is a process which leads to specific structural, biochemical and functional changes in multiple organs including the brain[176,177,178] and represents the major risk factor for the development of the most common neurodegenerative diseases like AD, Parkinson Disease, cerebrovascular disease and amyotrophic lateral sclerosis.[28] Age-related processes in the brain have been extensively studied[28,204] and changes in various lipids have been examined in several studies on cholesterol homeostasis.[23] Isoprenoids on the other hand, have received only scant attention in aging research. Age related changes in FPP and GGPP levels have not been reported, which is in stark contrast to their important biological roles. Dolichol levels increase with aging[83] and dolichols were identified as a potential biomarker of senescence.[76] Levels of dolichol were markedly higher in human brain tissue of aged individuals (e.g. approx. 19 vs. 26 µg/g ww hippocampus tissue in young and aged humans, respectively).[80,205] SPM of 18 and 28 month old C57BL/6 mice had a 5 fold and 11 fold increase, respectively, in dolichol levels when compared with 6 month old mice.[79] In the same study, it was found that dolichol had a greater fluidizing

effect on SPMs of young mice than aged mice. Increased dolichol content has been observed in brain tissue of individuals with AD and neuronal lipofuscinosis.[206,207,208] Neither has it been determined whether the elevated dolichol levels observed with increasing age and certain neurodegenerative diseases are injurious to cell function nor the mechanisms of such changes have been established.[209]

Ubiquinone levels were found to decrease with age in human brain tissue (e.g. approx. 14 vs. 8 µg/g ww hippocampus tissue in young and aged humans, respectively).[210] In rat brains however, the ubiquinone synthesis rate was shown to steadily increase with aging and ubiquinone levels (approx. 20 µg/g ww) were relatively constant throughout the entire life span.[192]

1.7.3.2. Prenylated proteins, synaptic plasticity and aging

The isoprenoids FPP and GGPP serve as substrates for the prenlyation of the small GTPases (see section 1.6). Their role is not well understood in the context of aging; although they are known to play a distinct role in synaptic plasticity (further details see section 1.8.5.). Long term potentiation (LTP) is one form of synaptic plasticity (section 1.8.5.), which underlies an age-dependant decline. However, the involved mechanisms still need to be elucidated.[211] A very recent study described the role of RhoB, besides other small GTPases in the regulation of dendritic and spine morphology.[212] The protein is expressed in the hippocampus and cortex, is induced during aging and has the ability to impact on actin regulation. Studies were carried out on RhoB knock-out mice and clearly demonstrated the involvement of RhoB in synaptic plasticity.[212]

1.7.3.3. The MVA-pathway and neurodegeneration

The MVA-pathway and its described various intermediates and end products (Figure 1) are involved in a wide range of crucial cell processes and functions including decisive signaling pathways. The distinct steps of the biosynthesis of different products involve a complex and not yet fully understood regulation of transcription, translation, activation and degradation. It is obvious that due to the involvement of such a large number of directly participating enzymes, abnormal functioning or misdirected regulation will lead to severe consequences for the cell. The most known disorders with a disrupted MVA-pathway homeostasis are the Smith-Lemli-Opitz syndrome, Huntington´s Disease and Niemann-Pick Disease, type C as mentioned

earlier.[187,188,189,190] However, implications of an abnormal MVA-pathway regulation in respect to neurodegenerative diseases, like AD have also been described earlier.[3,13] The following paragraphs will give a more detailed insight into AD pathology, will give some background information on the disease and will summarize recent knowledge of the possible implications of the mevalonate/isoprenoid/cholesterol pathway.

1.8. Alzheimer's Disease

1.8.1. Prevalence and characteristics

Alzheimer's disease (AD) is a progressive neurodegenerative disorder and accounts for an estimate of up to 80% of all dementia forms. In 2005 the number of people with AD worldwide was estimated to be 24 million and it is predicted that the number will increase to more than 80 million cases by 2040[213], a number equivalent to the population of Germany.

It is thought that the molecular pathology, describing the formation of senile amyloid beta (Aβ) plaques and neurofibrillary tangles, containing the tau protein, develops 10 – 20 years before the first symptoms occur.[214,215] The earliest observable signs are mostly recognized as memory lapses, semantic impairment and anomia[216], clinical symptoms, which are rather unspecific. As the disease progresses the cognitive deficits aggravate and become more noticeable for relatives. These changes become apparent as the patients tend to forget recently learned information and show strongly affected language skills. Patients experience mood swings and consequently they become more withdrawn. In the advanced stages of the disease severe memory deficits prevent the independence of the patients and the mood and behavioral changes normally become more dramatic. Finally the physically weakened patients mostly die as a consequence of secondary diseases like pneumonia.[217] The life expectancy of AD patients is mostly depending on age and the time point of diagnosis. Patients with a diagnosis in their 60s or early 70s usually have a time span of 7 – 10 years.[218]

1.8.2. Etiology

The most common form of AD is the sporadic type (SAD), which accounts for about 98% of all AD cases.[3] A minor proportion of AD cases occurs before the age of 65 and is known as early-onset AD. The majority of these patients inherit genetic mutations, which are then called familial AD (FAD) cases. The three major gene mutations which are known to be associated with FAD

are mutations in the presenilin 1 (PSEN 1) gene on chromosome 14, in the presenilin 2 (PSEN 2) gene on chromosome 1 and in the amlyoid precursor protein (APP) on chromosome 21.[219] Taken together these mutations lead to a preferential amyloidogenic processing of APP and increase the Aβ load in the brain.

A multitude of risk factors for SAD are discussed and intensively investigated. Besides the most important one, which is age[220] several other factors including nourishment, lifestyle and other diseases are up for debate.[221,222,223,224] Regarding genetics ApoE is the only well established risk factor for increasing the predisposition to develop SAD. ApoE is significantly involved in cholesterol transport in the periphery and in the CNS. The inheritance of the ApoE-ε4 allele, one of three different isoforms (ApoE- ε 2, ApoE- ε 3 and ApoE- ε 4) of the ApoE gene is linked to an increased risk to develop AD.[225,226] The exact mechanism underlying the ApoE involvement is not yet clarified and various interactions are under investigation.[227]

1.8.3. Diagnosis

Different forms of dementia can be roughly differentiated in primary and secondary forms. While primary forms like AD or vascular dementia are discrete diseases, secondary forms are a consequence of other neurological diseases like Pick's, Lewy bodies or Parkinson Disease. An exact diagnosis of AD is very complex and especially an early identification hard to achieve. Over the last years intensive research has been put into the discovery of reliable biomarkers in order to start an early therapeutic treatment and to monitor drug impact on disease progression.[228] Most studies focus on Aβ, phosphorylated and total tau, the major hallmarks of the disease forming extra- and intercellular plaques as well as intracellular tangles, respectively.[214,229] Ante mortem measurements as for example in the cerebrospinal fluid (CSF)[230] or imaging techniques based on magnetic resonance imaging (MRI) or X-ray computed tomography (CT) scans are most helpful tools to exclude other diseases. Besides 18-F-deoxy-glucose positron emission tomography (FDG-PET) the use of Pittsburgh Compound-B (PIB-PET) is one of the most studied and reliable amyloid imaging technique.[231] Despite these latest achievements and the use of state-of-the-art analytical techniques there are still shortcomings in terms of reliability and availability of such methods, not to mention the enormous costs simply for diagnosis.

On the other hand these clinical and scientific advances led in 2007 to a revision of the diagnostic markers defined by The National Institute of Neurological and Communicative Disorders and

Stroke, and the Alzheimer's Disease and Related Disorders Association (NINCDS-ADRDA) for the clinical diagnosis of AD.[232,233,234]

The clinical diagnosis is partly conducted with the help of test for cognitive impairment. These are for example the mini-mental status examination (MMSE), the global deterioration scale (GDS) and the cognitive part of the Alzheimer's Disease assessment scale (ADAS-Cog), which are compared in a study by Solomon et al.[235]

Despite all the advances a definite diagnosis of AD can only be carried out post mortem. Furthermore, by this histological analysis the disease progression can be defined according to Braak stages I – VI, as the pathology begins in the entorhinal area of the cortex, proceeding to the hippocampus and finally to the entire neocortex.[236] Full clinical dementia appears at about Braak stage IV. According to this definition neurofibrillary tangles and neuropil threads are the main characteristics in AD brain morphology.

A detailed description of AD etiology and neuropathology with its neurofibrillary tangels and amyloid plaques and a precise characterization of the formation and the processing of Aβ was recently published by our working group in form of two dissertations and the reader is referred to these two dissertations.[237,238]

.

1.8.4. Involvement of the MVA-pathway products and intermediates in AD

1.8.4.1. Cholesterol, statins and AD

The aforementioned two forms of AD, SAD and FAD show the same pathological hallmarks, Aβ plaques and tau tangles. Over the last decade the main body of research centered on APP and Aβ and innumerable investigations aimed to influence their synthesis, processing and the overall cell load.[239,240,241,242] Regarding these mechanisms cholesterol metabolism is of special interest and its association with AD is described briefly herein.

Based on evaluations of human studies there is a well investigated link between hypercholesterolemia and the development of AD.[3,243] The cholesterol link is further supported by the aforementioned inheritance of the ApoE-ε4 allele, as the only clearly demonstrated risk factor for the development of AD.[244] Albeit, it is worth mentioning that a recent review critically summarizes the latest studies on the cholesterol Aβ link, which challenges the question of the detrimental influence of high cholesterol levels.[245] Furthermore, the initially described beneficial

effects of cholesterol reducing statin intake in lowering the incidence for developing AD became disputable. Relying on retrospective evaluation of patient data the authors concluded a reduction in AD prevalence among patients with a statin treatment history.[246,247,248] These studies were later critically discussed by a prospective study with a small patient collective and over a relatively short period of 36 weeks. Aβ measurements after statin treatment could not substantiate the previous findings.[249] Another study was able to demonstrate a statin influence of human cerebral cholesterol homeostasis in clinical relevant doses, but did not succeed in showing changes in Aβ brain levels.[250]

A similar, not yet fully elucidated discrepancy was described by studies focusing on 24*S*-hydroxycholesterol in AD patients. A few publications by one group described elevated oxysterol levels in AD plasma, discussing it consequently as a possible early AD biomarker.[251,252] Authors from the same group revealed a cerebral 24*S*-hydroxycholesterol reduction in an advanced stage of the disease, while the 27*S*-hydroxy derivative was markedly elevated simultaneously.[29,253]

Taken together, the central cholesterol metabolism seems to be involved in AD pathology. This is further connected to lipid raft formation and Aβ generation. However, it remains a matter of discussion which MVA-pathway involving process underlies the development and progression of AD.[243]

Regarding the aforementioned statin investigations, it is well established that the HMG-CoA reductase inhibitors show a multitude of pharmacological effects beyond simply lowering cholesterol. This pleiotropic effects includes peripheral antithrombotic and plaque stabilizing mechanisms, improvements of endothelial function, antioxidative effects, a reduction of vascular inflammatory processes, etc.[254] Most of these effects are generally accepted to be due to a reduction of isoprenoids, notably FPP and GGPP reduction. Since it was shown that simvastatin, lovastatin and to a lower extent pravastatin cross the BBB in mice[255] it seems more than feasible that they also exert an inhibitory effect on the central mevalonate/isoprenoid/cholesterol pathway. However, it is questionable if the concentrations achieved by clinical doses in humans and the low concentrations measured in human CSF[256] are relevant.

1.8.4.2. Isoprenoids and neurodegeneration

The MVA-pathway and its several products are involved in a wide range of critical cell functions. Biosynthesis of different products involves a complex and not fully understood regulation of

transcription, translation, activation and degradation. Abnormal functioning or misdirected regulation of genes and protein products associated with the MVA-pathway will lead to severe consequences for the cell. A defective cholesterol homeostasis is causal for the Smith-Lemli-Opitz syndrome. Other disorders that have been at least partly linked to cholesterol are Huntington´s Disease, AD and the lysosomal storage disease Niemann-Pick type C.[187,188,189,190,257]

1.8.4.3. Isoprenoids in AD

There is some evidence that dolichol and ubiquinone levels are altered in AD.[210] Dolichol levels were decreased in all brain regions of AD patients (e.g. approx. 199 vs. 111 µg/g ww frontal cortex tissue from controls and Alzheimer's Disease, respectively).[210] In contrast, dolichyl phosphate levels increased in those regions that exhibited morphological changes (e.g. approx. 21 vs. 32 µg/g ww frontal cortex tissue from controls and Alzheimer's Disease, respectively). In the same study, a significant elevation in ubiquinone content was observed (e.g. approx. 13 vs. 17 µg/g ww frontal cortex tissue from controls and Alzheimer's Disease, respectively). It was concluded that the increase in the sugar carrier dolichyl phosphate might reflect an increased rate of glycosylation in the diseased brain whereas the increase in ubiquinone may be an attempt to protect the brain from oxidative stress.[210] A recent study reported increased oxidized ubiquinone levels in the cerebrospinal fluid of AD patients.[258] Experimental studies in animal AD models suggested that ubiquinone may protect against neuronal damage.[259] However, a synthetic analogue of ubiquinone (Idebenone) clinically failed to slow cognitive decline in AD.[260] However, the exact roles of dolichol and ubiquinone in AD pathogenesis have not been established yet.

There is evidence that prenylated small GTPases are involved in AD pathogenesis.[202,261] A straightforward prediction was that FPP and GGPP levels would be elevated in AD brains as compared with normal neurological controls.[3,262] However, due to methodological problems such data had not been reported.

Tong et al. described the first method for the simultaneous determination of FPP and GGPP in cultured cells.[94] Up to now, FPP and GGPP were determined in mouse embryonic fibroblasts and human cancer cells such as immortalized colorectal adenocarcinoma, myelogenous leukemia and multiple myeloma cells (Table 3a).[94,95,98,118] Cellular levels of FPP and GGPP are generally in the picomolar range as depicted in Table 3a, however significant differences in isoprenoid abundance can be observed between different cell lines. Moreover, the relative distribution between FPP and

GGPP varies between different cell lines. Such variances were also observed in mammalian tissue (Table 3b).[95]

Cell line	FPP	GGPP	unit	Reference
NIH3T3	0.125 ± 0.010	0.145 ± 0.008	pmol/10^{-6} cells	Tong et al.[94]
NIH3T3	0.131 ± 0.008	0.133 ± 0.003	nmol/g ww	Tong et al.[94]
K562	0.112 ± 0.008	0.238 ± 0.003	nmol/g ww	Tong et al.[95]
Caco-2	0.65 ± 0.02	-	pmol/well	Murthy et al.[118]
RPMI-8226	0.19 ± 0.001	0.29 ± 0,02	pmol/10^{-6} cells	Holstein et al.[263]
H929	0.16 ± 0.001	0.16 ± 0.02	pmol/10^{-6} cells	Holstein et al.[263]
U266	1.4 ± 0.001	0.58 ± 0.03	pmol/10^{-6} cells	Holstein et al.[263]
SY5Y-APP695	17.2 ± 1.2	13.4 ± 1.3	pmol/mg protein	Hooff et al.[264]

Tab. 3a. Levels of FPP and GGPP in different cell lines. Levels were determined using a fluorescence HPLC method[94] in mouse embryonic fibroblast cells (NIH3T3), in human immortalized myelogenous leukemia cells (K562), in human immortalized colorectal adenocarcinoma cells (Caco-2) and in human multiple myeloma cells (RPMI-8226, H929, U266). Human neuroblastoma SY5Y cell results were generated within the current work. Means ± SD.

Tissue	FPP	GGPP	unit	Reference
Mouse kiney[a]	0.320 ± 0.019	0.293 ± 0.035	nmol/g ww	Tong et al. 2008 [95]
Mouse liver[a]	0.326 ± 0.064	0.213 ± 0.029	nmol/g ww	Tong et al. 2008 [95]
Mouse heart[a]	0.364 ± 0.015	0.349 ± 0.023	nmol/g ww	Tong et al. 2008 [95]
Mouse brain[a]	0.355 ± 0.030	0.827 ± 0.082	nmol/g ww	Tong et al. 2008 [95]
Human brain[b]				
white matter	2.88 ± 1.04	14.34 ± 8,40	ng/mg protein	Hooff et al.[265]
grey matter	3.02 ± 1.32	9.66 ± 7.72	ng/mg protein	
Human brain[b]				
white matter	5.53 ± 0.63	11.88 ± 1.26	pmol/ mg protein	Eckert et al.[266]
grey matter	2.95 ± 0.25	7. 43 ± 0.81	pmol/ mg protein	
Alzheimer brain[b]	7.93 ± 0.91	18.61 ± 3.00	pmol/ mg protein	Eckert et al. [266]
white mater	4.03 ± 0.38	11.81 ± 1.69	pmol/ mg protein	
grey matter				

Tab. 3b. Leves of FPP and GGPP in different tissues.[95] Mouse tissue was isolated from athmic nu/nu mice. Human brain tissue results were generated within the current work. Means ± [a]SD, [b]SEM.

Compared to FPP, GGPP levels are lower in mouse kidney and liver tissue, equal in mouse heart tissue and higher in mouse brain tissue (Table 3b).[95] The differences in FPP and GGPP distribution may be due to the demand for intermediates of the MVA-pathway in specialized cells. There is a dearth of data on FPP and GGPP regulation and no more so than in brain.

It is well established that APP processing is influenced by cholesterol abundance[267,268,269,270] and that the reduction of cellular cholesterol levels using inhibitors of the MVA-pathway or extraction by methyl-β-cyclodextrin (MβCD) results in lower Aβ levels *in vitro* and *in vivo*.[271,272] However, evidence exists that FPP and GGPP are also involved in the cellular production of Aβ. It has previously been reported that γ-secretase is stimulated by geranylgeraniol[203] and incubation of H4 neuroglioma cells with FPP or GGPP were found to increase Aβ levels.[201] In those studies, APP processing was modified after incubation of cells with an extraordinarily high concentration of geranylgeraniol, FPP or GGPP (10 μM).

1.8.4.4. Prenylated proteins in AD

Prenylation of specific small GTPases has been associated with the processing of APP.[273] Activation of effectors downstream of prenylated small GTPases, such as the protein kinases ROCK (Rho associated coiled-coil forming protein kinase) have been implicated in APP metabolism.[274,275] GGPP stimulates γ- secretase to increase cleavage of APP and Aβ secretion[273] and inhibition of the Rho/Rock pathway reduced Aβ production.[276,277] Several small GTPases have been associated with AD in other pathways than those discussed in the preceding paragraph. There is evidence that Rab6 may be involved in APP processing and intracellular trafficking[278], Rab11 may contribute to vesicular transport[279] and Rac1 as a participant in Aβ induced generation of reactive oxygen species (ROS), which could damage neurons.[280] Moreover, Rac1 was shown to down-regulate transcriptional activity of the APP gene[281] and additionally, Rac1 and Rho-A appear to be involved in the production of actin-based morphological plasticity in dendrites and spines in hippocampal neurons.[282] Rab3 as a pre-synaptic protein was significantly reduced in AD brains.[283] Protein levels of Ras and Racl in both the cytosolic and membranous fractions and that of Rap2 in the cytosolic fraction were significantly decreased, while Rab8 was significantly increased in the membranous fraction in AD brains compared with controls.[284]

1.8.5. Prenylated proteins, synaptic plasticity and AD

Long-term storage of information is, at least in part, achieved by structural changes in neuronal connectivity, particularly changes in the structure and number of synapses. As a consequence, attention has focused on the rearrangement of specialized structures, termed dendritic spines, found at many synapses in the mammalian CNS. Increased synaptic activity has been shown to lead to LTP of synaptic efficiency via the formation of new spines.[285] Pronounced loss of neurites and synapses represents one of the most relevant histopathological lesions in AD brain with respect to neuronal function.[286,287,288] Failures of synaptic plasticity are thought to represent early events in AD.[289,290]

Synaptic plasticity is dependant on the structural regulation of the actin cytoskeleton in dendritic spines.[10,11,291] The Rho family of GTPases such as RhoA, Rac1, and Cdc42 monomeric G-proteins, are the major regulators in synaptic plasticity, both in dendrite morphogenesis and stability as well as in growth cone motility and collapse[6,8,9,10,11], affecting neuronal architecture and synaptic connectivity.[282] Small Rho proteins act as molecular switches between inactive GDP-bound and active GTP-bound forms under the regulation of several Rho GEFs and Rho GAPs (section 1.6.2.).[6,292] Representative of all Rho proteins, the role of Rac1 in synaptic function is highlighted: Rac1 is expressed in the adult mouse hippocampus[293], a brain area that exhibits robust synaptic plasticity and is crucial for the acquisition of associative memories.[294] In neurons, Rac1 is associated with neuronal development, participating in the morphological changes required for migration of newborn neurons to extension of axons and dendrites into proper target regions, and formation of synapses with appropriate partners. Its participation in neuronal morphogenesis is a contributor to synaptic plasticity and synapse formation.[295] *In vitro* studies in hippocampal slices indicated that activation of NMDA (N-methyl D-aspartate) receptors results in membrane translocation and activation of Rac1.[293,296] Furthermore, *in vivo* studies in adult mice revealed that Rac1 activation of NMDA receptors is linked with associative fear learning. Thus, Rac1 is recognized as an important molecule required for synaptic plasticity and is involved in the morphological changes observed at neuronal synapses during hippocampal learning and memory.[293,296] Recently, a small G-protein Rac dependant forgetting mechanism, which contributes to both passive memory decay and interference-induced forgetting was identified in Drosophila and it was suggested that Rac's role in actin cytoskeleton remodelling may contribute to memory erasure.[297] Recent studies described the Rac-specific GEF Tiam1 as a critical mediator of NMDA receptor-dependant spine developments. Tiam1 regulates spine and

dendrite development by activating Rac1- dependant signalling pathways which promote actin cytoskeletal re-organization and protein synthesis.[298] This process is triggered by the brain-derived neurotrophic factor (BDNF) and its tyrosine kinase receptor B (TrkB), which binds and phosphorylates Tiam 1, leading to activation of Rac-1 and induction of changes in cellular morphology.[299] TrkB activity is increased in aging and correlates with changes in cholesterol.[300] TrkB activates GGTase I, which mediates geranylgeranylation of Rac 1[273] and the GGTase I substrate GGPP acts on NMDA receptors and restores LTP dysfunction.[193] Hence, GGPP seems to be directly involved in Rac1 related actin cytoskeletal remodeling, which mediate dendritic spine formation, motility, and morphology, which are thought to be important for functional synaptic plasticity. FPP and GGPP levels in grey and white matter are speculated to be elevated in AD brains, which further suggests that abundance of prenylated small GTPases may be increased in AD.[3,261] Phospho-Rac/Cdc42 protein levels were increased in hippocampal membrane fractions isolated from AD brain and phospho-Rac/Cdc42 labeled only weakly and diffusely in hippocampal slices from normal controls, but appear as abnormal granular structures in AD brain.[301] The antibody used in that study detects endogenous levels of Rac1/Cdc42 only when phosphorylated at serine 71. Phosphorylation at that site may inhibit GTP binding of Rac1, attenuating the signal transduction pathway downstream of Rac1.[302] These findings are indicative for RhoA/Rac/Cdc42 dysfunction in AD brain. BDNF and its receptor TrkB also play important roles in synaptic plasticity and findings that BDNF and TrkB levels are severely decreased in the hippocampus and some cortical areas of AD patients[303,304,305] further support synaptic dysfunction in AD brain. Further, *in vitro* and *in vivo* findings support the idea that synaptic plasticity goes awry when levels of small GTPases are abnormally enhanced. Alzheimer related Aβ peptide increased the levels of the active GTP-bound form of RhoA in SH-SY5Y cells and increased levels of RhoA were found in neurons surrounding amyloid plaques in the cerebral cortex of APP(Swe) Tg2576 mice.[306] It was suggested in that study that Aβ-induced neurite outgrowth inhibition could be initiated through increased Rho GTPase activity that, in turn, phosphorylates the collapsin response mediator protein-2 and interferes with tubulin assembly in neurites.[306]

1.8.6. Prenylated proteins, oxidative stress and AD

AD elevated abundance of prenylated Rac1 could possibly also contribute to Rac1-NADPH oxidase-regulated generation of ROS causing oxidative stress, which has been reported in AD brain.[307,308,309] In the brain, microglia cells are prominent sources of ROS through expression of

the phagocyte oxidase, which generates superoxide ions. However, a recent study showed that microglia also express NADPH oxidases (NOX) and Rac1.[310] Immunohistochemical evaluations of NOX expression in human post-mortem tissue indicate that while microglia express high levels of the regulatory subunit gp91phox, moderate levels of gp91phox are also expressed in neurons.[311] Activation of NOX via Rac1 is a source of ROS generation in the brain[312], which plays a role in cerebral dysfunctions, such as stroke, BBB damage or seizure induced hippocampal damage.[313,314,315] A recent study found that NOX-associated redox pathways might participate in the early pathogenesis of AD. NOX expression and activity are up-regulated specifically in the temporal gyri of mild-cognitive-impaired (MCI) patients as compared to controls, but not in preclinical or late stage AD samples, and not in the cerebellum.[311] Moreover, *in vitro* studies identified Rac1 as an essential component of the Aβ signalling cascade leading to generation of ROS.[280]

1.9. Aims of the thesis

Aging represents the major risk factor for AD. In western countries a clear link is observed between a steadily increasing life expectancy and the prevalence of AD. Numerous publications indicate an involvement of cholesterol in both, brain aging and in AD. Analytical methods allow the measurement of cerebral cholesterol levels and its metabolites. Later ones are partially excreted into the blood-stream allowing the investigation of cholesterol turnover in the CNS by oxysterol analysis in the periphery. Although, data indicated that other MVA-pathway intermediates, especially FPP and GGPP also seem to be involved in cellular aging and AD progression, knowledge on relative or absolute isoprenoid brain levels and their regulation was clearly lacking. Impeding progress on advancing knowledge of FPP and GGPP regulation and on protein targets was mainly due to analytical difficulties and there was no technique available for the simultaneous quantification of FPP and GGPP levels in human brain tissue. Hence, the primary aim of the current work was to develop a validated method for the isolation and accurate, precise and sensitive quantification of FPP and GGPP levels in brain tissue. Moreover, further aims were to investigate the central regulation of these two key players of the MVA-pathway and to address their involvement in AD pathology and during aging.

FPP and GGPP are precursors of cellular lipids such as dolichol, ubiquinone and cholesterol. Furthermore, and of greatest relevance to the current work, the aforementioned molecules serve as substrates for the post-translational modification of members of the superfamily of small GTPases, including Rac1, RhoA and Cdc42. Small GTPases are crucial enzymes in a wide array of physiological processes. Due to their involvement in the activation of secondary effector pathways, a disease related modulation of intracellular abundance or localization potentially has critical effects on cell morphology and especially physiology. Their proper localization and functional activity in biological membranes primarily depends on the attachment of either of the two isoprenoids, FPP or GGPP.

As mentioned above, the involvement of the MVA-pathway in AD progression has been intensely discussed in literature. Previous studies mainly focused on cerebral and peripheral cholesterol and oxysterol levels, while more recent studies raised the interest in FPP and GGPP regulation in AD and during normal aging.

Due to the potential role of cholesterol in the onset and the progression of the AD, statins are discussed for their possible beneficial effects in AD. Statins are inhibitors of the rate limiting step of the MVA-pathway and therefore of the cholesterol synthesis. Hence, inhibition of mevalonate production may also affect the abundance of isoprenoids.

The development, validation and employment of a robust method for the quantification of FPP and GGPP in brain tissue was the pre-condition, required to begin to understand the isoprenoid homeostasis during aging and in AD. The knowledge of absolute levels of these two isoprenoids is the first step for a profound discussion of their involvement and regulation in the diseased stage. Furthermore, a comparison of isoprenoid levels in relation to cholesterol levels allows a better understanding of the regulation of the mevalonate/isoprenoid/cholesterol pathway.

To build upon the method for FPP and GGPP detection in human brain tissue, an extension of the analytical method was to demonstrate its applicability for measuring brain samples from *in vivo* studies in mice. Previous studies by our working group indicated cerebral statin levels after chronic treatment of animals. These studies suggested the potential for drug impact on the expression of an array of genes and on brain cholesterol levels. The aim of this part of the current work was to elucidate the impact of statin treatment on isoprenoid distribution in an *in vivo* model and to determine FPP and GGPP levels in various mouse models.

Since aging represents to most prominent risk factor for AD, the cerebral isoprenoid and cholesterol levels in three different generations of mice were investigated to further understand the physiological regulation of the mevalonate/isoprenoid/cholesterol pathway during brain aging processes.

A further goal of the current work was to detect differential effects of various mevalonate/isoprenoid/cholesterol pathway inhibitors on FPP and GGPP levels in an *in vitro* cell model using neuroblastoma derived SY5Y cells mimicking AD pathology in terms of Aβ formation. The aim of the current study was to provide information on isoprenoid regulation in this cell model under drug treatment using substances targeting this specific pathway.

After the successful implementation of the HPLC-FLD assay and the investigation of human AD brain samples the next technical aim of the current work was to transfer the method to a state of the art UHPLC-MS/MS system to significantly reduce analytical run times, while simultaneously increasing sensitivity. Over the last years MRM measurements on triple quadrupole mass spectrometers became the gold standard technique for absolute quantification and the number of new applications is increasing rapidly as the machine finds its way into an ever increasing number of laboratories.

2. MATERIALS

2.1. Chemicals

Chemical	Company / Source
[^{3}H]FPP (26.2 Ci/mmol)	Perkin Elmer, Waltham (USA)
[^{3}H]GGPP (23.0 Ci/mmol)	Perkin Elmer, Waltham (USA)
[^{14}C]- HMG-CoA	Sigma Aldrich, Munich
1-butanol	VWR International, Darmstadt
2-propanol	VWR International, Darmstadt
4-nonylphenol	Sigma Aldrich, Munich
Acetone	Merck, Darmstadt
Acetonitrile (ACN)	Carl Roth, Karlsruhe
Agar	Sigma Aldrich, Munich
Ammonium acetate	VWR International, Darmstadt
Ammonium hydroxide (NH_4OH) 28-30%	Alfa Aesar, Karlsruhe
Bovine Serum Albumin (BSA)	Sigma Aldrich, Munich
Brij 35	Sigma Aldrich, Munich
Bromphenol blue	Sigma Aldrich, Munich
Complete® protease inhibitor cocktail	Roche Diagnostics GmbH, Mannheim
D*-GCVLL (dansyl gly-cys-val-leu-leu)	Calbiochem, Darmstadt
D*-GCVLS (dansyl gly-cys-val-leu-ser)	Calbiochem, Darmstadt
Dansyl chloride	Sigma Aldrich, Munich
Diethyl ether	VWR International, Darmstadt
Diisopropyl ether	VWR International, Darmstadt
Dimethyl sulfoxide (DMSO)	Merck, Darmstadt
Dimethyl sulfoxide deuterated (C_2D_6OS)	Carl Roth, Karlsruhe
Dithiothreitol (DTT)	Sigma Aldrich, Munich
Dulbecco´s Phosphate Buffered Saline	Gibco/Invitrogen, Karlsruhe
Dulbecco´s Modified Eagle Medium (DMEM)	Gibco/Invitrogen, Karlsruhe
EDTA (K- and Na-salt)	Sigma Aldrich, Munich
Ethanol (EtOH)	Merck, Darmstadt
Ethyl acetate	VWR International, Darmstadt

Farnesyltransferase (FTase)	Jena Biosciences, Jena
Fetal Calf Serum (FCS)	Gibco/Invitrogen, Karlsruhe
Formic acid	Merck, Darmstadt
FTi 277	Calbiochem, Schwalbach
Gentamycine Sulfate (G418)	Gibco/Invitrogen, Karlsruhe
Geranylgeranyltransferase (GGTase)	Jena Biosciences, Jena
GGTi 286	Calbiochem, Darmstadt
Glucose-6-phosphate	Sigma Aldrich, Munich
Glucose-6-phosphate dehydrogenase	Sigma Aldrich, Munich
Glycine	Sigma Aldrich, Munich
Hank´s Balanced Salt solution (HBS)	Sigma Aldrich, Munich
HEPES	Merck, Darmstadt
Hybond P PVDF Membrane	GE Healthcare, Munich
Hydrochloric acid (HCl)	Merck, Darmstadt
Hygromycin B	Gibco/Invitrogen, Karlsruhe
Imidazole	Sigma Aldrich, Munich
KCl	Sigma Aldrich, Munich
KH_2PO_4	Sigma Aldrich, Munich
KOH	Sigma Aldrich, Munich
Lovastatin	MSD Sharp & Dohme GmbH, Haar
Methanol (MeOH)	Merck, Darmstadt
$MgCl_2$	Merck, Darmstadt
Milk powder (low-fat)	AppliChem, Darmstadt
Milli-Q Wasser	Millipore, Schwalbach
N-(5-dimethylamino-1-naphthalenesulfonyl)-1, 2-dioleoyl-sn-glycero-3-phosphoethanol-amine	Sigma Aldrich, Munich
Na_2CO_3	Merck, Darmstadt
NADP	Sigma Aldrich, Munich
NaF	Sigma Aldrich, Munich
n-hexane	Merck, Darmstadt
Non-essential amino acids MEM (100 x)	Gibco/Invitrogen, Karlsruhe
NuPAGE 4-12% gradient gels	Gibco/Invitrogen, Karlsruhe

NuPAGE MES SDS running buffer (20 x)	Gibco/Invitrogen, Karlsruhe
NuPAGE reducing agent (10 x)	Gibco/Invitrogen, Karlsruhe
NuPAGE sample buffer (4 x)	Gibco/Invitrogen, Karlsruhe
NuPAGE transfer buffer (20 x)	Gibco/Invitrogen, Karlsruhe
Octyl-β-D-glucopyranoside	Sigma Aldrich, Munich
OptiMEM	Gibco/Invitrogen, Karlsruhe
Penicillin/Streptomycin (PenStrep)	Gibco/Invitrogen, Karlsruhe
Petroleum ether	VWR International, Darmstadt
Phosphate buffered saline (PBS) (10 x)	Gibco/Invitrogen, Karlsruhe
Phosstop® phosphatase inhibitor	Roche Diagnostics GmbH, Mannheim
Preciset Cholesterol standards	Roche Diagnostics, Mannheim
Precision Plus, StrepTactin-Horse radish Peroxidase (HRP) Conjugate	Bio-Rad, Munich
Precision Plus, WesternC™, Protein standard	Bio-Rad, Munich
Pyruvate, sodium MEM	Gibco/Invitrogen, Karlsruhe
Rotiszint ecoplus	Carl Roth, Karlsruhe
Simvastatin (Zocor® 40 mg)	MSD Sharp & Dohme GmbH, Haar
Sodium azide (NaN_3)	VWR International, Darmstadt
Sodium chloride (NaCl)	Merck, Darmstadt
Sodium dodecyl sulfate (SDS)	Merck, Darmstadt
Sucrose	Sigma Aldrich, Munich
Super Signal® West Femto	Thermo Scientific, Bonn
Tetrahydrofuran	Merck, Darmstadt
Tris(hydroxymethyl)aminomethane (Tris)	Sigma Aldrich, Munich
Trypsin-EDTA (1 x)	Gibco/Invitrogen, Karlsruhe
U 18666A	Calbiochem, Darmstadt
Ultraglutamin	Gibco/Invitrogen, Karlsruhe
Vitamin solution MEM (100 x)	Gibco/Invitrogen, Karlsruhe
$ZnCl_2$	Merck, Darmstadt

All solvents for analytical procedures were of HPLC grade or higher.

Listed chemicals were purchased at the respective German subsidiary unless stated otherwise.

2.2. Western Blot Antibodies

Primary antibodies	kDa	Source	Catalogue #
GAPDH	36	Millipore, Schwalbach	MAB374
GGPPS	37	Abgent, Heidelberg	AP2419b
IL-13 alpha 2	50	Abcam, Cambridge (UK)	ab37631
NeuN	46	Millipore, Schwalbach	MAB377
Pan Rho + Rac(1,2,3) + Cdc42	21	Abcam, Cambridge (UK)	ab69091
Pan Ras (F-132)	21	Santa Cruz, Heidelberg	sc-32
Rac1 (C-11)	21	Santa Cruz, Heidelberg	sc-95
Secondary antibodies: anti-mouse, -rabbit, -goat		Santa Cruz, Heidelberg	sc-2055, sc-2054, sc-2961

All primary antibodies were diluted 1:1.000 and all secondary antibodies 1:10.000

2.3. Kits

Name	Company	Catalogue #
BCA Protein Assay reagent	Thermo Scientific, Bonn	23225
CHOD-PAP (Cobas^{TM}) Cholesterol kit	Roche Diagnostics, Mannheim	11491458 216 (Preciset Cholesterol standards not continued)

2.4. Laboratory equipment and materials

Name	Company
Biological samples / animals	
Human brain samples	Human brain and Spinal Fluid Center, Los Angeles (USA)
Pig brain	Metzgerei Friedrich Schreiber, Frankfurt
C57Bl/6 mice	Centre d'Elevage R. Janvier, Le Genest-St Isle (France)
SAMP1/KaHsD	Harlan-Winkelmann, Borchen (Germany)
SAMP8/TaHsD	Harlan-Winkelmann, Borchen (Germany)
HPLC columns/guard columns	
Ascentis® Express C18 RP (100 x 2.1 mm, 2.7 µm)	Sigma Aldrich, Munich
Security guard column C18 (4 x 2.0 mm)	Phenomenex, Aschaffenburg

	Nucleodur 100-5 C18 end-capped (250 x 4.0 mm)	Macherey-Nagel, Düren
	CC 8/4 Nucleodur 100-5 CN (8 x 4.0 mm)	Macherey-Nagel, Düren
	Zorbax SB-C18 (150 x 2.1 mm, 5 µm)	Agilent, Böblingen

Extraction		
	Extrelut®-NT1	Merck, Darmstadt
	Manifold (20 position)	Varian, Darmstadt
	Oasis® HLB 3cc, 60 mg	Waters, Eschborn
	Oasis® WAX	Waters, Eschborn
	Oasis® MAX	Waters, Eschborn
	Supelco DSC-CN	Sigma Aldrich, Munich
	Supelco DSC-Si	Sigma Aldrich, Munich
	Supelco DSC-diol	Sigma Aldrich, Munich
	Supelco DSC-18	Sigma Aldrich, Munich
	Strata X-AW	Phenomenex, Aschaffenburg
	Strata X	Phenomenex, Aschaffenburg
	Ion exchange column AG1-X8	Bio-Rad, Munich

Materials		
	(Ultra-) Centrifuge tubes	Beranek Laborgeräte, Weinheim
	HPTLC RP-18 W / UV $_{254}$ silica gel glass plates (5 x 20 cm, 0.25 mm)	Carl Roth, Karlsruhe
	Hybond ECL nitrocellulose Transfer Membrane	GE Healthcare, Munich
	Microplate, 96-well, IWAKI	Dunn Labortechnik, Asbach
	PVDF Transfer Membrane	GE Healthcare, Munich
	Reaction vials	Eppendorf, Hamburg
	Tissue culture dish, IWAKI	Dunn Labortechnik, Asbach

Laboratory equipment		
HPLC (1)		
	Jasco	Jasco, Gross-Umstadt

	DG-1580-53 Degasser	
	LG-980-02 Binary solvent mixer	
	PU-980 Pump	
	AS-950 Autosampler	
	Column thermostat	W.O. electronics, Langenzersdorf
	Gilson 122 Fluorometer	Gilson, Middleton (USA)
HPLC (2)		
	LaChrome Elite System	VWR-Hitachi, Darmstadt
	L-2130 pump (2x)	
	L-2200 Autosampler	
	Column oven	
	L-2485 Fluorescence detector	
UHPLC-MS		
	Waters Acquity system	Waters, Elstree (UK)
	API 4000 QTrap Sciex mass spectrometer	Applied Biosystems, Foster City (USA)
QFT 9.4 T triple-quadrupole Fourier transform ion cyclotron resonance (FT-ICR) mass spectrometer		IonSpec, Lake Forest (USA)
Further Equipment		
	Beckman GS-6R centrifuge	Beckman Coulter, Krefled
	Beckman J2-HS centrifuge (Rotor JA-20.1)	Beckman Coulter, Krefled
	Beckman L7 ultracentrifuge (Rotor SW41)	Beckman Coulter, Krefled
	Beckman Microfuge R (Rotor F241.5)	Beckman Coulter, Krefled
	Bio Rad Power Pac 300	Bio-Rad, Munich
	Biofuge pico (Heraeus)	Thermo Scientific, Bonn
	Bruker Avance 300 NMR	

	spectrometer	Bruker Daltonic, Bremen
	Canberra Packard Tricarb – 1900 scintillation counter	Canberra, Rüsselsheim
	Combi-tips	Eppendorf, Hamburg
	Cryo-vials, model Cryo-S	Greiner, Frickenhausen
	ELISA reader, Digiscan	ASYS Hitech, Eugendorf (AUT)
	Fortuna® Optima® glass Syringes	Poulten&Graf, Wertheim
	Gauge needle (1427a LL)	Acufirm, Dreieich
	Heraeus CO_2 incubator	Thermo Scientific, Bonn
	Incubator, GFL 4010	GFL, Burgwedel
	Laminar Flow box, Hera Safe	Thermo Scientific, Bonn
	Magnetic stirrer, IKA Combimag RCT	IKA® Werke, Staufen
	Pellet chow (standard 1320 maintenance diet)	Altromin, Lage
	pH-meter (Inolab)	WTW, Weilheim
	Pipettes (various volumes)	Gilson, Middleton (USA)
	Platform shaker, Promax 1020	Heidolph, Kehlheim
	Potter S	B.Braun, Melsungen
	Refrigerated Condensation Trap	Savant/ Thermo Scientific, Bonn
	Scale AB204	Mettler Toledo, Giessen
	SNAP i.d. Protein detection system	Millipore, Schwalbach
	Sonifier, Cell Disruptor B15	Branson, Danbury (USA)
	Speedvac® Plus SC210 A	Savant/ Thermo Scientific, Bonn
	Syringe pump	Harvard Apparatus, Holliston (USA)
	Transferpette® (2 – 200 µL)	Brand, Wertheim
	Ultra Turrax T_{25}	IKA® Werke, Staufen
	Ultrasonic bath, Sonorex Super RK 510H	Schalltec, Mörfelden-Waldorf
	Universal Hood II (Photometrics Cascade:1K camera)	Bio Rad, Munich
	Vacuum pump Millivac, Maxi SD1P014M04	Millipore, Schwalbach
	Vacuum pump, Diaphragm pump	Vaccubrand, Wertheim
	Vortex Genie 2	Scientific Industries, New York (USA)

Water bath (shaking), GFL 1083	GFL, Burgwedel
Xcell II™ Blot Module	Gibco/Invitrogen, Karlsruhe

2.5. Software

Name	**Company**
Analyst 1.4.2	Applied Biosystems, Foster City (USA)
Borwin 1.50	Jasco, Gross-Umstadt
EZ Chrome Elite®	VWR, Darmstadt
GraphPad Prism 4.0	GraphPad Software, La Jolla (USA)
MIDAS molecular formula calculator	NHMFL, Tallahassee (USA)
MS Office 2003	Microsoft, Redmond (USA)
Quantity One 4.6.5	Bio-Rad, Munich
Reference Manager Version 10	ISI Researchsoft, New York (USA)

2.6. Buffers and Solutions

2.6.1. General buffers

Buffers listed in the following section were prepared with Millipore water and the pH was adjusted using a pH meter, which was calibrated daily.

PBS - buffer

For the PBS buffer a concentrate (10 x) was used and diluted 1:10 using Millipore water. Sterile conditions were applied when necessary.

Tris-HCl – buffers

Buffer I	Tris HCl 50 mM, pH 7.4
Buffer II	Tris HCl 100 mM, pH 8.5
Buffer III	Tris HCl 5 mM, pH 7.4
Buffer IV	Tris HCl 5 mM, pH 8.5

Various – buffers

Buffer V	HEPES 10 mM, 0.32 sucrose, pH 7.4
Buffer VI	Buffer V, 0.25 mM Na-EDTA, pH 7.4
Buffer VII	0.1 M sucrose, 50 mM KCl, 40 mM KH_2PO_4, 30 mM K-EDTA
Buffer VIII	10 mM DTT in buffer VII
Buffer IX	17.5 mM NaCl, 25 mM glucose-6-phosphate, 5 mM NADP

Gradient solutions

Gradient 1	7.5% (w/v) ficoll, 0.25 mM Na-EDTA in buffer V
Gradient 2	14% (w/v) ficoll, 0.25 mM Na-EDTA in buffer V
Gradient 3	1.5 M sucrose, 10 mM HEPES, 0.25 mM Na-EDTA

2.6.2. Buffers and solutions for the isoprenoid isolation and derivatization

Reaction buffer

Reaction buffer used for the enzymatic reaction of the according dansyl-labels:

Dithiothreitol	5 mM
$MgCl_2$	5 mM
$ZnCl_2$	10 µM
O-β-D-Glucopyranosid	1% (m/v)
Tris-HCl (pH 7.5)	50 mM

Stop solution

Stop solution, used for the termination of the enzymatic reaction:

ACN /10% HCl	10 : 1 (v/v)

Dansyl-peptides

FPP substrate D*-GCVLS	50 µM in buffer I
GGPP substrate D*-GCVLL	50 µM in buffer I

Isoprenoid diluting solvent

Dilution agent used for isoprenoid solutions:

MeOH / 10 mM NH_4OH	7 : 3 (v/v)

Enzyme dilutions

FPTase	250 ng/µL reaction buffer
GGTase I	250 ng/µL reaction buffer

Phosphatase inhibitor mixture

NaF	100 mM
imidazole	200 mM

Elution mix 1 (for Extrelut®)

1-Butanol / H_2O / NH_4OH	10 : 2 : 1 (v/v/v)

Elution mix 2 (for SPE)

n-hexane / 2-propanol / NH_4OH	12 : 7 : 1 (v/v/v)

Elution mix 3 (for cell extraction)

1-Butanol / NH_4OH / EtOH	4 : 5 : 11 (v/v/v)

2.6.3. Western Blot buffers and solutions

TBST - solution

Tris-base	3 g
NaCl	8 g
TBS	500 mL
Tween 20	1 mL
H_2O	ad 1 liter

Running buffer

NuPage MES SDS running buffer (20x)	50 mL
H_2O	950 mL
NuPage Antioxidant	1 mL

Transfer buffer

NuPage transfer buffer	50 mL
Methanol	100 mL
H_2O	850 mL
NuPage Antioxidant	1 mL

Blocking solution

TBST (1x)	10 mL
Milk powder	750 mg

Azide- solution (100x)

Sodium azide	2%

Secondary antibody (sec. AB) solutions

TBST (1x)	10 mL
Sec. AB	3 µL
StrepTactin-HRP Conjugate	3 µL

2.6.4. Cell culture media and inhibitors

The following cultivation medium was used for the APP transfected (SH-SY5Y-APPwt) cells:

DMEM	500 mL
FCS	50 mL
MEM vitamins	5 mL
NEA	5 mL
Pyruvate	5 mL
P/S	3 mL
Hygromycin	3 mL

The following medium was used for the incubation with the various MVA-pathway inhibitors listed in Table 4:

OptiMem	500 mL
P/S	3 mL
Hygromycin	3 mL

Inhibitor	**Enzyme target**	**Solvent**	**concentration**
FTi 277	farnesyltransferase	DMSO	1 µM
GGTi 286	geranylgeranyltransferase	DMSO	1 µM
Lovastatin	HMG-CoA reductase	EtOH	5 µM
U 18666A	desmosterol reductase oxidosqualene cyclase	H_2O	1 µM

Tab. 4. Inhibitors for *in vitro* cell assays on human SY5Y cells (see section 3.6.). Depicted are the inhibitors, their respective enzyme target, the solvent they were dissolved in and the final concentration in the cell medium. An overview of the enzyme targets can be seen in Figure 41.

3. METHODS

3.1. Pre-column derivatization

Based on the work published by Tong et al. FPP and GGPP were determined using high performance liquid chromatography and fluorescence detection (HLPC-FLD) after pre-column labeling of FPP and GGPP using dansyl labeled pentapeptides.[94] The published method was modified as follows:

3.1.1. Standard prenylation assay (standard F-G-Assay)

The following solutions were combined in a reaction vial for the enzymatic attachement of FPP and GGPP to dansyl labeled pentapeptides (dansyl-glycine-cysteine(farnesyl)-valine-leucine-serine and dansyl-glycine-cysteine(geranylgeranyl)-valine-leucine-leucine, respectively) shown in Figure 5. This assay is referred to as standard F-G-Assay throughout the entire text. Concentrations ranging from 0.5–1000 ng/mL of FPP and GGPP were employed. The dansyl labeled FPP and GGPP derivatives are designated as FPP* and GGPP* throughout the entire text.

Reaction buffer	42 µL
FTase	1 µL
GGTase I	1 µL
FPP	1 µL
GGPP	1 µL
Dansyl-GCVLS (FTase substrate)	2 µL
Dansyl-GCVLL (GGTase I substrate)	2 µL
Total	50 µL

3.1.1.1. Incubation protocol I

The mixture of the F-G-Assay was incubated in a water bath for 120 min at 37 °C. Subsequently, the enzymatic reaction was terminated by the addition of 50 µL stop solution followed by a centrifugation step (15.000 x g; 5 min; 4 °C). For HPLC analysis 95 µL of the final solution were transferred to HPLC vials.

Both enzymes, farnesyltransferase (FTase) and the geranylgeranylteransferase I (GGTase I) were tested for their optimum concentrations. For each enzyme a prenylation assay, as described in section 3.1.1. was conducted with 46 µL reaction buffer and the respective enzyme, isoprenoid and dansyl-label. The enzyme concentrations tested were 62.5, 125, 250 and 1000 ng/µL.

3.1.1.2. Incubation protocol II

The mixture of the F-G-Assay was incubated in an Eppendorf thermomixer, comfort programmed for 90 or 120 min cycles (37 °C; per min: 10 sec; 500 rpm). Subsequently, the enzymatic reaction was terminated by the addition of 50 µL stop solution followed by a centrifugation step (15.000 x g; 5 min; 4 °C). For HPLC analysis 95 µL of the final solution were transferred to HPLC vials.

The incubation time for each enzymatic reaction was tested individually. The time dependant conversion of each isoprenoid to its respective dansyl-labeled product was monitored. Eight individual assays were prepared in a thermomixer and the reaction was terminated by the addition of 50 µL stop solution at the following time points: 0, 15, 30, 45, 60, 90, 120 and 180 min and processed as described above.

3.1.2. Prenylation assay following FPP and GGPP extraction

Following extraction from cells or tissue samples, dried residues from the applied extraction procedure were dissolved in 44 µL reaction buffer by vigorously mixing the reaction vial for 1 min, followed by 3 min in the ultrasonic bath. Subsequently 1 µL FTase, 1 µL GGTase and 2 µL of each dansyl-label were added and the mixture was incubated for 90 min as described in section 3.1.1.2.

3.2. Internal standard

3.2.1. Synthesis

The synthesis of dansyl-para nonylphenol (DNP) as the internal standard (IS) was conducted according to Naassner et al. with the following changes:[316]

For the chemical reaction 25 mg 4-n-nonylphenol were dissolved in 2 mL acetone, 25 µL 0.5 M Na_2CO_3 and 200 mg of dansyl chloride were added. The reaction mixture was stirred for 18 h at

room temperature (RT), the solution was evaporated to dryness under reduced pressure (400 mbar; 35 °C) and re-dissolved in 2 mL ACN.

3.2.2. Product confirmation using thin layer chromatography

Following synthesis of DNP the reaction product was firstly confirmed using thin layer chromatography. Commercially available, modified silica gel glass plates (HPTLC RP-18 W / UV_{254}) were used with the following mobile phase composition: Acetone/MeOH/H_2O (25:5:4 v/v/v). The product was detected under UV light (366 nm) with a retention factor (Rf-value) of 0.5. The silica gel showing the spot was scratched of the glass plate and collected in a reaction tube.

3.2.3. ^{1}H-NMR product confirmation

The silica gel with the product was scratched of the HPTLC plates and extracted with deuterated DMSO (C_2D_6SO) prior ^{1}H-NMR analysis. The solution was then subjected to a ^{1}H-NMR measurement (300 MHz) for product confirmation. ^{1}H-NMR spectra were measured on a Bruker AV 300 spectrometer. Chemical shifts were reported in parts per million (ppm) using tetramethylsilane (TMS) as an internal standard.

3.2.4. Preparative HPLC clean-up

Prior to the preparative clean-up via HPLC, the DNP solution (see section 3.2.1.) was centrifuged at 3000 x g for 5 min and the supernatant was transferred to HPLC vials. Repeated clean-up was conducted using a Nucleodur 100-5 C18 end-capped column and the fraction collector on the Jasco HPLC system. Chromatographic conditions are described in section 3.4.2.

Stock solution (2.8 µM) aliquots were evaporated to dryness and stored under nitrogen atmosphere at 4 °C in the dark.

3.3. FPP and GGPP extraction procedure for matrix samples

3.3.1. Sample preparation

Frozen tissue samples were homogenized with a rotor-stator homogenizer at 1100 rpm in 1.1 mL of buffer II containing 5 µL Halt® and 10 µL Phosstop® phosphatase inhibitor. Two 50 µL

aliquots of homogenate were retained for protein and total cholesterol determination (see section 3.8. and 3.9.). Subsequently, 1 mL homogenate was spiked with 15 µL of a 2.8 µM IS solution and vigorously mixed with 1 mL of buffer II.

3.3.2. Matrix assisted liquid/liquid extraction via Extrelut®

3.3.2.1. Generic Extrelut® protocol

A generic protocol for the Extelut®-NT1 columns is provided for the extraction of lipophilic compounds from aqueous solution with a volume of 0.1–1 mL. After the addition of the solution onto the columns and 15 min of incubation, the lipophilic compounds were eluted by the addition of an organic phase or a mixture thereof.

3.3.2.2. Adapted Extrelut® protocol

The matrix homogenate (section 3.3.1) was loaded onto an Extrelut®-NT1 column, and after 15 min washed of with three 2 mL steps of Elution-mix 1. The eluent was centrifuged (29.000 x g; 10 min; 4 °C) and the resulting supernatant decanted in a glass vial after evaporation to dryness under reduced pressure, in a SpeedVac (5 h; 55 °C; 30 mbar). The resulting residue was re-dissolved in 3.75 mL of 5% methanol in water (v/v). The solution was vigorously shaken for 1 min and placed in an ultrasonic bath for 10 min (see Figure 3).

3.3.3. Solid phase extraction (SPE)

3.3.3.1. Generic SPE protocol

A generic protocol for SPE applications is divided into the 5 following steps, all of which are carried out with negative pressure on a manifold:

Step 1: Conditioning (C)
Step 2: Equilibration (E)
Step 3: Sample (S)
Step 4: Wash (W)
Step 5: Elution (Elu)

During step C each solvent, which was subsequently used for step 3 – 5 was flushed through the column. In step 5 (E) the pure solvent in which the sample was present was employed. Finally, the whole volume of the sample was applied to the column (Step 3 (S)). For the following wash step (Step 4 (W)) a solution similar to that of the sample was chosen, generally a methanol or formic acid solution. Subsequently, the columns were dried under reduced pressure prior to eluting in the final step (Elu). During step 1 – 3 the columns were maintained wet.

3.3.3.2. Developed HLB protocol

Following the adapted Extrelut® protocol (section 3.3.2.2) further sample clean-up was conducted on a manifold connected to a vacuum pump using HLB solid phase extraction cartridges (3cc; 60 mg) pre-conditioned with 2 mL n-hexane, followed by 1 mL 2-propanol and 1 mL methanol. Afterwards, the columns were equilibrated with one tube volume of water. Following these initial conditioning steps (organic solvents) and the equilibration step (water), the solution resulting from the Extrelut® clean-up was introduced to the cartridges and washed with 1 mL of 2% methanol in water (v/v). For the final elution, 2 mL of Elution-mix 2 were applied to the columns and the eluent containing the isoprenoids was collected in 2 mL reaction vials. This solution was evaporated to dryness under reduced pressure in a SpeedVac (2 h; 55 °C; 30 mbar), prior the enzymatic pre-column derivatization (see Figure 3).

3.3.4. Extraction procedure for *in vitro* cell culture experiments

The isolation from cells was conducted according to Tong et al.[94] Cultivated cells were scraped from the cell culture dish, transferred to a reaction vial and centrifuged (1000 x g, 10 min; RT). The resulting cell pellet was washed with 1 mL PBS and subsequently centrifuged again under the same conditions. After the final centrifugation step the pellet was dissolved in 300 µL buffer I, containing 5 µL Halt® and 10 µL Phosstop® phosphatase inhibitor; the cells were constantly kept on ice. Following protein determination via the BCA assay (see 3.8.), 600 µg of total protein from the cell suspension were transferred to a vial and the volume for each sample was adjusted to maintain equal volumes in all vials, ready for extraction procedure and analysis.

For the calibration samples, 600 µg of SH-SY5Y cell suspension was used and was spiked as follows: 0, 5, 10, 20, 60 and 100 ng/mL for FPP and 0, 5, 10, 20, 75 and 100 ng/mL for GGPP.

To begin the isolation, 1 mL elution mix 3 (70 °C) was added to the cell suspension in each vial. Subsequently the mixture was shaken vigorously for 1 min and incubated in a thermomixer programmed for 20 min (70 °C; per min: 10 sec; 500 rpm). For further processing the samples were cooled to RT and centrifuged (9000 x g; 5 min; RT). The supernatant was transferred to a new vial and the pellet re-suspended by the addition of 1 mL elution mix 3 (70 °C) and subsequent sonication for 15 s. After vortexing the vials for one minute the samples were subjected to incubation in the thermomixer using the aforementioned conditions. After cooling the samples to RT and following centrifugation (9000 x g; 5 min; RT), the supernatants were combined and evaporated to dryness under reduced pressure in a SpeedVac (2 h; 55 °C; 30 mbar) and then subjected to enzymatic pre-column derivatization (see Figure 3).

For the calibration samples, un-spiked samples (endogenous control) were used to determine the endogenous FPP and GGPP levels (cell matrix). After measurement of the calibration curve, the peak areas for FPP and GGPP of the endogenous control were subtracted from each of the calibration samples.

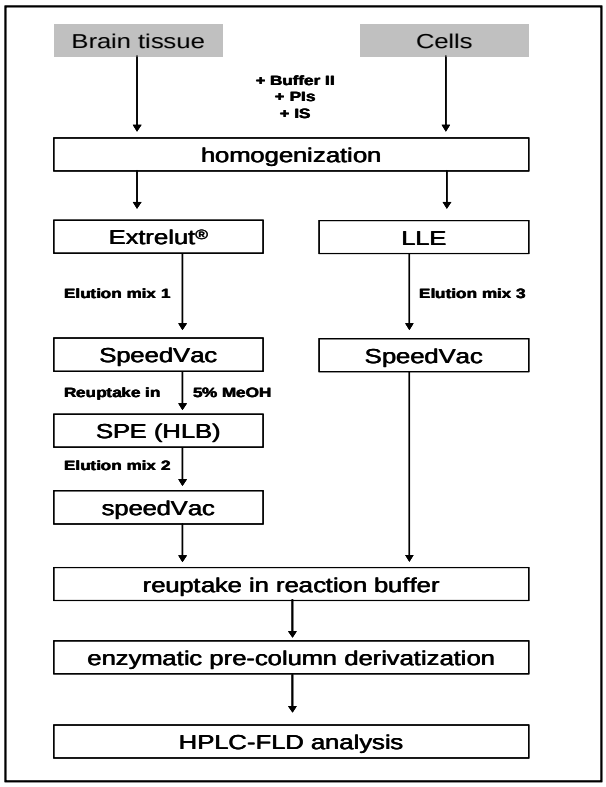

Fig. 3. Flow-chart of the final, complete sample preparation for brain tissue and cultured cells prior HPLC-FLD analysis.

3.4. Analytical methods

3.4.1. HPLC-FLD analysis (Jasco HPLC system)

The gradient elution and HPLC settings shown below describe the final settings for the routine analysis of standard F-G-Assays and for assays with matrix samples on the Jasco system.

Chromatographic conditions:

mobile Phase:	Solvent A	20 mM ammonium acetate in 40% ACN
	Solvent B	20 mM ammonium acetate in 90% ACN

gradient:

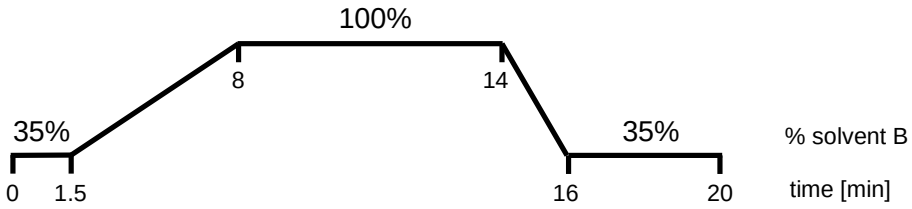

guard column:	Security guard column C18 (4 x 2.0 mm)
analytical column:	Ascentis® Express C18 RP (100 x 2.1 mm, 2.7 µm)
temperature:	35 °C
flow:	0.5 mL/min
injection volume:	80 µL
total run-time:	20 min
autosampler temperature:	4 °C
fluorescence wavelength:	excitation 340 nm / emission 525 nm

3.4.2. IS clean-up (Jasco HPLC system)

The settings for the gradient elution on the Jasco HPLC system with the fraction collector are described below. The preparative clean-up, following IS synthesis, was repeatedly conducted to ensure a higher purity of the IS.

Chromatographic conditions:

mobile Phase:	Solvent A	H_2O
	Solvent B	ACN

gradient:

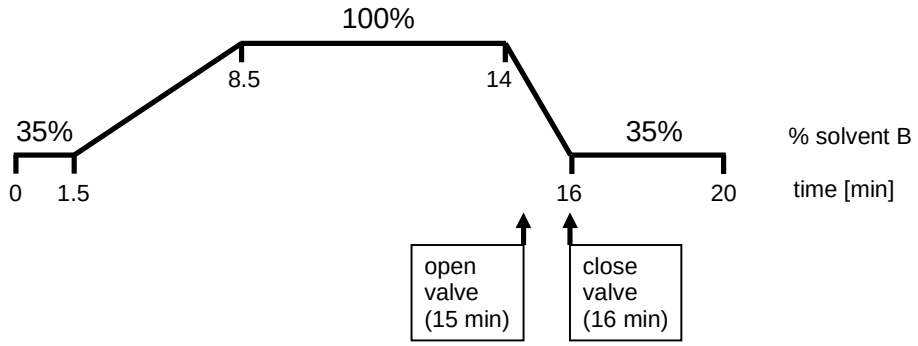

guard column:	CC 8/4 Nucleodur 100-5 CN (8 x 4.0 mm)
preparative column:	Nucleodur 100-5 C18 end-capped (250 x 4.0 mm)
temperature:	20 °C
flow:	1.5 mL/min
injection volume:	120 µL
total run-time:	20 min
autosampler temperature:	4 °C
fluorescence wavelength:	excitation 340 nm/emission 525 nm
fraction collector:	peak collection from 15–16 min

3.4.3. Comparative analysis (Hitachi HPLC–FLD system)

The gradient elution and HPLC settings shown below describe the final settings for the routine analysis of standard F-G-Assays and for assays with matrix samples on the LaChrome Elite system from Hitachi.

Chromatographic conditions:

mobile Phase:	Solvent A	20 mM ammonium acetate in 40% ACN
	Solvent B	20 mM ammonium acetate in 90% ACN

gradient:

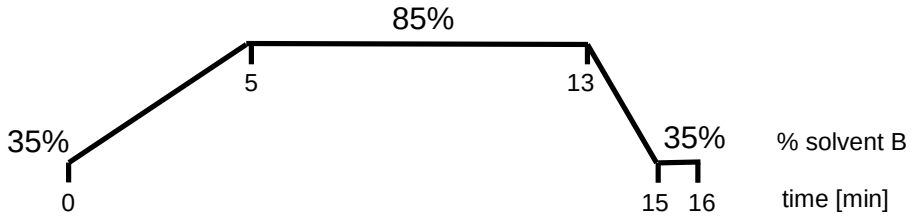

analytical column:	Ascentis® Express C18 RP (100 x 2.1 mm, 2.7 µm)
temperature:	20 °C
flow:	0.35 mL/min
injection volume:	1 - 75 µL
total run-time:	16 min
autosampler temperature:	RT
fluorescence wavelength:	excitation 320 nm/emission 520 nm

3.4.4. Fast separation analysis (UHPLC–MS/MS)

The gradient elution and UHPLC-MS/MS settings shown below describe the final settings for the routine analysis of standard F-G-Assays and for assays with matrix samples on the Waters Acquity system coupled to the QTrap 4000 triple quadrupole MS.

Chromatographic conditions:

mobile Phase:	Solvent A	20 mM ammonium acetate in water
	Solvent B	20 mM ammonium acetate in 90% ACN

gradient:

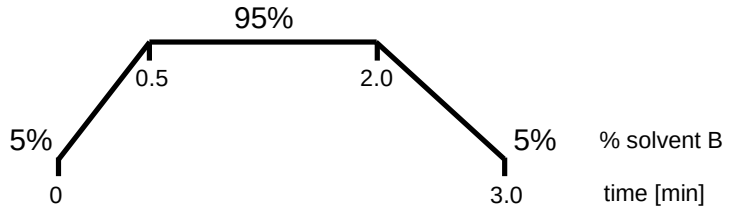

analytical column:	Ascentis® Express C18 RP (100 x 2.1 mm, 2.7 µm)
temperature:	20 °C
flow:	0.6 mL/min
injection volume:	10 µL (partial loop)
total run-time:	3 min
autosampler temperature:	10 °C

Mass spectrometer settings (API 4000 QTrap)

Ion source (turbo spray) dependant parameters

Ionization	ESI
Polarity	positive
Curtain gas (CUR)	10.0 a.u.
Collision gas pressure (CAD)	medium
IonSpray voltage (IS)	4500 V
Temperature (TEM)	600 °C
Ion source gas 1 (GS1)	40.0 a.u.
Ion source gas 2 (GS2)	0.0 a.u.
Interface heater (ihe)	On
De-clustering potential (DP)	120.0 V
Entrance potential (EP)	10.0 V
Collision energy (CE)	30.0 V
Collision cell exit potential (CXP)	10.0 V

3.4.5. Characterization of FPP* and GGPP* using FT-ICR MS

Accurate mass measurements were performed on a QFT 9.4 T triple-quadrupole Fourier transform ion cyclotron resonance MS (FT-ICR MS) in the negative ion mode. FPP* and GGPP* fractions were collected using the Jasco fraction collector while running spiked brain samples on the Jasco HPLC system. Solutions were infused into the ESI source after mixing with internal

mass calibration solution at a flow rate of 7 µL/min using a syringe pump. The needle potential of the ESI source was set to –3.8 kV, the cone voltage to –45 V and the extractor to –10 V. Ion accumulation times between 500 and 1000 ms in Q3 were used. Chirp excitation was performed at 155 V for 16 ms (from *m/z* 75 – 2500). Mass accuracies were calculated using the MIDAS molecular formula calculator software with atom constraints for C, H, N and O set to the respective number of atoms in the precursor ions.

3.5. Method validation

3.5.1. Validation samples for HPLC-FLD application

3.5.1.1. Human brain matrix

In order to minimize interference with endogenous FPP or GGPP sealed human frontal cortex samples from 8 different donors were thawed and kept at RT for 48 h prior to preparation. Following the storage at RT, the brain samples were homogenized with a rotor-stator homogenizer at 1100 rpm in buffer II resulting in a stock solution with 200 mg wet weight (ww) tissue per milliliter. Two separate batches from different brain samples were prepared, one for the calibration samples (CCs) and one for the quality control samples (QCs). 10 mL aliquots were stored at -20 °C for the duration of the validation and the measurement of the human brain study samples.

3.5.1.2. Calibration curve samples (CCs)

Separate stock solutions (1 mg/mL) of FPP and GGPP in MeOH/NH_4OH (7:3, v/v) were kept at -20 °C. Different working solutions containing FPP and GGPP were prepared by diluting the stock solution with the isoprenoid dilutent solution (see section 2.6.2.). The IS was prepared by dissolving the dried residue in an appropriate volume of acetonitrile resulting in a 2.8 µM solution. Calibration standards were prepared daily by adding 1 mL of brain homogenate to 1 mL buffer II spiked with 15 µL of IS solution, 5 µL Halt® and 10 µL Phosstop® phosphatase inhibitor and 10 µL of the appropriate FPP-GGPP working solutions, resulting in concentrations of 10, 20, 40, 60, 80, 100, 200 and 400 ng/mL for FPP and 50, 75, 100, 125, 150, 250, 500 and 1000 ng/mL for GGPP. A fresh set of CCs was prepared daily.

3.5.1.3. Quality control samples (QCs)

Analogue to the calibration standards (see section 3.5.1.2.) three different concentrations of QCs (FPP-GGPP: QC-L 30/80, QC-M 150/400 and QC-H 300/800 ng/mL; low, medium and high) were prepared in a different batch of human brain matrix. These QCs were prepared without the addition of the IS and phosphatase inhibitors prior to the validation and stored in 1 mL aliquots at -20 °C throughout the validation and the measurement of the human brain study samples. For each day the respective amount of QCs was thawed and prepared analogue to the CCs (see section 3.5.1.2), without the addition of isoprenoid standards.

3.5.2. Validation protocol

The preparation procedure combined with the analytical method was subjected to validation according to the latest FDA bioanalytical method validation guideline.[317]

Fundamental parameters to ensure the acceptability of the performance of a bioanalytical method are selectivity, linearity including the LLOQ, accuracy and precision (inter- and intraday), reproducibility, and stability.

Endogenous isoprenoid levels were removed from the tissue matrix as described in section 3.5.1.1. To ascertain sufficient degradation of FPP and GGPP chromatograms of zero samples (matrix sample spiked with IS), blank samples and spiked matrix samples were compared, respectively.

3.5.2.1. Selectivity

The selectivity of the method was shown by the comparison of blank and zero sample chromatograms from six brain homogenate samples of different origin to confirm the absence of interfering peaks.

3.5.2.2. Linearity

Linearity in brain homogenate was verified using five calibration curves measured on five separate days. Each standard curve consisted of eight non-zero calibration standards with concentrations ranging from 0.03 to 1.06 µmol (10 – 400 ng/mL) for FPP and 0.11 to 2.15 µmol (50 – 1000 ng/mL) for GGPP. The calibration curves were calculated by linear regression using weighting for both analytes. According the FDA requirements, the back-calculated values have to

be within 15% of the relative standard deviation (RSD) and 20% of RSD at the lower limit of quantification (LLOQ) of the nominal concentration. The acceptance criterion for the correlation coefficients (r^2) of the calculated regression curves was > 0.99.

3.5.2.3. Lower limit of quantification (LLOQ)

To determine the LLOQ, six different brain homogenate samples were spiked with FPP and GGPP at the lowest level of the calibration curve (10 ng/mL and 50 ng/mL, respectively) and re-calculated with a freshly prepared calibration curve.

3.5.2.4. Inter- and intraday accuracy and precision

The intraday accuracy and precision were determined by analyzing four replicates of each QC sample (in the lower, middle and upper range) together with a complete set of calibration standards in one analytical run within one day. The interday accuracy and precision were established by measuring four replicates of each QC sample on four consecutive days together with all calibration standards freshly prepared for each day. The mean, the standard deviation (SD), the RSD and bias were calculated.

3.5.2.5. Recovery

The recoveries of FPP and GGPP from brain homogenate were determined by analyzing triplicates of each QC sample (low, medium and high). Responses were compared to extracted blank brain homogenate (n=3 for each concentration) spiked with the same nominal concentrations prior to the prenylation assay. For further proof of reproducibility, both recoveries were additionally determined by analyzing each QC sample after extraction using [^{3}H]FPP and [^{3}H]GGPP. Counts were measured on a Canberra Packard Tricarb 1900 scintillation counter and referred to those obtained from samples spiked with the same nominal concentrations.

3.5.2.6. Stability

The stability of FPP and GGPP was tested in the presence of both phosphatase inhibitors (Halt® and Phosstop®) in brain homogenate (n=4) for two concentration levels (low and high) after storage at RT for 2 h, after three freeze and thaw cycles, and after storage for one and three

months at −80 °C. Furthermore, the auto sampler stability was tested using QC-M samples (n=4) and measured at the following time points: 0, 5, 10 and 20 h storage at 4 °C in the auto sampler.

3.5.3. Method transfer to the UHPLC-MS/MS application

In order transfer the fully validated HPLC-FLD method to a faster and more sensitive UHPLC-MS/MS application the following selected experiments were conducted to demonstrate the feasibility of the improved technique. The sample preparation protocol including the enzymatic derivatization of FPP and GGPP remained unchanged. Chromatic conditions and the applied MS settings are described in section 3.4.4.

3.5.3.1. Linearity and LLOQ

The 7-point calibration curves were measured in a concentration range of 5 – 250 ng/mL for both isoprenoids in an isoprenoid-free human blank brain homogenate (see section 3.5.1.1.). Calibration standards were prepared for the following concentrations for each isoprenoid: 5, 10, 40, 60, 100, 200, 250 ng/mL. The same weighting factors ($1/x^3$ and $1/x^2$ for FPP* and GGPP*, respectively) were used for the determination via HPLC-FLD and UHPLC-MS/MS.

The LLOQ was determined with five different brain homogenate samples, spiked with 5 ng/mL for FPP and GGPP, respectively. Values were recalculated with a freshly prepared calibration curve and met the criteria of the FDA guideline for bioanalytical method validation.[317] Samples without the addition of the respective dansyl-labeled pentapeptide were used as blank samples, which were run with each batch of samples.

3.5.3.2. Data correlation

For the correlation of the data generate via the HPLC-FLD and the UHPLC-MS/MS application, human brain samples were prepared as described in section 3.5.1.1. After the enzymatic conversion and addition of 100 µL stop solution 80 µL were analyzed via HPLC-FLD and 10 µL via UHPLC-MS/MS. Values were calculated with a calibration curve processed in the same manner.

3.6. Cell culture

3.6.1. Cultivation

Frozen SH-SY5Y-APP695 cells were gently thawed in a water bath at 37 °C. Before the cells were completely thawed they were transferred into falcon tubes (15 ml) containing fresh medium. After centrifugation (1000 x g; 10 min; RT) the resulting cell pellet was re-suspended in 1 mL fresh medium and transferred into a Petri dish with 10 mL medium.

Cells were grown to about 80-90% confluence, subsequently the medium was removed from the Petri dish and replaced by 10 mL of sterile PBS. After 2-3 min incubation the PBS was removed and 1 mL of trypsin was added, followed by another incubation of 2-3 min till half of the cells detached from the bottom of the plate. The trypsinization was stopped by the addition of 9 mL of fresh medium. Subsequently the cells were carefully triturated and a varying number (1: 3 to 1: 8 splits) of aliquots were taken and added to Petri dishes prepared with fresh medium. The maximum number of consecutive splits was 13 before new cells were thawed.

3.6.2. Inhibitor incubation protocols

For the incubation of the SH-SY5Y-APP695 cells with MVA-pathway inhibitors, it was necessary to exchange the FCS containing DMEM medium with serum free OptiMem medium (see section 2.6.4.). The cells are capable to circumvent reduced intracellular cholesterol levels, caused by inhibitors targeting the mevalonate (MVA-) pathway, by the uptake of cholesterol from the normal DMEM medium.

The selected inhibitors are listed in section 2.6.4. and the different targets within the MVA-pathway are shown in Figure 41. The following table (Table 5) gives an overview of the conditions for applied incubation protocols. Conditions were adapted from former studies in our working group.[238,270] Solvent controls were always performed.

Inhibitor	Incubation time / conditions
Lovastatin	24 h / 5 µM
FTi 277	24 h / 1 µM at the following time points: 0, 5, 10, 15, 20 h
GGTi 286	24 h / 1 µM at the following time points: 0, 5, 10, 15, 20 h
U 18666A	24 h / 1 µM

Tab. 5. Respective *in vitro* incubation conditions for each inhibitor applied in the cell experiments with human SY5Y cells.

3.7. Western Blot analysis

3.7.1. Sample preparation

Aliquots of the homogenate from either tissue or cell experiments were protected against endogenous proteases by the addition of 10 µL á 500 µL sample from a 1 mL (volume for 1 tablet) stock solution of Complete® protease inhibitor. Total protein was determined using the BCA method (see section 3.8.). All samples for one run were diluted to maintain the same protein concentration in the same total volume by the addition of buffer II. Subsequently sample buffer (10 x) and reducing agent (4 x) were added and the samples incubated for 10 min at 90 °C. After centrifugation (9000 x g; 2 min; RT) each sample was loaded on the gel. Depending on the matrix and antibody between 30 and 80 µg of protein were separated per lane.

3.7.2. Electrophoreses and transfer

Electrophoretic separation of the samples and the molecular weight marker (Precision Plus, WesternC™, protein standard) was achieved using a XCell II™ Blot Modul with a Bio Rad Power Pac 300 and the following settings: 8 min at 60 volts to collected the samples in the gel pockets followed by 190 volts for 40 min. The protein transfer was carried out using either polyvinylidene fluoride (PVDF) or nitrocellulose (NC) as the blotting membrane. The PVDF membranes were activated in methanol for 5 min before being transferred into transfer buffer for another 20 min. As for the NC membranes water was used instead of methanol. Using the above mentioned Blot module proteins were transferred from the gel to the membrane according to the manufacturers´ instructions at 30 volts for 2 hours.

3.7.3. Blot processing

To avoid unspecific binding of the applied antibody, as described in the following, the membranes were incubated with 7.5% fat free dry milk in TBST for 30 min at RT and washed with water before the antibody was applied. Depending on the primary antibody blots were incubated with the antibody solution under constant shaking for 2 h at RT or at 4 °C over night. Further processing was achieved by using the SNAP i.d protein detection system from Millipore. Membranes were washed with six 10 mL aliquots of TBST. Subsequently membranes were incubated for 10 min with 3 mL of the secondary antibody solution. After 10 min the washing procedure was repeated as described above.

For final detection the Thermo Fisher Super Signal® West Femto reagents were used. An aliquot of 500 µL of both solutions were combined with 500 µL of TBST prior incubation of the membrane for 5 min in the dark. Bands were detected and analyzed with the Quantity One software, in a Bio-Rad Universal Hood II equipped with a Photometrics Cascade: 1K camera.

3.8. BCA protein determination

Total protein amounts were determined using the BCA protein assay from Thermo Scientific. The assay was conducted in a 96-*well* plate format. Samples were diluted to an estimated protein concentration between 100 and 1000 µg/mL. Prior to the addition of the samples on the plate, Reagent A and B were mixed in a 50 : 1 (v/v) ratio. Furthermore, the BSA standard was prepared in the following concentrations: 0.1, 0.2, 0.33, 0.5 and 1 mg/mL. Depending on the sample volume, 10 or 25 µL standards were prepared and pipetted into the wells, 200 µL of the reagent A/B mixture was added and the plate incubated for 30 min at 37 °C. All values were measured in triplicates with the ELISA reader at 570 nm. The correlation coefficients (r^2) were > 0.99.

3.9. Total cholesterol determination

Total cholesterol levels were determined using the CHOD-PAP-method (cholesterol oxidase peroxidase 4-aminophenazone phenol method). Cholesterol Preciset standards were used in 50, 100, 200, 300 and 400 mg/dL (~ 1.29, 2.59, 5.17, 7.76 and 10.35 mmol/L). All samples and standards were measured in triplicates on a 96-*well* plate. To enhance solubilization of the cholesterol from the matrix, 10 µL of the sample/standard were incubated on the 96-*well* plate with 5 µL of the Brij35-solution (15% Brij35 in buffer III). After 15 min incubation time, 200 µL of the Roche cholesterol kit solution (section 2.3.) were added, followed by another 60 min of incubation time at RT. The photometric measurement was performed using an ELISA reader at 490 nm. All sample values were normalized to total protein.

3.10. Brain preparations

3.10.1. Crude fraction

The protocol for the purification of the crude membranes from brain tissue was adapted from Eckert et al. and modified for smaller tissue samples.[318] Frozen tissue was homogenized in 7.5

mL of buffer III (4 °C) using a rotor stator homogenizer at 1100 rpm. Pistil and glass vial were washed with 3 mL buffer III and solutions were combined prior centrifugation (48.000 x g; 20 min; 4 °C). The samples were kept at 4 °C at all times. The supernatant was discarded and the resulting pellet was re-dissolved in 10 mL buffer III (4 °C). The resulting suspension was homogenized using an Ultra Turrax at 13.500 rpm for 15 seconds. Subsequently the solution was centrifuged again with the aforementioned conditions. The resulting pellet was used for protein and cholesterol determinations.

3.10.2. Sub-cellular membranes

The protocol for the preparation of SPMs was adapted from Eckert et al. and was applied for either for whole mouse brains or single hemispheres (~200 – 400 mg ww).[318]

Frozen brain tissue was homogenized in 5 mL buffer VI using a rotor-stator homogenizer at 1100 rpm. Pistil and glass vial were rinsed with 2 mL buffer VI and solutions were combined prior to centrifugation (585 x g; 10 min; 4 °C). The pellet was discarded and the supernatant centrifuged at 17.400 x g for 20 min at 4 °C to remove heavy myelin and cell fragments. The resulting supernatant was either used for the preparation of brain peroxisomes (supernantant A – for further processing see section 3.10.3.) or centrifuged again under the same conditions. In case of the latter the pellets from both centrifugations were homogenized in 1.5 and 0.5 mL buffer V, respectively with an Ultra Turrax at 13.500 rpm for 15 s. The resulting suspension was transferred into an ultracentrifuge 15 mL Beckmann plastic tube followed by the injection of 3 mL gradient (via syringe) to form the bottom layer in the tube. Subsequently, 5 mL of gradient 2 were carefully layered to the bottom of the tube. The following centrifugation step, in an ultracentrifuge (87.300 x g; 60 min; 4 °C) yielded a protein layer between gradient 1 and 2 which was removed with a syringe and diluted (1:3) with buffer V. To further clean up the synaptosomes the suspension was subjected to centrifugation (14.600 x g; 20 min; 4 °C) and the pellet used for further processing by re-suspension in 2 mL buffer IV followed by another 5 mL buffer IV. The solution was kept on ice for one hour and shaken vigorously every 20 min to lyse the synaptosomes. Following the next centrifugation step (43.000 x g; 20 min; 4 °C) the pellet was re-suspended in 3 mL of water (4 °C), transferred to a ultracentrifuge tube and 3 mL gradient 3 were underlayed with a syringe to build the bottom layer. After ultracentrifugation (41.000 x g; 45 min; 4 °C) the top aqueous layer with the SPMs was removed and transferred into a centrifuge

tube while diluting it with 5 mL water (4 °C). The final centrifugation step (43.000 x g; 30 min; 4 °C) yielded the SPM pellet which was re-suspended in 1 mL buffer 1.

3.10.3. Peroxisomes preparation

For the preparation of the peroximsomes, the supernatant A from the preparation protocol of the SPMs (see section 3.10.2) was used and transferred into an ultracentrifuge tube. The solution was centrifuged (154.000 x g; 1.5 h; 4 °C) in an ultracentrifuge and the resulting pellet was re-suspended in 200 µL buffer VIII and stored at -80 °C prior to protein determination via BCA and activity measurements (see section 3.10.4.).

3.10.4. HMG-CoA reductase activity measurements

The HMG-CoA reductase activity assay was conducted with brain peroxisomes obtained from brains of the AD brain investigation (see section 3.11.1.3.). Activity of the HMG-CoA reductase was determined according to a modified protocol by Edwards et al. 1979.[319] Briefly, 200 µL of the re-suspended pellet was incubated together with 200 µL buffer IX, 10 µL glucose-6-phosphate dehydrogenase (2.2 units) and 90 µL HMG-CoA (containing 150 nmol ^{14}C with an activity of 0.34 Ci/mol, equal to 12.6 GBq) in a tempered water bath at 37 °C for one hour. The reaction was stopped by the addition of 30 µL KOH. The solution was further maintained at 37 °C for 30 min, to which 25 µl of bromphenol blue and 65 µL HCl (5N) were then added; the solution was incubated for approximately 1 h (37 °C), until a yellow color was apparent. Subsequently, this solution was centrifuged (10.060 x g; 3 min; RT) and the supernatant transferred to an ion exchange column. Elution was performed with 3.4 mL of water, whereas the first 0.9 mL of the eluate was discarded and the remaining 2.5 mL were combined with 2.5 mL scintillation cocktail, vortexed and radioactivity was measured via scintillation counting. The determined counts per minute (cpm) were re-calculated to the according protein values of the applied samples and declared in enzyme activity / mg protein / minute.

3.11. Tissue samples

3.11.1. Human brain samples

Human brain tissue samples were obtained from the Human Brain and Spinal Fluid Resource Centre (HBSFRC, LA, USA).

HBSFRC post mortem samples were prepared according to the brain bank protocols, provided on their homepage *[http://www.loni.ucla.edu/uclabrainbank/index.html]*, shipped on dry ice and stored at – 80 °C prior analysis. For tissue preparation prior analysis specific areas of the brain slices were cut on ice at 4 °C, followed by homogenization (as described in section 3.5.1.1.).

3.11.1.1. White and grey matter brain study

Frontal cortex brain slices from 5 different, neurological healthy donors (see relevant patient information in Table 7) were prepared and ~ 250 mg pieces of frozen white and grey matter were cut from each brain prior to homogenization. Besides visual differentiation (see Figure 4) into both areas an additional WB analysis was performed using NeuN as a neuronal marker for grey matter brain areas.

Fig. 4. Frozen tissue section (~2 x 2 cm) of human frontal cortex for the visual differentiation of white and grey matter prior the preparation.

3.11.1.2. Human brain study – analytical correlation

Post-mortem human brain samples from the cerebral cortex of each hemisphere of patients, who died of brain cancer were used to correlate measurements on the HPLC-FLD and the UHPLC-MS/MS system. All samples were obtained from the HBSFRC and a report including relevant patient information on disease progression, age, gender etc. can be found in Table 6. Tissue preparation of brain white matter samples was conducted upon visual differentiation.

	Left and right hemisphere (n = 7)
Demographic	
Age at death (years)	70 ± 9
Gender	3 female, 4 male
Histological	
Post mortem interval (h)	13.19 ± 2.69
Brain hemisphere (left:right)	1:6
WHO grade	6 times IV, 1 w/o classification

Tab. 6. Patient information of post mortem brain samples. At autopsy, brains were cut into coronal sections and a sample from each hemisphere was freshly frozen and stored at −80 °C. Glioblastoma multiforme (GBM) was the cause of death regarding this sample set and individual cancer progression was classified according to the WHO classification of tumors (I – IV) of the central nervous system.[320] Means ± SD.

3.11.1.3. Alzheimer's Disease brain study

Post-mortem brain samples from the frontal cortex of Alzheimer's Disease (AD) patients were compared to age-matched controls. All samples were obtained from the HBSFRC and a report including relevant patient information on disease progression, age, gender etc. can be found in Table 7. A careful separation of white and grey matter was conducted upon visual differentiation. Additional samples were collected for the HMG-CoA reductase assay and PCR analysis.

	Control (n = 13)	Alzheimer (n = 13)	P value
Demographic			
Age at death (years)	77.8 ± 3.5	80.4 ± 4.8	0.133
Gender	13 male	13 male	
Histological			
Post mortem interval (h)	15.0 ± 4.4	16.5 ± 5.0	0.433
Brain hemisphere (left:right)	0:13	3:10	
Braak – Stage (I-VI)	-	5.1 ± 0.7	

Tab. 7. Patient information of post mortem samples. At autopsy, brains were cut into coronal sections (2-4) and a sample of frontal cortex tissue of each sample was freshly frozen and stored at −80 °C. Patients were classified as AD or control (neurological healthy) cases according to the Consortium to Establish a Registry for Alzheimer's Disease (CERAD). CERAD have developed standardized instruments for the evaluation of individuals clinically diagnosed with AD.[321] Means ± SD.

3.11.2. Mouse brain tissue

All mice were maintained on a 12-h dark–light cycle at constant air temperature of 25 °C and with pelleted chow and tap water *ad libitum*. Animals were kept in separate groups of maximum 10 animals per cage according to their sex and age. All experiments were carried out according to the European Communities Council Directive (86/609/EEC)[322], after appropriate training of the personnel. Animal numbers were chosen according to the study design and statistical requirements. At the end of the study, animals were euthanized by cervical displacement 2 h after the last drug treatment. The cerebrum was removed and immediately snap frozen in liquid nitrogen, and stored at -80 °C prior to isolation and analysis.

3.11.2.1. Mouse strains

Three different mouse strains were used for the current work. All animals were kept under the conditions described in section 3.11.2.

C57Bl/6 mouse (♂ + ♀)

The C57Bl/6 mouse represents a multipurpose, easy to handle inbred mouse model widely used in research laboratories. Genetic modifications serve as models for human diseases.

Thy-1-APP transgenic mouse (♀)

The Thy-1 APP mice represent a C57Bl/6 transgenic mouse model possessing both the Swedish double and the London mutation. The human APP expression with both mutations is controlled by the murine Thy-1 promoter leading to a high and selective expression in neurons and consequently an accelerated plaque formation, becoming visible at an age of approximately 6 month.[323]

Mice used for the experiments described in the current work were of ~ 12 month of age.

3.11.2.2. Aging Study

Female and male C57Bl/6 mice were obtained in three different age-groups, young (3 month), middle-aged (12 month) and aged (24 month) from Janvier, France. The mice were kept for one week under the new conditions of the breeding facility prior to cervical displacement.

3.11.2.3. Sub-chronic simvastatin treatment study

The subchronic treatment study was conducted with simvastatin. The drug suspension (verum group) was prepared daily in 0.2% (w/v) aqueous agar gel at a final concentration of 10 mg/mL. Female C57Bl/6 mice (~3 month of age) received vehicle (control group) or 50 mg simvastatin/kg body weight daily for 21 days. The drug or vehicle solution was applied by oral gavage with a maximal dosing volume of 0.5 mL.

3.11.3. Pig brain tissue

Pig brain was used to partly during the method development (indicated in text) and to generate calibration curves for the evaluation of mouse brain data. This brain matrix was chosen to avoid sacrificing additional mice to generate data for technical samples, such as calibration standards. For tissue preparation frontal cortex samples were cut and homogenized (as described in section 3.5.1.1).

4. RESULTS

4.1. Method development

A systematic approach for the isolation and subsequent quantification of farnesyl- and geranylgeranylpyrophosphate (FPP and GGPP) in human brain tissue is described in the following. The step-by-step procedure includes the optimization of the enzymatic attachment of fluorescence tags to each analyte, the optimization of a HPLC method, including the introduction of an internal standard and the novel development of the simultaneous extraction of both isoprenoids from brain matrix.

4.1.1. HPLC method development

4.1.1.1. Background

The chemical structures of the two isoprenoids FPP and GGPP (see Figure 5) do not possess a distinct chemical group which would allow for a straightforward and accessible analysis via most commonly used HPLC detectors like ultraviolet light (UV), diode array detector (DAD) or via a mass spectrometer (MS). The enzymatic linkage via the farnesyl-geranylgeranyl assay (F-G-Assay) of either analyte to its respective dansyl-label enables the detection using a fluorescence detector (FLD), which was previously described by Tong and colleagues.[94] The dansyl-labeled FPP and GGPP are referred to as FPP* and GGPP* throughout the entire work (see Figure 5).

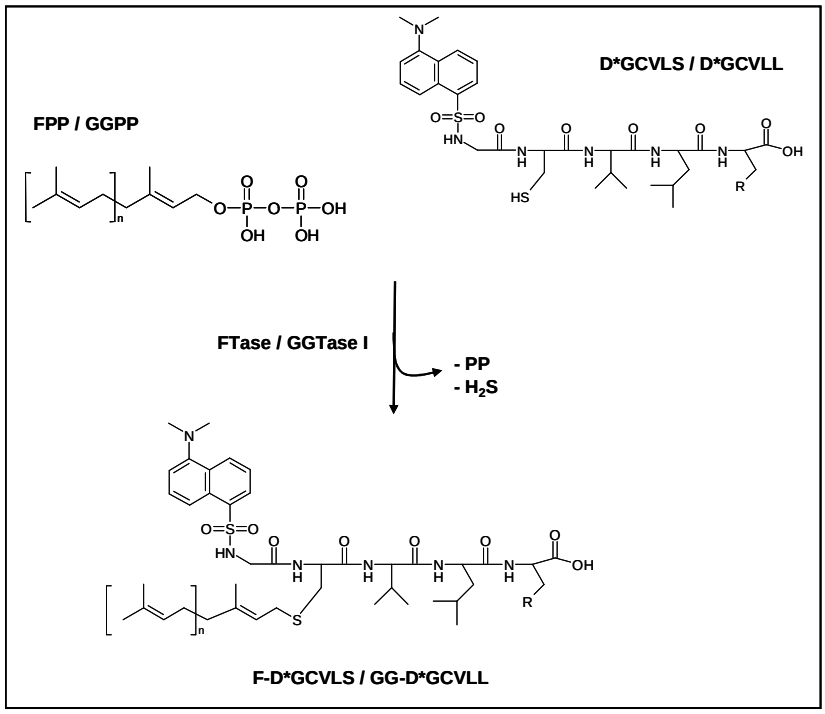

Fig. 5. Pre-column derivatization of FPP (n=2) and GGPP (n=3) to their specific dansyl labelled pentapeptide (R= -hydroxyl for D*GCVLS and R= -isopropyl for D*GCVLL) by specifically FTase or GGTase I. Enzymatic reaction occurs under hydrogen sulphide (H_2S) and diphophate (-PP) cleavage. Analytes detected after separation are FPP* (=F-D*GCVLS) and GGPP* (=GG-D*GCVLL).

4.1.1.2. Chromatographic conditions

Throughout the developmental stage of the F-G-Assay and the subsequent development of the isolation method, various solvent compositions, flow rates, columns, oven temperatures and analytical columns and combinations thereof were tested. Note: only experimental conditions which led to significant improvements of the method are mentioned in the following text.

The initial aim was to establish an analytical method for the separation and detection of both analytes (FFP* and GGPP*) after the F-G-Assay. For this purpose isoprenoid standards were applied in varying concentrations to the assay. The described assay conditions for the enzymatic pre-column derivatization (F-G-Assay) and the following HPLC-FLD detection were initially adapted and subsequently optimized (see section 3.1.). Firstly, various RP18 columns were tested under slightly varying HPLC conditions, with regards to flow rate and solvent composition in an isocratic or gradient elution. The most promising results were initially achieved with a Zorbax SB-C18 column. For each test run an F-G-Assay was prepared and the resulting solution was

injected into the HPLC system. Detailed settings of the system and conditions are summarized in Table 8.

Further optimization of the method, in terms of peak shape, could be achieved using a column with Fused Core™ technology (further details in section 4.1.3.).

4.1.1.3. Detector settings

Due to possible differences in solvent composition, eluting time and especially differences in the detector brand, it was necessary to adjust the FLD excitation and emission wavelengths. Measurements have to be performed with the detector set at the peak maximum for both wavelengths to obtain reproducible results. This was achieved by using identical injection volumes from the same HPLC vial for the analytical runs. Firstly, the excitation wavelength was gradually increased in 5 nm steps in the range of 320 to 355 nm. The maximum was determined to be 340 nm, which was used for the following emission wavelength scan. An emission scan from 500-540 nm indicated a maximum peak at 525 nm.

column	Zorbax SB-C18 (150 x 2.1 mm, 5 µm)
Gradient	*see section 3.4.1.*
flow rate	700 µL/min
oven temperature	20 °C
run time	23 min
FLD settings (excitation/emission wavelength)	340 / 525 nm
retention times (FPP/GGPP)	4.9 / 14.4 min

Tab. 8. Chromatographic conditions and fluorescence detector settings on the Jasco HPLC system with the Zorbax C18 column, adapted from Tong et al.[94]

4.1.2. Assay optimization

The conditions for the enzymatic reaction (F-G-Assay) described by Tong et al.[94] were adjusted and optimized. The following results were assessed by comparison of peak areas of each analyte after chromatographic separation and fluorescence detection.

4.1.2.1. Incubation settings

In the first set of experiments incubation protocol I was compared to incubation protocol II (see section 3.1.1.). Both incubation methods were carried out at 37 °C for 120 minutes. No differences were observed between both conditions and thus the thermomixer was favored due to easy handling.

Furthermore the incubation time for each enzymatic reaction was tested. In order to determine the time dependant conversion of both isoprenoids to their respecitve dansyl-labeled products, eight individual assays were prepared and the reactions were terminated at different time points. As depicted in Fig 6 a and b, complete conversion was achieved with an incubation time of 60 minutes. An additional 30 minutes were allowed to guarantee the reaction reached the plateau phase; hence a maximum incubation period of 90 minutes was selected for all experiments.

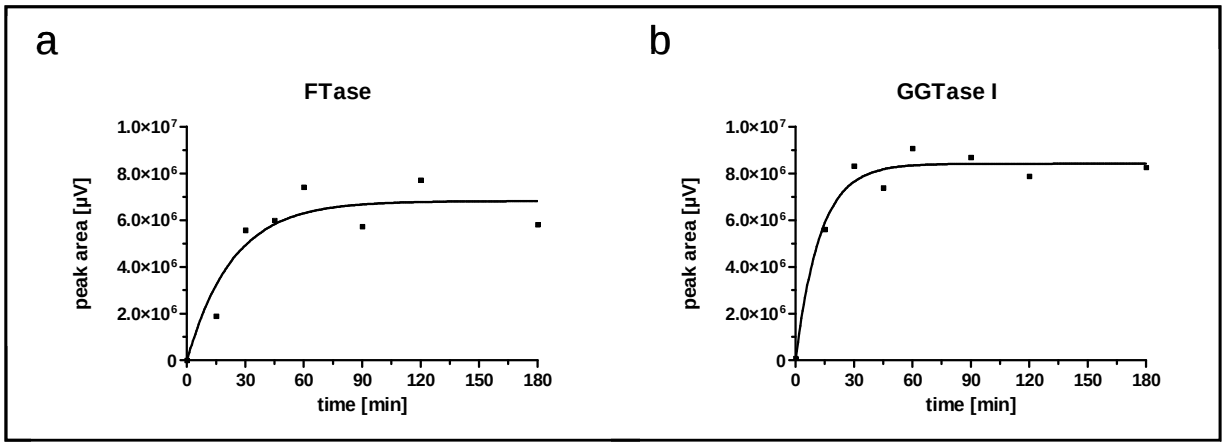

Fig. 6. Time dependant isoprenoid conversion by either transferase to their respective dansyl-labeled penta-peptide. Product enrichment (**a**) FPP* and (**b**) GGPP* at each time point was monitored by the FLD after HPLC separation. Peak areas are shown in µV.

4.1.2.2. Enzyme concentration, specificity and linearity

The amount of each enzyme needed for sufficient conversion of either isoprenoid to its dansyl-label was tested (data not shown). The optimal total amount of FTase and GGTase was found to be 250 ng/µL, respectively.

Furthermore, enzyme specificity was tested and each enzyme was incubated with combinations of FPP and GGPP (500 ng/ml, resp.) and the according dansyl labels. Of the eight possible combinations only the combinations of FPtase, FPP and dansyl-GCVLS and of GGPtase, GGPP and dansyl-GCVLL showed detectable peaks.

To further demonstrate linearity of the calibration curves both isoprenoids, FPP and GGPP, were individually added to the assay containing the respective enzyme, at the pre-determined concentration. The 5-point calibration curves were carried out in a range of 4-500 ng/mL and showed a minimum correlation of r^2 = 0.999 for both isoprenoids (see Figure 7 a and b). An exemplified chromatogram (Figure 7 c) shows the clear separation of the analyte.

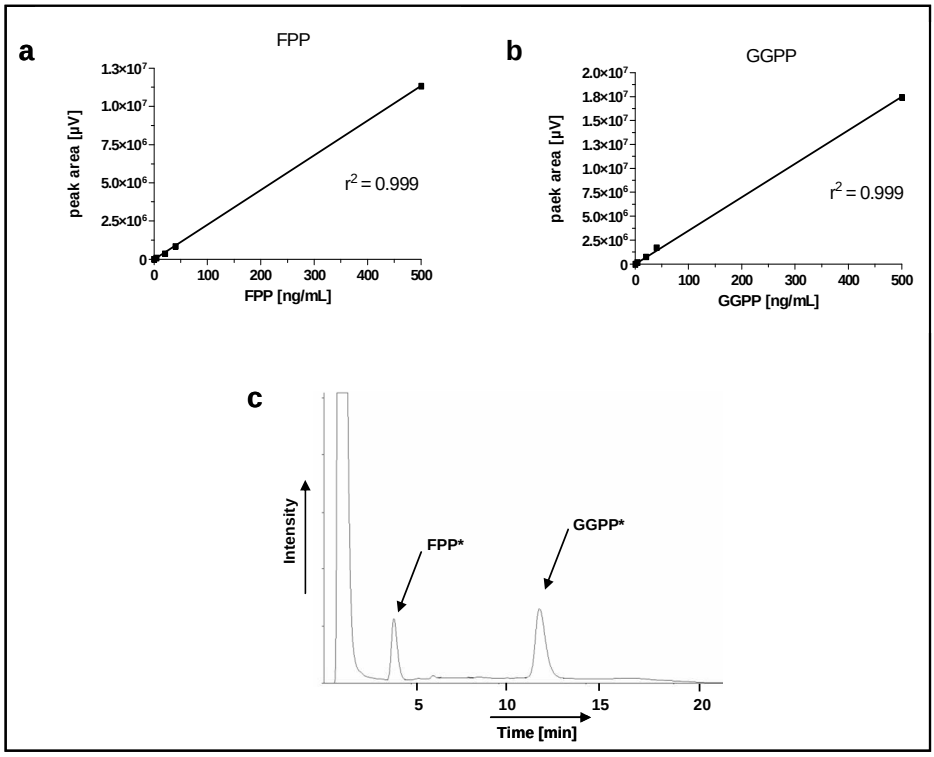

Fig. 7. (**a and b**) Five-point calibration curves (5 – 500 ng/mL) of FPP* and GGPP* after pre-column derivatization. The respective r^2-values are given in the graph. (**c**) Representative chromatogram of pure standard solutions after pre-column derivatization.

4.1.3. Implementation of a Fused Core™ RP18 column

The initial HPLC and F-G-Assay conditions were tested using the Zorbax SB-C18 column. Subsequent to these tests, further improvement of the method was achieved by the implementation of a rather novel column technology. The Ascentis® Express column, utilizing Fused Core™ technology was tested, which resulted in improved peak shapes and consequently, lower limits of detection (LODs).

The chromatograms in Fig 8 show a 2-step method transfer to the new column. The first step involved the replacement of the column and a reduction in the flow rate to 400 µL/min while the gradient remained constant (Figure 8 b). The second step was an adjustment of the gradient (Figure 8 c) (*note:* the injection volume was different for this run). The resulting enhanced peak width led to a 4-fold decrease in the LOD (see Table 9). During this transfer it became also obvious that a dansyl-labeled phospholipid, which was tested as an internal standard (IS) at that time (see also Figure 8) showed two baseline separated peaks (see chromatogram b at *Rt*= ~12 minutes) instead of one shown in the upper chromatogram at 7 minutes. This separation further points out the resolving capability of the newly applied column.

Settings	**Zorbax SB-C18**		**Ascentis® Express**	
Flow	0.7 mL/min		0.4 mL/min	
Gradient	time [min]	Solvent B [%]	time [min]	Solvent B [%]
	0 → 1.5	20	0 → 1.5	35
	1.5 → 4	20 → 55	1.5 → 8	35 → 100
	4 → 15	55	8 → 14	100
	15 → 18	55 → 20	14 → 16	100 → 35
	18 → 23	20	16 → 20	35
Run time	23 min		20 min	
Peak parameters	FPP* / GGPP*		FPP* / GGPP*	
Rt [min]	4.9 / 14.4		4.7 / 11.9	
LOD [ng/mL]	2 / 2		0.5 / 0.5	
Tailing factor	~ 1.4 / 1.7		~ 1.4 / 1.6	
FWHM [min]	~ 0.45 / 0.7		~ 0.23 / 0.33	

Tab. 9. A direct comparison of the HPLC settings using the Zorbax RP18 column compared to the Ascentis® Express analytical column. For both optimized methods flow rate, gradient conditions and total run time are described in the table. The lower part of the table describes the improvements in peak performance, including retention time (*Rt*), limit of detection (LOD), the tailing factor for peak symmetry and the peak width, depicted as full width at half maximum (FWHM).

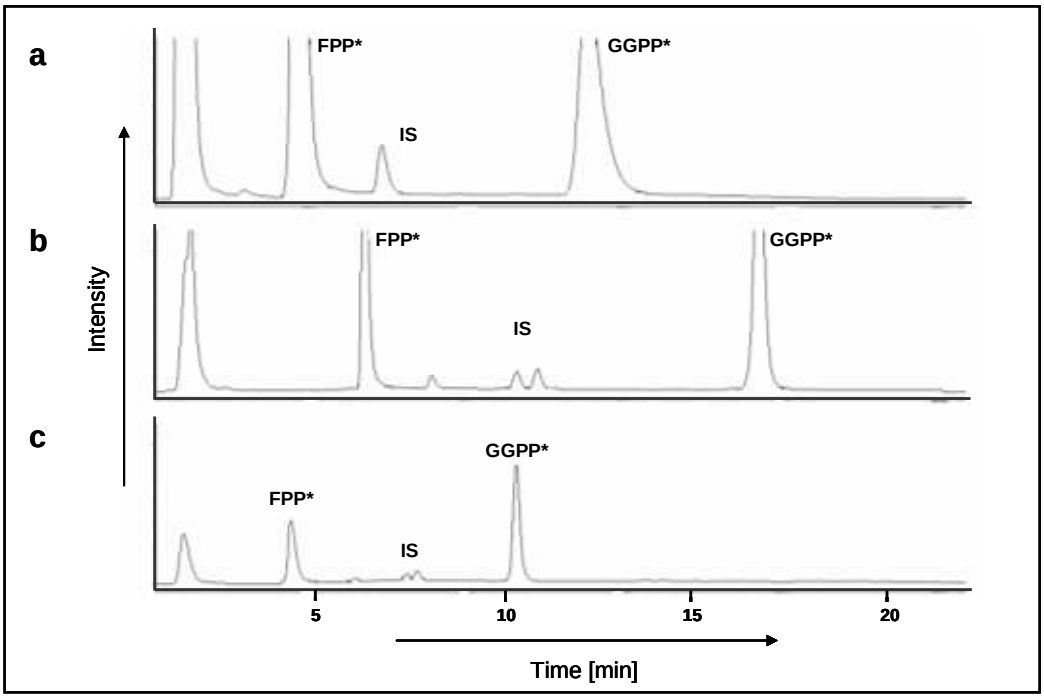

Fig. 8. Exemplified chromatograms for the method transfer from the (**a**) Zorbax RP18 column to the (**b and c**) Ascentis® Express column in two steps. Designated are the two analytes FPP* and GGPP* and the IS, showing two baseline separated peaks on the Ascentis® Express column. The chromatogram in (**c**) shows the optimized peak performance compared to chromatogram displayed in (**a**).

Lastly, a chromatographic overlay (Figure 9) on a different HPLC system (Hitachi HPLC system) clearly demonstrated the superiority of the Ascentis® Express column in respect to peak width and shape.

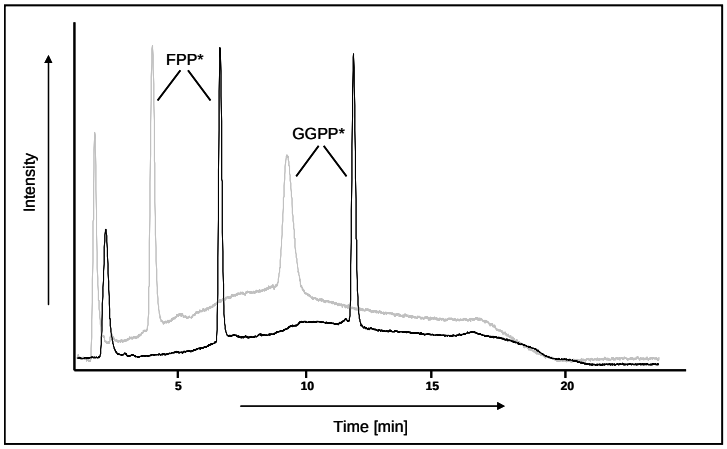

Fig. 9. Chromatographic overlay of two runs on the same HPLC system (Hitachi) injecting the same solution with the same injection volume. Grey trace shows the run on the Zorbax RP18 and the black trace on the Ascentis® Express column at same flow rates. FPP* and GGPP* are designated in both chromatograms.

4.1.4. FPP and GGPP extraction from brain matrix

Throughout the developmental phase of the isolation method for FPP and GGPP initial experiments for a specific type or combination of an extraction method were mostly conducted using spiked (FPP and GGPP were added in high concentrations, between 500 and 1000 ng/mL) water samples. All results were evaluated via HPLC fluorescence detection of FPP* and GGPP* following the pre-column F-G-Assay of the dried residues. Selected conditions were applied to matrix samples from either human, mouse (C57Bl/6) or pig brain and SY5Y cells. The applied matrix is indicated throughout the text.

4.1.4.1. Liquid/liquid extractions (LLE)

Tong and colleagues described a liquid/liquid extraction (LLE) for the isoprenoid extraction from cells.[94] As a straight-forward attempt this extraction procedure was applied to spiked brain matrix samples. Despite using very small amounts of tissue, between 10 and 30 mg of mouse brain homogenate, this isolation technique (see section 3.3.4.) resulted in rather impure extracts, containing relatively large amounts of un-precipitated protein. Consequently, the following enzymatic pre-column derivatization was employed and the resulting solution analyzed with the optimized HPLC-FLD method. No peaks were detectable at the respective retention times (*Rt*) of each analyte.

Based on these findings the initial experiments aimed to provide cleaner extracts by means of an extraction via a two phase hydrophilic-lipophilic system or the usage of different organic solvents.

4.1.4.1.1. LLE using a 2-phase system

A screening for solvents was conducted to determine the best conditions for the LLE. Based on the chemical properties of the isoprenoids with a hydrophilic head group attached to a lipophilic chain, initial extraction solvents consisted of an organic solvent and water, generating a 2-phase LLE system. 1-butanol, diethyl ether, petroleum ether, diisopropyl ether and ethyl acetate were chosen. A typical work-up of the samples was as follows: 1 mL of spiked water samples were extracted twice for 15 minutes with 1 mL of the according solvent after which the organic phases were combined and dried under reduced pressure. The dried residue was subjected to the F-G-Assay followed by HPLC-FLD analysis. Petroleum ether itself resulted in impurities in the F-G-

Assay impeding the enzymatic reaction and no signal of the analytes was detected after HPLC separation; the isolation via diethyl- and diisopropyl ether and ethyl acetate also showed no signal of the analytes. 1-butanol however, was an effective extracting solvent but led to lower peak intensities, as compared to the isolation method used by Tong et al.[94]

4.1.4.1.2. LLE using a 1-butanol solution

Bruenger and Rilling[92] and later Tong et al.[94], used a 1-butanol based extraction solvent. On the basis of the preliminary results as described under section 4.1.4.1. these two methods were compared for the isoprenoid extraction from spiked mouse brain samples. For this purpose a mouse cerebrum was homogenized in 3 mL Buffer II and divided in 3 x 1 mL aliquots. One sample was processed as described in section 4.1.4.1 and the other two aliquots were processed as followed. NH_4OH solution was added to the mixture resulting in a 150 mM ammoniac solution. Subsequently, 1.2 mL 1-butanol saturated with water was added and each mixture was immediately homogenized using an ultraturax for 1 minute. Following centrifugation (20.000 x g; 5 min; RT) the upper, butanol layer was removed and retained. The extraction was repeated and the supernatants were combined and dried under reduced pressure.

All three extractions led to a high degree of impurities in the following F-G-Assay, which completely inhibited the enzymatic reaction.

4.1.4.1.3. LLE using different organic solvents

The results from the solvent screening described under section 4.1.4.1.1., in addition to the fact that the isoprenoids are provided by the distributor in an ammoniac solution and that previous work conducted by Tong et al.[94] as well as by Bruenger and Rilling[92] described the utilization of an ammoniac solvent, demonstrated the necessity of incorporating NH_4OH into the mixture.

The following set of experiments evaluated the extraction power, the influence of protein in the matrix and the stability of the isoprenoids using SY5Y cells. To further evaluate these results with respect to overall recovery, a standard F-G-Assay was used as a reference. The first experiment aimed to generate a cleaner extract using an ammoniac n–hexane/isopropanol mixture (Elution mix 2) instead of a 1-butanol/methanol mixture (Elution mix 3= equals the mixture used by Tong et al.[94]) to generate an ammoniac two phase system. Therefore, the Elution mix 3 was compared to extractions using Elution mix 2 and an ammoniac diethyl ether solution. Table 10

shows the conditions and the relative FLD response (peak areas) for FPP* and GGPP* compared to the F-G-Assay. The results indicate a similar extraction power of the Elution mix 2 as compared to the Elution mix 3. The ether based extraction was unsatisfactory, although in comparison to the pure ether (section 4.1.4.1.1.) the mixture including NH_4OH showed improvements. Under non-alkaline conditions no peaks were detectable. In general, this result showed no improvement over the previously published extraction method using cell matrix and was therefore not further investigated. Nevertheless, the enhanced solubility of the isoprenoids in Elution mixture 2 was used for the subsequent SPE applications (section 4.1.4.3.).

Extracting solvent **Protocol**	Elution mix 2 *section 3.3.4.*	Elution mix 3 *section 3.3.4.*	Dieethylether/NH_4OH (95:5 v/v) - addition of solvent - 3 min sonification - 10 min shaking at RT → centrifugation (3000 x g; 10 min; RT)
Recovery [%]			
FPP	62.9	70.5	13.0
GGPP	46.0	62.9	24.3

Tab. 10. A direct comparison of three different protocols using different organic solvents. Elution efficiency was assessed by relative recovery compared to a standard F-G-Assay.

4.1.4.2. Matrix assisted LLE (Extrelut®)

The preliminary results obtained from the development of the method described in section 4.1.4.1.2. indicated the need for a cleaner extraction procedure leading to pure extracts. Isolations using Extrelut® columns represents a common approach for the extraction, e.g. of drugs from body fluids.[324] The diatomaceous earth filling of the columns absorbs proteins and contaminants retaining drugs or metabolites for the subsequent organic elution. Hence the suitability of this technique for the current method was tested using mouse brain as biological matrix. Following the generic protocol (section 3.3.2.1.) for Extrelut®, samples were added to the column and incubated for 15 minutes prior to elution. Four combinations of eluent solvents were tested, as summarized in Table 11. The chromatograms (data not shown) displayed a significant injection

peak, at a retention time similar to that of FPP, interfering considerably with the detection of FPP; this was due to impurities in the samples. Only the Elution mix 3 and the basic alkaline MeOH/CH_3CN/acetone mixture resulted in detectable peaks of GGPP but with very low intensities (Figure 10). Overall, the chromatograms showed high background noise due to impurities.

Eluting solvent	THF/ethyl acetate/n-henxane/2-propanol (160:160:160:15 v/v/v/v)	Elution mix 3	Ethyl acetate	MeOH/NH_4OH /CH_3CN/acetone (40:65:30:30 v/v/v/v)
Protocol	15 min incubation			
Peak detection				
FPP	-	-	-	-
GGPP	-	+	-	+

Tab. 11. A direct comparison of four different organic solvents mixtures for the elution from the Extrelut® columns. Feasibility of the protocol was judged by the detection of a peak after enzymatic conversion. + stands for a detection of a peak at the respective *Rt*. - stands for the absence of an assignable peak at the respective *Rt*.

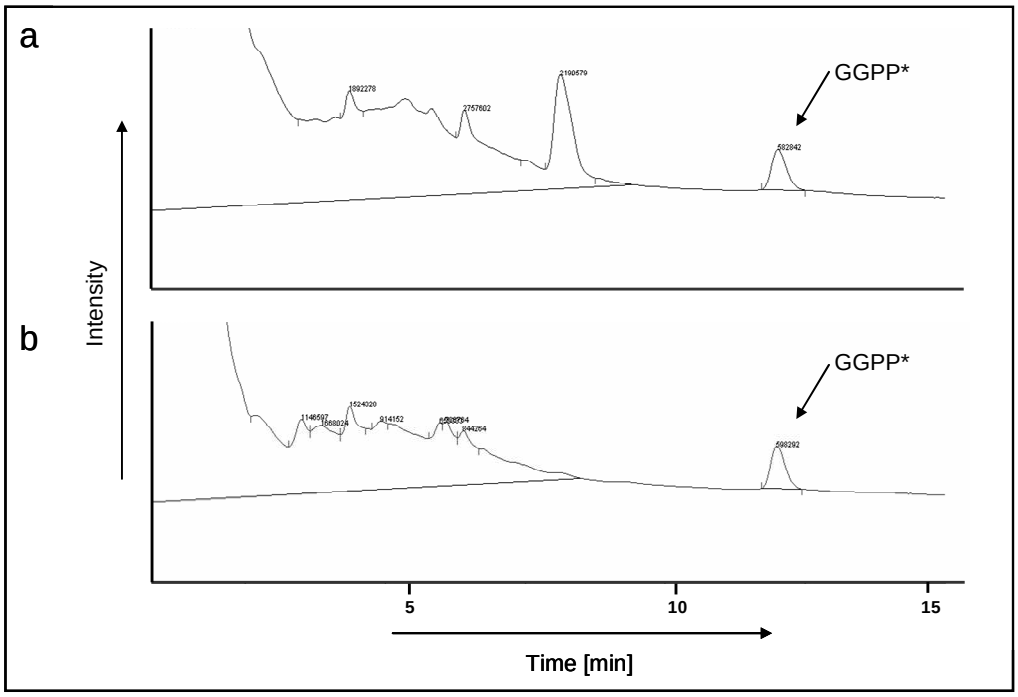

Fig. 10. Chromatograms after elution with (**a**) Elution mix 3 and (**b**) the basic alkaline MeOH/CH3CN/acetone mixture (see Table 11), resulting in detectable peaks of only GGPP*. Chromatograms show a high background noise within the first 8 – 9 minutes. Chromatograms are cut off after 15 minutes to highlight the impurities coming of the column after sample injection.

4.1.4.3. Solid phase extraction (SPE)

Prior experiments using liquid/liquid based extractions (sections 4.1.4.1. and 4.1.4.2.) indicated proteins as a major source of contamination. Consequently, the development of the current extraction procedure included steps for protein precipitation (PPT) in combination with solid phase extraction (SPE).

4.1.4.3.1 Comparative SPE extractions in reversed and normal phase mode

A preliminary experiment was carried out to determine whether FPP and GGPP eluted preferably under reversed or normal phase conditions (RP and NP, resp.). Therefore, the isoprenoids were dissolved in an organic solvent (n-hexane) and in water. Table 12 summarizes the experimental set-up and the final conditions.

SPE-phase		DCS-CN	DSC-Si	DSC-diol
Protocol	[mL]			
Conditioning (C)	1	n-hexane	H_2O	
	1	2-propanol	MeOH	
	1	MeOH	1-butanol	
Equilibrating (E)	2	H_2O	n-hexane	
Sample (S)	1	spiked H_2O	spiked 1-butanol/n-hexane (1:1 v/v)	
Elution (Elu)	2	Elution mix 2	MeOH/H_2O (1:1 v/v)	

Tab. 12. SPE protocols for three different (-CN = cyano, -Si = silanol and diol) SPE cartridges and the applied solvents for each step of the protocol (conditioning (C), equilibrating (E), sample loading (S) and elution (Elu) step).

For FPP the two NP extractions (DSC-Si and DSC-diol) led to higher peak intensities as compared to the RP condition (DSC-CN) but revealed the opposite for GGPP. Overall, the recovery, as determined by a comparative F-G-Assay, using the same isoprenoid concentrations, was low.

4.1.4.3.2. SPE extraction from an organic solvent in reversed phase mode

The previous experiment (section 4.1.4.3.1.) did not elucidate the optimal conditions for the isolation procedure and therefore modifications of the method were required.

Table 13 shows the final protocol which was used; n-hexane was selected as the organic solvent. Neither test condition resulted in peaks for either isoprenoid. The following experiments were conducted under the assumption that the isoprenoids were not retained sufficiently when the samples were loaded onto the column.

The experiment was repeated with the phenomenex X-AW SPEs (Table 13) while the fraction form the sample load and the elution step were collected and combined, dried, derivatized and measured. However, this did not lead to any significant improvements in the level of detection of FPP and GGPP.

SPE-phase		Oasis WAX	Strata X-AW	DSC-NH_2	Oasis MAX
Protocol	[mL]				
C	1		H_2O		
	1		MeOH		
E	2		n-hexane		
S	1		spiked n-hexane		
Elu 1	2		10% MeOH inH_2O		
Elu 2	2		2-propanol/MeOH (1:1 v/v)		

Tab. 13. SPE protocols for four different (-WAX and –X-AW= weak anion exchanger (two different companies), -NH_2 = amino and –MAX = strong anion exchanger) SPE cartridges and the applied solvents for each step of the protocol (conditioning (C), equilibrating (E), sample loading (S) and elution (Elu) step). Two elution steps were conducted separately (Elu 1 and Elu 2).

4.1.4.3.3. SPE extraction using anion exchanger cartridges

Previous experiments tested various anionic stationary phases for their potential to retain the two isoprenoids. However, elution with *pure* organic solvents did not result in a detectable amount of the isoprenoids; therefore the following set of experiments was designed to determine the influence of the pH of the spiked solution. In the following experiments samples were prepared in a range from pH 1-12 (Table 14 and Figure 11).

As clearly shown in the graph (Figure 11) the acidified spiked water sample (pH 1) led to very low intensities of the two isoprenoids. A neutral or basic character of the spiked water resulted in improved recoveries in combination with the X-AW and the WAX cartridges. The DSC-NH_2 and MAX SPEs resulted in poor signals and were consequently excluded from further testing.

SPE-phase		**Oasis WAX***	**Strata X-AW**	**DSC-NH_2**	**Oasis MAX**
Protocol	[ml]				
C	1	MeOH (2x)	MeOH	MeOH (2x)	MeOH
	1		CH_3CN		
E	2		H_2O		
S	1		spiked H_2O at pH 1, 6-7 and 12		
Wash (W)	1	2% MeOH	2% MeOH	2% FA	5% NH_4OH
Elu 1	1	MeOH	NH_4OH/MeOH / CH_3CN (1:7:12 v/v/v)	5% NH_4OH in MeOH	2% FA in MeOH
Elu 2	2	5% NH_4OH in MeOH	2% NH_4OH in CH_3CN		

* Generic protocol

Tab. 14. Optimized SPE protocols for four different (-WAX and –X-AW= weak anion exchanger (two different companies), -NH_2 = amino and –MAX = strong anion exchanger) SPE cartridges and the applied solvents for each step of the protocol (conditioning (C), equilibrating (E), sample loading (S), wash (W) and elution (Elu) step). Two elution steps were collected separately (Elu 1 and Elu 2). * The Oasis-WAX protocol was the generic protocol as recommended by the supplier. For each protocol samples were applied at pH 1, 6-7 and 12.

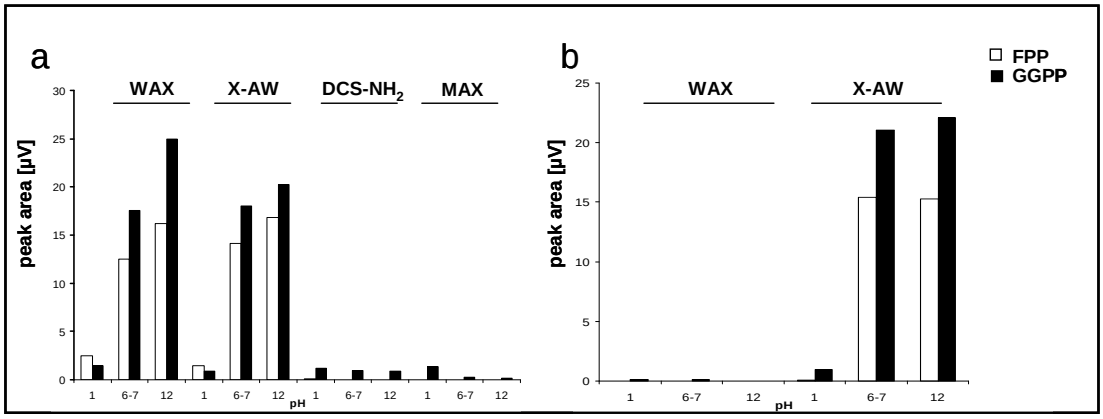

Fig. 11. Comparison of peak intensities after (**a**) elution step 1 and (**b**) elution step 2 in dependency of the pH of the sample solution (see Table 14 for applied conditions).

A repetition of the experiments using the generic WAX protocol (Table 14) for both the X-AW and WAX cartridges could not reproduce previous findings. The wash step with 2% formic acid (FA) was suspected to be the critical step of the applied protocol. Consequently the strata X-AW protocol was further developed.

The following experiments attempted to improve the design of the previously employed protocol at a neutral pH. Initially all conditions were kept constant (Table 14) except for modifications of the elution step. For both protocols only one elution step was conducted and an acetonitrile conditioning step was included; a summary of the adapted conditions and results is shown in Table 15. The results show the relative recoveries compared to a standard F-G-Assay with the same FPP and GGPP concentrations. In brief, the X-AW cartridges with a 1 mL 2% MeOH wash step and the previously used 5% NH_4OH solution in MeOH yielded a superior 85% recovery for FPP and 75% for GGPP.

Strata X-AW		**Protocol 1**	**Protocol 2**
Protocol	[mL]		
C	1	CH_3CN	
	1	MeOH	
E	2	H_2O	
S	1	spiked H_2O at pH 7	
W	1	2% MeOH	
Elu	2	NH_4OH/MeOH/ CH_3CN (1:7:12 v/v/v)	5% NH_4OH in MeOH
Recovery [%]			
FPP		42.5	84.5
GGPP		11.5	75.1

Tab. 15. Comparison of two varying elution conditions using Strata X-AW SPE cartridges. Shown are the applied solvents for each step of the protocol (conditioning (C), equilibrating (E), sample loading (S), wash (W) and elution (Elu) step). Results are shown as relative recovery compared to a standard F-G-Assay.

4.1.4.3.4. SPE extraction using lipophilic and mixed mode interactions

The following experiment studied the pH dependency of the spiked water samples with 3 different stationary phases (Table 16). Acidic (pH 1) and neutral (pH 6-7) conditions were chosen for the sample solutions. For all three cartridges the same protocol was followed. The second, separately collected elution step was conducted with an alkaline solvent to increase the hydrophilic properties of the isoprenoids for a facilitated elution.

SPE-phase		**HLB**	**Strata X**	**DSC-18**
Protocol	[mL]			
C	2		MeOH	
	2		CH_3CN	
E	2		H_2O	
S	1		spiked H_2O at pH 1 and 6-7	
W	1		2% MeOH	
Elu 1	1		MeOH/ CH_3CN (3:7 v/v)	
Elu 2	2		NH_4OH/MeOH/ CH_3CN (1:7:12 v/v/v)	

Tab. 16. Application of the identical protocol for three different SPE phases (HLB = hydrophilic/lipophilic balance, -X = RP18 phase, DSC-18 = RP18 phase). Shown are the applied solvents for each step of the protocol (conditioning (C), equilibrating (E), sample loading (S), wash (W) and elution (Elu) step). Two elution steps with different solvent compositions were conducted separately (Elu 1 and Elu 2). For each protocol samples were applied at pH 1 and 6-7.

Figure 12 summarizes the results of the tested mixed mode (HLB) and lipophilic interactions based (Strata X and DSC-18) cartridges. The Discovery DCS-18 columns proved to be unsuitable under these conditions. The results obtained with the Oasis HLB and Strata X showed good intensities for both columns, which was emphasized when both fractions were applied. The latter resulted in the highest signals for the extraction using the HLB cartridges, when a neutral solution was applied.

As a result further investigations were undertaken to improve the mixed mode HLB protocol.

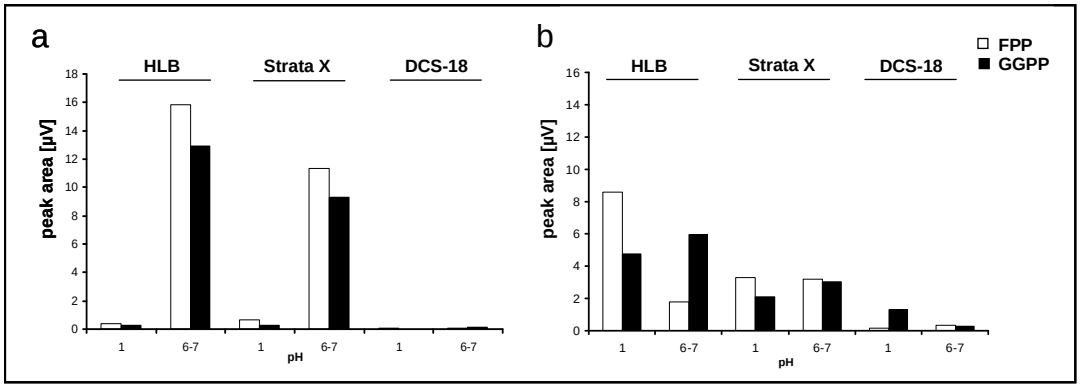

Fig. 12. Comparison of peak intensities after (**a**) elution step 1 and (**b**) elution step 2 in dependency of the pH of the sample solution (see Table 16 for applied conditions).

4.1.5. Optimization of the HLB protocol

4.1.5.1. Influence of the elution solvent

To simplify the 2-step elution method described under section 4.1.4.3.4. the following experiment was planned to show the influence of the chemical properties of the eluting mixture. All solvents contained the identical concentration of NH_4OH, and the organic composition was varied. As shown in Table 17, 4 different eluting solvents (highlighted solvents are varied) were tested without further modification of the protocol. In summary, a direct correlation between the lipophilicity of the organic phase (eluent) and the ability to disrupt lipophilic interactions was observed.

HLB		**Protocol 1**	**Protocol 2**	**Protocol 3**	**Protocol 4**
Protocol	[mL]				
C	1		CH_3CN		
	1		MeOH		
E	2		H_2O		
S	1		spiked H_2O at pH 7		
W	1		2% MeOH		
Elu	2	NH_4OH/ **MeOH**/ CH_3CN (1:3:16 v/v/v)	NH_4OH/ **MeOH**/ CH_3CN (1:7:12 v/v/v	NH_4OH/ **2-propanol**/ CH_3CN (1:7:12 v/v/v)	NH_4OH/ MeOH/ **acetone** (1:7:12 v/v/v)
Recovery [%]					
FPP		61.5	63.8	51.3	68.6
GGPP		23.2	24.2	75.0	82.2

Tab. 17. Optimization of the HLB protocol by varying the elution solvent composition. Shown are the applied solvents for each step of the protocol (conditioning (C), equilibrating (E), sample loading (S), wash (W) and elution (Elu) step). Results are shown as relative recoveries compared to a standard F-G-Assay.

Further modifications were required and implemented as discussed in the following sections.

From the aforementioned eluting solvents, (Table 17) the acetone mixture was selected to generate an elution profile by collecting four 1 mL steps and measuring the individual isoprenoid concentrations. Table 18 shows the recoveries of the individual elution steps in comparison to a standard F-G-Assay.

Elution step	1	2	3	4	**Total recovery**
FPP recovery [%]	58.6	4.1	1.5	1.1	**65.2**
GGPP recovery [%]	56.7	3.5	1.8	1.4	**63.4**

Tab. 18. Elution profile for Protocol 4 (Table 17) by applying 4 individual 1 mL elution steps. Results are shown as relative recovery for each elution step compared to a standard F-G-Assay. Total recovery is given as the sum of all 4 steps.

As shown in Table 18 the highest intensity was detected in the 1st fraction but detectable levels were also observed in the other 3 fractions. These results indicated that the organic solvent composition was not optimal for a complete elution of the analytes (2 mL collection). It was assumed that this specific organic composition lacked the capacity required to completely disrupt the lipophilic interactions and hence a mixture containing n-hexane was employed in future experiments (section 4.1.5.3.). N-hexane was selected since it has the highest eluting power in a RP system.

The experimental setup previously employed was also applied for the mixture containing n-hexane. Elution steps were collected in 500 µL increments. The elution profiles show a complete elution after 2 mL for FPP and GGPP (Figure 13 a and b). Consequently a 2 mL elution step was chosen for further testing.

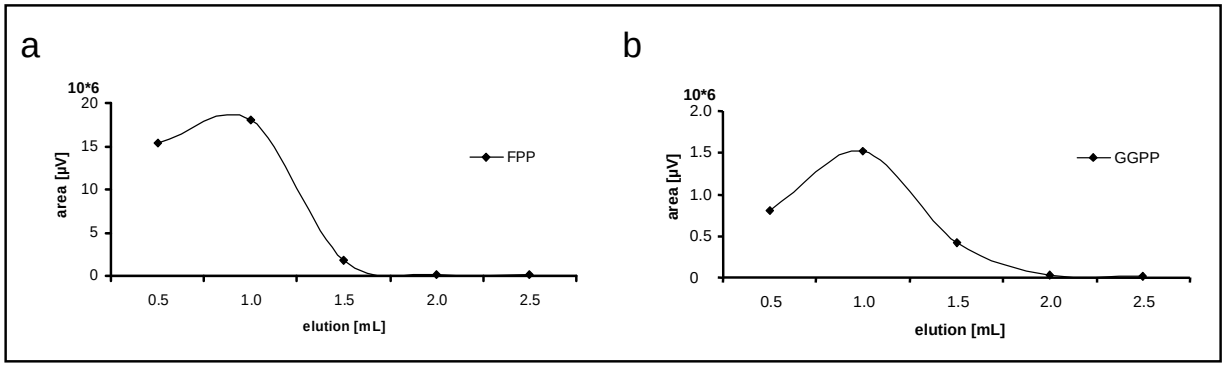

Fig. 13. HLB elution profiles using n-hexane for (**a**) FPP and (**b**) GGPP with 0.5 mL elution steps, separately collected and measured. Peak areas are given as µV.

4.1.5.2. Wash/elution profiles

The following experimental procedure addressed the question of the influence of the composition of the wash solution on the recovery of the analytes. Commonly used wash solvents for the HLB SPE cartridges are water/MeOH or 2% formic acid (FA) mixtures. For the current screening, MeOH/water solutions in 10% increments, in a range from 0-100% MeOH were tested. Furthermore, a wash step using 2% FA in water was tested in parallel. All wash steps were carried out with 2 mL and subsequently the eluent, following the protocol mentioned above (section 4.1.5.1.), was collected and measured (Figure 14).

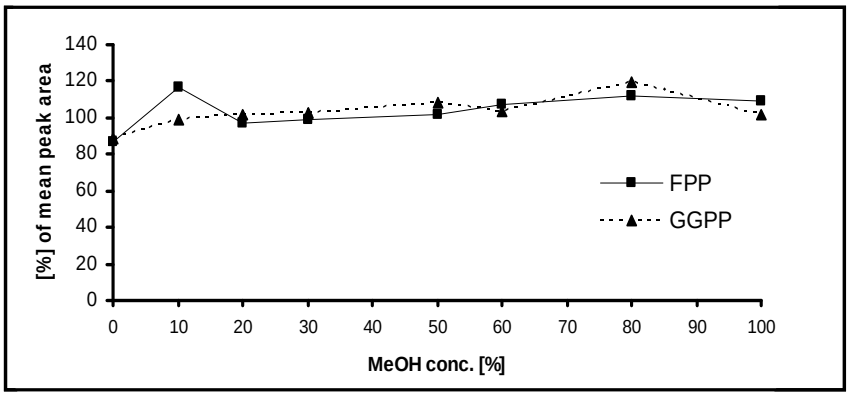

Fig. 14. Wash/elution profiles for FPP and GGPP with increasing methanol concentrations. Elution steps were separately collected and measured. Results are shown as relative recovery compared to a standard F-G-Assay.

Figure 14 shows no significant influence of increasing methanol concentrations over the entire range from 0 – 100% MeOH. In stark contrast the wash step with 2% FA in water resulted in a complete signal loss.

4.1.5.3. Comparison of the HLB and X-AW protocol

Summarizing the result of the previous screening assays from spiked water samples two methods showed feasible results. To further focus the investigations on one single method the following two experiments were carried out. In a first step the developed protocol for the strata X-AW cartridges (section 4.1.4.3.3.) was compared with the Oasis HLB protocol (section 4.1.5.1.). Figure 15 shows the results from the direct comparison in relative recovery compared to a standard F-G-Assay. There was a roughly 20% better recovery for FPP with the HLB protocol while there was no difference concerning GGPP.

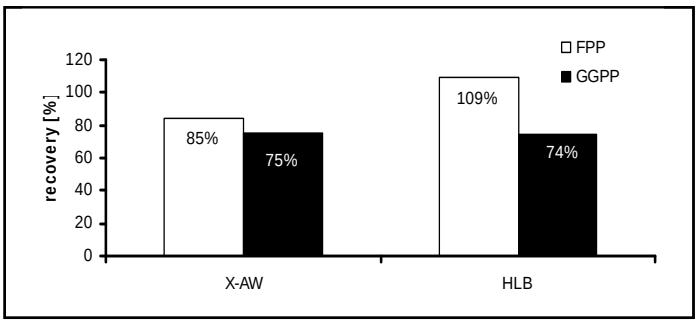

Fig. 15. Relative comparison of the FPP and GGPP recoveries of the employed X-AW and HLB protocol compared to a standard F-G-Assay.

Since part of the retention mechanism for the HLB cartridges is based on lipophilic interactions the following experiment addressed the question of how a spiked, partly organic sample solution would influence the retention during the wash and elution step. Therefore, both steps were collected separately and measured after the enzymatic reaction. The sample solution consisted of 12.5% ACN based on the following reasons. Common SPE applications are carried out after a PPT step mostly using an organic solvent such as ACN. Relying on the manufacturer's specifications organic concentration in the sample solution should not exceed 12.5%.

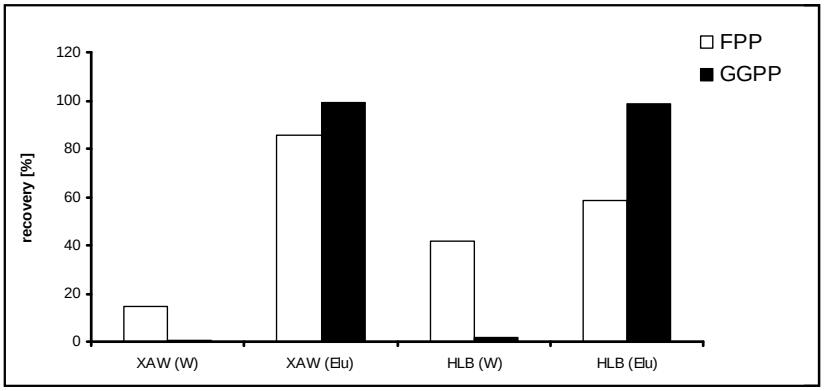

Fig. 16. Comparison of the optimized X-AW and HLB protocol after the application of a sample solution containing 12.5 % ACN. The wash (W) and elution (Elu) step were collected and measured separately. Results are shown as relative recovery compared to a standard F-G-Assay.

Overall the results shown in Figure 16 revealed that the application of a partly organic sample solution hampered a sufficient retention during the wash step. Furthermore, the additional comparison of the X-AW and HLB protocol under these conditions showed a 13% better total recovery for FPP and a 9% reduced total recovery for the HLB protocol.

Summarizing and interpreting the results above, the HLB protocol was determined to be the most adequate method for use in future experiments employing matrix samples.

4.1.6. Employment of the HLB protocol for spiked cell matrix

4.1.6.1. HLB application with untreated cell homogenate

Further investigations of the hitherto developed HLB protocol addressed the potential influence of matrix components on the extraction and the subsequent detection. For this purpose homogenates from SY5Y cells were spiked and used as matrix samples. For the homogenate a total of approximately 8 million cells was collected and re-suspended in 1 mL water, spiked with FPP and GGPP and sonified. The HLB protocol (section 4.1.5.1.) was applied and the eluate processed via the standard protocol. The chromatograms showed very low intensities for both peaks, mostly due to a very high degree of impurities after re-uptake of the dried residue for the F-G-Assay.

4.1.6.2. HLB application with pre-treated cell matrix

Two main reasons could be accounted for the dramatic drop of signal intensities when the unprocessed cell homogenate was extracted (section 4.1.6.1). Firstly, under conditions which allow enzymatic activity of endgogenous phosphatases, in cells or tissue, might cleave off the diphosphate of the isoprenoids. Secondly, the cell components, mostly proteins and membrane lipids might partly pass the column and hamper the sensitive enzymatic conversion of either isoprenoid to its dansyl-label. Another possibility is that these structures might bind the isoprenoids and prevent them from being eluted during the SPE extraction. To investigate these possible influences the following experiments were conducted: one sample treated with a PPT step, one sample mixed with phosphatase inhibitor (PI) from Roche Diagnostics and one sample with the PI and the PPT step (Figure 17). The PPT was conducted using 1:1 ACN (maintained at -20 °C) and the samples were diluted to 12.5 % ACN in water and during the HLB protocol the wash step was omitted.

The results (Figure 17) clearly demonstrated the inhibitory effect of the PI on the activity of the endogenous phosphatases and furthermore underscored the importance of the PPT step.

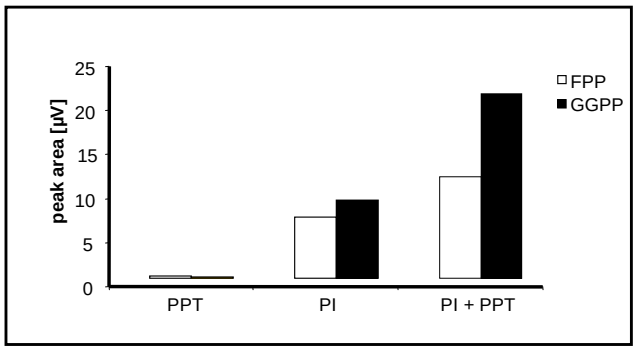

Fig. 17. Influence of the sample pre-treatment, including protein precipitation (PPT) and the employment of a phosphatase inhibitor (PI). Results are shown as comparative peak intensities for FPP* and GGPP* deriving from the identical spiked concentrations.

4.1.6.3. Influence of phosphatase inhibitors

The findings described under section 4.1.6.2 clarified the importance of the addition of a phosphatase inhibitor. Due to their composition different PIs most likely exert varying effects on various phosphatases. In regard to the current application it was questioned whether different inhibitors have diverse effects in preventing the degradation of either FPP or GGPP, hence a series of experiments was conducted to test the commercially available Halt® PI versus a mixture of NaF/imidazole. Both inhibitor mixtures were separately added to cell homogenates and extracted thereafter. The results are displayed in Figure 18 a and show for the NaF/imidazole mixture an equal inhibiting effect on the degradation of FPP like seen with the Halt® PI. The effect on the protection of GGPP is strongly reduced.

The second set of experiments investigated the already tested Halt® PI versus the Phosstop® PI, which is also commercially available. The tests were conducted in mouse brain homogenates with 3 samples per group (Figure 18 b).

As shown in Figure 18 b there was a significant difference regarding the potency of each PI. These findings strongly support the idea that the Halt® PI had a stronger effect on preventing the degradation of GGPP and the Phosstop® inhibited phosphatase activity, which led to reduced levels of FPP. Since the NaF/immidazole mixture had similar effects on FPP as the Halt® PI but was less effective in preventing the degradation of GGPP further experiments in matrix were carried out using a combination of both commercially available PIs (Halt® and Phosstop®).

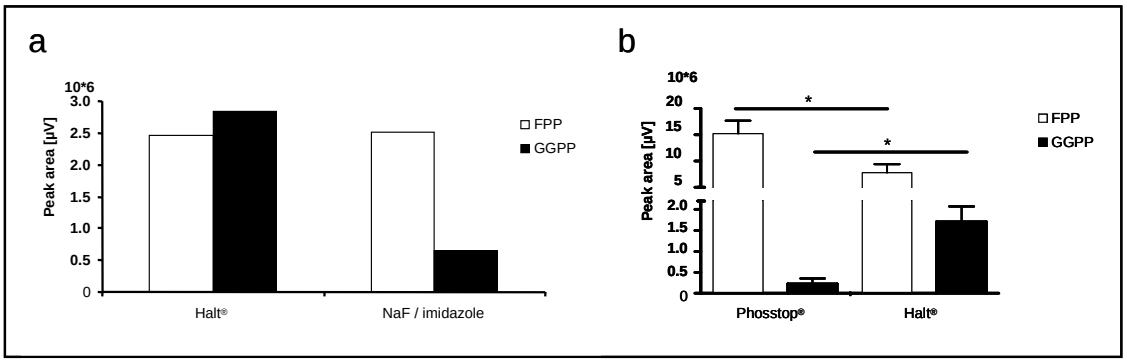

Fig. 18. Influence of phosphatase inhibitors on the recovery of FPP and GGPP levels. (**a**) Comparison of Halt® and a mixture of sodium fluoride and imidazole. (**b**) Comparison of Phosstop® and Halt® phosphatase inhibitor (n=3). Means ± SD; *p<0.05.

4.1.7. Employment of the HLB protocol with spiked brain matrix samples

Based on the previous results, the HLB application was tested on more complex biological matrix-brain homogenates. Preliminary tests were conducted with spiked pig brain homogenates in buffer II with both PIs (Halt® and Phosstop®). The ultimate aim of this set of experiments was to determine the best combination of a LLE or a PPT step with the developed HLB protocol. Therefore, different approaches were selected, the most relevant of which are listed below:

- extraction of fatty acid esters
- PPT with ACN (section 4.1.6.2.)
- LLE as described by Tong et al.[94]
- LLE as described by Bruenger and Rilling[92]
- LLE with a NH_4OH/MeOH solution combined with an 1-butanol extraction

However, each of the aforementioned set of conditions led to clogging of the HLB column and hence early termination or in instances where the protocol could be fully executed, large amounts of impurities in the F-G assay, resulted in incomplete enzymatic reaction and hence low levels of detection of FPP and GGPP. Consequently, none of the aforementioned protocols will be further discussed.

4.1.8. Two dimensional clean-up using Extrelut® and HLB

Previous test runs (section 4.1.7.) revealed that an isoprenoid isolation from complex matrices e.g. brain homogenates, with a single clean up step, using either liquid/liquid based procedures or solid phase extraction, did not lead to satisfactory results. Contamination of the extracted samples hampered the sensitive enzymatic reactions of the F-G-Assay. The experiment described herein presents a combination of the two extraction procedures (two dimensional extraction), Extrelut® and solid phase extraction (HLB protocol).

The first set of experiments addressed the issue of determining the adequate elution mixture for the initial Extrelut® step using spiked buffer II samples. The eluting solvents used for the Extrelut® step are shown in Table 19. These samples were dried under reduced pressure and the resulting pellet was re-dissolved in 5% MeOH and applied to the HLB protocol shown in Table 17. The results are shown as relative peak areas (Table 18) with condition 3 set as the 100% reference.

Protocol	**1**	**2**	**3**	**4**
Sample	spiked Buffer II			
Incubation	15 min			
Extrelut® elution mix	1-Butanol/	n-hexane/	H_2O-saturated	n-hexane
3 x 2 mL	NH_4OH/EtOH	2-propanol /	1-butanol /	
	4:5:11 (v/v/v)	NH_4OH	NH_4OH	
		12:7:1 (v/v/v)	10:1 (v/v)	
	evaporation to dryness and reuptake in 5 mL 5% MeOH			
HLB protocol	section 4.1.5.1.			
Recovery [%]				
FPP	40.9	117.8	100.0	-
GGPP	28.4	19.0	100.0	-

Tab. 19. Comparison of four different organic mixtures for the elution of FPP and GGPP of the Extrelut® columns combined with a unique SPE protocol (as shown in section 4.1.5.1.). Relative recoveries are shown in comparison with protocol number 3, overall showing the highest peak intensities. Protocol 4 did not show any detectable peaks.

The recoveries shown in Table 19 indicated that a simple organic solvent such as n-hexane is inappropriate to elute the isoprenoids. The most convincing results in this experimental setup

were achieved via elution with the settings under number 3. Despite the fact that the recovery for FPP was higher with the n-hexane/2-propanol/NH_4OH mix, the overall recovery for both isoprenoids was superior when the H_2O-saturated 1-butanol / NH_4OH 10:1 (v/v) was applied (→ Elution mix 1).

An identical experimental setup as described in Table 19 protocol 1-3 was repeated with spiked matrix samples (mouse brain homogenate). After elution of the Extrelut® columns, the solutions from all three solvents resulted in un-dissolved residues. To separate the solid residue from the solutions a centrifugation step was included and the supernatant processed as described for the HLB protocol (section 4.1.5.3.). Overall, the HLB application and enzymatic conversion was most successful in combination with the 1-butanol elution mix (Table 19 protocol 3), resulting in the highest peak intensities.

4.1.9. Employment of an internal standard

4.1.9.1. A dansyl-labeled phospholipid as internal standard

N-(5-dimethylamino-1-naphthalenesulfonyl)-1, 2-dioleoyl-sn-glycero-3-phosphoethanol-amine (DP) was initially chosen as a possible internal standard (IS) candidate. The compound is commercially available, has a dansyl label comparable to the analytes. Furthermore, the general structure of phospholipids with their polar head group and the lipophilic tail section resembles that of the isoprenoids. At first glance, the chromatogram of the IS appeared ideal, as the retention time (*Rt* = 7.1 min) lay between that of the two isoprenoids. As described in section 4.1.3., the implementation of the Ascentis® Express HPLC column, revealed the instability of this specific phospholipid under these test conditions. As shown in the chromatograms (Figure 8) the single peak which occurred at 7.1 min (Figure 8 a) after separation on the Zorbax SB-C18 column, was revealed to be two overlapping peaks which were baseline separated on the Ascentis® Express (*Rt* ~ 12 min) (Figure 8 b). These findings terminated future work employing DP as a potential IS.

4.1.9.2. DNP as internal standard

Dansyl-para nonylphenol (DNP)[316] offeres structural similarity to FPP* and GGPP* and was tested as an IS. It was synthesized as described in section 3.2.1. Subsequent to synthesis, DNP

was isolated via RP- high performance thin layer chromatography (RP-HPTLC) (section 3.2.2.) and its identity confirmed via ^{1}H-NMR; the spectrum and signals are shown in Figure 19.

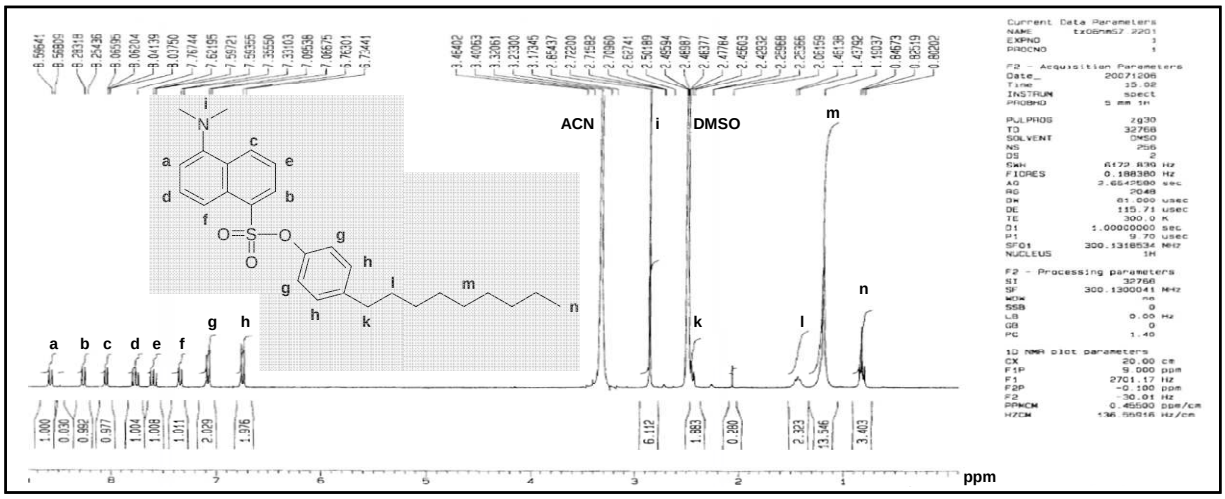

Fig. 19. 300 MHz ^{1}H-NMR spectrum of DNP after HPTLC clean-up. Instrumental settings are displayed on the right and the chemical structure of DNP with the signal assignment given in the spectrum. The acetonitrile (ACN) and dimethyl sulfoxide (DMSO) signals are from impurities of the extraction and NMR solution (deuterated DMSO).

After HPLC separation (Figure 20), the peak for DNP had a retention time of 11.6 min, occurring shortly after GGPP*. Hence it was concluded that DNP could effectively be used in combination with the current conditions of the isolation method developed for FPP and GGPP.

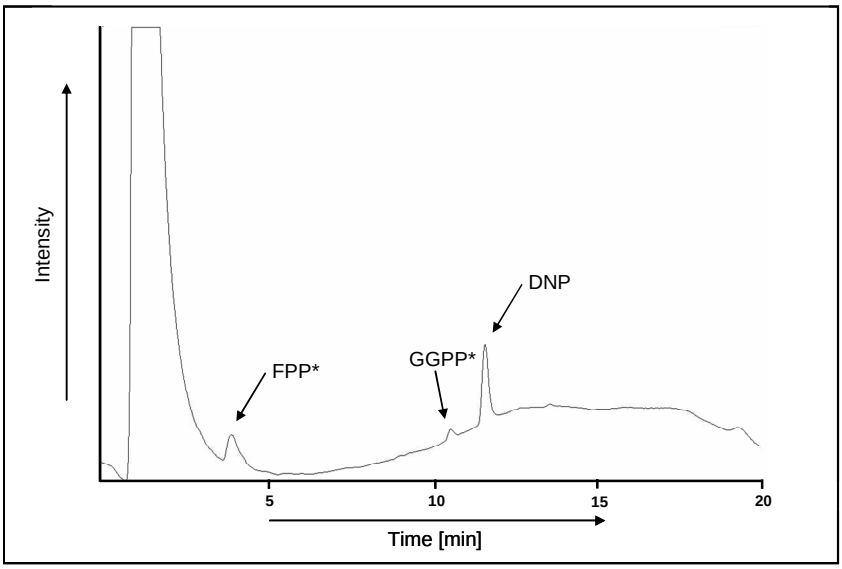

Fig. 20. Exemplified HPLC-FLD chromatogram showing the peaks for FPP* (*Rt*=4.1 min), GGPP* (*Rt*=11.0) and the newly implemented DNP (*Rt*=11.6 min) as the IS for the application.

Based on these findings the combined extraction procedure as described in the flow chart (see Figure 3), was used together with DNP as an IS for the quantification of endogenous FPP and GGPP levels.

4.2. Method employment

The following study illustrates the validation of the aforementioned (see 4.1.8.) extraction and determination of endogenous FPP and GGPP levels in human brain tissue. Importantly, the procedure meets all criteria outlined by the Food and Drug Administration (FDA) for a full method validation for bioanalytical methods.[317] These criteria include selectivity, analyte confirmation, linearity, stability, accuracy, precision and repeated measurements at the lower limit of quantification (LLOQ). The technique shown here also makes use of a weighting factor for the calibration curves to improve accuracy.

4.2.1. Validation results

4.2.1.1. Selectivity

"*Selectivity is the ability of an analytical method to differentiate and quantify the analyte in the presence of other components in the sample.*" [317]

Initially, the degradation of endogenous FPP and GGPP levels in the two brain homogenate batches was shown. Therefore, zero samples were prepared (section 3.5.2.) and subjected to the enzymatic reaction. The resulting samples showed no detectable isoprenoid concentrations and no other interfering peaks. To further ensure the consistency of this brain matrix, samples were spiked before and after storage at room temperature and analyzed, showing again no significant differences in their chromatograms.

Furthermore, the selectivity of the assay was successfully demonstrated when no significant interfering signals were observed in six blank brain homogenate samples of different origin at the retention times for FPP* (*Rt* = 4.1 min) and GGPP* (*Rt* = 11.0 min), as well as in the related zero samples spiked with the IS (*Rt* = 11.6 min).

4.2.1.2. Analyte confirmation

Following selectivity it was essential to characterize each analyte (FPP* and GGPP*) to confirm the identity. The separated peaks were collected after the FLD and measured via high accuracy

FT-ICR mass spectrometry (MS). The spectra are shown in Figure 21 and the measured accurate masses for FPP* and GGPP* corresponded well to the calculated exact masses (<5 ppm measurement uncertainties for all experiments), thus confirming the identities of the derivatized isoprenoids.

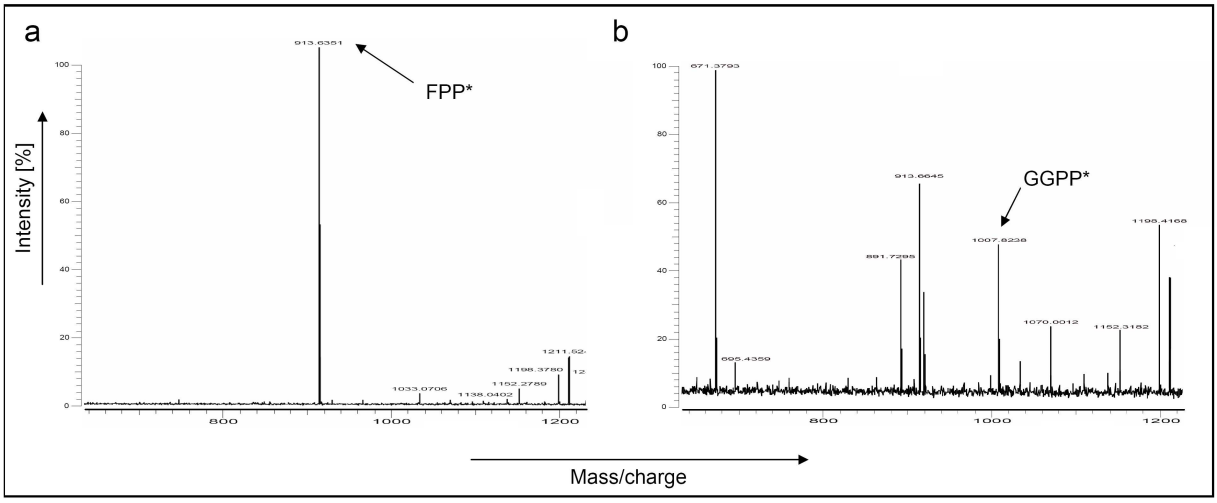

Fig. 21. Accurate mass measurements of (**a**) FPP* (*m/z* 913.635) and (**b**) GGPP* (*m/z* 1007.823) after manual HPLC peak collection from spiked human brain samples. Measurements were conducted on a FT-ICR MS in negative ion mode (< 5 ppm measurement uncertainties for both experiments).

4.2.1.3. Linearity

Good linearity was shown over the investigated calibration range of 10–400 ng/mL for FPP and 50–1000 ng/mL for GGPP in human brain homogenate on five consecutive days. The best fit for the calibration curves was achieved using a weighting factor of $1/x^3$ for FPP and $1/x^2$ for GGPP evaluated by comparing the r^2 values and the sums of the absolute values of the relative errors for the calibration curves using different weighting factors (Table 20 a and b).

Relative error (% RE) of various curve weighting values for FPP					
nominal conc. (ng/mL)	$1/x^0$	$1/x$	$1/x^{0.5}$	$1/X^2$	$1/x^3$
10	201.9	40.4	106.7	-4.7	-0.5
20	97.9	26.2	54.1	15.2	4.3
40	30.4	0.6	11.0	2.8	-11.4
60	26.2	13.9	16.4	24.9	4.7
80	12.3	6.6	6.5	19.1	-1.0
100					
200	0.0	8.3	2.1	26.8	3.5
400	4.1	18.7	9.5	41.1	14.6
sum of abs %-RE	372.9	114.8	206.3	134.5	**39.9**
r^2	0.959	0.896	0.933	0.834	**0.995**

Relative error (% RE) of various curve weighting values for GGPP					
nominal conc. (ng/mL)	$1/x^0$	$1/x$	$1/x^{0.5}$	$1/X^2$	$1/x^3$
50	3.5	15.9	-22.8	-6.8	-3.7
75	21.9	28.8	4.9	12.0	11.6
100	0.0	0.0	0.0	0.0	0.0
125	3.0	6.3	-6.9	-4.7	-6.3
150	3.1	5.4	-5.0	-4.3	-6.5
250					
500	4.7	3.4	3.0	-1.8	-5.9
1000	-1.9	-3.8	-2.4	-7.8	-12.1
sum of abs %-RE	38.2	63.8	45.0	**37.4**	46.1
r^2	0.993	0.969	0.997	**0.991**	0.985

Tab. 20. Overview over the evaluation of various weighting factors for the calibration curves for (**a**) FPP* and (**b**) GGPP*. The best fit calibration curves (highlighted in dark grey) were determined by comparing the r^2 values and the sums of the absolute values of the relative errors (% RE). Rows with missing RE values were excluded in accordance with the FDA guideline.[317]

The results are summarized in Table 21. The correlation coefficients (r^2) were consistently greater than 0.992 and 0.989, resulting in mean values of 0.994 ± 0.0012 and 0.991 ± 0.0014 for FPP and GGPP, respectively. The relative deviations of the calculated standard concentrations

from their nominal values were always less than 15% for all values including the LLOQ and thus meeting the FDA requirements.[317]

FPP		weighting factor	correlation coefficient
calibration range	10 - 400 ng/ml	$1/x^3$	$r^2 > 0.992$
	(~ 0.03 – 1.06 µmol)		0.994 ± 0.0012
slope	0.030415 ± 0.015836		
intercept	0.318673 ± 0.268067		
GGPP			
calibration range	50 - 1000 ng/ml	$1/x^2$	$r^2 > 0.989$
	(~ 0.11 – 2.15 µmol)		0.991 ± 0.0014
slope	0.010204 ± 0.006947		
intercept	-0.15870 ± 0.124934		

Tab. 21. Summary of the results for the determination of linearity for FPP and GGPP in human brain tissue using the evaluated weighting factors evaluated in Table 20.

4.2.1.4. Lower limit of quantification (LLOQ)

Determination of the LLOQ at 10 ng/mL for FPP and at 50 ng/mL for GGPP was carried out in six spiked human brain homogenate samples, yielding an average of 9.8 ng/mL ± 4.3% (bias -2.1%) for FPP and 45.6 ng/mL ± 6.2% (bias -8.9%) for GGPP. The general criteria for accuracy and precision for the lowest quantification level were thus fulfilled. An overlay in Figure 22 illustrates a chromatogram at the LLOQ (lower trace) compared to its respective blank sample (upper trace).

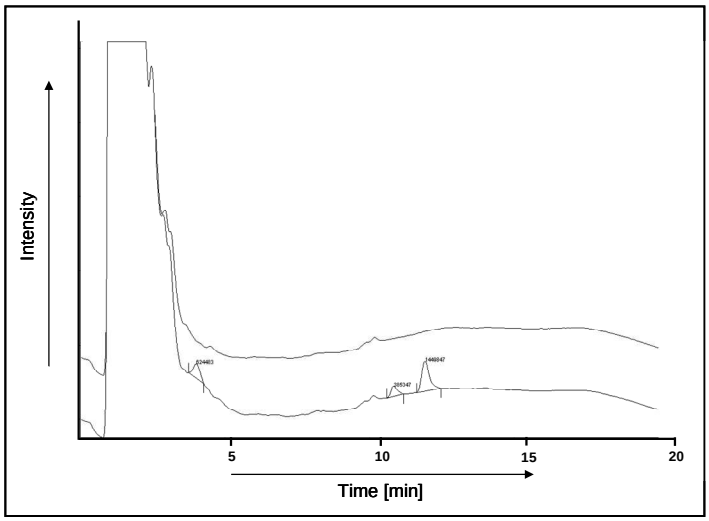

Fig. 22. Representative chromatograms at the LLOQ. Upper trace, blank brain homogenate; lower trace, FPP (*Rt*=4.1 min) and GGPP (*Rt*=11.0) at the LLOQ, DNP as the IS at *Rt*=11.6 min.

4.2.1.5. Accuracy and Precision

The values for intra- and inter-day accuracy and precision are summarized in Table 22, fulfilling the international acceptance criteria for bioanalytical method validation, requiring a maximum of 15% RSD for the respective values of each QC.[317]

Intra- and Interday Accuracy and Precision in brain homogenates

FPP

	nominal concn (ng/mL)	mean calc. concn (ng/mL)	accuracy (bias %)	precision (% CV)
intraday	30	29.1	-2.9	8.7
(n=4)	150	153.9	2.6	4.5
	300	285.3	-4.9	6.1
interday	30	29.5	-1.8	11.3
(n=4)	150	147.5	-1.7	9.7
	300	303.7	1.2	9.3

GGPP

	nominal concn (ng/mL)	mean calc. concn (ng/mL)	accuracy (bias %)	precision (% CV)
intraday	80	84.8	6.0	5.2
(n=4)	400	428.3	7.1	4.6
	800	825.5	3.2	8.8
interday	80	79.9	-0.2	8.8
(n=4)	400	426.2	6.5	6.0
	800	823.5	2.9	8.1

Tab. 22. Summary of the intra- and interday accuracy and precision for FPP and GGPP in human brain homogenates.

4.2.1.6. Recovery

A wide spectrum of SPE materials LLE procedures was screened during the developmental phase of this study. The best results were obtained using the combined approach of matrix-assisted LLE (Extrelut®) and the HLB (Figure 3 and section 4.1.8.). The recoveries for FPP and GGPP were determined in the low, medium and high range of the calibration curves. Mean recovery values for FPP were 64.6, 63.1 and 52.9% and 15.0, 16.2 and 26.5% for GGPP, respectively. Despite relatively poor recoveries, especially for GGPP, the results were reproducible throughout the validation. This was further confirmed by the recovery tests using ^{3}H-FPP and ^{3}H-GGPP, yielding a FPP retrieval of 54% for all three concentrations; GGPP retrieval at the low, medium and high concentration ranges was 18.5, 12.7 and 23.1%, respectively. A summary of these findings can be found in Table 23.

Sample	FPP / ^{3}H-FPP [%]	GGPP / ^{3}H-GGPP [%]
QC-L		
mean	64.6 / 54.0	15.0 / 18.5
SD	0.70	0.95
RSD [%]	1.09	6.32
QC-M		
mean	63.1 / 54.0	16.2 / 12.7
SD	2.58	0.44
RSD [%]	4.08	2.74
QC-H		
mean	52.9 / 54.0	26.5 / 23.1
SD	3.06	1.29
RSD [%]	5.77	4.87

Tab. 23. Summary of the recoveries for FPP and GGPP using QC samples at three different concentrations / QC samples spiked with deuterated FPP and GGPP at three different concentrations.

4.2.1.7. Stability

The stability tests showed no significant degradation of FPP or GGPP in brain homogenate after storage at room temperature, in the presence of two phosphatase inhibitors, at -80 °C for 1 and 3 months and after three freeze and thaw cycles. Storage of FPP* and GGPP* in the autosampler showed unsatisfying results for 20 h at 4 °C due to degradation of the analytes and IS, whereas results measured at the other time points showed acceptable results as noted in Table 24.

Stability data of FPP and GGPP under various experimental conditions (n=3)						
condition	**nominal conc. [ng/mL]**		**accuracy (bias %)**		**precision (% CV)**	
	FPP	GGPP	FPP	GGPP	FPP	GGPP
2 h at RT	30	80	6.2	1.1	1.1	3.4
	300	800	-8.3	2.3	2.2	8.3
1 F/T cycle	30	80	13.4	13.5	1.2	1.8
	300	800	4.1	9.4	5.3	1.2
3 F/T cycles	30	80	9.5	11.3	1.0	4.2
	300	800	12.0	9.3	2.9	1.1
1 month at -80°C	30	80	6.0	11.8	7.9	4.0
	300	800	2.2	11.9	9.2	3.2
3 month at -80°C	30	80	-6.2	7.9	3.1	3.8
	300	800	12.0	12.6	3.4	2.6
autosampler (n=4)			FPP*	GGPP*	FPP*	GGPP*
0 h	150	400	-10.1	8.5	9.2	6.1
5 h	150	400	-7.5	9.4	6.2	0.4
10 h	150	400	-11.9	11.7	2.6	3.2
20 h	150	400	-67.6	33.5	69.0	7.3

Tab. 24. Summary of the stability tests for FPP and GGPP under various conditions. Autosampler stability was tested for FPP* and GGPP*. Highlighted values are outside the acceptance criteria of the FDA guideline.[317]

4.2.1.8. Partial validation for mouse brain samples

The developed and validated method for the detection of endogenous brain FPP and GGPP levels was primarily designed for studies in post mortem human AD brains to assess a possible isoprenoid disturbance in the course of the disease. A more than obvious shortcoming of this kind of matrix is its availability or much more the possibility of generating data from *in vivo* studies.

In order to bypass the latter limitation the following experiments were carried out to obtain *in vivo* brain data from mouse studies. However, brain matrix from pig was investigated for its feasibility.

According to the FDA guideline for bioanalytical method validation[317] a partial validation can range from a simple comparison of the calibration curves to an intensive validation, similar to that described in section 4.2. In the context of this work it was found to be adequate to limit the partial validation to a comparison of the calibration curves for FPP and GGPP in human, pig and

mouse brain matrix. For all three isolations the identical protocol was applied (section 4.1.8.), including the IS and the weighting factor for the calculation of the concentrations. The calibration curves which are displayed (Figure 23) show the nominal and calculated concentrations. Table 25 gives the according correlation coefficients, the calculated concentrations and their variation from the nominal values.

FPP	r^2 = 0.998 ± 0.0009		
Nominal conc. [ng/mL]	Mean calculated conc. [ng/mL]	RSD [%]	Bias [%]
10	9.96	0.82	-0.43
20	20.5	4.17	2.49
40	39.38	3.09	-1.55
70	66.39	5.05	-5.15
100	95.37	8.43	-4.63
200	221.91	0.70	10.96
400	444.32	2.46	11.08
GGPP	r^2 = 0.995 ± 0.0035		
50	47.84	3.95	-4.31
80	83.69	3.47	4.61
100	110.80	n.d.	10.80
150	150.00	8.27	0.0
250	253.34	3.02	1.33
500	462.32	5.33	-7.54
1000	1023.02	5.97	2.30

Tab. 25. Summary of the partial validation for mouse brain samples. Calibration curves were generated in human, mouse and pig brain. The mean of three values are mentioned together with the calculated RSD and bias. n.d. = not determined

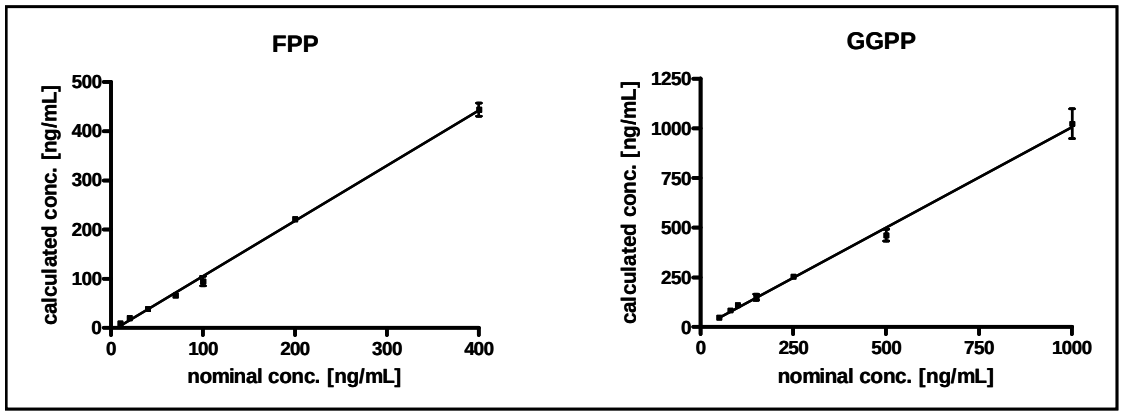

Fig. 23. Linearity for (**a**) FPP and (**b**) GGPP. Calibration curves were generated in human, mouse and pig brain and the means of the three values were plotted against the nominal concentration; variations are given as means ± SD. Concentrations, exact values and r^2-values are shown in Table 25.

Overall, these results indicate that the extraction and detection methods which have been developed thus far are suitable for application on *in vivo* brain tissue samples acquired from mice.

4.3. Method transfer to an UHPLC-MS/MS application

Although the majority of the data presented in the current work were generated by the fully validated HPLC-FLD application a technical aim of the current work was to show the possibility to transfer the newly developed method to an ultra-fast and highly sensitive UHPLC-MS/MS system. This method transfer implicated the capability of providing larger separation efficiencies, much faster run times and greater sensitivity leading to lower detection limits in comparison to fluorescent detection. The instrument chosen for this application was an electrospray ionisation (ESI) triple quadrupole (QqQ) mass spectrometer hyphenated with an UHPLC system.

4.3.1. Determination of the MRM settings

All initial experiments for the development of this method were carried out from standard F-G-Assay using high concentrations of isoprenoids (i.e. 250ng/mL). The first step was a direct infusion into the ESI source of the API 4000 QTrap linear ion trap (QqLIT) mass spectrometer via a syringe pump at a flow rate of 5 µl/min. In addition to providing optimal signal intensity for each analyte, specific fragmentation patterns were also recognized for each prenylated peptide through product ion scans. Ions relating to FPP* and GGPP* were clearly visible in both the negative and positive ionisation mode; however, the positive mode yielded higher ionisation efficiencies and better signal intensities (data not shown). On determining sufficient signal

intensities in the positive ion mode, the compounds were subjected to low energy collision induced dissociation (CID). The according product ion (MS^2) mass spectra for FPP* and GGPP* are shown in Figures 24 a and b. The prominent product ions were observed at *m/z* 810 and 878 for FPP* and GGPP*, respectively. These fragment ions are consistent with a loss of the C-terminal amino acid, serine (-105 Da) and leucine (-131 Da), respectively. These product ions were chosen for MRM analysis and signal intensities were optimized mainly by adjusting the collision energy (CE), ionspray voltage (IS), temperature (TEM) and collision gas pressure (CAD). Moreover, these parameters were further fine-tuned after the employment of the chromatographic separation and resulted in the final settings described in section 3.4.4.

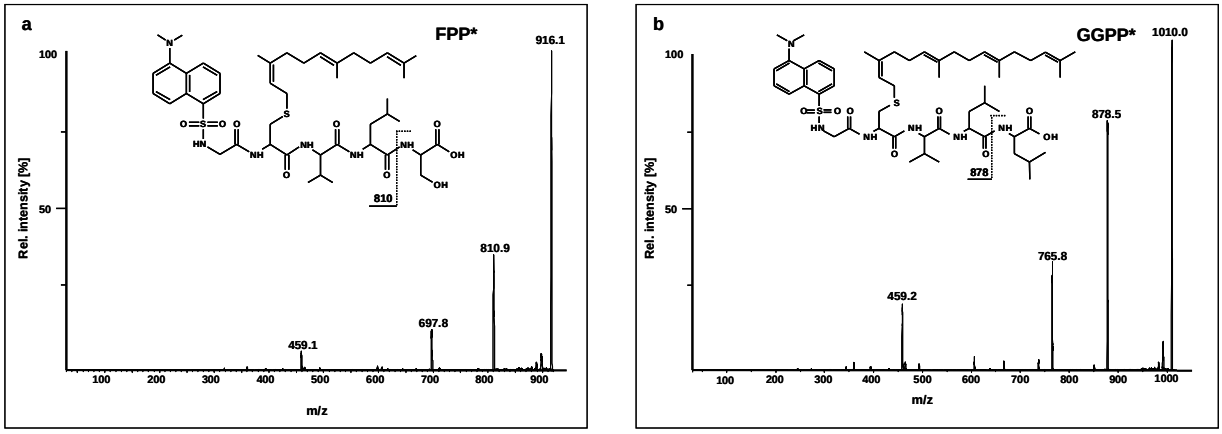

Fig. 24. Representative product ion scans (MS^2) for each analyte. Both spectra show the parent ion (*m/z* 916 for FPP* (**a**) *m/z* 1010 for GGPP* (**b**). Furthermore, the complete structures of both analytes with their respective transitions are shown (*m/z* 916 → 810 (**a**) and *m/z* 1010 → 878 (**b**))

4.3.2. Analyte confirmation

Due to the combined triple quadrupole (QqQ)-LIT instrument employed, further fragmentation could be monitored. The product ion of interest was selected in the third quadrupole (Q3) before undergoing further fragmentation in the LIT. This is known as MS^3 analysis and was employed to verify the product ion identification through structural elucidation. As shown by the representative MS^3 spectrum of FPP* in Figure 25, further mass peaks were observed which could be unequivocally assigned to fragments of the parent molecule (Figure 25). An analogue fragmentation pattern was achieved for GGPP* (data not shown).

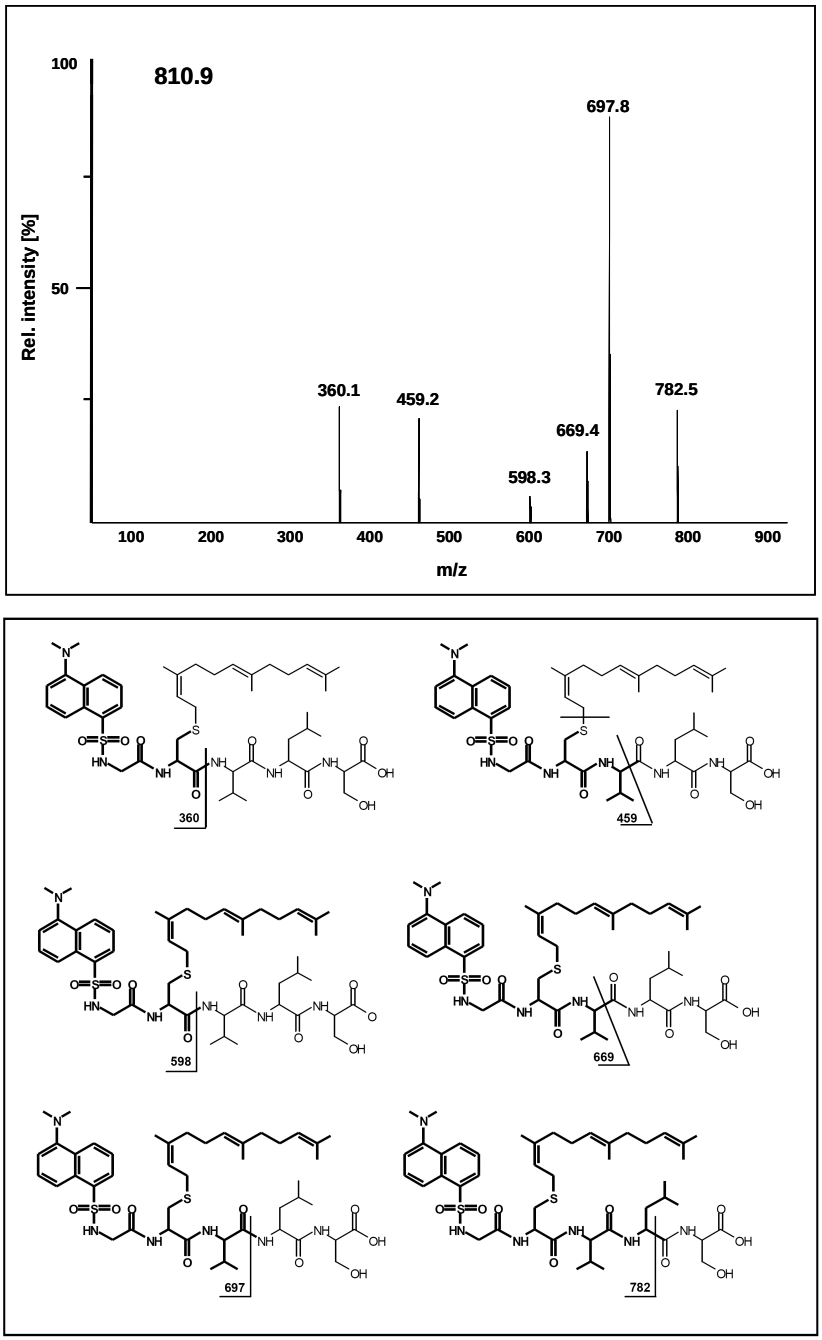

Fig. 25. Rrepresentative MS^3 spectrum of FPP* and the corresponding fragment peaks of *m/z* 810. The according fragments are shown with their chemical structures and the site of fragmentation.

4.3.3. Adjustments of the chromatographic separation on the UHPLC system

The chromatographic analysis of the two analytes was transferred from the original HPLC method to a UHPLC separation, greatly reducing total chromatographic run time from 20 min to only 3 min using the same column with same dimensions on both systems. Consequently, the

retention time for FPP* was reduced from 4.1 to 1.08 min and for GGPP* from 12.1 to 1.56 min. The backpressure on the UHPLC system was at no point higher than 550 bar at a flow rate of 600 µL/min at 20 °C. Figure 26 a shows a representative MRM chromatogram of the newly developed method and Figure 26 b illustrates the chromatographic improvements, especially concerning analysis time (20 min to 3 min) and peak performance achieved by the implementation of the UHPLC separation compared to the HPLC system and finally shows the optimized UHPLC-MRM chromatogram in direct comparison.

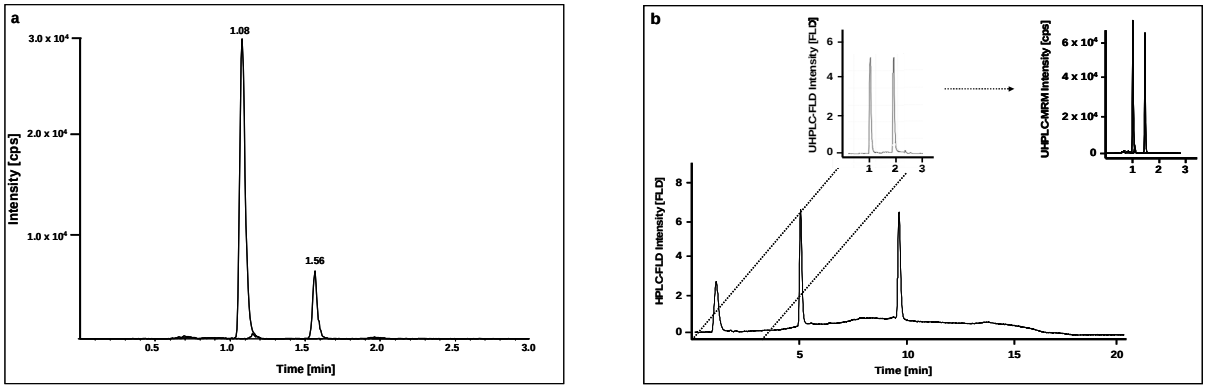

Fig. 26. (**a**) Representative UHPLC-MS/MS (MRM) chromatogram at the LLOQ for FPP* (*Rt*=1.08 min) and GGPP* (*Rt*=1.56 min). (**b**) Illustration of the improvements achieved by the method transfer from the HPLC-FLD system (lower chromatogram) to the UHPLC-FLD and finally to the UHPLC-MRM method.

4.3.4. Linearity and LLOQ

Improvements in selectivity and sensitivity were achieved by using MRMs on a state-of-the-art triple quadrupole MS system. With only one eights of the previously reported injection volume of 80 µL the LLOQ was determined at 5 ng/mL, equivalent to 12.5 pg absolute amount of FPP and GGPP per injection, respectively. This represents a 16 fold increase in sensitivity for FPP* and 80 fold for GGPP* as compared to the HPLC-FLD assay and consequently allowing the preparation of smaller tissue samples for the isolation of endogenous FPP and GGPP. The RSD at the level of the LLOQ were 7.4% for FPP* and 12.3% for GGPP* and were well within the acceptance criteria of the FDA guideline.[317] Subsequently, linearity was determined over a calibration range from 5 and 250 ng/mL for both isoprenoid. Blank samples showed no interfering peaks. While the best fit for the calibration was achieved using a weighting factor of $1/x^3$ for FPP and $1/x^2$ for GGPP, the correlation coefficients were greater than 0.9964 for FPP and

0.9937 for GGPP. The calculated standard concentrations were always within 15% RSD of the nominal concentration.

4.3.5. Matrix effects

To further ensure the absence of interfering ion suppression in the ESI source of the mass spectrometer at the time of retention of FPP* and GGPP*, infusion chromatograms were conducted separately for each analyte. The total ion count (TIC) chromatograms in Figure 27 a and b depict that there was no matrix interference from the brain homogenate samples at the respective retention times of the analytes.

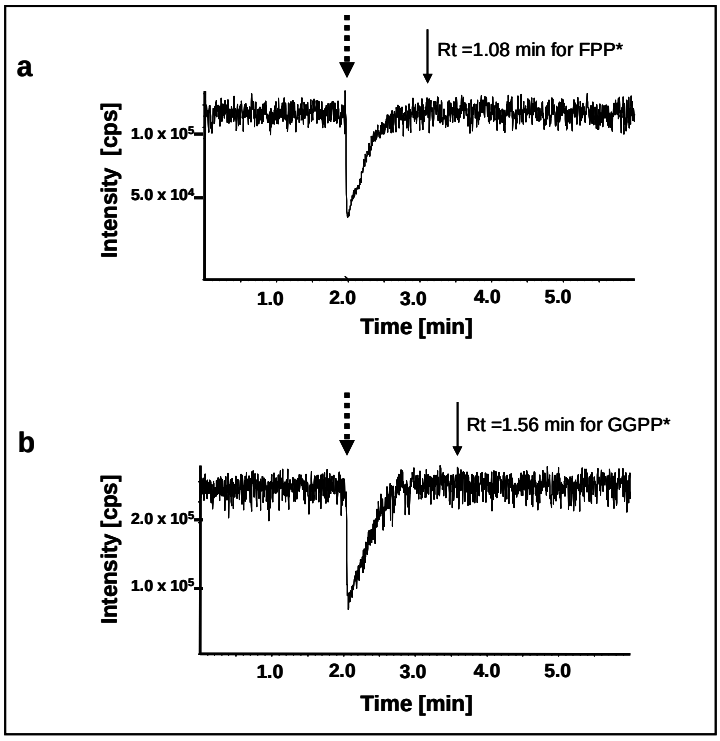

Fig. 27. Infusion chromatograms for (**a**) FPP* and (**b**) GGPP*. ---> marks the time point for the injection on the UHPLC system. → indicate the retention time of FPP* and GGPP* under normal separation conditions, respectively.

4.3.6. HPLC-FLD and UHPLC-MS/MS correlation

For a final assessment of the method transfer from the HPLC-FLD to the UHPLC-MS/MS system the correlation of FPP and GGPP concentrations obtained from both systems were calculated, respectively. For this cross-validation 14 human brain samples were prepared and the

resulting solution after the pre-column derivatization was divided into two aliquots and to be measured on each system separately. Concentrations of the samples were back calculated using a calibration curve processed identically. Results shown in Figure 28 a and b show a correlation of 0.9254 for the FPP* and 0.9530 for the GGPP* results, respectively.

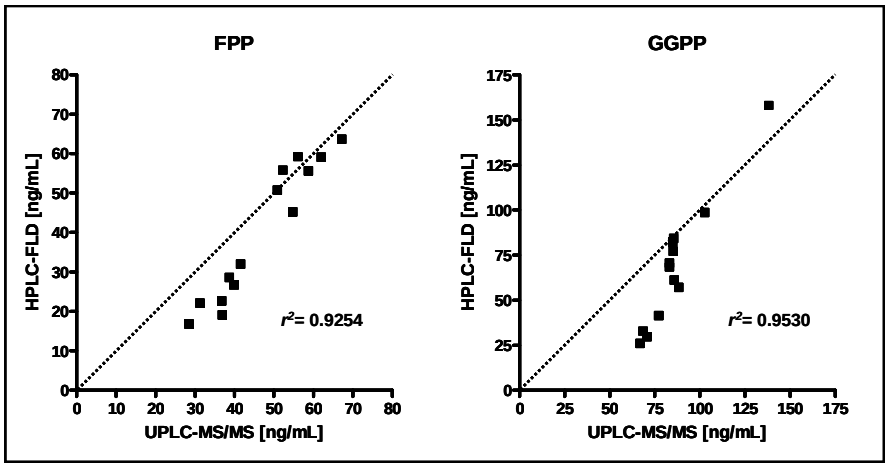

Fig. 28. Data correlation for (**a**) FPP and (**b**) GGPP results obtained from the identical solutions via the HPLC-FLD and UHPLC-MS/MS method. The *dashed lines* correspond to the ideal behavior (slope = 1) and the correlation coefficients (n=14) are shown, respectively.

4.4. Analysis of human brain samples

4.4.1. White and grey matter distribution

White and grey matter brain samples from 5 different human frontal cortex specimens were prepared and analyzed for their FPP and GGPP levels according to the developed and validated HPLC-FLD method described in section 4.2. The specific patient information can be viewed in Table 7. The results of these experiments are summarized in Table 26. This data clearly demonstrated a significantly higher concentration of GGPP in all samples as compared to FPP and a much higher abundance in the white matter, which is expressed in the ratio in Table 26. FPP shows a less distinct distribution between the two areas.

Results of human frontal cortex samples – white and grey matter				
Sample		FPP concentration (pmol/mg protein)	GGPP concentration (pmol/mg protein)	ratio FPP/GGPP
1	white	9.7	61.8	0.16
	grey	10.2	50.0	0.20
2	white	9.9	36.2	0.27
	grey	8.4	24.2	0.35
3	white	7.9	27.8	0.28
	grey	11.3	15.6	0.72
4	white	6.3	18.9	0.33
	grey	7.3	9.3	0.79
5	white	3.4	14.7	0.23
	grey	2.4	8.2	0.29

Tab. 26. Results for human frontal cortex white and grey matter samples. Concentrations are given in pmol/mg protein. The ratio depicts the higher concentration of GGPP compared to FPP.

4.4.2. Post mortem interval (PMI)

The herein described study addressed the question of whether, varying post mortem intervals (PMI), the period between the time of death and the time of removal of the brain, could have an influence on isoprenoid degradation. A delay between the time of death and the brain removal and subsequent deep freezing of the brain could result in depletion of FPP and GGPP due to lysis of the tissue and especially due to the activity of endogenous phosphatases. Previous investigations described in section 4.1.6.3. clearly demonstrated a loss of FPP and GGPP when homogenates were co-incubated without PIs.

Brain samples (grey matter) were selected according to their PMI and divided into short and long PMI groups, 3.38 +/- 0.31 hours; age: 79.25 +/- 3.97 years and 11.75 +/- 0.77 hours; age: 78.0 +/- 1.47 years, respectively. The concentrations of FPP and GGPP which were measured in both sets are shown in Figure 29 a and b. The results demonstrate no influence of a longer PMI as compared to the short PMI. Furthermore, the results again showed a higher abundance of GGPP compared to FPP.

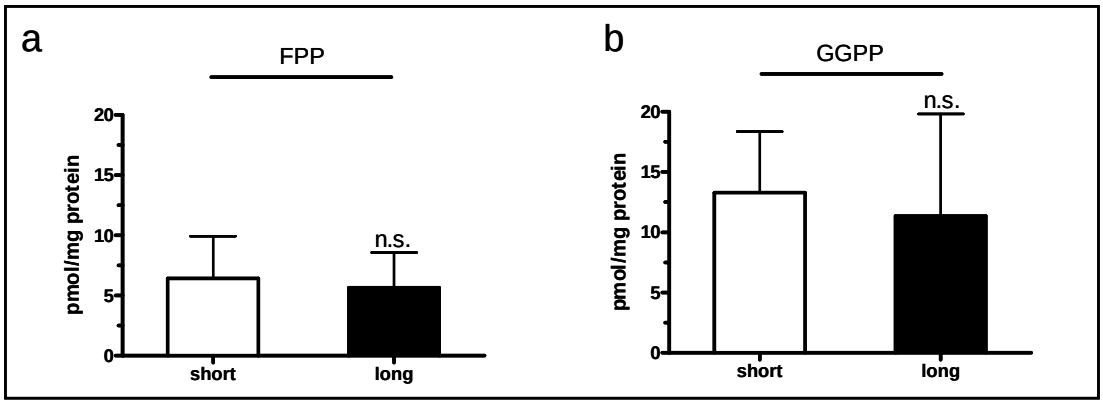

Fig. 29. Influence of the PMI on (**a**) FPP and (**b**) GGPP concentrations. Concentrations were compared between short (3.38 ± 0.31 hours) and long (11.75 ± 0.77 hours) PMI in human grey matter samples. Means ± SD; n.s. = non significant (unpaired t-test), (n=4).

4.4.3. Human AD brain investigation

As mentioned in the introduction, multiple members of the family of small GTPases may be involved in the onset and the progression of AD. All of these proteins require an isoprenylation/prenylation step with either FPP or GGPP for correct function. Hence, the study described herein focused on the abundance of the isoprenoids, FPP and GGPP in AD.

In order to determine the abundance of the isoprenoids in the grey and white matter, a clear separation of both areas in the brain samples was essential. The successful preparation was confirmed by western blot analysis using a neuronal cell nucleus marker protein (NeuN) (Figure 30).

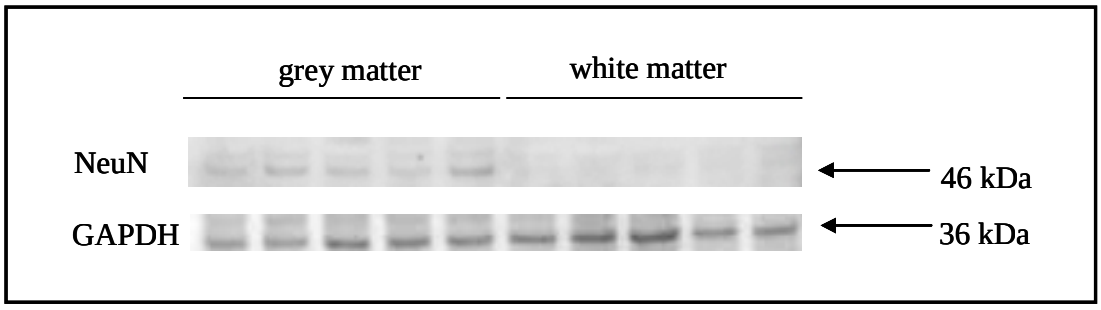

Fig. 30. Preparation of human brain tissue from control and AD samples. Quality of separation of grey from white matter was confirmed by enrichment of the protein NeuN, which is a marker of neuronal cell bodies in grey matter. Protein abundance was determined by western blot analysis (n=5).

To further investigate the specificity of the isoprenoid elevation, the study included separate white and grey matter frontal cortex samples from each patient. The relevant patient information is shown in Table 7 and the protocol for the brain preparation is described in section 3.3.1.

FPP and GGPP levels were determined simultaneously using the aforementioned established and validated HPLC-FLD method (section 4.2.). An overlay of representative chromatograms is shown in Figure 31 a. Figure 31 b depicts that GGPP levels were significantly higher in brain tissue of AD patients (56%) as compared with control samples. FPP levels were also significantly higher in the AD brain tissue (36%) (Figure 31 b). In both, AD patients and controls, GGPP levels were markedly higher than FPP levels and these data are in accordance with the results reported in section 4.4.2.

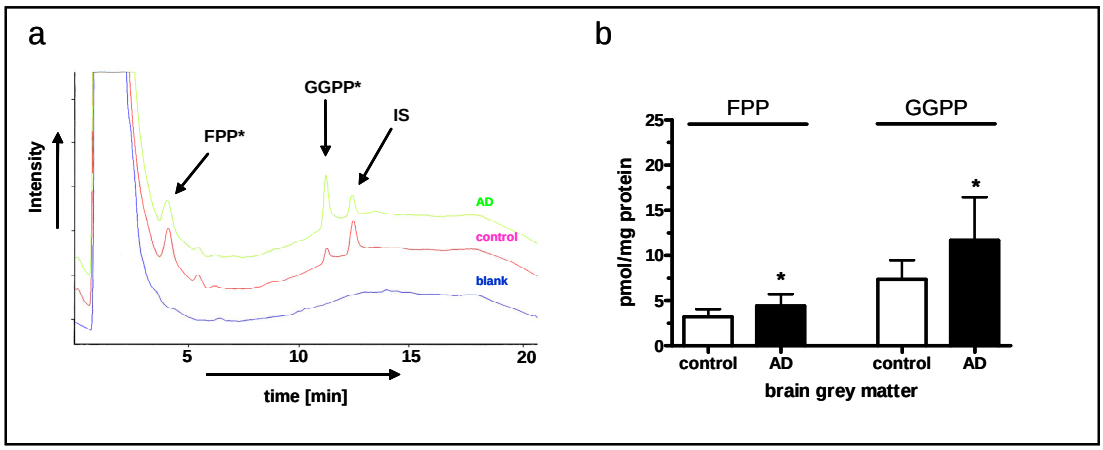

Fig. 31. Elevated FPP and GGPP levels in the frontal cortex grey matter of male AD brain compared with controls. (**a**) Representative chromatographic overlay of grey matter brain samples. Upper trace: AD sample; middle trace: control sample; lower trace: blank sample. (**b**) Endogenous FPP and GGPP levels in human brain grey matter in the control and AD group. Means ± SD, *p<0.05; (n=13).

In order to determine if this up regulation was due to an increased enzyme activity of the FPPS and GGPPS protein or if a transcriptional regulation was involved, mRNA data of the previously mentioned matrix samples were investigated. The FPPS and GGPPS mRNA levels were quantified via qRT-PCR. These measurements were carried out in the laboratories of Prof. W.G. Wood. The results from these experiments were in accordance with the previous findings on elevated FPP and GGPP levels. In summary, the gene expression of FPP synthase (FPPS) and GGPP synthase (GGPPS) was confirmed and the increase in FPP levels in the frontal cortex of

AD affected brain was associated with a significant up-regulation of FPPS expression at the mRNA level as depicted in Figure 32. GGPPS mRNA levels were also increased however no statistically significant differences were observed (Figure 32).

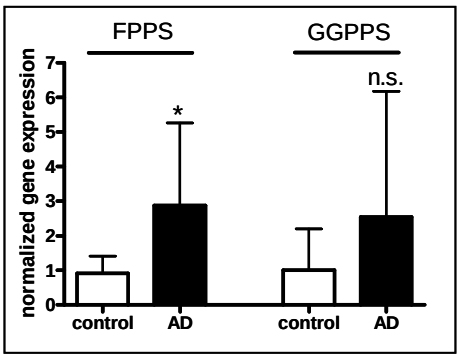

Fig. 32. Gene expression of the FPP and GGPP synthase in human AD and control brain samples. Gene expression was determined by qRT-PCR (data kindly provided by Prof. W.G. Wood). Data were normalized to GAPDH and results are shown as means ± SD; *p<0.05; n.s. = non significant; (n=10).

Contrary to the findings on altered isoprenoid levels, cholesterol levels and gene expression of HMG-CoA reductase were similar in AD and control samples (see Fig 33 a and b). Gene expression was again determined in the laboratory of Prof. W.G. Wood and cholesterol data was determined from the same homogenate, as from which the isoprenoids were measured.

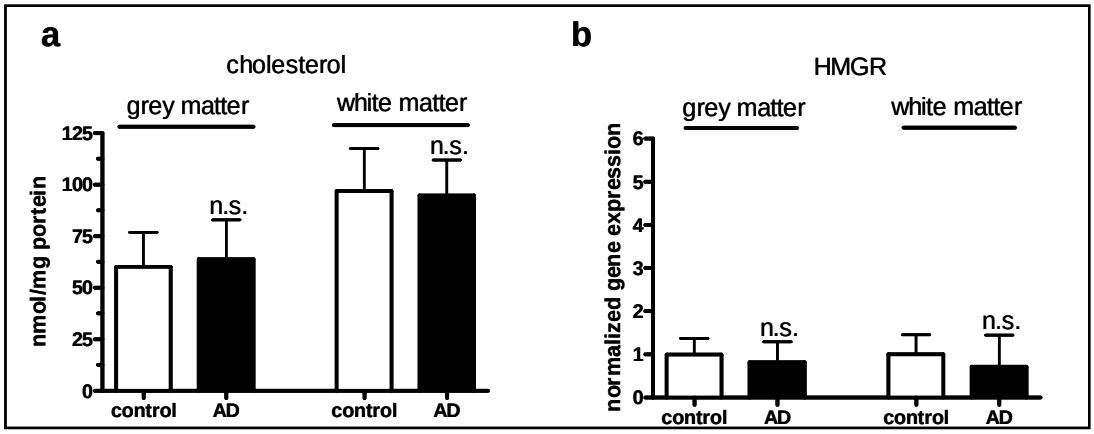

Fig. 33. Cholesterol levels and HMG-CoA reductase gene expression in brain grey and white matter tissue of AD and control subjects. (**a**) Cholesterol levels in brain tissue of control and AD samples; (n=13). (**b**) Gene expression of HMG-CoA reductase (HMGR) in brain tissue of controls and AD samples. Gene expression was determined in grey and white matter by qRT-PCR (data kindly provided by Prof. W.G. Wood). Data were normalized to GAPDH and results are shown as means ± SD; n.s. = non significant; (n=10).

The specificity of the isoprenoid elevation is further supported by similar observations in white matter brain tissue (Figure 34). Here, the same AD brains show a 59% and 43% elevation for GGPP and FPP, respectively. Again this observation is not accompanied by an alteration of the cholesterol concentration (Figure 33 a).

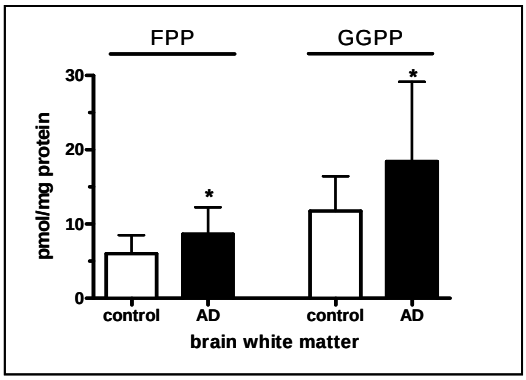

Fig. 34. Elevated FPP and GGPP levels in the frontal cortex white matter of male AD brain samples compared to controls. Means ± SD, *p<0.05; (n=13).

Further investigations addressed the question whether elevated HMG-CoA reductase expression levels or its activation status are accountable for increased isoprenoid abundance.

Based on the aforementioned statement, the identical AD and control samples used for the determination of endogenous FPP and GGPP were subjected to an HMG-CoA reductase activity assay and as described in the previous paragraph, measured for their mRNA levels by qRT-PCR in the laboratory of Prof. W.G.Wood.

Note: HMG-CoA reductase is inactive in the phosphorylated form. For this reason it was essential for this experiment to work with phosphatase inhibitors during sample preparation. Interestingly, the results revealed that the mRNA levels were unaltered (see Figure 35 b) in both the grey and white matter of the diseased brain while the activity was significantly reduced by 39% in the grey matter. A reduction by 34% in the white matter was statistically not significant.

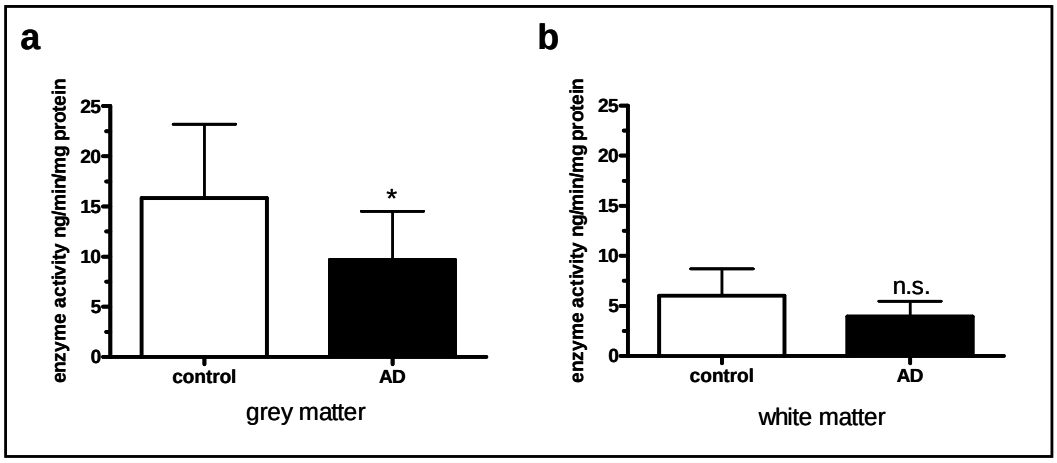

Fig. 35. HMG-CoA reductase activity in brain grey (**a**) and white matter (**b**) tissue of AD and control subjects. Means ± SD; n.s. = non significant; *p<0.05; (n=10).

These results are strongly linked to the unaltered cholesterol levels and clearly demonstrated a specific elevation of the isoprenoids and their respective synthases.

4.5. *In vivo* mouse studies

4.5.1. Mouse simvastatin study

To establish if FPP and GGPP regulation were more susceptible to perturbation than cholesterol, FPP, GGPP and cholesterol levels were determined in the brains of mice, chronically treated (21 days) with the HMG-CoA reductase inhibitor, simvastatin. Figure 36 b shows the differences between the treated and the control group. An exemplified chromatogram from either treatment group is compared to a blank sample, see Figure 36 a.

The overall findings from this trial show that FPP and GGPP are significantly reduced by 52% and 33%, respectively. Cholesterol levels were also reduced but to a lower extent (22%) as shown in Figure 36 c.

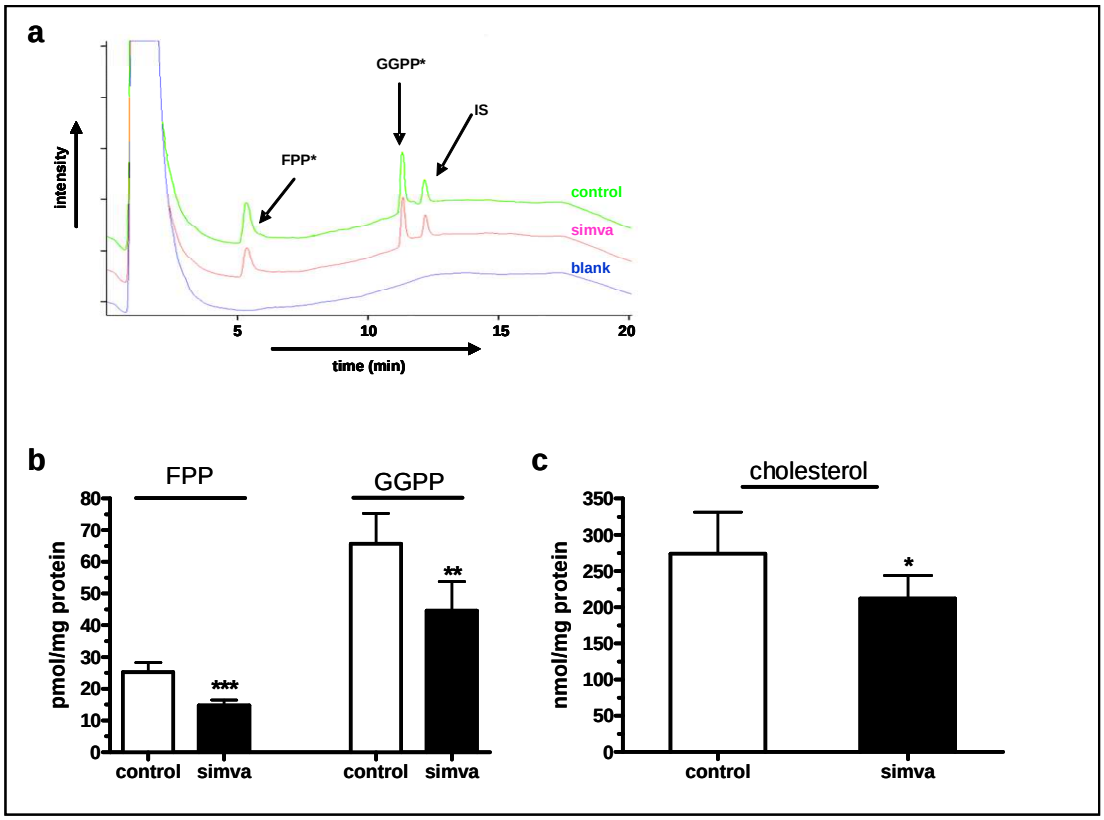

Fig. 36. Brain FPP, GGPP and cholesterol levels in female C57Bl/6 mice (3 month of age) treated with the HMG-CoA reductase inhibitor simvastatin. (**a**) Representative chromatographic overlay of mouse brain samples. Upper trace: control, middle trace: simvastatin treated sample and lower trace: blank sample. (**b**) FPP and GGPP levels in the cerebrum of control and simvastatin treated mice. (**c**) Brain cholesterol levels in control and simvastatin treated mice. Results are shown as means ± SD; ***p<0.001, **p<0.01 and *p<0.05; (n=6).

In contrast to the findings in AD post-mortem brain tissue (section 4.4.4.) these results demonstrate that an inhibition of the HMG-CoA reductase affects both isoprenoid and cholesterol levels, albeit at varying magnitude and this effect is reflected when correlating the data from the control and treatment group. Figure 37 a shows a correlation of r^2= 0.824 ($p < 0.0001$) of the GGPP to its immediate precursor FPP and Figure 37 b demonstrates the correlation (r^2=0.3449; $p = 0.0447$) of FPP as a precursor for cholesterol.

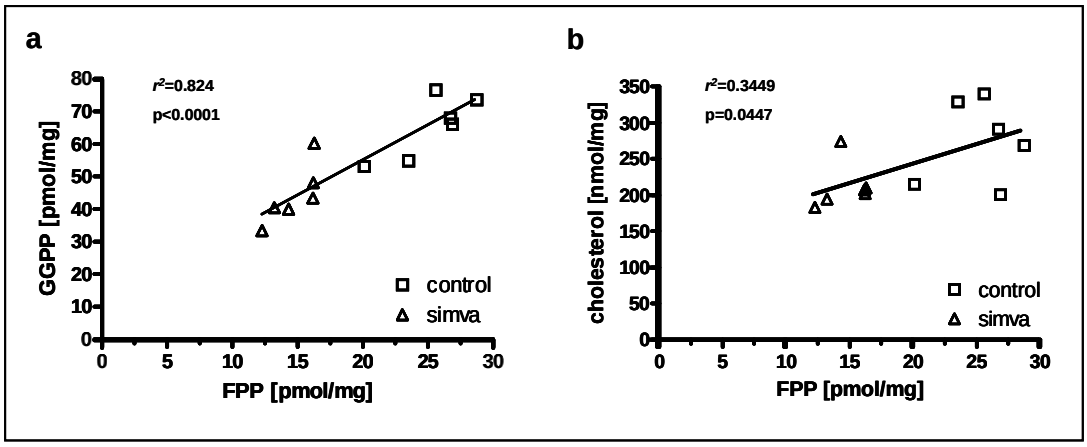

Fig. 37. Data correlation of FPP and its downstream product. Results are taken from the *in vivo* mouse simvastatin study (see Fig. 36). (**a**) Correlation of FPP and its immediate product GGPP. (**b**) Correlation of FPP and the endproduct of the MVA-pathway cholesterol. Goodness of correlation is shown as the correlation coefficient (r^2) and the statistical significance. Data are shown as pmol or nmol / mg protein (n=12).

To further investigate the potential effects of reduced isoprenoid levels in this *in vivo* model on prenylation of proteins, western blot analysis was conducted using a PanRac and a PanRas antibody. The PanRac antibody detects antigenic determinants common to Rac1, Rho A and Cdc42 all of which are geranylgeranylated. The second antibody was raised against antigenic determinants which are common to H-, K- and N-Ras which are farnesylated. Figure 38 a and b show a reduction in band intensities for both antibodies following simvastatin treatment. One could clearly observe an enhanced effect of the drug treatment for the farnesylated proteins, showing a significant ($p = 0.026$) reduction by 27% (Figure 38 b). The impact on gernaylgeranylation with 15% was statistically not significant ($p = 0.2471$) (Figure 39 b).

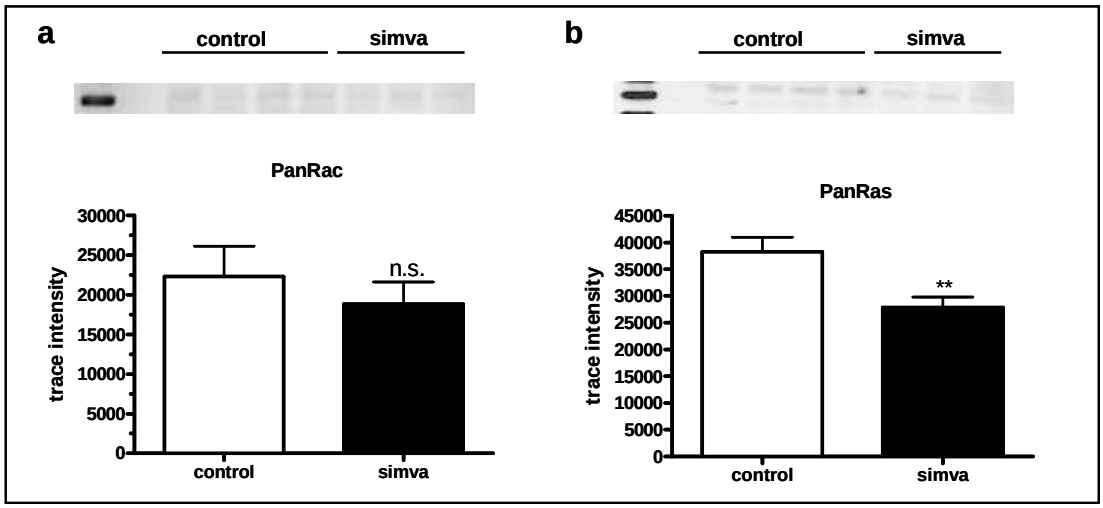

Fig. 38. Western blot analysis of mouse brain homogenate after chronic simvastatin treatment (female C57Bl/6 mice; 3 month of age). (**a**) 21 kDa band of the PanRac (geranylgeranylated proteins) antibody in control brain and brain homogenate of treated mice. According graph shows the evaluation of band intensities. (**b**) 21 kDa band of the PanRac (farnesylated proteins) antibody in control brain and brain homogenate from treated mice. According graph shows the evaluation of the band intensities. Means ± SD, n.s. = non significant; **p<0.01; (n=4 for control and n=3 for simvastatin group).

4.5.2. The transgenic mouse model – Thy-1 APP_{SL} mice

After examination of human AD brains and of mouse brains after chronic simvastatin administration we further investigated if a transgenic mouse model, widely discussed to mimic AD would show a comparable isoprenoid distribution as demonstrated in humans. The Thy-1 APP mice comprise the double Swedish mutation and the London mutation, leading to higher yields of the Aβ peptide and consequently to plaque formation.

We investigated brains of 12 month old Thy-1 APP female mice and their age matched wild type controls. The results shown in Figure 39 a-c depict no significant changes of isoprenoid or cholesterol levels in the transgenic mouse model when compared for each group. However, the calculation of a two-way ANOVA, show a significant ($p<0.0001$) difference when calculated over both variables, FPP and GGPP.

In summary, elevated isoprenoid levels in AD affected brains were observed, however, cholesterol levels remained unchanged. The subsequent *in vivo* simvastatin study in mice indicated the possibility to reduce endogenous isoprenoid and cholesterol levels in the central nervous system (CNS). Furthermore, this study demonstrated a downstream effect of altered isoprenoid abundance, on members of the small GTPases. Nevertheless, in this experimental setup the transgenic mouse model did not produce similar findings in terms of the isoprenoid levels, as compared to human AD brains.

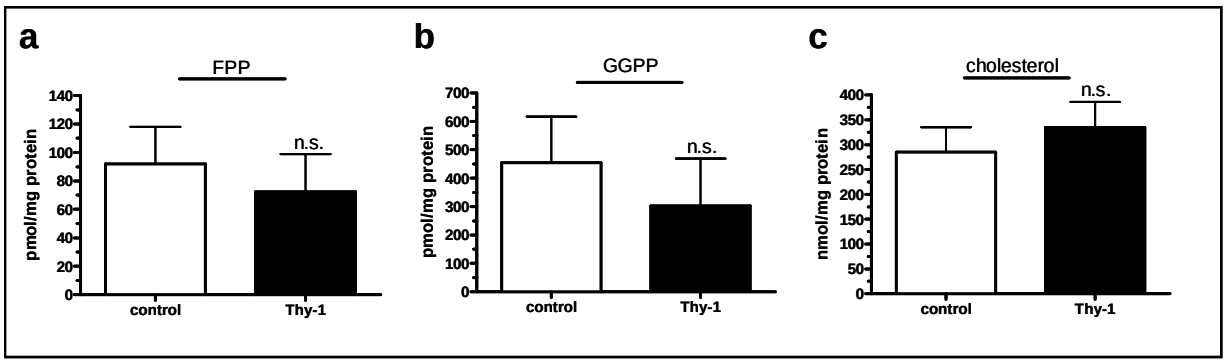

Fig. 39. Brain FPP, GGPP and cholesterol levels in female Thy-1 APP mice and controls (12 month of age). (**a**) FPP, (**b**) GGPP and (**c**) cholesterol levels in the cerebrum of Thy-1 APP mice and their respective controls. Means ± SD; n.s. = non significant; (n=5).

4.5.3. MVA-pathway alterations in aged mice

We demonstrated significant alterations in isoprenoid levels in human AD brain versus controls. All brains in this study were from male donors and their age (section 3.11.1.3.) ranged from roughly 75 to 85 years. We next addressed the question how isoprenoid and cholesterol levels are physiologically regulated during the process of aging. Therefore, brains from three different C57Bl/6 mouse age groups, young (3 month), middle-aged (12 month) and aged (24 month) were investigated.

A pilot study was conducted to address the question whether FPP and GGPP abundance is dependant on the gender of the mice. For this experiment the isoprenoid levels were compared between female and male mice in the aforementioned three different age groups. The results are displayed in a table format (Table 27) listing the mean values and respective SD values from each group and sex. Furthermore, the p-values for the inter-group comparisons are given. The results show no gender dependant differences in FPP and GGPP levels in the brains of female and male C57Bl/6 mice.

C57Bl/6	**Female**		**Male**		
	mean conc. [ng/mg protein]	+/- SD	mean conc. [ng/mg protein]	+/- SD	p- value
FPP					
young	41.04	10.89	36.89	3.48	0.4404
middle	38.28	6.08	35.14	9.99	0.5640
aged	46.66	5.99	53.46	3.44	0.1429
GGPP					
young	226.8	70.16	205.7	48.42	0.5945
middle	268.7	51.04	204.8	72.64	0.1464
aged	359.3	106.2	357.7	77.89	0.9841

Tab. 27. Cerebral FPP and GGPP levels of young (3 month), middle (12month) and aged (24 month) C57Bl/6 mice. Means ± SD; (n=5).

Since the human AD study was conducted with brains derived from male donors and no obvious difference was visible according to the sex of the mouse, further research focused on male mice. The results from the table concerning the three different generations of male mice are included in Figure 40 to emphasize the actual differences in isoprenoid levels. There is no significant elevation of FPP and GGPP levels between the 3 and the 12 month old mice. Significant changes are apparent as the mice reach approximately 24 month, as shown by significantly elevated levels of both isoprenoids between both the young and the aged, and the middle-aged and the aged group. In average FPP levels were elevated by 48% in the aged (24 month) group. GGPP levels were subjected to an even greater increase of 73% on average.

In terms of cholesterol levels, a close correlation with the isoprenoid levels became apparent. Specifically, only the aged group depicted elevated total cholesterol levels in brain homogenate. Though the mean elevation in the 24 month old group became obvious, the difference in concentrations failed to reach the level of statistical significance. However, cholesterol measurement in the crude fraction of the identical brain did show a significant increase over age ($p = 0.0322$, one-way ANOVA) (data no shown).

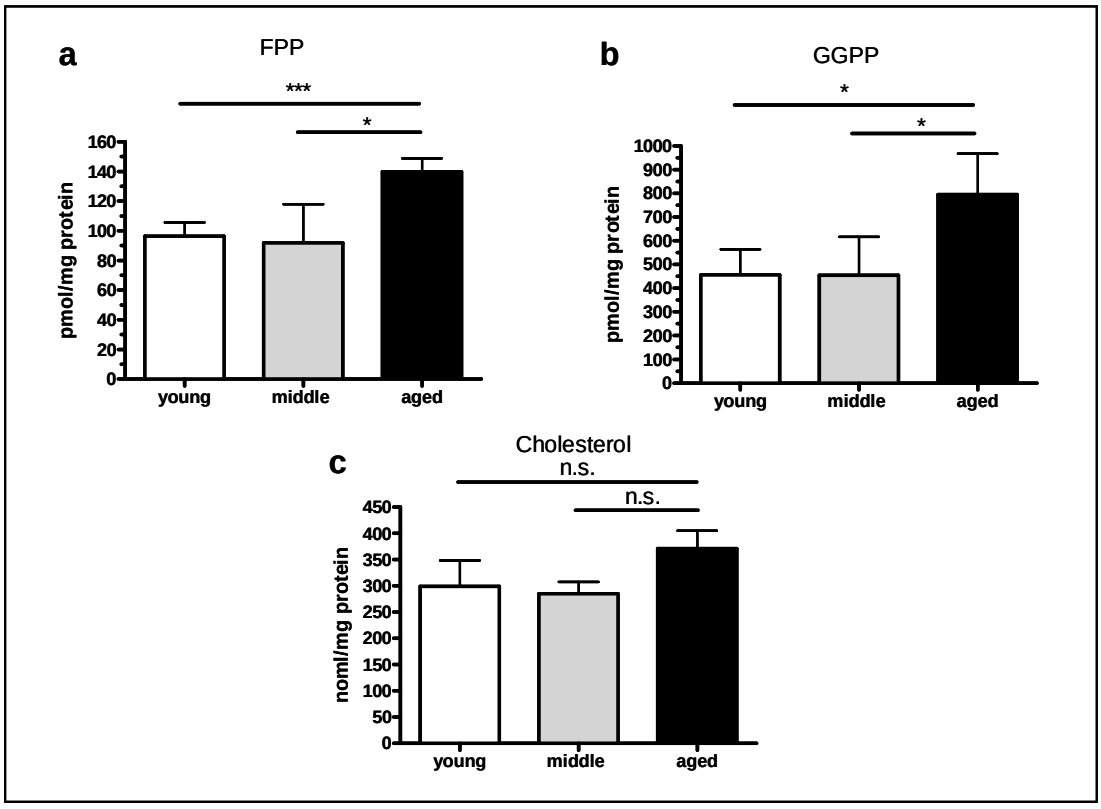

Fig. 40. Brain FPP, GGPP and cholesterol levels in three different age groups, young (3 month), middle (12 month) and aged (24 month). (**a)** FPP, (**b**) GGPP and (**c**) cholesterol levels in the cerebrum of male C57Bl/6 mice. Means ± SD; n.s. = non significant, ***p<0.001, **p<0.01 and *p<0.05; (n=5).

4.6. *In vitro* screening of selected MVA-pathway inhibitors

In vitro cell-culturing is a simple biological model for testing the impact of a drug on a specific metabolic pathway(s). Usually effects can be screened via various methods including measurements of metabolite formation; however this generally involves a cumbersome sample preparation.

A common and widely used cell model in AD research is the neuroblastoma derived SH-SY5Y cell line and a derivative of this cell line, mimicking AD pathology with respect to Aβ formation, are SH- SY5Y-APP wt cells. As previously shown by our group, certain inhibitors of the MVA-pathway reduce cholesterol levels, have an influence on membrane fluidity, leaflet composition and cellular Aβ load.[238]

Different inhibitors and slightly varying conditions were chosen to investigate the effects of specific enzyme inhibition on FPP and GGPP levels in SH-SY5Y-APP cells. Absolute isoprenoid and choletsterol levels in these cells are depicted in the following table (Table 28).

SH-SY5Y-APP	FPP		GGPP		Cholesterol	
	mean conc. [pmol/mg protein]	± SD	mean conc. [pmol/mg protein]	± SD	mean conc. [pmol/mg protein]	± SD
	17.2	1.3	13.4	1.3	381.1	8.5

Tab. 28. Absolute FPP, GGPP and cholesterol concentrations measured in untreated SH-SY5Y-APP cells. Means ± SD; (n=9).

As mentioned in the materials and methods section (section 3.6.2.) several inhibitors were previously tested in our working group for their influence on the parameters given in Table 29.[238,270] As demonstrated in the abbreviated outline of the MVA-pathway (Figure 41), the inhibitors were selected based on their level of inhibition of the pathway, relative to the isoprenoids.

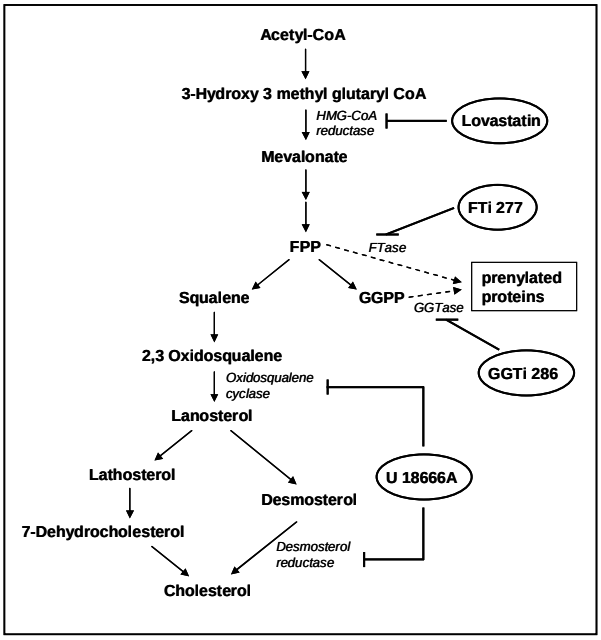

Fig. 41. Abbreviated mevalonate/isoprenoid/cholesterol pathway. Highlighted are the inhibitors, applied in the *in vitro* experiments (see Table 29) as well as their respective enzyme target. A complete overview of the pathway can be seen in Figure 1.

Lovastatin, belonging to the group of "statins" was used to inhibit the first and rate-limiting step of the whole MVA-pathway. Farnesyltransferase inhibitor FTi 277 and geranylgeranyltransferase inhibitor GGTi 286, were chosen to block those enzymes using FPP and GGPP as substrates. Moreover, U 18666A was selected as an inhibitor of cholesterol synthesis, following the

branching point of FPP towards cholesterol synthesis. Conditions were applied as previously used as described in the dissertation of I. Peters. [238,270]

	Cholesterol	FPP-Transfer	GGPP-Transfer
Lovastatin	⇩	⇩	⇩
GGTi 286	⇔	⇔	⇩
FTi 277	⇔	⇩	⇔
U 18666A	⇩	⇔	⇔

Tab. 29. Effect table of different inhibitors on cholesterol levels and FPP- and GGPP- transfer to the respective dansyl labels. Results were evaluated via fluorescence spectroscopy and are adapted from the dissertation from I.Peters.[238,270]. ⇔ symbolizes unaffected results under the respective treatment compared to control cells and ⇩ stands for a reduction.

The same treatment scheme used in section 4.6.1. were applied for the determination of FPP and GGPP.

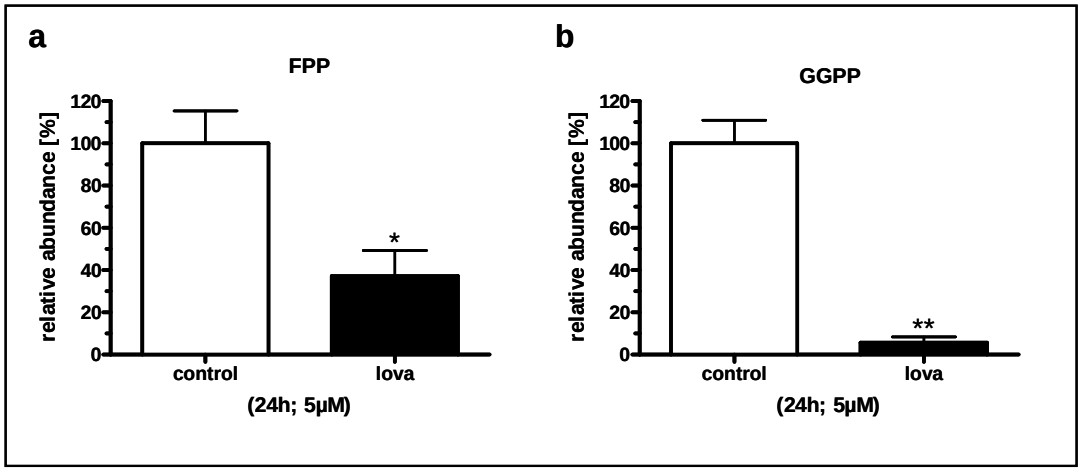

Fig. 42. SH-SY5Y-APP isoprenoid levels incubated 24 h with 5 µM lovastatin. (**a**) 63% relative reduction of FPP and (**b**) 94% relative reduction of GGPP. Means ± SD, n.s. = non significant; **p<0.01; (n=2).

Figure 42 a and b illustrate that the 24 h lovastatin (5 µM) treatment had a strong effect on the cellular isoprenoid levels. FPP levels were significantly ($p = 0.0456$) decreased by 63%, while the impact on GGPP ($p = 0.0072$) was even stronger and reached 94% reduction in average.

To further understand the effects of blocking the MVA-pathway (downstream from FPP) by the aforementioned inhibitors, the following set of experiments was carried out. Cells were incubated for 24 hours with U 18666A (1 µM), an inhibitor of the desmosterol reductase and the oxidosqualene cyclase. The results in Figure 43 clearly show an FPP elevation of 56% ($p = 0.0006$) while GGPP levels were unchanged.

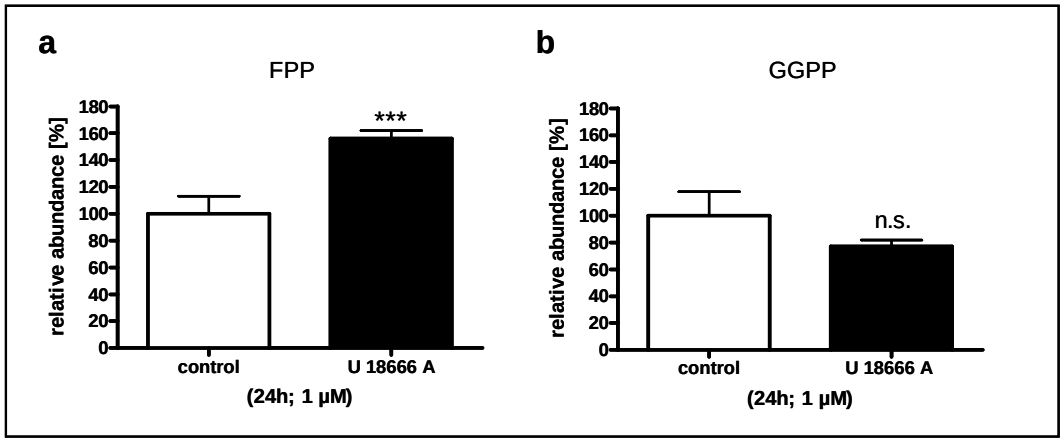

Fig. 43. SH-SY5Y-APP isoprenoid levels incubated 24 h with 1 µM U 18666 A. (**a**) 56% relative elevation of FPP and (**b**) unchanged GGPP levels. Means ± SD, n.s. = non significant; ***$p<0.001$; (n=4).

The last experimental setup aimed to provide information on isoprenoid levels when either transferase was blocked. FTi 277 and GGTi 286 block specifically those enzymes, respectively which use FPP and GGPP as a substrate for post translational modifications. These two experiments were designed, taking the possible instability of the drugs into account. Each inhibitor was added at time points 0, 5, 10, 15 and 20 hours (1 µM respectively) to give a cumulative concentration of 5 µM, respectively. The two graphs in Figure 44 a and b display for FTi 277 a significant ($p = 0.0034$) FPP reduction by 24% while GGPP levels were unaltered ($p = 0.1175$). The GGTi 286 treatment had no significant influence on isoprenoid abundance in this experimental setup.

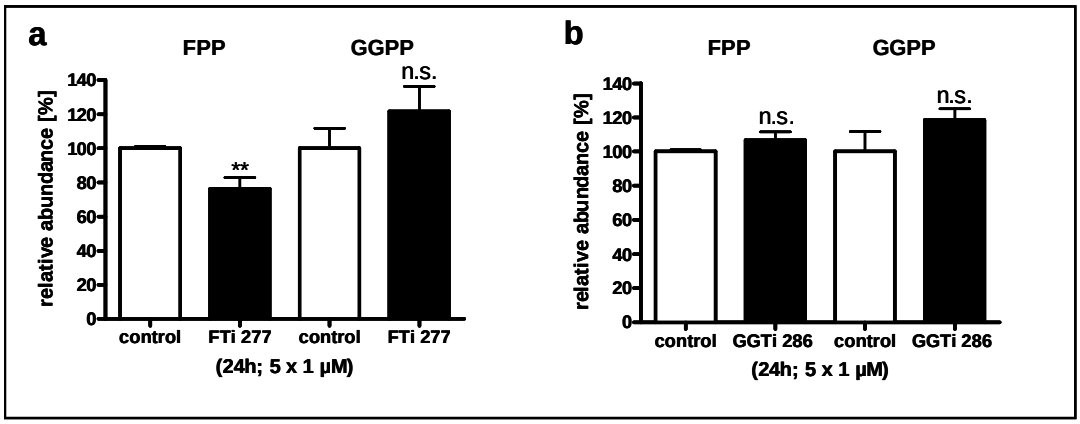

Fig. 424. SH-SY5Y-APP isoprenoid levels incubated 24 h with 1 µM FTi 277 and GGTi 286, freshly added at the following time points: 0, 5, 10, 15 and 20 hours. (**a**) Influence of FTi 277 on FPP and GGPP levels. (**b**) Influence of GGTi 286 on FPP and GGPP. Means ± SD, n.s. = non significant; **p<0.01; (n=3).

5. DISCUSSION

5.1. Previous studies of FPP ad GGPP quantification

As described in the introduction, FPP and GGPP are precursors for various end-products of the MVA-pathway. Their function, regulation and role in cell physiology have been previously discussed in detail.[1,17,83,325] Despite their critical roles in a wide array of fundamental cell processes, our knowledge on the cellular regulation of the two isoprenoids FPP and GGPP is limited. Preventing advancement was mainly due to analytical difficulties concerning a robust isolation technique and a sensitive detection method. The analytical progress in detecting FPP and GGPP now allows investigations of isoprenoid regulation *in vitro* and *in vivo*, which is documented herein.

Researchers have investigated peripheral isoprenoid/protein complexes via methods including mass spectrometry[127], and semi-quantitative immunoassays.[12,326] A major shortcoming of earlier described methods was the determination of solely FPP[85,92,93]; moreover, these methods were cumbersome and costly due the use of radio labeled substrates. Data contained within the current work, on the determination of the free isoprenoids, is crucial in elucidating the regulatory mechanisms governing isoprenylation. An impressive amount of research has focused specifically on brain cholesterol distribution and regulation[327,328], but also on the longer chain isoprenoids or derivatives dolichol, ubiquinone and HemeA.[329,330]

FPP is the precursor for not only cholesterol but also for dolichol, ubiquinone and HemeA. Additionally, like GGPP it is a substrate for the isoprenylation of distinct members of the small GTPases.[331,332] There is a lack of data regarding FPP and GGPP tissue concentrations using valid detection methods.

The most relevant work for the sensitive detection of FPP and GGPP involved the enzymatic coupling of both compounds to their respective dansyl labeled pentapeptides.[94] This method was initially applied for the determination of cellular levels (*in vitro*). A modified method was published for the determination of FPP and GGPP in mouse tissues, including the brain[95] (for a method comparison please also refer to Table 30).

The method described by Tong and colleagues[94] comprised the derivatization of the two isoprenoids to their respective dansyl-labeled pentapeptides and subsequent fluorescence detection. Similar methods were also reported by Saisho et al. who applied a fluorescence tag, 9-antroylcyanide, after alkaline phosphatase conversion of the diphosphate to farnesol.[93] This reaction however is limited by the generated FPP–FOH gradient.

5.2. Method development

5.2.1. Modifications to the pre-existing assay conditions

The enzymatic reaction with the subsequent HPLC-FLD separation and detection method was adapted from Tong et al.[94] Changes in assay conditions and the settings for the chromatographic separation were necessary to optimize the method. The incubation time of the enzymatic reaction was shortened from two hours to 1.5 hours. The most relevant change was achieved by the implementation of the Fused Core® column technology of the Ascentis® Express column. The physicochemical nature of the column bed particles with an impenetrable 1.7 µM core, covered by a porous 0.5 µM silica layer, led to a reduced mass transfer and consequently, to an increased peak efficiency.[333,334] Improvements upon the published method by Tong and colleagues were as follows:

1. Retention time and peak shape of both analytes were improved, including tailing factor and peak width, which led to a 4-fold increased detection limit upon the separation on the Zorbax column
2. Flow rate was noticeably reduced in two steps from 1 mL/min[94] to 0.7 mL/min on the Zorbax column. Using the the Ascentis® Express column further reduced the flow rate to 0.4 mL/min.

Additional changes to the FLD settings were necessary to achieve optimal peak intensities.

5.2.2. Development of a robust FPP and GGPP isolation procedure from tissue

An aim of the current work was to establish a robust isolation method for FPP and GGPP from brain tissue samples, before enzymatically labeling both isoprenoids (section 3.1.1.) and quantify FPP* and GGPP* reproducible. Obtaining clean residues from the extraction for the enzymatic

conversion and analytical studies represented a precondition, since residues potentially inhibit the activity of the converting enzymes and lead to high chromatographic background noise.

5.2.2.1. Liquid/liquid extraction (LLE)

Initially, a LLE for FPP and GGPP from small tissue samples (~20 mg) was conducted according to Tong and colleagues.[94] The method was successfully applied to cell homogenates but not for tissue samples, such as for brain homogenate. A high degree of impurities, most likely due to irremovable precipitated proteins and lipids inhibited the enzymatic activity of the FTase and GGTase. Consequently, there was a demand for a new isolation technique. First attempts, as shown in the preliminary experiments, aimed to test various organic solvents for an optimized LLE based extraction. The solvents were selected for their compatibility with the diphosphates, with respect to solubility and stability. As suggested by Tong et al., experiments were carried out under ammoniac conditions, which prevented the hydrolysis of the phosphate esters of the pyrophophates.[94] The utilization of organic solvents added to the solubility of the isoprenoids. Furthermore, initial experiments were carried out with spiked water samples, which were hypothesized to deliver recoveries close to 100% due to the absence of matrix interference.
Saisho et al. showed n-hexane to be suitable for the isolation.[93] Bruenger et al. used ammoniac dieethylether and 1-butanol[92] similar to Tong et al.[94], mixtures of these organic solvents with NH_4OH were employed and tested for the isolation of FPP and GGPP in the current work. Based on these experiments it was concluded that NH_4OH was needed for the stability of both isoprenoids. As for the organic solvents the n-hexane and 1-butanol mixtures were shown to be suitable with recoveries between 45 and 70% from spiked cell homogenates. Nevertheless, LLE conditions failed to show clean residues for the enzymatic reaction when applied to tissue homogenate.

As an enhancement of common liquid/liquid based extractions a matrix assisted LLE was subsequently employed. This technique was previously used in collaboration with our group for the extraction of exogenous compounds from brain matrix[324] and was tested for the current application to provide cleaner sample extracts. The diatomaceous earth filling of the columns is used to retain proteins, lipids, ions etc. and organic solvents are selected to allow for elution of the desired analyte. However, attempts with several different organic elution solvents continuously resulted in high degrees of impurity, limiting the detection of FPP* and GGPP*. The impurities led to a high background noise during the initial 15 minutes of the analytical run,

severely impeding FPP* and GGPP* detection. There was no detectable peak for FPP* due to co-eluting impurities, while the impact on GGPP* detection was less significant due to the declining baseline signal. The detection of a GGPP* peak was taken as a proof for the enzymatic reaction to occur, but at this point a partial impairment due to impurities could not be excluded.

5.2.2.2. Solid phase extraction (SPE)

5.2.2.2.1. Normal phase or reversed phase mechanisms

To overcome the issue of impurities after the LLE or matrix assisted LLE another conventionally used sample preparation step was investigated. Even though over the last couple of years new and sophisticated isolation techniques and tools were brought onto the market SPE remains the most widespread isolation technique for the isolation of drugs and/or metabolites from organic matrix samples.[335] Due to their large diversity in size, format and especially packing materials (from various suppliers), these cartridges are almost universally applicable for small molecules. The basic underlying mechanism is retention via various interactions between the analyte and the stationary phase of the cartridge.

Similar to HPLC columns, SPE cartridges can be used under normal phase (NP) and reversed phase (RP) mode. The NP mode describes a more or less hydrophilic analyte in a mostly aprotic solvent. The elution power of applied elution solvents increases with an increasing dielectric constant. The RP mode describes the contrary. The physicochemical properties of FPP and GGPP clearly separate each molecule in a hydrophilic head group and a lipophilic tail theoretically allowing both aforementioned mechanisms. The C20 chain of GGPP allows the molecule to have stronger lipophilic interactions than the C15 FPP.

According to the suppliers (Sigma-Aldrich) description, the Discovery® cyanopropyl bonded phase (DSC-CN) SPE cartridges can be used for RP mode of lipophilic analytes in aqueous solutions, while they are less retentive for polar analytes in NP mode when compared to the silica (DSC-Si) or the dihydroxy (DSC-Diol) bonded sorbents under the same conditions.

With respect to the aforementioned details, the first SPE experiment was designed to determine the most favorable conditions. Interestingly, the comparison of the NP and RP mode showed a better retention for FPP under NP conditions for both cartridges. GGPP with the longer lipophilic tail group was retained stronger on the DSC-CN phase. However, the recoveries were insufficient

and the results conflicting and hence required fine-tuning. From these initial results a general conclusion as to whether the NP or RP mode would result in better recoveries could not be met and further stationary phases with varying conditions needed to be tested.

5.2.2.2.2. Anionic interaction mechanism

Further screening of SPE cartridges and modifications of the applied protocols were necessary. Therefore, it was tested whether ionic interactions of the isoprenoid diphosphate groups with amino groups of the stationary phase would occur. Initial experiments with four different sorbent bound amine-groups for the interaction with anionic structures were tested. To determine a possible influence of the different amine functions of the cartridges, identical protocols were applied for all cartridges. The sample was applied in a neutral solution and the elution steps only varied in their organic composition; neither the elution steps nor the eluate from the sample step showed significant analyte concentrations after enzymatic conversion. In order to confirm that analyte loss did not occur due to instability of the diphosphate groups but due to a firm binding of the isoprenoids to the functional groups of the cartridge filling, the pH of the sample solution was modified to acidic, neutral and basic conditions. Furthermore, the protocols for the four different anion exchanger cartridges were slightly modified.

The acidic pH of the sample solution or the addition of formic acid both resulted in almost complete analyte loss, which most likely occurred due to acidic hydrolysis of the diphosphates of both isoprenoids. The comparison of the Oasis® WAX and Strata X-AW SPEs, both weak anion exchangers, clearly revealed the advantage of an alkaline elution. The difference between the first and the second elution step showed a clear dependency of the pH of the eluting solvents; the addition of NH_4OH facilitated the elution of both isoprenoids with the organic solvent because the strong base led to a deprotonated, neutral functional group of the sorbent and shifted the equilibrium of the diphosphate towards the anionic form. Consequently the ionic interactions were enhanced and retention of the analytes did not occur. This was observed without any major influence at pH values between 6 and 12 of the sample solution. The two elution steps on the X-AW cartridges yielded the best results and consequently that protocol was selected for further optimization as compared to mixtures containing acetonitrile.

A critical step during SPE procedures for recovery is the elution step and the composition of the deployed solution. The elution conditions require a complete offset of any kind of chemical interactions between the analyte and the stationary phase. Results from a comparison of two different ammoniac elution solvents with different organic composition revealed that methanol as the more polar and protic solvent had the higher elution power.

5.2.2.2.3. Mixed mode and apolar interaction mechanism

As described in the previous section isoprenoids were shown to be possibly retained on the SPE cartridges via ionic interactions of their polar diphosphate group. Further screening assays were conducted to test whether lipophilic-lipophilic interactions of the apolar carbohydrate chains could result in an optimized retention during the sample loading step. Moreover, these interactions were compared to mixed mode SPEs. Mixed mode SPE cartridges like the hydrophilic-lipophilic balance (HLB) from Oasis® offer a possible retention via polar and apolar interactions of the stationary phase with the analyte and were therefore designed to be applicable for a wide spectrum of analytes.

Two mixed mode (HLB and Strata X) and a purely C_{18} (DSC-18) phase were subjected to the identical protocol. Samples were applied in solutions with a pH of 1 and 6-7. A solution under basic conditions was not tested, since a strong basic environment would lead to multiple negatively charged isoprenoids, consequently hampering the apolar interactions with the stationary phase. Overall, it was confirmed that again an acidic pH led to significant analyte loss. Furthermore, in contrast to the previously described pH dependency of the anion exchanger columns (section 5.2.2.2.2.) during elution, the alkalinization of the eluent in this experimental setup did not have a relevant impact, suggesting that the basic mechanism relies purely on apolar interactions. The eluate on the DSC-18 phase did not show a significant analyte concentration most likely due to a strong retention.

In summary, the HLB cartridges showed the strongest signal intensities under the tested conditions and were therefore used for further improvements of the protocol.

In order to achieve a complete elution with preferably small amounts of solvent, several ammoniac solvent compositions were compared. The screening revealed the need for a strong organic solvent in terms of eluting power on a RP system. Based on the lowest dielectric constant of the most common organic solvents n-hexane was chosen and tested in an elution profile assay. For the test conditions five separate 500 µL steps of a n-hexane/2-propanol/NH_4OH mixture were applied to the cartridges during the elution step. Each volume was collected and measured separately and revealed a full elution after the third step.

During the aforementioned test runs the main focus was to achieve adequate analyte retention and subsequently a complete elution. For matrix samples it is further important to include a wash step into the SPE protocol during which impurities on the column bed are reduced and analyte concentration is not affected. Such steps are especially important to overcome ion suppression when measuring on a MS system but are also necessary to lower background noise in common HPLC detectors like FLD or UV. Additionally in the case of the current application, the wash step was necessary to provide cleaner samples for the enzymatic reaction. The most commonly used wash solvents are mixtures of methanol and formic acid. The latter was applied in a 2% solution and resulted in a complete analyte loss, due to the earlier mentioned acidic inorganic ester hydrolysis of the diphosphates. Methanol was used in concentrations up to 100% and did not reveal any significant analyte loss during the wash/elution profiling.

The subsequent SPE screening led to two distinct protocols with two different SPE cartridges. Directly comparing the two protocols the HLB method was slightly superior and was thereafter employed for spiked SY5Y cell matrix analysis. Cell matrix was chosen to demonstrate matrix interference on a lower level than tissue samples. Cells are a less complex system concerning the abundance of potentially interfering compounds, especially lipids. This was demonstrated by the direct application of tissue homogenate samples, which led to an immediate clogging of the cartridges. However, results with SY5Y matrix were not satisfactory due to one of the following reasons or combinations thereof:

- analyte loss due to endogenous phosphatase(s) activity preventing the enzymatic conversion of the free alcohols

- low concentration of FPP* and GGPP* due to impurities hindering the enzymatic conversion
- low detection due to a high degree of impurities resulting in a poor signal to noise ratio
- low elution from FPP and GGPP from the SPE due to matrix interactions

5.2.2.2.3. Improvements of the HLB application

Limitations to the HLB protocol developed thus far, in terms of purity of the eluate, required modifications of the protocol. One main contributor to the failure of the SPE application with cell matrices was thought to be the activity of endogenous phosphatases. Preliminary tests showed that despite handling the samples at 4 °C, distinct analyte loss occurred. Experiments with phosphatase inhibitors clearly showed the beneficial effect of the enzyme suppression in terms of higher recoveries for both isoprenoids. The two commercially available inhibitors and a mixture of imidazole and sodium fluoride, acting on alkaline and acid phosphatase were compared. The markedly higher effect of the Halt® compared to the Phosstop® inhibitor on GGPP and vice versa on FPP degradation, resulted in a combinatorial mixture for further experiments. In summary, the introduction of two different phosphatase inhibitors suppressed phosphatase activity sufficiently.

To overcome the problem of a high degree of impurities from brain matrix samples leading to column clogging and/or possibly reducing isoprenoid recovery, several pre-SPE sample preparation attempts were tested. The most promising approach was the combination of PPT and the HLB protocol, which is a widely used approach for plasma samples.

However, none of the approaches including the PPT overcame the aforementioned problems and the detection of FPP and GGPP remained strongly impeded or completely hindered.

As shown in section 4.1.4.2. the amplification of LLE with a matrix assisted LLE led to partly detectable peaks and was therefore tested in combination with the SPE protocol developed as a possible approach for the FPP and GGPP isolation from matrix samples. The earlier mentioned problematic background in the chromatograms was the result of a high degree of impurities which were not retained on the Extrelut® columns. In the following set of experiments this problem was overcome by the combination of the Extrelut® extraction and the HLB protocol to result in a two dimensional sample clean-up procedure (section 4.1.8.). Based on previous findings during the development of the SPE protocol, NH_4OH containing mixtures were compared to pure n-hexane for the elution from the Extrelut® column. As previously shown the alkalization of the eluent was necessary for the extraction of the isoprenoids. Overall, the best

results were obtained by elution with a water saturated 1-butanol mixture, similar to a solvent used by Bruenger et al.[92] Following the Extrelut® elution a centrifugation step was implemented in order to remove dissolved proteins and to prevent column clogging of the SPE cartridges.

5.2.3. Precision and internal standard

One of the key factors in quantitative analytics is the precision of a measurement.[317] Precision, also often referred to as reproducibility describes the closeness of individual data points of repeated measurements, from a single homogenous sample, under identical conditions. Variations during analytical runs mainly originate from varying injection volumes of the HPLC autosampler, differences in detector sensitivity or from sample loss during analyte clean-up steps. To compensate for these errors, calibration standards are used to validate the results. The most commonly used methods are the standard addition method and the external or internal calibration, while the latter is the gold standard and often preferentially used because of its higher precision.[336] The ideal IS, when using fluorescence detection is chemically inert, elutes closely to the analyte but not at the same *Rt* and its chemical structure largely, if not completely (e.g. stereoisomers) resembles the analyte. The *Rt* and structure might even be the same when a mass based detector is used. In such cases the heavy isotope labeled forms of the analyte are optimal internal standards.[337] In respect to the method developed within the current body of work, the internal calibration technique was chosen due to the extensive sample clean-up and the associated possible sample loss.

The implementation of an internal standard was a significant improvement over previously described methods detecting FPP and GGPP without an IS.[92,94,95] Concerning the structural similarities between the IS and the analyte the following section illustrates the challenges associated with the application described in the current work.

The assay for the simultaneous determination of FPP and GGPP contained two structurally slightly different analytes. Moreover, due to the intermediate enzymatic reaction the analytes are structurally very different for the sample preparation steps and for the HPLC-FLD detection (Figure 5). Furthermore, stability of the IS was an issue due to the long drying steps (approx. 5 h after the Extrelut® and 2 hours after the HLB step) in the SpeedVac during sample preparation (Figure 3). An ideal non-radioactive IS for this application would be a compound undergoing the

same enzymatic conversion to one of the dansyl-labeled pentapeptides. However, limited commercial availability and a time consuming synthesis severely limited the possibility for applying such an IS. Furthermore, subsequent studies would have been necessary to determine the influence of an additional compound during the enzymatic reaction. The implementation of ^{14}C-radioactive labeled FPP and GGPP would have been a possible route; however technical limitations prevented the use of its implementation e.g. radioactive laboratory facilities for HPLC-FLD. Furthermore, the development of a non-radioactive method would provide a simplified technique and would target a wider audience.

Hence, to satisfy the aforementioned requirements, 1, 2-dioleoyl-sn-glycero-3-phosphoethanol-amine was chosen as an IS which offered a lipophilic carbohydrate chain attached to a dansyl head-group and was commercially available. It showed a *Rt* (7.1 min) between FPP* and GGPP*, however, it was deemed inadequate due to its chemical instability under the experimental conditions employed.

Further investigations led to DNP as an appropriate IS and synthesis conducted as described by Naassner et al.[316]as the compound was commercially not available. Preparative clean-up via HPLC provided a clean IS, characterized by means of a 300 MHz H-NMR spectrum and HPLC-FLD measurements of DNP solutions e.g. good peak to noise ratio and absence of interfering peaks. The *Rt* of the IS was 1.1 min after the elution of GGPP*.
Overall, DNP as an IS has some shortcomings concerning its structure, as compared to the analytes (Figure 19) but was nevertheless shown to be a suitable candidate as shown by the implementation in the method validation, described in the following paragraphs.

5.3. Method validation

The method development as described in the proceeding paragraphs was consequently fully validated, including within-run and between-run accuracy and precision proving the reproducibility of the assay and the accuracy of the results. Concentrations were back-calculated using an eight-point calibration curve. The terminology “validation” is very variable, ranging from a simple proof of linearity to full validations described by the Food and Drug Administration (FDA) or the International Conference on Harmonisation of Technical

Requirements for Registration of Pharmaceuticals for Human Use (ICH). The complexity of the FDA guideline will be discussed in the following paragraphs.

After the successful method development for the extraction and detection of FPP and GGPP from cellular brain matrices, subsequent experiments were conducted to prove the validity of the method and appropriateness for quantitative analysis of human brain samples.

The initial step was the FPP* and GGPP* analyte confirmation by high accuracy FT-ICR MS measurements. FPP* and GGPP* peak fractions were collected from spiked tissue samples after HPLC separation and analyzed subsequently with high mass accuracy on the FT-ICR MS. The measured accurate masses for FPP* and GGPP* corresponded well with the calculated exact masses (<5ppm), thus confirming the identity of the labeled isoprenoids.

The following method validation procedures met all criteria outlined by the FDA for full method validation of bioanalytical methods.[317] These criteria included selectivity, linearity, stability, accuracy, precision, recovery and repeated measurements at the lower limit of quantification (LLOQ). The technique developed in the current work also employed a weighting factor for the calibration curves to improve accuracy. The following sections briefly depict each single aforementioned criterion and its importance in the development of the method.

5.3.1. Selectivity

The major challenge for establishing the selectivity of this method was the presence of endogenous FPP and GGPP levels in all brain samples. Additional to the analyte confirmation, it was necessary to clearly demonstrate that the observed peaks for FPP* and GGPP* only originated from the two isoprenoids FPP and GGPP. Therefore, it was required to obtain an isoprenoid free matrix, which was achieved by storage of the homogenized tissue batch at RT; endogenous phosphatases degraded endogenous pyrophosphate pools. The resulting zero and blank samples showed no interfering peaks at the respective retention times and thus demonstrated the selectivity of the method.

5.3.2. Linearity

The calibration range for each isoprenoid was chosen according to test runs of brain samples prior the validation. From these trials it became apparent that GGPP abundance was higher in human brain samples and consequently the calibration range was shifted to higher concentrations. Furthermore, the LOD and LLOQ for GGPP were higher for GGPP than for FPP.

A common method to obtain a good curve fit in bioanalytics is the use of a weighting factor, which proved to be beneficial for both analytes. Consequently, all correlation coefficients (r^2) were greater than 0.99 for both analytes and the relative deviation values (calculated vs. nominal) were lower than 15%, thus fully meeting the FDA requirements.[317]

5.3.3. LLOQ

Within the calibration range the LLOQ is given special interest. Peak area and the peak-to-noise ratio become very small leading to possibly greater variability between the measured and true values. Separate measurements of six individual spiked brain samples at the LLOQ revealed accuracy and precision values below 10%, well within the FDA allowance of 20% variation.[317]

5.3.4. Accuracy and Precision

Intra- and inter-day accuracy and precision describes the closeness of single measurements from their true value and the variation from each other within different measurements on one day and within consecutive days. The FDA accepts 15% variation[317] and with the fulfillment of these requirements, isoprenoid values obtained with the developed method were shown to be reproducible. The samples which were chosen for these tests were in the lower, middle and upper calibration range, but with distinct nominal concentrations from the standard samples. Moreover, these QC samples were taken from different brain homogenates than the calibration samples to exclude any matrix dependency.

5.3.5. Recovery

During the developmental stage of the method a wide range of extraction methods and materials were tested. Challenges were encountered in sufficiently extracting and determining FPP and GGPP from brain samples. As discussed earlier, the physiochemical properties of the isoprenoids impede a simple sample preparation and as a downside of the double clean-up step, employing

matrix assisted LLE and SPE, analyte loss was somewhat problematic. The recoveries were determined in two different ways. Firstly, by utilizing the developed method to analyze samples which were spiked before and after the clean-up steps. Secondly, the experiments were repeated with radioactive labeled FPP and GGPP, without the intermediate enzymatic reaction, to exclude any interference from the enzymatic conversion of the isoprenoids on overall recovery. These data substantiated the primary findings. Overall the determinations of the recoveries in the low, medium and upper concentration range were reproducible.

5.3.6. Stability

Tests for the stability of an analyte can cover a whole spectrum of different conditions. Depending on the nature of the sample, the preparation, handling and the applied analytical procedures, these experiments should be designed to investigate all possible influencers for the analyte at hand. For the current application storage conditions were of highest importance, including long-time storage and freeze-thaw cycles, stability at RT and in the autosampler. The results revealed an excellent stability of the analytes under the applied conditions with the exception of long time (> 10 h) storage in the autosampler, in the dark at 4 °C. Consequently, all experiments were planned and executed so that all samples could be measured within a 10 h time span.

5.3.7. Partial method validation for mouse brain samples

Earlier studies by our group revealed detectable lovastatin and simvastatin and to a lower extent pravastatin levels in the brains of chronically treated mice. These studies, as well as further studies with simvastatin in guinea pigs showed a cerebral influence of statins on the expression of various genes.[255,338] The developed method presented herein, enables the expansion of previously published *in vitro* statin studies[202,274] and to test the influence of mevalonate/isoprenoid/cholesterol pathway inhibitors on APP processing *in vivo*.

For the interpretation of the pharmacological modulation of isoprenoid levels and its impact on Aβ production, the measurement of cerebral FPP and GGPP levels is essential.

It appears less reliable to measure statin effects on brain cholesterol levels for two reasons: (1) enzymes of the isoprenoid and prenylation pathway have a higher affinity to FPP than the squalene synthase leading to cholesterol;[123] consequently FPP and GGPP concentrations might be

far more susceptible to fluctuations in upstream mevalonate abundance and (2) FPP and GGPP are intermediates, consequently having a higher turnover in the cell than the end-product cholesterol[123] and thus acting as a more sensitive indicator for the activity of the MVA-pathway. Thus, FPP and GGPP measurements will add further information to cholesterol determinations.

Following this notion it was of interest for the current work if cerebral isoprenoid levels were influenced by chronic simvastatin treatment in mice. Moreover, further investigations were conducted to measure age-dependant changes of cholesterol and isoprenoid regulation in the CNS. Due to sample availability such studies are far more feasible to be measured in rodents than in humans. Due to these reasons the isolation of FPP and GGPP and with subsequent quantification was further extended to measure isoprenoid levels in mouse brains. As explained in the results section (section 4.2.1.8.) pig brain homogenate was used for the calibration standards in studies with mouse brain samples. Therefore, the calibration curves in human brain matrix were compared to the identical nominal concentrations in pig and mouse brain matrices. An overlay of the three calibration curves showed alignment with the calculated results within the accepted variations and the r^2 values for the linear regression of the mean values were greater than 0.99. Consequently the method was also applied for mouse brain samples.

5.3.8. Method transfer to an UHPLC-MS/MS system

Prior the method transfer the assay was fully validated according to the latest FDA guideline.[317] This validation showed the robustness of the sample preparation which was unchanged for the method transfer. Moreover, the previously described pre-column derivatization technique for FPP and GGPP via enzymatic coupling to their respective dansyl-labeled pentapeptides was kept for the UHPLC-MS/MS assay for the following reasons. Firstly, the enzymatic removal of the pyrophosphate group greatly increases hydrophobicity and thus chromatographic retention of the isoprenoids on reversed-phase HPLC columns. Secondly, the increased proton affinity from the label strongly enhances the ionization efficiency for FPP* and GGPP*. And finally, the fluorescent activity of the label allows the complementary analysis of the same FPP and GGPP containing samples by HPLC-FLD.

The assay was shown to be linear from 5 to 250 ng/ml and the LLOQ (5 ng/ml for both analytes) were determined accordingly. Furthermore, and important for LC-MS analysis, infusion chromatograms clearly showed no interference of co-eluting compounds with signal intensities of both analytes at their respective retention times.

Finally, a direct comparison of results obtained by the two methods, HPLC-FLC and UHPLC-MS/MS, revealed a good correlation of the data, although a slight positive bias for the UHPLC-MS/MS method can be observed close to the quantification limit. Transferring the data to a Bland-Altman-plot also revealed this bias for both analytes (data not shown) but values were still considered acceptable as all values were within 1.96 times of the standard deviation of the differences calculated for each value obtained from both assays.

5.4. Method comparisons

The rational for the development of a new isolation technique for FPP and GGPP was the fact that previous studies by Tong and colleagues focused on the detection of the two isoprenoids in *in vitro* models.[94] Prior the onset of the current work there was no method available for the simultaneous determination of FPP and GGPP in tissue. The current work builds upon the analytical method developed by Tong and colleagues.[94] It demonstrates an optimized analytical protocol in combination with a newly developed isolation technique for these isoprenoids from human and rodent brain tissue. The incorporation of an internal standard allowed for the first time a state of the art method validation according to the most recent guideline for bioanalytical method validation. The publication of an article by Tong and colleagues describing the detection of endogenous isoprenoid level in mouse brain[95], parallel to the herein described work was lacking the incorporation of an internal standard and the description of a data validation. The main differences between the mentioned methods are described in Table 30.

Furthermore, the current work depicts the method transfer to a much faster, more sensitive and selective UHPLC-MS/MS method. The development of this analytical method was mainly conducted to provide a platform for a high-throughput screening of bigger sample sets combined with the benefit of using smaller tissue fractions in the future.

Method	**HPLC-FLD**	**UHPLC-MS/MS**	**HPLC-FLD**	**HPLC-FLD**
(publication)	(Hooff et al. 2008)[265]	(Hooff et al. 2010)[339]	(Tong et al. 2005)[94]	(Tong et al. 2008)[95]
Run time [min]	20	3	22	22
Flow rate [µL/min]	400	600	1000	1000
Rt [min]				
FPP	4.7	1.08	8.4	8.4
GGPP	11.9	1.56	16.9	16.9
IS	DNP	-	-	-
Validated assay	full	partial	-	-
Detection in				
cells	-	-	X	X
tissue [mg]	X	X	-	X

Tab. 30. Overview over the newly developed and published methods for the simultaneous quantification of endogenous FPP and GGPP levels using liquid chromatography. Rt = retention time, IS = internal standard, - = not applicable, X = detection was shown in publication.

5.5. Analysis of human brain samples

5.5.1. Sample pre-examinations

(A) An initial examination was conducted to evaluate grey and white matter isoprenoid distributions under physiological conditions in aged human brain samples. In analogy to higher cholesterol levels in white matter compared to grey matter[20] isoprenoid levels were suspected to show a similar distribution pattern.

After the careful validation of the method, human grey and white frontal cortex samples from five different donors were subjected to the developed method.

The results were the first reported determinations of isoprenoids in human brains. They revealed that GGPP abundance was significantly higher in the white matter compared to grey matter samples (Table 31).

	mean white matter conc. ± SD [ng/mg protein]	mean grey matter conc. ± SD [ng/mg protein]	p-value (paired t-test)
GGPP	14.34 +/- 8.4	9.66 +/- 7.73	0.0007
FPP	2.84 +/- 1.03	3.02 +/- 1.32	0.62

Tab. 301. Concentrations of FPP and GGPP in human brain grey and white matter. The table depicts the mean values, SD and the statistically significant higher concentration of GGPP in the white matter compared to grey matter abundance (n=5).

A possible explanation for these findings might be the higher cholesterol abundance in the white matter leading in a negative feedback mechanism to reduced mevalonate turnover into the cholesterol pathway, while simultaneously maintaining biosynthesis of vital non-sterol isoprenoids.[13] FPP concentrations are generally lower and show a less distinct distribution.[95] A plausible explanation for this observation is that FPP is the branch point of the mevalonate/cholesterol/isoprenoid pathway providing the substrate for two separate pathways including four different enzymes, which diminishes the FPP precursor pool, as explained in the introduction (Figure 1).[3]

(B) It was further investigated if the PMI would influence isoprenoid concentrations, due to a possible degradation in post-mortem tissue. As shown by Olaisen, brain temperature remains almost constant for approximately two hours after death before it starts dropping exponentially.[340] The maintenance of temperature and even a slow decline still enables physiological processes, including enzyme activity to occur in tissue, even after blood flow and therefore the supply of most importantly oxygen has stopped. In tissues biochemical processes are immediately disturbed after blood flow interruption. Therefore, the PMI possibly changes cell physiological conditions. Although measured brain temperatures were not available for the samples investigated, one can assume a significant difference in average temperature, during the time of brain removal between the short (Ø = 3.38 h) and long (Ø = 11.75 h) PMI groups. In summary, PMIs and sample treatment and their associated possible alterations are a general issue and should be addressed as part of an investigation.[341,342]

Consequently, for the investigations described in the current work, samples were assigned to two groups with short and long PMI; donors from both groups were of similar average age. However,

the current data clearly demonstrated that the longer interval between the death of the patient and the removal of the brain had no influence on the isoprenoid levels.

(C) As the final pre-examination, selected samples were subjected to western blot analysis to confirm the quality of the visual (Figure 4) separation of grey and white matter within a sample. Recently, it has been reported that changes in grey matter of human AD brains is associated with hypo-metabolism, especially regarding neuropsychiatric symptoms and behaviour.[343,344] In order to determine the abundance of the isoprenoids in the grey matter, a clear separation of grey and white matter in the brain samples was essential. Hence, anti-NeuN antibody that specifically indicates grey matter was used in Western blot analysis. NeuN was previously shown to be a useful histological marker for neuronal structures, areas with high densities of neuron cell bodies associated with the grey matter.[345]

5.5.2. Investigation of AD brain samples

The proceeding investigations demonstrated the independence of isoprenoid levels from PMI time. Moreover, the preparation technique for white and grey matter from human frontal cortex samples was proven to be reliable. Important to the following AD brain study was the detection of differences in isoprenoid concentrations in the two areas of the frontal cortex samples, consequently leading to the investigation of both, white and grey matter samples of AD patients and the comparison to controls.

As mentioned in the introduction, the mevalonate/isoprenoid/cholesterol pathway has generated much attention with regards to AD.[3,261] Of particular interest has been the proposed involvement of the two isoprenoids FPP and GGPP via their function in prenylating small GTPases. One of the protective effects of statins in brain has been attributed to a reduction in FPP and GGPP levels.[3,13] In spite of the keen interest in isoprenoids and AD, evidence supporting involvement of isoprenoids has only been indirect due to a lack of a quantitative analytical method for determining FPP and GGPP levels. These assumptions were based either on elevated levels of prenylated small GTPases in AD[124,261,278] or on well characterized models in which statins were able to reduce the Aβ load and ROS production via an isoprenoid dependant way.[346]

The current work provides for the first time data indicating that homeostasis of FPP and GGPP but not cholesterol is specifically altered in brain tissue of male AD patients (mean Braak stage 5.1). The conclusion is based on the following: both FPP and GGPP levels were significantly

higher in brain tissue of male AD patients as compared with male control samples of similar age. Brain cholesterol levels on the other hand did not differ between the two groups. Furthermore, HMG-CoA reductase gene (HMGR) expression was similar between the AD and control group and the determination of HMG-CoA reductase activity even revealed a slight reduction in the AD brain samples as compared to controls. The results are in line with a report by Omkumar et al. 1992 describing a negative feed-back mechanism on HMG-CoA reductase activity by increased concentrations of ubiqinone outsite the CNS.[347] This hypothetical mechanism is supported by reports on elevated ubiquinone levels in AD affected brains.[206] Furthermore, results from the investigated AD brains showed significantly elevated gene expression of FPPS, substantiating the findings of elevated isoprenoid levels. The up-regulation of FPPS is a key finding as it is a precursor of both isoprenoids (GGPP, dolichol, ubiquinone), and of cholesterol (Figure 1).[13]

Regulation of FPP and GGPP is not as well understood as cholesterol regulation and this especially applies to the brain. Low cellular cholesterol levels are sensed by SCAP, which in turn triggers a cascade of events ultimately leading to the up-regulation of the HMG-CoA reductase and increased mevalonate production.[348] Mevalonate is the upstream precursor of several products including FPP. Synthesis of FPP involves the enzyme FPPS and condensation reactions of IPP and GPP. As shown in the present study, both FPP levels and FPPS gene expression were elevated in male AD brains. What has not been clearly established is if changes in FPP levels are detected by SCAP leading to activation of the SREBP-2. In an *in vitro* model, employing Caco-2 cells treated with lovastatin (mevalonate depleted), the addition of exogenous FPP did not alter mature SREBP-2 abundance; whereas replenishing mevalonate counteracted the effects of lovastatin on mature SREBP-2.[118] Based on elevated FPP levels and FPPS gene expression in contrast to unchanged cholesterol levels and HMG-CoA reductase gene expression, a tentative conclusion is that the increase in FPP levels in AD brain may not involve the SCAP/SREBP-2 pathway.

GGPP levels but not cholesterol levels were significantly higher in AD brain. FPP serves as a precursor of both GGPP and cholesterol. One interpretation of the data is a possible shunting of FPP to GGPP and away from cholesterol. This hypothesis is supported by earlier findings of elevated GGPP-derived ubiquinone levels in AD brains.[206] The same study revealed decreased FPP-derived dolichol levels substantiating the FPP shunt into the GGPP pathway and into protein prenylation, supported by findings of elevated Ras gene expression[349] proteins which depend on farnesylation.[350]

Furthermore, the current work showed an elevated GGPP synthase gene expression in AD affected brains compared to healthy control brains, however it did not reach significance. It is possible in the case of GGPP that enzymatic activity of GGPPS may be a critical regulatory contributor to its synthesis. The underlying mechanisms for increased GGPP as well as FPP levels in AD brain tissue are unknown. A speculative explanation may involve proteins that are prenylated by the two isoprenoids. It was reported that both FPP and GGPP levels were increased when reticulocyte cytosol was incubated with recombinant protein substrates for FPP and GGPP prenylation, respectively.[116]

Figure 45 summarizes findings from the current work in context with previously published data regarding AD pathology and the regulation of intermediates and products of the mevalonate/isoprenoid/cholesterol pathway.

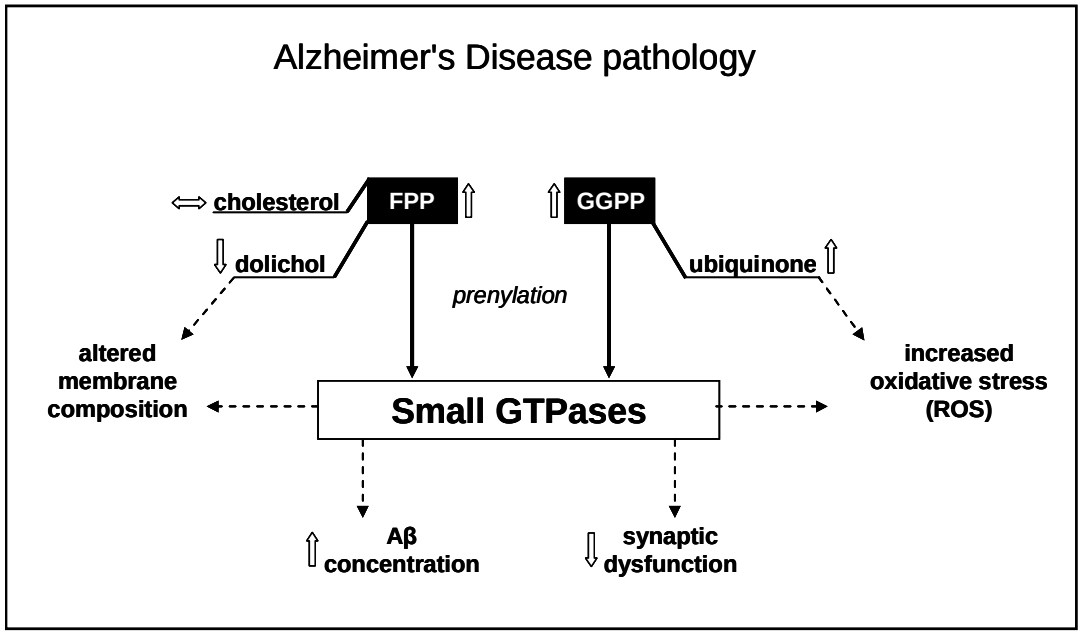

Fig. 45. Isoprenoids, small GTPases and Alzheimer's Disease. Levels of the isoprenoids ubiquinone, dolichol, dolichyl-phosphate (dolichyl-P) farnesyl- (FPP) and geranylgeranylpyrophosphate (GGPP) were reported to be modified in AD brain. It is known for many years that the long-chain isoprenoid dolichol is decreased in post-mortem AD brain tissue, while dolichyl-P and ubiquinone are elevated. Data from the current work showed that FPP and GGPP levels were significantly higher in brain tissue of AD patients, while cholesterol levels were unchanged. These data indicate distinct alterations of isoprenoid metabolism within the mevalonate/isoprenoid/cholesterol pathway. FPP and GGPP play a fundamental role in prenylation of small GTPases, which function as molecular switches in various signalling pathways. In AD pathology, small GTPases have been connected with oxidative stress, the generation of Aβ and synaptic dysfunction (for further details, refer to the text).

In summary, the results of this study show that FPP and GGPP levels in grey and white matter were elevated in male AD frontal cortex brain tissue with an average Braak stage core of 5.1. While further work is needed to unequivocally demonstrate that FPP and GGPP regulation is

altered in AD, including studies examining brain tissue of other neurodegenerative diseases and other brain areas, the present findings support results of an increased abundance of certain prenylated small GTPases, as it has been shown for Rab8 and Rab6 in AD brain.[3,261,284] However, other small GTPases including Rab3 were shown to be down-regulated[283], leading to the speculation that post-translational unmodified small GTPases are involved in triggering mevalonate turnover, to yield higher isoprenoid levels. Following this notion, the underlying mechanisms governing protein prenylation remain to be elucidated and the specific role of certain Ras family members in AD pathology need to be unravelled.

Such investigations together with the findings described in the current work may have utility in the development of new drugs similar to bisphosphonates which inhibit FPPS but can bypass the blood brain-barrier.

5.6. Analysis of *in vivo* brain samples

5.6.1. Pharmacological intervention of the brain MVA-pathway

Although it has been previously hypothesized that statin treatment would lead to a reduction in brain FPP and GGPP levels[262], no published data was available. For a better understanding of the regulation of the mevalonate/isoprenoid/cholesterol pathway in the CNS an *in vivo* mouse study was conducted. C57B1/6 mice were chronically treated with simvastatin and the results of this study represent the first report on endogenous FPP and GGPP levels in mouse brains after statin treatment.

Similar to the earlier described findings in human white and grey matter of control and AD brain samples, GGPP levels were higher than FPP levels in the investigated mouse brain samples. Those results are consistent with a simultaneous published report on FPP and GGPP levels in mouse brain.[95] Table 3 b shows a comparison between the findings described in literature and the data described in the current work. Both studies are similar in respect to the relative abundance of both isoprenoids. Interestingly, the report described by Tong and colleagues also depicted absolute concentrations in kidney, liver and heart[95] showing substantially different abundance of FPP and GGPP (Table 3 b). An explanation for such differences is not well understood and future studies are needed.

Concerning the findings of higher GGPP than FPP levels in the identical samples there is some evidence that more proteins are prenylated by GGPP than by FPP.[351] Other authors conclude a more or less even distribution of farnesyl- and geranylgeranylated proteins.[123] As discussed earlier, a straight forward explanation accounts solely for the utilization of FPP. The FPP pool serves as a supply for the synthesis of cholesterol, GGPP and longer chain isoprenoids and for protein prenylation, while GGPP is used for only two of such processes, namely protein prenylation and longer chain isoprenoid synthesis, reducing its turnover rate as compared to FPP.
As for the simvastatin effect, it has been previously proposed[3] that HMG-CoA reductase inhibition would reduce brain FPP and GGPP levels but such data had not been reported due to analytical difficulties of isolation and detection sensitivity of FPP and GGPP. The effects of statin induced HMG-CoA reductase inhibition was effectively illustrated by data on brain FPP and GGPP levels, compared to those of the placebo group. The results revealed that simvastatin had a greater effect on reducing FPP levels followed by reductions in GGPP and cholesterol levels. These data fulfilled the rational expectation that brain simvastatin levels[255] decrease intermediates of the MVA-pathway. The data sets collected during this study showed a good correlation especially when blotting the measured FPP against GGPP levels, as FPP is the immediate precursor. The correlation of FPP and its downstream product cholesterol is less significant, albeit visible. These results nicely demonstrate the downstream effect of the inhibition of the HMG-CoA reductase as the rate limiting step of the mevalonate/isoprenoid/cholesterol pathway

It would appear that HMG-CoA reductase inhibition does not have an equal effect on the downstream products of mevalonate. The consequences of these differential effects on isoprenoids and cholesterol on cellular function are unclear. One possibility is that there is a gradient of cellular effects based on the magnitude of reduction in the individual lipids with FPP associated cell functions more affected.
In relation to the earlier described AD brain findings it is worth mentioning that HMG-CoA reductase inhibition affected both, isoprenoid and cholesterol levels in brain tissue of chronically treated mice. In the contrary, regulation of FPP and GGPP in the diseased AD brain appears to be altered which may not involve HMG-CoA reductase.

Finally, homogenate from simvastatin treated and control mouse brains was subjected to semi-quantitative WB analysis using a PanRas antibody directed against members of farnesylated Ras

proteins (H-, N- and K-Ras) and an antibody detecting a common epitope on geranylgeranylated Rac-family members (Rac1, RhoA and Cdc42). The mean reduction in specific protein abundance was pronounced in the farnesylated proteins (PanRas antibody), possibly correlating to the stronger effect of simvastatin treatment on FPP than GGPP levels. Overall the statin treatment markedly reduced protein abundance of the investigated small GTPases. It is worth mentioning that the antibodies employed did not differentiate between post-translationally modified and unmodified proteins since the epitope regions did not involve the prenylation site. These findings are in line with recent reports showing simvastatin induced reduction of different members of the small GTPases in cell membranes.[12,202] One possible implication concerning the widely discussed beneficial effects of statins in AD might be through reducing the prenylation status of small GTPases like Rab6, which was found to be elevated in AD brains. Rab6 is thought to be involved in APP processing.[261,278] Other GTPases are also thought to have a putative role in AD pathology but remain to be elucidated.[3]

5.6.2. The transgenic Thy-1 APP mouse model

The Thy-1 APP mice represent a transgenic mouse model of the C57Bl/6 mice posessing both the Swedish double and the London mutation. The 751 amino acid form of human APP with both mutations is controlled by the murine Thy-1 promoter, which leads to a high and selective expression in neurons.[323] Furthermore, a Kozack element was introduced into the DNA sequence of the APP to yield higher gene expression. The amino acid sequence of APP contains the Kunitz protease inhibitor region, which has been shown to result in altered APP processing leading to higher Aβ levels in cell culture.[352] As a result, plaque formation is accelerated and the first plaques appear at an age of approximately 6 months.

Due to the presence of these AD hallmarks this FAD model is widely used to mimic AD/SAD findings and to study Aβ lowering attempts. Nevertheless, it should be emphasized at this point that this and other animal models for AD can only reflect a relatively small portion of the characteristics of AD, which go far beyond a simple accumulation of Aβ.[353]

Thy-1 APP mice FPP, GGPP and cholesterol levels were unchanged as compared to their non-transgenic counterparts, although there was a significant reduction of FPP and GGPP in the Thy-1 mice calculated over both variables (two-way ANOVA). These results show that induced APP mutations and associated elevated Aβ levels are not necessarily related to higher isoprenoid levels as seen in human AD brains.

5.6.3. Aging

5.6.3.1. MVA-pathway alterations during aging

Earlier described findings showed elevated isoprenoid levels in the grey and white matter of male AD patients versus healthy age matched controls. Individuals from this study were between 75 and 85 years of age. Age is the major risk factor for developing AD[220,354] and levels of the isoprenoids FPP and GGPP during senescence were completely unknown. However, reports on MVA-derived cholesterol and the longer chain isoprenoids ubiquinone and dolichol are available. It is crucial to elucidate and understand physiological regulation of FPP and GGPP during aging, due to their fundamental role in the MVA-pathway and for cellular processes in general. Recently published reports strongly implicated the small GTPases as signalling players during aging[355], consequently involving the isoprenoids FPP and GGPP in senescence. Another recent report was able to demonstrate a constant and significant increase in HMGR gene expression in the cortex and hippocampus of rats ranging from 6 to 24 month of age.[21] These data are not supported by findings of HMG-CoA reductase protein levels in rats between 3 and 24 month of age of a different strain. But the same study revealed a higher activity of the HMG-CoA reductase by a possible impaired phosphorylation/dephosphorylation mechanism leading to dolichol accumulation in the brain.[83] The authors hypothesized an alteration of the activity of branch point enzymes of the mevalonate/isoprenoid/cholesterol pathway.

Based on these aforementioned speculations, three generations of male C57Bl/6 mice at the age of 3, 12 and 24 months (young, middle-aged and aged) were investigated. The findings clearly revealed an age-dependant elevation of FPP, GGPP and cholesterol brain levels. Interestingly, the endogenous levels between 3 and 12 month old animals of all three investigated analytes were unchanged and only the aged group showed a strong increase, which was significant for the two isoprenoids. These data substantiate the findings of the previously mentioned study of an age-dependant modulation of branch point enzyme activities and/or abundance.[83]

To the author's knowledge, the CNS mevalonate/isoprenoid/cholesterol pathway is widely unaffected by a regulation of sex hormones. Most gender derived discrepancies concerning brain characteristics described in the literature are more or less in the context of a hormonal regulation, recently reviewed by Tobet et al.[356] The current findings of the comparison of the FPP and GGPP levels between male and female mice also seem to be unaffected by the gender. Interpretation of such data should be evaluated carefully with regard to species and gender, as various proteins

were described to be differentially expressed in brain tissue[357] and consequently involved metabolites might also vary.

5.6.3.2. Alterations in the Rho GTPases during aging

As described in detail in the introduction (section 1.6.), members of the Rho family of small GTPases including RhoA, Rac1, and Cdc42 monomeric G-proteins are claimed to be participants in Aβ induced ROS generation[282] and in a down-regulation of transcriptional activity of the APP gene.[283] Furthermore, Rac1 and RhoA are major regulators in the production of actin-based morphological plasticity in dendrites and spines of hippocampal neurons.[6,8,9,10,11,284] Neuronal Cdc42, Rac1 and RhoA appear to play a role in the plasticity of the adult mammalian brain, affecting neuronal architecture, synaptic connectivity and efficacy.[282] It is therefore of valuable interest to study protein expression of these small GTPases in senescence, for a better understanding of the physiology in respect to AD pathology

The aforementioned possible shunt of mevalonate derived products into the isoprenoid/GGPP pathway during aging was demonstrated by strongly elevated FPP and especially GGPP levels, in the aged mouse brain. The isoprenoid GGPP represents the physiological substrate for prenylation of the ´classical´ Rho family members (e.g.: Rac1, RhoA, Cdc42).[166] A straightforward prediction of the findings presented in the current work would point to an elevation of such proteins, as a consequence of the elevated substrate GGPP.

However, studies following this work by our working group revealed significantly reduced levels of Rho proteins (unpublished data). These western blot results support the notion of an impaired synaptic plasticity and LTP during senescence.[211]

Continuative studies of our working group also revealed significantly reduced FTase and GGTase levels (unpublished data) explaining elevated isoprenoid levels as a consequence of an insufficient abundance of small GTPases via a yet unknown mechanism. A different approach could explain these findings by a down-regulation of the transferases as a consequence of an abnormal upregulation of isoprenoid production, consequently also leading to a decreased small GTPases abundance. Either of the explanations has yet to be substantiated by further investigations of expression levels both on gene and protein level.

Data from *in vitro* prenyltransferase activity assays using a fluorescence labeled C-terminal H-Ras motive has been reported.[358] The study was conducted to investigate prenylation of the artificial peptide (resembling the H-Ras C-terminus) after incubation with various inhibitors on

different levels of the MVA-pathway. These experiments showed a clear correlation of decreased isoprenoid levels with a reduction in membrane anchoring, hence prenylation, of the artificial peptide under physiological conditions.[358] As a shortcoming of this method isoprenoid levels were not determined and it should be noted that this high-throughput assay was developed to study an inhibitor screening assay rather than investigating physiological cell processes. Moreover, for an interpretation of the physiological regulation, as for example in aging or under pathological conditions like AD, it is clear that one would need to investigate prenylation of several members of the small GTPases as they are known to be differentially regulated.[3,123] Such studies on a gene, protein and activity level will provide additional information to previously published reports on protein isoprenylation with genetically engineered animals.[359] In respect to AD, a complete understanding of physiological processes concerning the activation of distinct members of the small GTPases, is necessary to address abnormal regulations during the onset and the progression of the disease.

5.7. *In vitro* modulation of the mevalonate/cholesterol/isoprenoid pathway

Despite their aforementioned crucial role in a wide array of fundamental cell processes, our knowledge on the cellular regulation of the two isoprenoids FPP and GGPP is limited. This was mainly due to analytical difficulties concerning a robust isolation technique and a sensitive detection method. Recent analytical progress together with the method developed in the current work has allowed investigations into a better understanding of isoprenoid regulation via *in vitro* and *in vivo* models.[94,95]

Tong and colleagues described the first method for the simultaneous determination of FPP and GGPP in cultured cells.[94] To the present day, FPP and GGPP were determined by the same group in a few different cell lines, including mouse embryonic fibroblasts and human cancer cells such as immortalized colorectal adenocarcinoma, myelogenous leukemia and multiple myeloma cells.[94,95,118,263] For a summary of the various cell concentrations see Table 3 a. The current work describes for the first time FPP and GGPP levels in cultured neuronal cells (Table 28). Cellular levels of FPP and GGPP are generally in the picomolar range as depicted in Table 3, however significant differences in isoprenoid abundance can be observed between different cell lines. Moreover, the relative distribution between FPP and GGPP varies between different cell lines. As depicted in the results section, GGPP levels are 22% lower, as compared to FPP in SY5Y-APP695 cells. Lower levels of GGPP have also been reported for U266 cells (- 59%).[263]

However, in other cell lines levels of GGPP are equal or higher as compared to FPP (Table 3 a).[94,95,118] Such variances were also observed in mammalian tissue. Compared to FPP, GGPP levels are lower in mouse kidney and liver tissue, equal in mouse heart tissue and higher in mouse and human brain tissue (Table 3 b).[95] It can be speculated that depending on the demand for intermediates of the MVA-pathway, specialized cells may differentially regulate the production of FPP and GGPP.

The results from the chronically treated mice showed a reduction for FPP and GGPP of 52% and 32%, respectively (section 4.5.1.). In comparison, a 24 h incubation with 5 µM lovastatin lowered FPP and GGPP by 63% and 94% in SY5Y-APP695 cells, respectively. Our data are in line with recent findings, which demonstrated a statin induced reduction in FPP- and GGPP-levels by 69% and 77% in NIH3T3 cells, respectively.[94] Moreover, lovastatin treatment of human multiple myeloma cells and Caco-2 cells also significantly reduced both, FPP and GGPP levels.[98,118]

To investigate *in vitro* MVA-pathway inhibition on a more distinct level, further experiments with neuronal SY5Y cells were conducted with inhibitors targeting different levels of the mevalonate/isoprenoid/cholesterol pathway (Figure 41). Previous experiments within our working group showed a cholesterol reduction following U 18666A and lovastatin treatment.[238] Moreover, FTi 277 and GGTi 286 treatment led to specific reduction of FTase and GGTase activity. Lovastatin, as an upstream inhibitor markedly reduced both isoprenoid levels. Furthermore, inhibition of both the oxidosqualen cyclase down-stream of squalene synthase and the desmosterol reductase by U 18666A (section 4.6.2.), led to a 56% elevation of FPP. GGPP on the other hand was unchanged compared to control cells. These data substantiate recent reports showing that inhibition of squalene synthase using zaragozig acid, significantly elevated FPP and reduced GGPP levels in NIH3T3 mouse embryonic fibroblast cells.[94]

It has been shown that inhibition of FPPS using zolendronic acid modulates FPP and GGPP levels in human multiple myeloma cells.[98] Until now there has been a lack of evidence proving the effects of FTase or GGTase inhibition on cellular FPP and GGPP levels. Herein however, it was demonstrated that inhibition of FTase significantly decreased FPP levels, while inhibition of GGTase I had no effect in this experimental setup.

It is well established that the reduction of cellular cholesterol levels using inhibitors of the MVA-pathway or extraction by methyl beta cyclodextrin (MβCD) results in lower Aβ levels *in vivo* and *in vitro* AD models.[271,272,362] However, evidence exists that FPP and GGPP are also involved in

the cellular production of Aβ. It has been previously reported that γ-secretase is stimulated by GGPP[203] and both FPP and GGPP were found to increase Aβ levels in H4 neuroglioma cells, expressing the Alzheimer relevant amyloid precursor protein APP695NL.[201] The data presented in the current work demonstrate that modulation of the mevalonate/isoprenoid/cholesterol pathway results in changes of cholesterol as well of isoprenoid levels in human neuronal cells. Previous investigations, under identical conditions, showed that Aβ levels were specifically reduced when cholesterol levels were lowered by inhibitors of the HMG-CoA reductase, while selective inhibition of either farnesylation or geranylgeranylation did not affect Aβ production (section 4.6.2.). A summary of the data from both studies indicates that changes in endogenous cholesterol levels rather than isoprenoid levels, account for the observed modifications in Aβ production. Accordingly, it is well established that APP processing is influenced by cholesterol abundance.[267,268,269,270] During the interpretation of the current results one must consider that excess of FPP or GGPP has not been investigated in the present study. Moreover, in the aforementioned studies APP processing in cells was modified after incubation of cells with micro-molar FPP and GGPP concentrations. The present findings demonstrated endogenous FPP and GGPP levels in the picomolar range, which may not significantly interfere with Aβ production.[201,203]

If isoprenoids do not affect Aβ metabolism, the question remains how elevated levels of FPP and GGPP could contribute to AD progression. In addition to the earlier discussed functions of members of the Rho family of small GTPases, for example RhoA, Rac1, and Cdc42 are also the major regulators in synaptic plasticity, both in dendrite morphogenesis and stability, as well as in growth cone motility.[6,8,9,10,11] Synaptic degeneration is a striking characteristic of AD and there is evidence that certain small GTPases are associated with AD.[261,283,284,301] Phosphorylated Rac/Cdc42 protein levels were increased in hippocampal membrane fractions and abnormal distributed in hippocampal slices isolated from AD brain .[301] Rab-6, which is involved in the cellular regulation of vesicular transport, is increased in AD brain.[124,186,261] These proteins cannot function properly unless prenylated by FPP or GGPP and we propose that FPP and GGPP are up-regulated in AD.

6. SUMMARY

Over the last years there has been an increasing interest in the involvement of the MVA-pathway and of members of the small GTPases, in the development and progression of AD. Earlier investigations mainly focused on the role of cholesterol in disease pathology. This research was supported by retrospective cohort studies, initially showing beneficial effects of the long-term intake of cholesterol lowering statins, on the incidence of the development of sporadic AD. Subsequent prospective studies were not able to substantiate these findings resulting in a fading interest in the cholesterol - AD connection. However, in more recent literature increasing attention has been paid to the isoprenoids, FPP and GGPP, due to their crucial role in the post-translational modifications of members of the superfamily of small GTPases. In AD, these proteins were amongst others shown to be involved in mechanisms affecting APP processing, ROS generation and synaptic plasticity. A major factor impeding the clarification of the role of the MVA-pathway intermediates in these mechanisms was the lack of a sensitive and accurate method to determine FPP and GGPP levels in brain tissue.

Hence, a state of the art HPLC-FLD method for the quantification of the isoprenoids FPP and GGPP in brain tissue was successfully developed. After the introduction of a double clean-up step from complex brain matrix samples and the synthesis of an appropriate IS (DNP), the method was fully validated according to the latest FDA guideline for bioanalytical method validation. Criteria included measurements at the LLOQ, linearity, determination of the recovery, accuracy, precision and stability tests. Furthermore, this method was transferred to a faster and more sensitive, state of the art UHPLC-MS/MS application. Additionally, the method was shown to be applicable for mouse brain tissue and data was generated from an *in vivo* mouse simvastatin study and for different mouse models. The method was adapted to allow for the routine in-house analysis of samples from *in vitro* cell experiments.

According to the aims of the thesis (section 1.9.), the current work describes for the first time absolute isoprenoid concentrations in human frontal cortex white and grey matter. Furthermore, this is the first report of isoprenoid levels in the frontal cortex of human AD brains.

Further results were shown from mouse brains originating from different mouse models, including the Thy-1 APP mouse model mimicking AD pathology in terms of Aβ formation or C57Bl/6 mice at different ages. AD prevalence can be clearly correlated with increasing age.

Therefore, three different generations of mice were investigated. The study demonstrated constant isoprenoid and cholesterol levels in the first half of their life followed by a significant increase of FPP and GGPP in the second half (between 12 and 24 month of age). Cholesterol levels were also elevated in the aged group, but again the effect was less pronounced than shown for the isoprenoids. These results lead to the tentative conclusion that cerebral isoprenoid levels are elevated during aging and that this accumulation is amplified during AD leading to accelerated neuronal dysfunction.

In a different mouse study, using the C57Bl/6 mice, *in vivo* drug intervention with the HMG-CoA reductase inhibitor simvastatin revealed strong inhibition of the rate limiting step of the mevalonate/isoprenoid/cholesterol pathway and resulted in the first report of significantly reduced FPP and GGPP levels in brain tissue of statin treated mice. These results open for the first time the possibility to monitor drug effects on cerebral isoprenoid levels and correlate these data with a modulation of APP processing, which was shown by our group in previous studies. Interestingly, apart from the isoprenoid reduction following statin treatment the reduction of brain cholesterol was also significant but to a lesser extent. These findings support the notion that isoprenoid levels are more susceptible to statin treatment than cholesterol levels. Furthermore, this suggests a strong cellular dependence on FPP and GGPP, as the pool seems to be easily depleted, which finally could lead to cell death. The first investigations of farnesylated Ras and geranylgeranylated Rac protein levels by means of immuno-blotting, substantiated the notion of a decreased abundance of prenylated small GTPases under statin influence as a consequence of reduced isoprenoid levels. These findings demonstrate for the first time a correlation of FPP and GGPP levels with the abundance of small GTPases.

These findings together with the results from the AD study prove that isoprenoid levels are not strictly subject to the same regulation as cholesterol levels (mevalonate/isoprenoid/cholesterol pathway). To further understand the physiological regulation in the cell, *in vitro* experiments with different inhibitors of the mevalonate/isoprenoid/cholesterol pathway were conducted. These results confirmed the isoprenoid and cholesterol reducing effects of statin treatment as observed in the aforementioned *in vivo* mouse study. Interestingly, cholesterol synthesis inhibition targeted after FPP as the branch point, led to significantly elevated FPP levels. FTase inhibition led to

significantly reduced FPP levels, whereas inhibition of the GGTase I did not show a significant change of either isoprenoid levels.

The following serves as a concise summary of the results from the current work:

1. Development, validation and implementation of a HPLC-FLD method for the simultaneous absolute quantification of FPP and GGPP in human and mouse brain tissue.
2. Elevated FPP, GGPP and cholesterol levels in the white matter of the human frontal cortex compared to the gray matter.
3. Elevated FPP and GGPP levels in human AD brains, while cholesterol levels were unchanged.
4. Unchanged FPP, GGPP and cholesterol levels in the Thy-1 APP mouse model.
5. Reduced FPP, GGPP and cholesterol levels after chronic simvastatin treatment in an *in vivo* mouse model.
6. Elevated FPP, GGPP and cholesterol levels only between middle aged and aged mice, not between young and middle aged mice.
7. Reduced FPP, GGPP and cholesterol levels after lovastatin treatment in an *in vitro* SY5Y cell model; elevated FPP levels after inhibition of cholesterol synthesis downstream of FPP; reduction of FPP levels after FTase inhibition.
8. Method transfer to a faster, more sensitive and selective UHPLC-MS/MS method for future studies with a higher sample volume or more detailed analysis of distinct brain regions

In conclusion, data from the human AD brains, *in vitro* and *in vivo* studies and the aging study in mice has allowed for a better understanding and deeper insight into isoprenoid regulation in the brain under physiological conditions, in the diseased stage and after drug administration. The developed analytical techniques and the data can be used to substantiate further investigations on a gene and protein level concerning the isoprenoid synthases, transfersases and distinct members of the small GTPases.

7. ZUSAMMENFASSUNG

Unter Einbezug von Gen-Expressionsdaten und Protein Gehalten ist es für das Grundverständnis von biologischen Prozessen von elementarer Bedeutung spezielle Metabolite in ausgewählten Biosynthesewegen quantitativ zu erfassen. Hierzu ist es eine Analytik unabdingbar die den strengen Auflagen, wie sie in der Arzneistoffforschung und im klinischen Bereich vorzufinden sind, genügt.

Im Zusammenhang mit der Entstehung und dem Fortschreiten der Alzheimer Demenz (AD) spielt speziell der Mevalonat-Biosyntheseweg eine bedeutsame Rolle. Frühere Arbeiten beschäftigten sich hauptsächlich, gestützt durch die Ergebnisse retrospektiver Studien mit Statinen, mit der Rolle des Cholesterins. Diese Studien deuteten darauf hin, dass die Langzeiteinnahme von Statinen das Risiko für das Auftreten der sporadischen AD verringerte. Folgende prospektive Studien konnten positive Effekte der Statine auf den Krankheitsbeginn und -verlauf aber nicht eindeutig klären, was möglicher Weise daran liegt, dass retrospektive Studien einen längeren Beobachtungszeitraum einschließen und möglicherweise frühe Krankheitsphasen erfassen. Statine sind kompetitive Inhibitoren der 3-Hydroxy-3-Methylglutaryl-Coenzym-A-(HMG-CoA-)Reduktase, ausgehend von Acetoacetyl-CoA einem der ersten und der geschwindigkeitsbestimmenden Schritte auf dem Weg der endogenen Synthese von Cholesterin über den Mevalonat-Biosyntheseweg.

Aktuellere Arbeiten richten den Fokus der Forschung stärker auf die ebenfalls aus dem Mevalonat-Biosyntheseweges entstammenden Isoprenoide, Farnesyl- (FPP) und Gernaylgeranylpyrophosphat (GGPP). Statine als Inhibitoren der HMG-CoA Reduktase hemmen die Bildung von Mevalonat und somit sowohl die Cholesterin– als auch die FPP- und GGPP-Synthese. Beide Isoprenoide sind maßgeblich an der post-translationalen Modifikation von Proteinen aus der Familie der kleinen Rho-GTPasen (RhoA, Rac1, Cdc42, etc.) beteiligt. Bezüglich der AD konnte gezeigt werden, dass bestimmte Mitglieder dieser Familie in Mechanismen involviert sind die an der Entstehung von reaktiven Sauerstoffspezies (ROS) und neurotoxischem Amyloid beta beteiligt sind. Weiterhin spielen sie bei der synaptischen Plastizität eine zentrale Rolle. Bisherige Forschungen zur Aufklärung der genauen biochemischen Funktion

von FPP und GGPP sowie deren Regulation, speziell in Hirngewebe, wurden durch das Fehlen einer sensitiven und validen Analytik eingeschränkt.

Die vorgelegte Arbeit beschreibt die Entwicklung, Validierung und erfolgreiche Anwendung einer HPLC-Fluoreszenz Methode zur Quantifizierung der beiden Isoprenoide FPP und GGPP in Hirngewebe. Der Erarbeitung eines komplexen Protokolls zur Methodenaufarbeitung und der Synthese eines geeigneten internen Standards folgte eine komplette Validierung nach den aktuellen FDA Richtlinien für bioanalytische Methodenvalidierung. Anhand der Richtlinien wurden Linearität, Quantifizierungslimit, Wiederfindung, Genauigkeit, Präzision und Stabilität überprüft. Dies stellt ein Novum dar, da derartige Untersuchungen zur Reproduzierbarkeit üblicherweise nur für Xenobiotika durchgeführt werden. Des Weiteren wurde diese Methode auf eine schnellere, sensitivere und selektivere, hoch-moderne UHPLC-MS/MS Methode übertragen und neben der Validierung der Methode für humane Hirnproben wurde auch die Übertragbarkeit auf Mäusehirne gezeigt. Eine weitere analytische Methode wurde zur Untersuchung der Isoprenoid Spiegel von *in vitro* Versuchen adaptiert und für die Routine-Untersuchung im Labor implementiert.

Entsprechend der Zielsetzung dieser Arbeit wurden erstmalig FPP und GGPP Konzentrationen in der weißen und grauen Substanz des menschlichen frontalen Kortex quantifiziert. Weiter konnten unter Verwendung der neu etablierten Methode zum ersten Mal erhöhte FPP und GGPP Spiegel im frontalen Kortex von AD Patienten verglichen mit gleichaltrigen Kontroll-Hirn Proben nachgewiesen werden. Für die Cholesterin Spiegel der identischen Proben konnten gezeigt werden, dass diese unverändert waren, was frühere Arbeiten bestätigt.

Die vorgelegte Arbeit liefert weiterhin neue Ergebnisse zu der Korrelation von cerebralen Isoprenoid- und Cholesterin-Spiegeln in einem *in vivo* Thy-1 APP Maus-Model, welches typischer Weise herangezogen wird um den, der AD zugrunde liegenden Amyloid beta Metabolismus zu untersuchen. Weiter wurden Studien an einem Alterungsmodell mit C57Bl/6 Mäusen durchgeführt, die eine zunächst (zwischen Mäusen im Alter zwischen 3 und 12 Monaten) unveränderte FPP und GGPP Homöostase zeigten, während in der dritten und ältesten Gruppe (24 Monate) ein signifikanter Anstieg zu verzeichnen war. Diese Ergebnisse wurden auch durch die gemessenen Cholesterin Spiegel reflektiert, die ebenfalls nur im Alter erhöht waren. Da das

Auftreten der AD deutlich mit dem Alter korreliert führten diese Ergebnisse, zusammen mit den Daten von den humanen AD Hirnproben zu der Hypothese, dass Isoprenoid Spiegel mit dem Alter im Gehirn ansteigen und dieser Effekt bei der AD möglicherweise potenziert ist. In weiteren *in vivo* Versuchen mit C57Bl/6 Mäusen konnte erstmalig der pharmakologische Effekt von Simvastatin auf die Gehalte von FPP und GGPP im Gehirn gezeigt werden. Die orale Verabreichung des HMG-CoA Reduktase Inhibitors für 21 Tage führte zu stark reduzierten FPP und GGPP Konzentrationen im Gehirn der behandelten Tiere. Cholesterin wurde durch die Behandlung ebenfalls reduziert, wobei dieser Effekt vergleichsweise schwach ausgeprägt war. Dies lässt darauf schließen, dass Isoprenoid-Spiegel sensibler auf eine Hemmung der HMG-CoA Reduktase reagieren als Cholesterin-Spiegel. Diese Ergebnisse lassen sich mit der Literatur in Einklang bringen, dass die Zelle primär von einem gegebenen FPP und GGPP Pool abhängig ist. Hier findet ein erhöhter Umsatz statt, welcher primär der Isoprenylierung von lebenswichtigen Proteinen aus der Familie der kleinen GTPasen dient.

Unter Einbeziehung der Isoprenoid- und Cholesterin Daten aus der AD Studie und der Ergebnisse der Simvastatin Behandlung an Mäusen erlauben diese Daten die Interpretation, dass die jeweiligen Endprodukte (Isoprenoide und Cholesterin) einer unterschiedlichen Regulation innerhalb des Biosyntheseweges unterliegen. Diese Erkenntnis führte zu der neuartigen Bezeichnung des Mevalonat-Biosyntheseweges als Mevalonat/Isoprenoid/Cholesterin-Biosyntheseweg. Um weitere Einblicke in die physiologische Regulation dieses speziellen Biosyntheseweges zu erlangen, wurden einerseits in mehreren Kooperationen eine ganze Reihe von weiteren Metaboliten des Mevalonat-Biosyntheseweges an dem zuvor beschriebenen *in vivo* Alterungsmodels untersucht (Daten noch in Bearbeitung). In der Gesamtheit wurden, wie oben beschrieben bei FPP und GGPP die stärksten Veränderungen im hohen Alter festgestellt, was die bedeutende Rolle der beiden Isoprenoide in diesem Biosyntheseweg unterstreicht. Andererseits wurden im Zellmodel (SY5Y Zellen) unterschiedliche Inhibitoren des Mevalonat/Isoprenoid/Cholesterin-Biosyntheseweges untersucht. Hierbei konnte der Statin-Effekt aus dem *in vivo* Versuch ebenfalls *in vitro* gezeigt werden. Inhibition der Squalensynthase, die den Cholesterin-Biosyntheseweg nach der FPP Synthesestufe hemmt, führte zu signifikant erhöhten FPP Spiegel, was auf eine Akkumulation des Isoprenoids hindeutet. Eine Hemmung des für die Farnesylierung verantwortlichen Enzyms, der FTase, zeigte eine signifikante Erniedrigung

der FPP Spiegel, was gegebenenfalls auf einen shunt in Richtung GGPP und Geranylgeranylierung schliessen lässt.

Die in dieser Arbeit durchgeführten Untersuchungen zeigen die erfolgreiche Anwendung zur Untersuchung des Effekts unterschiedlicher Inhibitoren des Biosyntheseweges, was zukünftig gezielte Studien zum Einfluss von Arzneistoffen auf die cerebralen Isoprenoid Spiegel ermöglicht. Im Zusammenhang mit AD können diese Methoden zu eine Korrelation mit einer modifizierten APP (Amyloid Precursor Protein) Prozessierung herangezogen werden. Der Einfluss auf die Prozessierung war und ist Gegenstand von Untersuchungen in unserer Gruppe, und diese Methoden vermögen zusätzliche Informationen zu diesen speziellen Metaboliten liefern. Ausserdem bilden diese Untersuchungen die Grundlage für weitere Forschungen an den prenylierten Proteinen (kleine GTPasen), in wieweit deren zelluläre Expression, Aktivierung und Funktionalität von diesen beiden Isoprenoiden abhängig ist. Erste immuno-chemische Untersuchungen von farnesylierten Ras und geranylgeranylierten Rac Proteinen mittels semi-quantitativer Western Blot Analysen deuteten darauf hin, dass die Expression dieser Proteine unter Statin Behandlung reduziert ist, was als Konsequenz der verminderten Isoprenoid-Spiegel interpretiert werden kann.

Zusammenfassend und übersichtlich dargestellt zeigen die folgenden Punkte die wichtigsten Ergebnisse der vorgelegten Arbeit:

1. Entwicklung, Validierung und Anwendung einer neuartigen Methode zur zeitgleichen Quantifizierung von FPP und GGPP in Hirngewebe von Menschen und Mäusen.
2. Erhöhte FPP, GGPP und Cholesterin Spiegel in der weißen Substanz des menschlichen frontalen Kortex, verglichen zur grauen Substanz.
3. Erhöhte FPP und GGPP in humanen Hirnproben (frontaler Kortex) von AD Patienten; Cholesterin unverändert.
4. Unveränderte FPP, GGPP und Cholesterin Spiegel im Thy-1 APP Mausmodel
5. Erniedrigte FPP, GGPP und Cholesterin Spiegel nach chronischer Simvastatin Behandlung *in vivo*.
6. Erhöhte FPP, GGPP und Cholesterin Spiegel in alten Mäusen verglichen zu jungen und mittel-alten Mäusen.

7. Erniedrigte FPP, GGPP und Cholesterin Spiegel nach Lovastatin Behandlung *in vitro*; erhöhte FPP Spiegel nach Hemmung der Cholesterin-Synthese folgend auf FPP; erniedrigte FPP Spiegel nach FTase Inhibition.
8. Methoden Transfer auf ein schnelleres, empfindlicheres und selektives UHPLC-MS/MS System für zukünftige Studien mit einer höheren Probenanzahl oder einer detaillierteren Analyse von spezifischen Hirnregionen.

Schlussfolgernd kann man sagen, dass die Daten der AD Hirn-Studie und von de *in vivo* und *in vitro* Versuchen erstmalig einen tieferen Einblick in die cerebrale Regulation des Isoprenoid-Zweiges des Mevalonat/Isoprenoid/Cholesterin-Biosyntheseweg erlauben. Die Ergebnisse der Arbeit beruhen auf einer neu entwickelten und validierten Analytik. Sie zeigen unterschiedliche Regulationsmechanismen unter dem Einfluss des Alterns, der Alzheimer Krankheit und unter pharmakologischer Beeinflussung des Mevalonat-Biosyntheseweges im Vergleich zu physiologischen Bedingungen. Die entwickelten analytischen Methoden und die im Laufe der Arbeit gesammelten Daten können dahingehend verwendet werden, zukünftige Studien bezüglich des Mevalonate-Biosyntheseweges auf Gen und Protein Ebene zu untermauern. Des Weiteren bieten sie die Grundlage für die Studie ausgewählter Proteine aus der Familie der kleinen GTPasen. Diese Proteine und deren Regulation spielen nicht nur bei neurodegenerativen Krankheiten wie der Alzheimer Demenz eine Rolle sondern sind auch speziell in der Krebsforschung seit langem als Arzneistoff-Targets bekannt.

8. APPENDIX

8.1. Figure and Table legends

8.2. References

References

(1) Brown, M. S.; Goldstein, J. L. Multivalent Feedback Regulation of HMG CoA Reductase, a Control Mechanism Coordinating Isoprenoid Synthesis and Cell Growth. *J. Lipid Res.* **1980,** *21,* 505-517.

(2) Hall, A. Rho GTPases and the Control of Cell Behaviour. *Biochem. Soc. Trans.* **2005,** *33,* 891-895.

(3) Cole, S. L.; Vassar, R. Isoprenoids and Alzheimer's Disease: a Complex Relationship. *Neurobiol. Dis.* **2006,** *22,* 209-222.

(4) Gelb, M. H.; Brunsveld, L.; Hrycyna, C. A.; Michaelis, S.; Tamanoi, F.; Van Voorhis, W. C.; Waldmann, H. Therapeutic Intervention Based on Protein Prenylation and Associated Modifications. *Nat. Chem. Biol.* **2006,** *2,* 518-528.

(5) Konstantinopoulos, P. A.; Karamouzis, M. V.; Papavassiliou, A. G. Post-Translational Modifications and Regulation of the RAS Superfamily of GTPases As Anticancer Targets. *Nat. Rev. Drug Discov.* **2007,** *6,* 541-555.

(6) Linseman, D. A.; Loucks, F. A. Diverse Roles of Rho Family GTPases in Neuronal Development, Survival, and Death. *Front Biosci.* **2008,** *13,* 657-676.

(7) Pfeffer, S.; Aivazian, D. Targeting Rab GTPases to Distinct Membrane Compartments. *Nat. Rev. Mol. Cell Biol.* **2004,** *5,* 886-896.

(8) Govek, E. E.; Newey, S. E.; Van Aelst, L. The Role of the Rho GTPases in Neuronal Development. *Genes Dev.* **2005,** *19,* 1-49.

(9) Ramakers, G. J. Rho Proteins, Mental Retardation and the Cellular Basis of Cognition. *Trends Neurosci.* **2002,** *25,* 191-199.

(10) Schubert, V.; Dotti, C. G. Transmitting on Actin: Synaptic Control of Dendritic Architecture. *J. Cell Sci.* **2007,** *120,* 205-212.

(11) Sekino, Y.; Kojima, N.; Shirao, T. Role of Actin Cytoskeleton in Dendritic Spine Morphogenesis. *Neurochem. Int.* **2007,** *51,* 92-104.

(12) Cordle, A.; Koenigsknecht-Talboo, J.; Wilkinson, B.; Limpert, A.; Landreth, G. Mechanisms of Statin-Mediated Inhibition of Small G-Protein Function. *J. Biol. Chem.* **2005,** *280,* 34202-34209.

(13) McTaggart, S. J. Isoprenylated Proteins. *Cell Mol. Life Sci.* **2006,** *63,* 255-267.

(14) Reiss, A. B.; Siller, K. A.; Rahman, M. M.; Chan, E. S.; Ghiso, J.; de Leon, M. J. Cholesterol in Neurologic Disorders of the Elderly: Stroke and Alzheimer's Disease. *Neurobiol. Aging* **2004,** *25,* 977-989.

(15) Kovacs, W. J.; Faust, P. L.; Keller, G. A.; Krisans, S. K. Purification of Brain Peroxisomes and Localization of 3-Hydroxy-3-Methylglutaryl Coenzyme A Reductase. *Eur. J. Biochem.* **2001,** *268,* 4850-4859.

(16) Buhaescu, I.; Izzedine, H. Mevalonate Pathway: a Review of Clinical and Therapeutical Implications. *Clin. Biochem.* **2007,** *40,* 575-584.

(17) Holstein, S. A.; Hohl, R. J. Isoprenoids: Remarkable Diversity of Form and Function. *Lipids* **2004,** *39,* 293-309.

(18) CLAYTON, R. B.; BLOCH, K. The Biological Conversion of Lanosterol to Cholesterol. *J. Biol. Chem.* **1956,** *218,* 319-325.

(19) GOODMAN, D. S.; AVIGAN, J.; STEINBERG, D. Studies of Cholesterol Biosynthesis. V. The Time Course and Pathway of the Later Stages of Cholesterol Biosynthesis in the Livers of Intact Rats. *J. Biol. Chem.* **1963,** *238,* 1287-1293.

(20) Dietschy, J. M.; Turley, S. D. Cholesterol Metabolism in the Brain. *Curr. Opin. Lipidol.* **2001,** *12,* 105-112.

(21) Perovic, M.; Mladenovic, D. A.; Smiljanic, K.; Tanic, N.; Rakic, L.; Ruzdijic, S.; Kanazir, S. Expression of Cholesterol Homeostasis Genes in the Brain of the Male Rat Is Affected by Age and Dietary Restriction. *Biogerontology.* **2009**.

(22) Turley, S. D.; Burns, D. K.; Dietschy, J. M. Preferential Utilization of Newly Synthesized Cholesterol for Brain Growth in Neonatal Lambs. *Am. J. Physiol* **1998,** *274,* E1099-E1105.

(23) Dietschy, J. M.; Turley, S. D. Thematic Review Series: Brain Lipids. Cholesterol Metabolism in the Central Nervous System During Early Development and in the Mature Animal. *J. Lipid Res.* **2004,** *45,* 1375-1397.

(24) Bjorkhem, I.; Lutjohann, D.; Diczfalusy, U.; Stahle, L.; Ahlborg, G.; Wahren, J. Cholesterol Homeostasis in Human Brain: Turnover of 24S-Hydroxycholesterol and Evidence for a Cerebral Origin of Most of This Oxysterol in the Circulation. *J. Lipid Res.* **1998,** *39,* 1594-1600.

(25) Lutjohann, D.; Breuer, O.; Ahlborg, G.; Nennesmo, I.; Siden, A.; Diczfalusy, U.; Bjorkhem, I. Cholesterol Homeostasis in Human Brain: Evidence for an Age-Dependent Flux of 24S-Hydroxycholesterol From the Brain into the Circulation. *Proc. Natl. Acad. Sci. U. S. A* **1996,** *93,* 9799-9804.

(26) Griffiths, W. J.; Wang, Y.; Alvelius, G.; Liu, S.; Bodin, K.; Sjovall, J. Analysis of Oxysterols by Electrospray Tandem Mass Spectrometry. *J. Am. Soc. Mass Spectrom.* **2006,** *17,* 341-362.

(27) Lund, E. G.; Guileyardo, J. M.; Russell, D. W. CDNA Cloning of Cholesterol 24-Hydroxylase, a Mediator of Cholesterol Homeostasis in the Brain. *Proc. Natl. Acad. Sci. U. S. A* **1999,** *96,* 7238-7243.

(28) Farooqui, A. A.; Ong, W. Y.; Horrocks, L. A.; Chen, P.; Farooqui, T. Comparison of Biochemical Effects of Statins and Fish Oil in Brain: the Battle of the Titans. *Brain Res. Rev.* **2007,** *56,* 443-471.

(29) Heverin, M.; Bogdanovic, N.; Lutjohann, D.; Bayer, T.; Pikuleva, I.; Bretillon, L.; Diczfalusy, U.; Winblad, B.; Bjorkhem, I. Changes in the Levels of Cerebral and Extracerebral Sterols in the Brain of Patients With Alzheimer's Disease. *J. Lipid Res.* **2004,** *45,* 186-193.

(30) Meaney, S.; Heverin, M.; Panzenboeck, U.; Ekstrom, L.; Axelsson, M.; Andersson, U.; Diczfalusy, U.; Pikuleva, I.; Wahren, J.; Sattler, W.; Bjorkhem, I. Novel Route for Elimination of Brain Oxysterols Across the Blood-Brain Barrier: Conversion into 7alpha-Hydroxy-3-Oxo-4-Cholestenoic Acid. *J. Lipid Res.* **2007,** *48,* 944-951.

(31) Leoni, V.; Masterman, T.; Patel, P.; Meaney, S.; Diczfalusy, U.; Bjorkhem, I. Side Chain Oxidized Oxysterols in Cerebrospinal Fluid and the Integrity of Blood-Brain and Blood-Cerebrospinal Fluid Barriers. *J. Lipid Res.* **2003,** *44,* 793-799.

(32) Bjorkhem, I. Crossing the Barrier: Oxysterols As Cholesterol Transporters and Metabolic Modulators in the Brain. *J. Intern. Med.* **2006,** *260,* 493-508.

(33) Keller, R. K.; Small, M.; Fliesler, S. J. Enzyme Blockade: a Nonradioactive Method to Determine the Absolute Rate of Cholesterol Synthesis in the Brain. *J. Lipid Res.* **2004,** *45,* 1952-1957.

(34) Zhang, Y.; Appelkvist, E. L.; Kristensson, K.; Dallner, G. The Lipid Compositions of Different Regions of Rat Brain During Development and Aging. *Neurobiol. Aging* **1996,** *17,* 869-875.

(35) Funfschilling, U.; Saher, G.; Xiao, L.; Mobius, W.; Nave, K. A. Survival of Adult Neurons Lacking Cholesterol Synthesis in Vivo. *BMC. Neurosci.* **2007,** *8,* 1.

(36) Mauch, D. H.; Nagler, K.; Schumacher, S.; Goritz, C.; Muller, E. C.; Otto, A.; Pfrieger, F. W. CNS Synaptogenesis Promoted by Glia-Derived Cholesterol. *Science* **2001,** *294,* 1354-1357.

(37) Harr, S. D.; Uint, L.; Hollister, R.; Hyman, B. T.; Mendez, A. J. Brain Expression of Apolipoproteins E, J, and A-I in Alzheimer's Disease. *J. Neurochem.* **1996,** *66,* 2429-2435.

(38) Kester, M. I.; Verwey, N. A.; van Elk, E. J.; Blankenstein, M. A.; Scheltens, P.; van der Flier, W. M. Progression From MCI to AD: Predictive Value of CSF Abeta42 Is Modified by APOE Genotype. *Neurobiol. Aging* **2009**.

(39) Ohm, T. G.; Hamker, U.; Cedazo-Minguez, A.; Rockl, W.; Scharnagl, H.; Marz, W.; Cowburn, R.; Muller, W.; Meske, V. Apolipoprotein E and Beta A4-Amyloid: Signals and Effects. *Biochem. Soc. Symp.* **2001,** 121-129.

(40) Poirier, J. Apolipoprotein E, Cholesterol Transport and Synthesis in Sporadic Alzheimer's Disease. *Neurobiol. Aging* **2005,** *26,* 355-361.

(41) Igbavboa, U.; Hamilton, J.; Kim, H. Y.; Sun, G. Y.; Wood, W. G. A New Role for Apolipoprotein E: Modulating Transport of Polyunsaturated Phospholipid Molecular Species in Synaptic Plasma Membranes. *J. Neurochem.* **2002,** *80,* 255-261.

(42) Singer, S. J.; Nicolson, G. L. The Fluid Mosaic Model of the Structure of Cell Membranes. *Science* **1972,** *175,* 720-731.

(43) Jacobson, K.; Sheets, E. D.; Simson, R. Revisiting the Fluid Mosaic Model of Membranes. *Science* **1995,** *268,* 1441-1442.

(44) Anderson, R. G.; Jacobson, K. A Role for Lipid Shells in Targeting Proteins to Caveolae, Rafts, and Other Lipid Domains. *Science* **2002,** *296,* 1821-1825.

(45) Maxfield, F. R.; Mondal, M. Sterol and Lipid Trafficking in Mammalian Cells. *Biochem. Soc. Trans.* **2006,** *34,* 335-339.

(46) Ohvo-Rekila, H.; Ramstedt, B.; Leppimaki, P.; Slotte, J. P. Cholesterol Interactions With Phospholipids in Membranes. *Prog. Lipid Res.* **2002,** *41,* 66-97.

(47) Igbavboa, U.; Avdulov, N. A.; Schroeder, F.; Wood, W. G. Increasing Age Alters Transbilayer Fluidity and Cholesterol Asymmetry in Synaptic Plasma Membranes of Mice. *J. Neurochem.* **1996,** *66,* 1717-1725.

(48) Igbavboa, U.; Eckert, G. P.; Malo, T. M.; Studniski, A. E.; Johnson, L. N.; Yamamoto, N.; Kobayashi, M.; Fujita, S. C.; Appel, T. R.; Muller, W. E.; Wood, W. G.; Yanagisawa, K. Murine Synaptosomal Lipid Raft Protein and Lipid Composition Are Altered by Expression of Human ApoE 3 and 4 and by Increasing Age. *J. Neurol. Sci.* **2005,** *229-230,* 225-232.

(49) Fielding, C. J.; Fielding, P. E. Cholesterol and Caveolae: Structural and Functional Relationships. *Biochim. Biophys. Acta* **2000,** *1529,* 210-222.

(50) Ferrari, A.; Pellegrini, V.; Arcangeli, C.; Fittipaldi, A.; Giacca, M.; Beltram, F. Caveolae-Mediated Internalization of Extracellular HIV-1 Tat Fusion Proteins Visualized in Real Time. *Mol. Ther.* **2003,** *8,* 284-294.

(51) Nabi, I. R.; Le, P. U. Caveolae/Raft-Dependent Endocytosis. *J. Cell Biol.* **2003,** *161,* 673-677.

(52) Parton, R. G.; Simons, K. The Multiple Faces of Caveolae. *Nat. Rev. Mol. Cell Biol.* **2007,** *8,* 185-194.

(53) Harder, T.; Scheiffele, P.; Verkade, P.; Simons, K. Lipid Domain Structure of the Plasma Membrane Revealed by Patching of Membrane Components. *J. Cell Biol.* **1998,** *141,* 929-942.

(54) Simons, M.; Kramer, E. M.; Thiele, C.; Stoffel, W.; Trotter, J. Assembly of Myelin by Association of Proteolipid Protein With Cholesterol- and Galactosylceramide-Rich Membrane Domains. *J. Cell Biol.* **2000,** *151,* 143-154.

(55) Simons, K.; Ehehalt, R. Cholesterol, Lipid Rafts, and Disease. *J. Clin. Invest* **2002,** *110,* 597-603.

(56) Hering, H.; Lin, C. C.; Sheng, M. Lipid Rafts in the Maintenance of Synapses, Dendritic Spines, and Surface AMPA Receptor Stability. *J. Neurosci.* **2003,** *23,* 3262-3271.

(57) Raunser, S.; Haase, W.; Franke, C.; Eckert, G. P.; Muller, W. E.; Kuhlbrandt, W. Heterologously Expressed GLT-1 Associates in Approximately 200-Nm Protein-Lipid Islands. *Biophys. J.* **2006,** *91,* 3718-3726.

(58) Garner, A. E.; Smith, D. A.; Hooper, N. M. Visualization of Detergent Solubilization of Membranes: Implications for the Isolation of Rafts. *Biophys. J.* **2008,** *94,* 1326-1340.

(59) Owen, D. M.; Williamson, D.; Rentero, C.; Gaus, K. Quantitative Microscopy: Protein Dynamics and Membrane Organisation. *Traffic.* **2009,** *10,* 962-971.

(60) Heerklotz, H. Triton Promotes Domain Formation in Lipid Raft Mixtures. *Biophys. J.* **2002,** *83,* 2693-2701.

(61) Heffer-Lauc, M.; Lauc, G.; Nimrichter, L.; Fromholt, S. E.; Schnaar, R. L. Membrane Redistribution of Gangliosides and Glycosylphosphatidylinositol-Anchored Proteins in Brain Tissue Sections Under Conditions of Lipid Raft Isolation. *Biochim. Biophys. Acta* **2005,** *1686 3,* 200-208.

(62) Mann, M. Functional and Quantitative Proteomics Using SILAC. *Nat. Rev. Mol. Cell Biol.* **2006,** *7,* 952-958.

(63) Zheng, Y. Z.; Foster, L. J. Contributions of Quantitative Proteomics to Understanding Membrane Microdomains. *J. Lipid Res.* **2009**.

(64) Eckert, G. P. Manipulation of Lipid Rafts in Neuronal Cells. *The Open Biology Journal* **2010,** *3,* 32-38.

(65) Liang, P. H. Reaction Kinetics, Catalytic Mechanisms, Conformational Changes, and Inhibitor Design for Prenyltransferases. *Biochemistry* **2009,** *48,* 6562-6570.

(66) Rodriguez-Concepcion, M.; Boronat, A. Elucidation of the Methylerythritol Phosphate Pathway for Isoprenoid Biosynthesis in Bacteria and Plastids. A Metabolic Milestone Achieved Through Genomics. *Plant Physiol* **2002,** *130,* 1079-1089.

(67) Kavanagh, K. L.; Dunford, J. E.; Bunkoczi, G.; Russell, R. G.; Oppermann, U. The Crystal Structure of Human Geranylgeranyl Pyrophosphate Synthase Reveals a Novel Hexameric Arrangement and Inhibitory Product Binding. *J. Biol. Chem.* **2006,** *281,* 22004-22012.

(68) Ernster, L.; Dallner, G. Biochemical, Physiological and Medical Aspects of Ubiquinone Function. *Biochim. Biophys. Acta* **1995,** *1271,* 195-204.

(69) Lenaz, G.; Genova, M. L. Mobility and Function of Coenzyme Q (Ubiquinone) in the Mitochondrial Respiratory Chain. *Biochim. Biophys. Acta* **2009,** *1787,* 563-573.

(70) Kalen, A.; Appelkvist, E. L.; Chojnacki, T.; Dallner, G. Nonaprenyl-4-Hydroxybenzoate Transferase, an Enzyme Involved in Ubiquinone Biosynthesis, in the Endoplasmic Reticulum-Golgi System of Rat Liver. *J. Biol. Chem.* **1990,** *265,* 1158-1164.

(71) Houten, S. M.; Frenkel, J.; Waterham, H. R. Isoprenoid Biosynthesis in Hereditary Periodic Fever Syndromes and Inflammation. *Cell Mol. Life Sci.* **2003,** *60,* 1118-1134.

(72) Distelmaier, F.; Koopman, W. J.; van den Heuvel, L. P.; Rodenburg, R. J.; Mayatepek, E.; Willems, P. H.; Smeitink, J. A. Mitochondrial Complex I Deficiency: From Organelle Dysfunction to Clinical Disease. *Brain* **2009,** *132,* 833-842.

(73) Rotig, A.; Appelkvist, E. L.; Geromel, V.; Chretien, D.; Kadhom, N.; Edery, P.; Lebideau, M.; Dallner, G.; Munnich, A.; Ernster, L.; Rustin, P. Quinone-Responsive Multiple Respiratory-Chain Dysfunction Due to Widespread Coenzyme Q10 Deficiency. *Lancet* **2000,** *356,* 391-395.

(74) Valnot, I.; Kleist-Retzow, J. C.; Barrientos, A.; Gorbatyuk, M.; Taanman, J. W.; Mehaye, B.; Rustin, P.; Tzagoloff, A.; Munnich, A.; Rotig, A. A Mutation in the Human Heme A:Farnesyltransferase Gene (COX10) Causes Cytochrome c Oxidase Deficiency. *Hum. Mol. Genet.* **2000,** *9,* 1245-1249.

(75) Chojnacki, T.; Dallner, G. The Biological Role of Dolichol. *Biochem. J.* **1988,** *251,* 1-9.

(76) Parentini, I.; Cavallini, G.; Donati, A.; Gori, Z.; Bergamini, E. Accumulation of Dolichol in Older Tissues Satisfies the Proposed Criteria to Be Qualified a Biomarker of Aging. *J. Gerontol. A Biol. Sci. Med. Sci.* **2005,** *60,* 39-43.

(77) Marino, M.; Girelli, A. M.; Leoni, S.; Trentalance, A. Variations of Hepatic Dolichols During Rat Development. *Biochim. Biophys. Acta* **1990,** *1047,* 192-194.

(78) Vigo, C.; Grossman, S. H.; Drost-Hansen, W. Interaction of Dolichol and Dolichyl Phosphate With Phospholipid Bilayers. *Biochim. Biophys. Acta* **1984,** *774,* 221-226.

(79) Wood, W. G.; Sun, G. Y.; Schroeder, F. Membrane Properties of Dolichol in Different Age Groups of Mice. *Chem. Phys. Lipids* **1989,** *51,* 219-226.

(80) Andersson, M.; Appelkvist, E. L.; Kristensson, K.; Dallner, G. Age-Dependent Changes in the Levels of Dolichol and Dolichyl Phosphates in Human Brain. *Acta Chem. Scand. B* **1987,** *41,* 144-146.

(81) Bergamini, E.; Bizzarri, R.; Cavallini, G.; Cerbai, B.; Chiellini, E.; Donati, A.; Gori, Z.; Manfrini, A.; Parentini, I.; Signori, F.; Tamburini, I. Ageing and Oxidative Stress: a Role for Dolichol in the Antioxidant Machinery of Cell Membranes? *J. Alzheimers. Dis.* **2004,** *6,* 129-135.

(82) Carroll, K. K.; Guthrie, N.; Ravi, K. Dolichol: Function, Metabolism, and Accumulation in Human Tissues. *Biochem. Cell Biol.* **1992,** *70,* 382-384.

(83) Pallottini, V.; Marino, M.; Cavallini, G.; Bergamini, E.; Trentalance, A. Age-Related Changes of Isoprenoid Biosynthesis in Rat Liver and Brain. *Biogerontology.* **2003,** *4,* 371-378.

(84) James, M. J.; Kandutsch, A. A. Inter-Relationships Between Dolichol and Sterol Synthesis in Mammalian Cell Cultures. *J. Biol. Chem.* **1979,** *254,* 8442-8446.

(85) Keller, R. K.; Adair, W. L., Jr.; Ness, G. C. Studies on the Regulation of Glycoprotein Biosynthesis. An Investigation of the Rate-Limiting Steps of Dolichyl Phosphate Biosynthesis. *J. Biol. Chem.* **1979,** *254,* 9966-9969.

(86) Yamada, K.; Yokohama, H.; Abe, S.; Katayama, K.; Sato, T. High-Performance Liquid Chromatographic Method for the Determination of Dolichols in Tissues and Plasma. *Anal. Biochem.* **1985,** *150,* 26-31.

(87) Turpeinen, U. Liquid-Chromatographic Determination of Dolichols in Urine. *Clin. Chem.* **1986,** *32,* 2026-2029.

(88) Garrett, T. A.; Guan, Z.; Raetz, C. R. Analysis of Ubiquinones, Dolichols, and Dolichol Diphosphate-Oligosaccharides by Liquid Chromatography-Electrospray Ionization-Mass Spectrometry. *Methods Enzymol.* **2007,** *432,* 117-143.

(89) Ward, W. C.; Guan, Z.; Zucca, F. A.; Fariello, R. G.; Kordestani, R.; Zecca, L.; Raetz, C. R.; Simon, J. D. Identification and Quantification of Dolichol and Dolichoic Acid in Neuromelanin From Substantia Nigra of the Human Brain. *J. Lipid Res.* **2007,** *48,* 1457-1462.

(90) Tang, P. H.; Miles, M. V.; DeGrauw, A.; Hershey, A.; Pesce, A. HPLC Analysis of Reduced and Oxidized Coenzyme Q(10) in Human Plasma. *Clin. Chem.* **2001,** *47,* 256-265.

(91) Teshima, K.; Kondo, T. Analytical Method for Ubiquinone-9 and Ubiquinone-10 in Rat Tissues by Liquid Chromatography/Turbo Ion Spray Tandem Mass Spectrometry With 1-Alkylamine As an Additive to the Mobile Phase. *Anal. Biochem.* **2005,** *338,* 12-19.

(92) Bruenger, E.; Rilling, H. C. Determination of Isopentenyl Diphosphate and Farnesyl Diphosphate in Tissue Samples With a Comment on Secondary Regulation of Polyisoprenoid Biosynthesis. *Anal. Biochem.* **1988,** *173,* 321-327.

(93) Saisho, Y.; Morimoto, A.; Umeda, T. Determination of Farnesyl Pyrophosphate in Dog and Human Plasma by High-Performance Liquid Chromatography With Fluorescence Detection. *Anal. Biochem.* **1997,** *252,* 89-95.

(94) Tong, H.; Holstein, S. A.; Hohl, R. J. Simultaneous Determination of Farnesyl and Geranylgeranyl Pyrophosphate Levels in Cultured Cells. *Anal. Biochem.* **2005,** *336,* 51-59.

(95) Tong, H.; Wiemer, A. J.; Neighbors, J. D.; Hohl, R. J. Quantitative Determination of Farnesyl and Geranylgeranyl Diphosphate Levels in Mammalian Tissue. *Anal. Biochem.* **2008,** *378,* 138-143.

(96) Song, L. Detection of Farnesyl Diphosphate Accumulation in Yeast ERG9 Mutants. *Anal. Biochem.* **2003,** *317,* 180-185.

(97) Vallon, T.; Ghanegaonkar, S.; Vielhauer, O.; Muller, A.; Albermann, C.; Sprenger, G.; Reuss, M.; Lemuth, K. Quantitative Analysis of Isoprenoid Diphosphate Intermediates in Recombinant and Wild-Type Escherichia Coli Strains. *Appl. Microbiol. Biotechnol.* **2008,** *81,* 175-182.

(98) Holstein, S. A.; Tong, H.; Kuder, C. H.; Hohl, R. J. Quantitative Determination of Geranyl Diphosphate Levels in Cultured Human Cells. *Lipids* **2009**.

(99) Henneman, L.; van Cruchten, A. G.; Denis, S. W.; Amolins, M. W.; Placzek, A. T.; Gibbs, R. A.; Kulik, W.; Waterham, H. R. Detection of Nonsterol Isoprenoids by HPLC-MS/MS. *Anal. Biochem.* **2008,** *383,* 18-24.

(100) Sakakura, Y.; Shimano, H.; Sone, H.; Takahashi, A.; Inoue, N.; Toyoshima, H.; Suzuki, S.; Yamada, N. Sterol Regulatory Element-Binding Proteins Induce an Entire Pathway of Cholesterol Synthesis. *Biochem. Biophys. Res. Commun.* **2001,** *286,* 176-183.

(101) Kennelly, P. J.; Rodwell, V. W. Regulation of 3-Hydroxy-3-Methylglutaryl Coenzyme A Reductase by Reversible Phosphorylation-Dephosphorylation. *J. Lipid Res.* **1985,** *26,* 903-914.

(102) Brown, M. S.; Goldstein, J. L. The SREBP Pathway: Regulation of Cholesterol Metabolism by Proteolysis of a Membrane-Bound Transcription Factor. *Cell* **1997,** *89,* 331-340.

(103) Weber, L. W.; Boll, M.; Stampfl, A. Maintaining Cholesterol Homeostasis: Sterol Regulatory Element-Binding Proteins. *World J. Gastroenterol.* **2004,** *10,* 3081-3087.

(104) Horton, J. D. Sterol Regulatory Element-Binding Proteins: Transcriptional Activators of Lipid Synthesis. *Biochem. Soc. Trans.* **2002,** *30,* 1091-1095.

(105) Smith, J. R.; Osborne, T. F.; Goldstein, J. L.; Brown, M. S. Identification of Nucleotides Responsible for Enhancer Activity of Sterol Regulatory Element in Low Density Lipoprotein Receptor Gene. *J. Biol. Chem.* **1990,** *265,* 2306-2310.

(106) Yang, T.; Espenshade, P. J.; Wright, M. E.; Yabe, D.; Gong, Y.; Aebersold, R.; Goldstein, J. L.; Brown, M. S. Crucial Step in Cholesterol Homeostasis: Sterols Promote Binding of SCAP to INSIG-1, a Membrane Protein That Facilitates Retention of SREBPs in ER. *Cell* **2002,** *110,* 489-500.

(107) Wang, L.; Schuster, G. U.; Hultenby, K.; Zhang, Q.; Andersson, S.; Gustafsson, J. A. Liver X Receptors in the Central Nervous System: From Lipid Homeostasis to Neuronal Degeneration. *Proc. Natl. Acad. Sci. U. S. A* **2002,** *99,* 13878-13883.

(108) Abildayeva, K.; Jansen, P. J.; Hirsch-Reinshagen, V.; Bloks, V. W.; Bakker, A. H.; Ramaekers, F. C.; de Vente, J.; Groen, A. K.; Wellington, C. L.; Kuipers, F.; Mulder, M. 24(S)-Hydroxycholesterol Participates in a Liver X Receptor-Controlled Pathway in Astrocytes That Regulates Apolipoprotein E-Mediated Cholesterol Efflux. *J. Biol. Chem.* **2006,** *281,* 12799-12808.

(109) Repa, J. J.; Liang, G.; Ou, J.; Bashmakov, Y.; Lobaccaro, J. M.; Shimomura, I.; Shan, B.; Brown, M. S.; Goldstein, J. L.; Mangelsdorf, D. J. Regulation of Mouse Sterol Regulatory Element-Binding Protein-1c Gene (SREBP-1c) by Oxysterol Receptors, LXRalpha and LXRbeta. *Genes Dev.* **2000,** *14,* 2819-2830.

(110) Wang, Y.; Muneton, S.; Sjovall, J.; Jovanovic, J. N.; Griffiths, W. J. The Effect of 24S-Hydroxycholesterol on Cholesterol Homeostasis in Neurons: Quantitative Changes to the Cortical Neuron Proteome. *J. Proteome. Res.* **2008,** *7,* 1606-1614.

(111) Radhakrishnan, A.; Ikeda, Y.; Kwon, H. J.; Brown, M. S.; Goldstein, J. L. Sterol-Regulated Transport of SREBPs From Endoplasmic Reticulum to Golgi: Oxysterols Block Transport by Binding to Insig. *Proc. Natl. Acad. Sci. U. S. A* **2007,** *104,* 6511-6518.

(112) Dawson, P. A.; Metherall, J. E.; Ridgway, N. D.; Brown, M. S.; Goldstein, J. L. Genetic Distinction Between Sterol-Mediated Transcriptional and Posttranscriptional Control of 3-Hydroxy-3-Methylglutaryl-Coenzyme A Reductase. *J. Biol. Chem.* **1991,** *266,* 9128-9134.

(113) Sever, N.; Yang, T.; Brown, M. S.; Goldstein, J. L.; DeBose-Boyd, R. A. Accelerated Degradation of HMG CoA Reductase Mediated by Binding of Insig-1 to Its Sterol-Sensing Domain. *Mol. Cell* **2003,** *11,* 25-33.

(114) Runquist, M.; Parmryd, I.; Thelin, A.; Chojnacki, T.; Dallner, G. Distribution of Branch Point Prenyltransferases in Regions of Bovine Brain. *J. Neurochem.* **1995,** *65,* 2299-2306.

(115) Ericsson, J.; Runquist, M.; Thelin, A.; Andersson, M.; Chojnacki, T.; Dallner, G. Distribution of Prenyltransferases in Rat Tissues. Evidence for a Cytosolic All-Trans-Geranylgeranyl Diphosphate Synthase. *J. Biol. Chem.* **1993,** *268,* 832-838.

(116) Lutz, R. J.; McLain, T. M.; Sinensky, M. Feedback Inhibition of Polyisoprenyl Pyrophosphate Synthesis From Mevalonate in Vitro. Implications for Protein Prenylation. *J. Biol. Chem.* **1992,** *267,* 7983-7986.

(117) Sagami, H.; Morita, Y.; Ogura, K. Purification and Properties of Geranylgeranyl-Diphosphate Synthase From Bovine Brain. *J. Biol. Chem.* **1994,** *269,* 20561-20566.

(118) Murthy, S.; Tong, H.; Hohl, R. J. Regulation of Fatty Acid Synthesis by Farnesyl Pyrophosphate. *J. Biol. Chem.* **2005,** *280,* 41793-41804.

(119) Fukuchi, J.; Song, C.; Ko, A. L.; Liao, S. Transcriptional Regulation of Farnesyl Pyrophosphate Synthase by Liver X Receptors. *Steroids* **2003,** *68,* 685-691.

(120) Inoue, S.; Simoni, R. D. 3-Hydroxy-3-Methylglutaryl-Coenzyme A Reductase and T Cell Receptor Alpha Subunit Are Differentially Degraded in the Endoplasmic Reticulum. *J. Biol. Chem.* **1992,** *267,* 9080-9086.

(121) Ravid, T.; Doolman, R.; Avner, R.; Harats, D.; Roitelman, J. The Ubiquitin-Proteasome Pathway Mediates the Regulated Degradation of Mammalian 3-Hydroxy-3-Methylglutaryl-Coenzyme A Reductase. *J. Biol. Chem.* **2000,** *275,* 35840-35847.

(122) Sebti, S. M. Protein Farnesylation: Implications for Normal Physiology, Malignant Transformation, and Cancer Therapy. *Cancer Cell* **2005,** *7,* 297-300.

(123) Winter-Vann, A. M.; Casey, P. J. Post-Prenylation-Processing Enzymes As New Targets in Oncogenesis. *Nat. Rev. Cancer* **2005,** *5,* 405-412.

(124) Takai, Y.; Sasaki, T.; Matozaki, T. Small GTP-Binding Proteins. *Physiol Rev.* **2001,** *81,* 153-208.

(125) Boettner, B.; Van Aelst, L. The Role of Rho GTPases in Disease Development. *Gene* **2002,** *286,* 155-174.

(126) Luo, L. Rho GTPases in Neuronal Morphogenesis. *Nat. Rev. Neurosci.* **2000,** *1,* 173-180.

(127) Appels, N. M.; Rosing, H.; Stephens, T. C.; Schellens, J. H.; Beijnen, J. H. Quantification of Farnesylmethylcysteine in Lysates of Peripheral Blood Mononuclear Cells Using Liquid Chromatography Coupled With Electrospray Tandem Mass Spectrometry: Pharmacodynamic Assay for Farnesyl Transferase Inhibitors. *Anal. Chem.* **2006,** *78,* 2617-2622.

(128) Casey, P. J.; Seabra, M. C. Protein Prenyltransferases. *J. Biol. Chem.* **1996,** *271,* 5289-5292.

(129) Leung, K. F.; Baron, R.; Seabra, M. C. Thematic Review Series: Lipid Posttranslational Modifications. Geranylgeranylation of Rab GTPases. *J. Lipid Res.* **2006,** *47,* 467-475.

(130) Leung, K. F.; Baron, R.; Ali, B. R.; Magee, A. I.; Seabra, M. C. Rab GTPases Containing a CAAX Motif Are Processed Post-Geranylgeranylation by Proteolysis and Methylation. *J. Biol. Chem.* **2007,** *282,* 1487-1497.

(131) Casey, P. J.; Thissen, J. A.; Moomaw, J. F. Enzymatic Modification of Proteins With a Geranylgeranyl Isoprenoid. *Proc. Natl. Acad. Sci. U. S. A* **1991,** *88,* 8631-8635.

(132) Zhang, F. L.; Casey, P. J. Protein Prenylation: Molecular Mechanisms and Functional Consequences. *Annu. Rev. Biochem.* **1996,** *65,* 241-269.

(133) Huang, C. C.; Casey, P. J.; Fierke, C. A. Evidence for a Catalytic Role of Zinc in Protein Farnesyltransferase. Spectroscopy of Co2+-Farnesyltransferase Indicates Metal Coordination of the Substrate Thiolate. *J. Biol. Chem.* **1997,** *272,* 20-23.

(134) Zhang, F. L.; Casey, P. J. Influence of Metal Ions on Substrate Binding and Catalytic Activity of Mammalian Protein Geranylgeranyltransferase Type-I. *Biochem. J.* **1996,** *320 (Pt 3),* 925-932.

(135) Hightower, K. E.; Huang, C. C.; Casey, P. J.; Fierke, C. A. H-Ras Peptide and Protein Substrates Bind Protein Farnesyltransferase As an Ionized Thiolate. *Biochemistry* **1998,** *37,* 15555-15562.

(136) Moores, S. L.; Schaber, M. D.; Mosser, S. D.; Rands, E.; O'Hara, M. B.; Garsky, V. M.; Marshall, M. S.; Pompliano, D. L.; Gibbs, J. B. Sequence Dependence of Protein Isoprenylation. *J. Biol. Chem.* **1991,** *266,* 14603-14610.

(137) Roskoski, R., Jr.; Ritchie, P. Role of the Carboxyterminal Residue in Peptide Binding to Protein Farnesyltransferase and Protein Geranylgeranyltransferase. *Arch. Biochem. Biophys.* **1998,** *356,* 167-176.

(138) James, G. L.; Goldstein, J. L.; Brown, M. S. Polylysine and CVIM Sequences of K-RasB Dictate Specificity of Prenylation and Confer Resistance to Benzodiazepine Peptidomimetic in Vitro. *J. Biol. Chem.* **1995,** *270,* 6221-6226.

(139) Zhang, F. L.; Kirschmeier, P.; Carr, D.; James, L.; Bond, R. W.; Wang, L.; Patton, R.; Windsor, W. T.; Syto, R.; Zhang, R.; Bishop, W. R. Characterization of Ha-Ras, N-Ras, Ki-Ras4A, and Ki-Ras4B As in Vitro Substrates for Farnesyl Protein Transferase and Geranylgeranyl Protein Transferase Type I. *J. Biol. Chem.* **1997,** *272,* 10232-10239.

(140) Reid, T. S.; Terry, K. L.; Casey, P. J.; Beese, L. S. Crystallographic Analysis of CaaX Prenyltransferases Complexed With Substrates Defines Rules of Protein Substrate Selectivity. *J. Mol. Biol.* **2004,** *343,* 417-433.

(141) Sousa, S. F.; Fernandes, P. A.; Ramos, M. J. Farnesyltransferase Inhibitors: a Detailed Chemical View on an Elusive Biological Problem. *Curr. Med. Chem.* **2008,** *15,* 1478-1492.

(142) Armstrong, S. A.; Hannah, V. C.; Goldstein, J. L.; Brown, M. S. CAAX Geranylgeranyl Transferase Transfers Farnesyl As Efficiently As Geranylgeranyl to RhoB. *J. Biol. Chem.* **1995,** *270,* 7864-7868.

(143) Adjei, A. A. Blocking Oncogenic Ras Signaling for Cancer Therapy. *J. Natl. Cancer Inst.* **2001,** *93,* 1062-1074.

(144) Joberty, G.; Tavitian, A.; Zahraoui, A. Isoprenylation of Rab Proteins Possessing a C-Terminal CaaX Motif. *FEBS Lett.* **1993,** *330,* 323-328.

(145) Thoma, N. H.; Iakovenko, A.; Goody, R. S.; Alexandrov, K. Phosphoisoprenoids Modulate Association of Rab Geranylgeranyltransferase With REP-1. *J. Biol. Chem.* **2001,** *276,* 48637-48643.

(146) Manandhar, S. P.; Hildebrandt, E. R.; Schmidt, W. K. Small-Molecule Inhibitors of the Rce1p CaaX Protease. *J. Biomol. Screen.* **2007,** *12,* 983-993.

(147) Porter, S. B.; Hildebrandt, E. R.; Breevoort, S. R.; Mokry, D. Z.; Dore, T. M.; Schmidt, W. K. Inhibition of the CaaX Proteases Rce1p and Ste24p by Peptidyl (Acyloxy)Methyl Ketones. *Biochim. Biophys. Acta* **2007,** *1773,* 853-862.

(148) Tam, A.; Nouvet, F. J.; Fujimura-Kamada, K.; Slunt, H.; Sisodia, S. S.; Michaelis, S. Dual Roles for Ste24p in Yeast a-Factor Maturation: NH2-Terminal Proteolysis and COOH-Terminal CAAX Processing. *J. Cell Biol.* **1998,** *142,* 635-649.

(149) Dai, Q.; Choy, E.; Chiu, V.; Romano, J.; Slivka, S. R.; Steitz, S. A.; Michaelis, S.; Philips, M. R. Mammalian Prenylcysteine Carboxyl Methyltransferase Is in the Endoplasmic Reticulum. *J. Biol. Chem.* **1998,** *273,* 15030-15034.

(150) Chelsky, D.; Ruskin, B.; Koshland, D. E., Jr. Methyl-Esterified Proteins in a Mammalian Cell Line. *Biochemistry* **1985,** *24,* 6651-6658.

(151) Wright, L. P.; Philips, M. R. Thematic Review Series: Lipid Posttranslational Modifications. CAAX Modification and Membrane Targeting of Ras. *J. Lipid Res.* **2006,** *47,* 883-891.

(152) Appelkvist, E. L.; Aberg, F.; Guan, Z.; Parmryd, I.; Dallner, G. Regulation of Coenzyme Q Biosynthesis. *Mol. Aspects Med.* **1994,** *15 Suppl,* s37-s46.

(153) Dietrich, L. E.; Ungermann, C. On the Mechanism of Protein Palmitoylation. *EMBO Rep.* **2004,** *5,* 1053-1057.

(154) Smotrys, J. E.; Linder, M. E. Palmitoylation of Intracellular Signaling Proteins: Regulation and Function. *Annu. Rev. Biochem.* **2004,** *73,* 559-587.

(155) Otth, C.; Mendoza-Naranjo, A.; Mujica, L.; Zambrano, A.; Concha, I. I.; Maccioni, R. B. Modulation of the JNK and P38 Pathways by Cdk5 Protein Kinase in a Transgenic Mouse Model of Alzheimer's Disease. *Neuroreport* **2003,** *14,* 2403-2409.

(156) Schmidt, A.; Hall, A. Guanine Nucleotide Exchange Factors for Rho GTPases: Turning on the Switch. *Genes Dev.* **2002,** *16,* 1587-1609.

(157) Bernards, A.; Settleman, J. GAP Control: Regulating the Regulators of Small GTPases. *Trends Cell Biol.* **2004,** *14,* 377-385.

(158) Olofsson, B. Rho Guanine Dissociation Inhibitors: Pivotal Molecules in Cellular Signalling. *Cell Signal.* **1999,** *11,* 545-554.

(159) Wennerberg, K.; Rossman, K. L.; Der, C. J. The Ras Superfamily at a Glance. *J. Cell Sci.* **2005,** *118,* 843-846.

(160) Repasky, G. A.; Chenette, E. J.; Der, C. J. Renewing the Conspiracy Theory Debate: Does Raf Function Alone to Mediate Ras Oncogenesis? *Trends Cell Biol.* **2004,** *14,* 639-647.

(161) Downward, J. Targeting RAS Signalling Pathways in Cancer Therapy. *Nat. Rev. Cancer* **2003,** *3,* 11-22.

(162) Appels, N. M.; Bolijn, M. J.; Chan, K.; Stephens, T. C.; Hoctin-Boes, G.; Middleton, M.; Beijnen, J. H.; de Bono, J. S.; Harris, A. L.; Schellens, J. H. Phase I Pharmacokinetic and Pharmacodynamic Study of the Prenyl Transferase Inhibitor AZD3409 in Patients With Advanced Cancer. *Br. J. Cancer* **2008,** *98,* 1951-1958.

(163) Brunner, T. B.; Hahn, S. M.; Gupta, A. K.; Muschel, R. J.; McKenna, W. G.; Bernhard, E. J. Farnesyltransferase Inhibitors: an Overview of the Results of Preclinical and Clinical Investigations. *Cancer Res.* **2003,** *63,* 5656-5668.

(164) Ridley, A. J. Rho Proteins, PI 3-Kinases, and Monocyte/Macrophage Motility. *FEBS Lett.* **2001,** *498,* 168-171.

(165) Bishop, A. L.; Hall, A. Rho GTPases and Their Effector Proteins. *Biochem. J.* **2000,** *348 Pt 2,* 241-255.

(166) Roberts, P. J.; Mitin, N.; Keller, P. J.; Chenette, E. J.; Madigan, J. P.; Currin, R. O.; Cox, A. D.; Wilson, O.; Kirschmeier, P.; Der, C. J. Rho Family GTPase Modification and Dependence on CAAX Motif-Signaled Posttranslational Modification. *J. Biol. Chem.* **2008,** *283,* 25150-25163.

(167) Pereira-Leal, J. B.; Seabra, M. C. Evolution of the Rab Family of Small GTP-Binding Proteins. *J. Mol. Biol.* **2001,** *313,* 889-901.

(168) Bergbrede, T.; Chuky, N.; Schoebel, S.; Blankenfeldt, W.; Geyer, M.; Fuchs, E.; Goody, R. S.; Barr, F.; Alexandrov, K. Biophysical Analysis of the Interaction of Rab6a GTPase With Its Effector Domains. *J. Biol. Chem.* **2009,** *284,* 2628-2635.

(169) Kimura, T.; Kaneko, Y.; Yamada, S.; Ishihara, H.; Senda, T.; Iwamatsu, A.; Niki, I. The GDP-Dependent Rab27a Effector Coronin 3 Controls Endocytosis of Secretory Membrane in Insulin-Secreting Cell Lines. *J. Cell Sci.* **2008,** *121,* 3092-3098.

(170) Zerial, M.; McBride, H. Rab Proteins As Membrane Organizers. *Nat. Rev. Mol. Cell Biol.* **2001,** *2,* 107-117.

(171) Zhu, H.; Liang, Z.; Li, G. Rabex-5 Is a Rab22 Effector and Mediates a Rab22-Rab5 Signaling Cascade in Endocytosis. *Mol. Biol. Cell* **2009,** *20,* 4720-4729.

(172) Pechlivanis, M.; Kuhlmann, J. Hydrophobic Modifications of Ras Proteins by Isoprenoid Groups and Fatty Acids--More Than Just Membrane Anchoring. *Biochim. Biophys. Acta* **2006,** *1764,* 1914-1931.

(173) Li, H. Y.; Cao, K.; Zheng, Y. Ran in the Spindle Checkpoint: a New Function for a Versatile GTPase. *Trends Cell Biol.* **2003,** *13,* 553-557.

(174) Weis, K. Regulating Access to the Genome: Nucleocytoplasmic Transport Throughout the Cell Cycle. *Cell* **2003,** *112,* 441-451.

(175) Memon, A. R. The Role of ADP-Ribosylation Factor and SAR1 in Vesicular Trafficking in Plants. *Biochim. Biophys. Acta* **2004,** *1664,* 9-30.

(176) Caserta, M. T.; Bannon, Y.; Fernandez, F.; Giunta, B.; Schoenberg, M. R.; Tan, J. Normal Brain Aging Clinical, Immunological, Neuropsychological, and Neuroimaging Features. *Int. Rev. Neurobiol.* **2009,** *84,* 1-19.

(177) Loerch, P. M.; Lu, T.; Dakin, K. A.; Vann, J. M.; Isaacs, A.; Geula, C.; Wang, J.; Pan, Y.; Gabuzda, D. H.; Li, C.; Prolla, T. A.; Yankner, B. A. Evolution of the Aging Brain Transcriptome and Synaptic Regulation. *PLoS. One.* **2008,** *3,* e3329.

(178) Yankner, B. A.; Lu, T.; Loerch, P. The Aging Brain. *Annu. Rev. Pathol.* **2008,** *3,* 41-66.

(179) O'Brien, J. S.; Sampson, E. L. Lipid Composition of the Normal Human Brain: Gray Matter, White Matter, and Myelin. *J. Lipid Res.* **1965,** *6,* 537-544.

(180) Lutjohann, D. Cholesterol Metabolism in the Brain: Importance of 24S-Hydroxylation. *Acta Neurol. Scand. Suppl* **2006,** *185,* 33-42.

(181) Wood, W. G.; Schroeder, F.; Igbavboa, U.; Avdulov, N. A.; Chochina, S. V. Brain Membrane Cholesterol Domains, Aging and Amyloid Beta-Peptides. *Neurobiol. Aging* **2002,** *23,* 685-694.

(182) Cutler, R. G.; Kelly, J.; Storie, K.; Pedersen, W. A.; Tammara, A.; Hatanpaa, K.; Troncoso, J. C.; Mattson, M. P. Involvement of Oxidative Stress-Induced Abnormalities in Ceramide and Cholesterol Metabolism in Brain Aging and Alzheimer's Disease. *Proc. Natl. Acad. Sci. U. S. A* **2004,** *101,* 2070-2075.

(183) Besshoh, S.; Chen, S.; Brown, I. R.; Gurd, J. W. Developmental Changes in the Association of NMDA Receptors With Lipid Rafts. *J. Neurosci. Res.* **2007,** *85,* 1876-1883.

(184) Gimpl, G.; Burger, K.; Fahrenholz, F. Cholesterol As Modulator of Receptor Function. *Biochemistry* **1997,** *36,* 10959-10974.

(185) Kuehnle, K.; Ledesma, M. D.; Kalvodova, L.; Smith, A. E.; Crameri, A.; Skaanes-Brunner, F.; Thelen, K. M.; Kulic, L.; Lutjohann, D.; Heppner, F. L.; Nitsch, R. M.; Mohajeri, M. H. Age-Dependent Increase in Desmosterol Restores DRM Formation and Membrane-Related Functions in Cholesterol-Free DHCR24-/- Mice. *Neurochem. Res.* **2009,** *34,* 1167-1182.

(186) Scheuer, K.; Stoll, S.; Paschke, U.; Weigel, R.; Muller, W. E. N-Methyl-D-Aspartate Receptor Density and Membrane Fluidity As Possible Determinants of the Decline of Passive Avoidance Performance in Aging. *Pharmacol. Biochem. Behav.* **1995,** *50,* 65-70.

(187) Karten, B.; Peake, K. B.; Vance, J. E. Mechanisms and Consequences of Impaired Lipid Trafficking in Niemann-Pick Type C1-Deficient Mammalian Cells. *Biochim. Biophys. Acta* **2009,** *1791,* 659-670.

(188) Porter, F. D. Smith-Lemli-Opitz Syndrome: Pathogenesis, Diagnosis and Management. *Eur. J. Hum. Genet.* **2008,** *16,* 535-541.

(189) Schweitzer, J. K.; Krivda, J. P.; D'Souza-Schorey, C. Neurodegeneration in Niemann-Pick Type C Disease and Huntington's Disease: Impact of Defects in Membrane Trafficking. *Curr. Drug Targets.* **2009,** *10,* 653-665.

(190) Valenza, M.; Rigamonti, D.; Goffredo, D.; Zuccato, C.; Fenu, S.; Jamot, L.; Strand, A.; Tarditi, A.; Woodman, B.; Racchi, M.; Mariotti, C.; Di Donato, S.; Corsini, A.; Bates, G.; Pruss, R.; Olson, J. M.; Sipione, S.; Tartari, M.; Cattaneo, E. Dysfunction of the Cholesterol Biosynthetic Pathway in Huntington's Disease. *J. Neurosci.* **2005,** *25,* 9932-9939.

(191) Thelen, K. M.; Falkai, P.; Bayer, T. A.; Lutjohann, D. Cholesterol Synthesis Rate in Human Hippocampus Declines With Aging. *Neurosci. Lett.* **2006,** *403,* 15-19.

(192) Andersson, M.; Aberg, F.; Teclebrhan, H.; Edlund, C.; Appelkvist, E. L. Age-Dependent Modifications in the Metabolism of Mevalonate Pathway Lipids in Rat Brain. *Mech. Ageing Dev.* **1995,** *85,* 1-14.

(193) Kotti, T.; Head, D. D.; McKenna, C. E.; Russell, D. W. Biphasic Requirement for Geranylgeraniol in Hippocampal Long-Term Potentiation. *Proc. Natl. Acad. Sci. U. S. A* **2008,** *105,* 11394-11399.

(194) Alegret, M.; Silvestre, J. S. Pleiotropic Effects of Statins and Related Pharmacological Experimental Approaches. *Methods Find. Exp. Clin. Pharmacol.* **2006,** *28,* 627-656.

(195) Russell, R. G.; Watts, N. B.; Ebetino, F. H.; Rogers, M. J. Mechanisms of Action of Bisphosphonates: Similarities and Differences and Their Potential Influence on Clinical Efficacy. *Osteoporos. Int.* **2008,** *19,* 733-759.

(196) Swanson, K. M.; Hohl, R. J. Anti-Cancer Therapy: Targeting the Mevalonate Pathway. *Curr. Cancer Drug Targets.* **2006,** *6,* 15-37.

(197) Capell, B. C.; Erdos, M. R.; Madigan, J. P.; Fiordalisi, J. J.; Varga, R.; Conneely, K. N.; Gordon, L. B.; Der, C. J.; Cox, A. D.; Collins, F. S. Inhibiting Farnesylation of Progerin Prevents the Characteristic Nuclear Blebbing of Hutchinson-Gilford Progeria Syndrome. *Proc. Natl. Acad. Sci. U. S. A* **2005,** *102,* 12879-12884.

(198) Rajanikant, G. K.; Zemke, D.; Kassab, M.; Majid, A. The Therapeutic Potential of Statins in Neurological Disorders. *Curr. Med. Chem.* **2007,** *14,* 103-112.

(199) Dunn, S. E.; Youssef, S.; Goldstein, M. J.; Prod'homme, T.; Weber, M. S.; Zamvil, S. S.; Steinman, L. Isoprenoids Determine Th1/Th2 Fate in Pathogenic T Cells, Providing a Mechanism of Modulation of Autoimmunity by Atorvastatin. *J. Exp. Med.* **2006,** *203,* 401-412.

(200) Paintlia, A. S.; Paintlia, M. K.; Khan, M.; Vollmer, T.; Singh, A. K.; Singh, I. HMG-CoA Reductase Inhibitor Augments Survival and Differentiation of Oligodendrocyte Progenitors in Animal Model of Multiple Sclerosis. *FASEB J.* **2005,** *19,* 1407-1421.

(201) Kukar, T.; Murphy, M. P.; Eriksen, J. L.; Sagi, S. A.; Weggen, S.; Smith, T. E.; Ladd, T.; Khan, M. A.; Kache, R.; Beard, J.; Dodson, M.; Merit, S.; Ozols, V. V.; Anastasiadis, P. Z.; Das, P.; Fauq, A.; Koo, E. H.; Golde, T. E. Diverse Compounds Mimic Alzheimer Disease-Causing Mutations by Augmenting Abeta42 Production. *Nat. Med.* **2005,** *11,* 545-550.

(202) Ostrowski, S. M.; Wilkinson, B. L.; Golde, T. E.; Landreth, G. Statins Reduce Amyloid-Beta Production Through Inhibition of Protein Isoprenylation. *J. Biol. Chem.* **2007,** *282,* 26832-26844.

(203) Urano, Y.; Hayashi, I.; Isoo, N.; Reid, P. C.; Shibasaki, Y.; Noguchi, N.; Tomita, T.; Iwatsubo, T.; Hamakubo, T.; Kodama, T. Association of Active Gamma-Secretase Complex With Lipid Rafts. *J. Lipid Res.* **2005,** *46,* 904-912.

(204) Mattson, M. P.; Magnus, T. Ageing and Neuronal Vulnerability. *Nat. Rev. Neurosci.* **2006,** *7,* 278-294.

(205) Pullarkat, R. K.; Reha, H. Accumulation of Dolichols in Brains of Elderly. *J. Biol. Chem.* **1982,** *257,* 5991-5993.

(206) Edlund, C.; Soderberg, M.; Kristensson, K. Isoprenoids in Aging and Neurodegeneration. *Neurochem. Int.* **1994,** *25,* 35-38.

(207) Wolfe, L. S.; Ng Ying Kin, N. M.; Palo, J.; Bergeron, C.; Kotila, M.; Varonen, S. Dolichols Are Elevated in Brain Tissue From Alzheimer's Disease, but Not in Urinary Sediment From Alzheimer's Disease and Down's Syndrome. *Neurochem. Pathol.* **1985,** *3,* 213-221.

(208) Ng Ying Kin, N. M.; Palo, J.; Haltia, M.; Wolfe, L. S. High Levels of Brain Dolichols in Neuronal Ceroid-Lipofuscinosis and Senescence. *J. Neurochem.* **1983,** *40,* 1465-1473.

(209) W.G.WOOD, U. I. G. P. E. W. E. M. Cholesterol-A Janus Faced Molecule in the Central Nervous System. In *Neural Membranes and Transport*; Lajtha, A. R. M. E. A., Ed.; Plenum: New York, 2007.

(210) Edlund, C.; Soderberg, M.; Kristensson, K.; Dallner, G. Ubiquinone, Dolichol, and Cholesterol Metabolism in Aging and Alzheimer's Disease. *Biochem. Cell Biol.* **1992,** *70,* 422-428.

(211) Bergado, J. A.; Almaguer, W. Aging and Synaptic Plasticity: a Review. *Neural Plast.* **2002,** *9,* 217-232.

(212) McNair, K.; Spike, R.; Guilding, C.; Prendergast, G. C.; Stone, T. W.; Cobb, S. R.; Morris, B. J. A Role for RhoB in Synaptic Plasticity and the Regulation of Neuronal Morphology. *J. Neurosci.* **2010,** *30,* 3508-3517.

(213) Ferri, C. P.; Prince, M.; Brayne, C.; Brodaty, H.; Fratiglioni, L.; Ganguli, M.; Hall, K.; Hasegawa, K.; Hendrie, H.; Huang, Y.; Jorm, A.; Mathers, C.; Menezes, P. R.; Rimmer, E.; Scazufca, M. Global Prevalence of Dementia: a Delphi Consensus Study. *Lancet* **2005,** *366,* 2112-2117.

(214) Buchhave, P.; Blennow, K.; Zetterberg, H.; Stomrud, E.; Londos, E.; Andreasen, N.; Minthon, L.; Hansson, O. Longitudinal Study of CSF Biomarkers in Patients With Alzheimer's Disease. *PLoS. One.* **2009,** *4,* e6294.

(215) Tiraboschi, P.; Hansen, L. A.; Thal, L. J.; Corey-Bloom, J. The Importance of Neuritic Plaques and Tangles to the Development and Evolution of AD. *Neurology* **2004,** *62,* 1984-1989.

(216) Huff, F. J.; Corkin, S.; Growdon, J. H. Semantic Impairment and Anomia in Alzheimer's Disease. *Brain Lang* **1986,** *28,* 235-249.

(217) Forstl, H.; Kurz, A. Clinical Features of Alzheimer's Disease. *Eur. Arch. Psychiatry Clin. Neurosci.* **1999,** *249,* 288-290.

(218) Zanetti, O.; Solerte, S. B.; Cantoni, F. Life Expectancy in Alzheimer's Disease (AD). *Arch. Gerontol. Geriatr.* **2009,** *49 Suppl 1,* 237-243.

(219) Rocchi, A.; Pellegrini, S.; Siciliano, G.; Murri, L. Causative and Susceptibility Genes for Alzheimer's Disease: a Review. *Brain Res. Bull.* **2003,** *61,* 1-24.

(220) Gao, S.; Hendrie, H. C.; Hall, K. S.; Hui, S. The Relationships Between Age, Sex, and the Incidence of Dementia and Alzheimer Disease: a Meta-Analysis. *Arch. Gen. Psychiatry* **1998,** *55,* 809-815.

(221) Dosunmu, R.; Wu, J.; Basha, M. R.; Zawia, N. H. Environmental and Dietary Risk Factors in Alzheimer's Disease. *Expert. Rev. Neurother.* **2007,** *7,* 887-900.

(222) Friedland, R. P.; Fritsch, T.; Smyth, K. A.; Koss, E.; Lerner, A. J.; Chen, C. H.; Petot, G. J.; Debanne, S. M. Patients With Alzheimer's Disease Have Reduced Activities in Midlife Compared With Healthy Control-Group Members. *Proc. Natl. Acad. Sci. U. S. A* **2001,** *98*, 3440-3445.

(223) Ownby, R. L.; Crocco, E.; Acevedo, A.; John, V.; Loewenstein, D. Depression and Risk for Alzheimer Disease: Systematic Review, Meta-Analysis, and Metaregression Analysis. *Arch. Gen. Psychiatry* **2006,** *63*, 530-538.

(224) Patterson, C.; Feightner, J. W.; Garcia, A.; Hsiung, G. Y.; MacKnight, C.; Sadovnick, A. D. Diagnosis and Treatment of Dementia: 1. Risk Assessment and Primary Prevention of Alzheimer Disease. *CMAJ.* **2008,** *178*, 548-556.

(225) Corder, E. H.; Saunders, A. M.; Strittmatter, W. J.; Schmechel, D. E.; Gaskell, P. C.; Small, G. W.; Roses, A. D.; Haines, J. L.; Pericak-Vance, M. A. Gene Dose of Apolipoprotein E Type 4 Allele and the Risk of Alzheimer's Disease in Late Onset Families. *Science* **1993,** *261*, 921-923.

(226) Saunders, A. M.; Strittmatter, W. J.; Schmechel, D.; George-Hyslop, P. H.; Pericak-Vance, M. A.; Joo, S. H.; Rosi, B. L.; Gusella, J. F.; Crapper-MacLachlan, D. R.; Alberts, M. J.; . Association of Apolipoprotein E Allele Epsilon 4 With Late-Onset Familial and Sporadic Alzheimer's Disease. *Neurology* **1993,** *43*, 1467-1472.

(227) Mahley, R. W.; Weisgraber, K. H.; Huang, Y. Apolipoprotein E4: a Causative Factor and Therapeutic Target in Neuropathology, Including Alzheimer's Disease. *Proc. Natl. Acad. Sci. U. S. A* **2006,** *103*, 5644-5651.

(228) Blennow, K.; Zetterberg, H. Cerebrospinal Fluid Biomarkers for Alzheimer's Disease. *J. Alzheimers. Dis.* **2009,** *18*, 413-417.

(229) Kester, M. I.; van der Vlies, A. E.; Blankenstein, M. A.; Pijnenburg, Y. A.; van Elk, E. J.; Scheltens, P.; van der Flier, W. M. CSF Biomarkers Predict Rate of Cognitive Decline in Alzheimer Disease. *Neurology* **2009,** *73*, 1353-1358.

(230) Mattsson, N.; Blennow, K.; Zetterberg, H. CSF Biomarkers: Pinpointing Alzheimer Pathogenesis. *Ann. N. Y. Acad. Sci.* **2009,** *1180*, 28-35.

(231) Rabinovici, G. D.; Jagust, W. J. Amyloid Imaging in Aging and Dementia: Testing the Amyloid Hypothesis in Vivo. *Behav. Neurol.* **2009,** *21*, 117-128.

(232) Blacker, D.; Albert, M. S.; Bassett, S. S.; Go, R. C.; Harrell, L. E.; Folstein, M. F. Reliability and Validity of NINCDS-ADRDA Criteria for Alzheimer's Disease. The National Institute of Mental Health Genetics Initiative. *Arch. Neurol.* **1994,** *51*, 1198-1204.

(233) Dubois, B.; Feldman, H. H.; Jacova, C.; Dekosky, S. T.; Barberger-Gateau, P.; Cummings, J.; Delacourte, A.; Galasko, D.; Gauthier, S.; Jicha, G.; Meguro, K.; O'brien, J.; Pasquier, F.; Robert, P.; Rossor, M.; Salloway, S.; Stern, Y.; Visser, P. J.; Scheltens, P.

Research Criteria for the Diagnosis of Alzheimer's Disease: Revising the NINCDS-ADRDA Criteria. *Lancet Neurol.* **2007,** *6*, 734-746.

(234) McKhann, G.; Drachman, D.; Folstein, M.; Katzman, R.; Price, D.; Stadlan, E. M. Clinical Diagnosis of Alzheimer's Disease: Report of the NINCDS-ADRDA Work Group Under the Auspices of Department of Health and Human Services Task Force on Alzheimer's Disease. *Neurology* **1984,** *34*, 939-944.

(235) Solomon, P. R.; Adams, F. A.; Groccia, M. E.; DeVeaux, R.; Growdon, J. H.; Pendlebury, W. W. Correlational Analysis of Five Commonly Used Measures of Mental Status/Functional Abilities in Patients With Alzheimer Disease. *Alzheimer Dis. Assoc. Disord.* **1999,** *13*, 147-150.

(236) Braak, H.; Braak, E. Neuropathological Stageing of Alzheimer-Related Changes. *Acta Neuropathol.* **1991,** *82*, 239-259.

(237) Reham Mahmoud Abdel-Kader. Molecular and cellular mechanisms of Ginkgo biloba extract [EGb 761®] in improving age-related and ß-amyloid induced neuronal dysfunctions. 2009. Fachbereich Biochemie, Chemie und Pharmazie der Johann Wolfgang Goethe-Universität in Frankfurt am Main.
Ref Type: Thesis/Dissertation

(238) Imke Peters. Untersuchungen zur Membranfluidität als regulatorisches Element der APP-Prozessierung. 2007. Fachbereich Biochemie, Chemie und Pharmazie der Johann Wolfgang Goethe-Universität in Frankfurt am Main.
Ref Type: Thesis/Dissertation

(239) Marks, N.; Berg, M. J. APP Processing Enzymes (Secretases) As Therapeutic Targets: Insights From the Use of Transgenics (Tgs) and Transfected Cells. *Neurochem. Res.* **2003,** *28*, 1049-1062.

(240) Selkoe, D. J. Alzheimer's Disease: Genes, Proteins, and Therapy. *Physiol Rev.* **2001,** *81*, 741-766.

(241) Vassar, R. BACE1: the Beta-Secretase Enzyme in Alzheimer's Disease. *J. Mol. Neurosci.* **2004,** *23*, 105-114.

(242) Vassar, R.; Kovacs, D. M.; Yan, R.; Wong, P. C. The Beta-Secretase Enzyme BACE in Health and Alzheimer's Disease: Regulation, Cell Biology, Function, and Therapeutic Potential. *J. Neurosci.* **2009,** *29*, 12787-12794.

(243) Reid, P. C.; Urano, Y.; Kodama, T.; Hamakubo, T. Alzheimer's Disease: Cholesterol, Membrane Rafts, Isoprenoids and Statins. *J. Cell Mol. Med.* **2007,** *11*, 383-392.

(244) Papassotiropoulos, A.; Wollmer, M. A.; Tsolaki, M.; Brunner, F.; Molyva, D.; Lutjohann, D.; Nitsch, R. M.; Hock, C. A Cluster of Cholesterol-Related Genes Confers Susceptibility for Alzheimer's Disease. *J. Clin. Psychiatry* **2005,** *66,* 940-947.

(245) Stefani, M.; Liguri, G. Cholesterol in Alzheimer's Disease: Unresolved Questions. *Curr. Alzheimer Res.* **2009,** *6,* 15-29.

(246) Jick, H.; Zornberg, G. L.; Jick, S. S.; Seshadri, S.; Drachman, D. A. Statins and the Risk of Dementia. *Lancet* **2000,** *356,* 1627-1631.

(247) Rockwood, K.; Kirkland, S.; Hogan, D. B.; MacKnight, C.; Merry, H.; Verreault, R.; Wolfson, C.; McDowell, I. Use of Lipid-Lowering Agents, Indication Bias, and the Risk of Dementia in Community-Dwelling Elderly People. *Arch. Neurol.* **2002,** *59,* 223-227.

(248) Wolozin, B.; Kellman, W.; Ruosseau, P.; Celesia, G. G.; Siegel, G. Decreased Prevalence of Alzheimer Disease Associated With 3-Hydroxy-3-Methyglutaryl Coenzyme A Reductase Inhibitors. *Arch. Neurol.* **2000,** *57,* 1439-1443.

(249) Hoglund, K.; Wiklund, O.; Vanderstichele, H.; Eikenberg, O.; Vanmechelen, E.; Blennow, K. Plasma Levels of Beta-Amyloid(1-40), Beta-Amyloid(1-42), and Total Beta-Amyloid Remain Unaffected in Adult Patients With Hypercholesterolemia After Treatment With Statins. *Arch. Neurol.* **2004,** *61,* 333-337.

(250) Fassbender, K.; Stroick, M.; Bertsch, T.; Ragoschke, A.; Kuehl, S.; Walter, S.; Walter, J.; Brechtel, K.; Muehlhauser, F.; Von Bergmann, K.; Lutjohann, D. Effects of Statins on Human Cerebral Cholesterol Metabolism and Secretion of Alzheimer Amyloid Peptide. *Neurology* **2002,** *59,* 1257-1258.

(251) Lutjohann, D.; Papassotiropoulos, A.; Bjorkhem, I.; Locatelli, S.; Bagli, M.; Oehring, R. D.; Schlegel, U.; Jessen, F.; Rao, M. L.; Von Bergmann, K.; Heun, R. Plasma 24S-Hydroxycholesterol (Cerebrosterol) Is Increased in Alzheimer and Vascular Demented Patients. *J. Lipid Res.* **2000,** *41,* 195-198.

(252) Papassotiropoulos, A.; Lutjohann, D.; Bagli, M.; Locatelli, S.; Jessen, F.; Buschfort, R.; Ptok, U.; Bjorkhem, I.; Von Bergmann, K.; Heun, R. 24S-Hydroxycholesterol in Cerebrospinal Fluid Is Elevated in Early Stages of Dementia. *J. Psychiatr. Res.* **2002,** *36,* 27-32.

(253) Bretillon, L.; Siden, A.; Wahlund, L. O.; Lutjohann, D.; Minthon, L.; Crisby, M.; Hillert, J.; Groth, C. G.; Diczfalusy, U.; Bjorkhem, I. Plasma Levels of 24S-Hydroxycholesterol in Patients With Neurological Diseases. *Neurosci. Lett.* **2000,** *293,* 87-90.

(254) Liao, J. K.; Laufs, U. Pleiotropic Effects of Statins. *Annu. Rev. Pharmacol. Toxicol.* **2005,** *45,* 89-118.

(255) Johnson-Anuna, L. N.; Eckert, G. P.; Keller, J. H.; Igbavboa, U.; Franke, C.; Fechner, T.; Schubert-Zsilavecz, M.; Karas, M.; Muller, W. E.; Wood, W. G. Chronic Administration of Statins Alters Multiple Gene Expression Patterns in Mouse Cerebral Cortex. *J. Pharmacol. Exp. Ther.* **2005,** *312,* 786-793.

(256) Botti, R. E.; Triscari, J.; Pan, H. Y.; Zayat, J. Concentrations of Pravastatin and Lovastatin in Cerebrospinal Fluid in Healthy Subjects. *Clin. Neuropharmacol.* **1991,** *14,* 256-261.

(257) Yanagisawa, K. Cholesterol and Pathological Processes in Alzheimer's Disease. *J. Neurosci. Res.* **2002,** *70,* 361-366.

(258) Isobe, C.; Abe, T.; Terayama, Y. Increase in the Oxidized/Total Coenzyme Q-10 Ratio in the Cerebrospinal Fluid of Alzheimer's Disease Patients. *Dement. Geriatr. Cogn Disord.* **2009,** *28,* 449-454.

(259) Yang, X.; Yang, Y.; Li, G.; Wang, J.; Yang, E. S. Coenzyme Q10 Attenuates Beta-Amyloid Pathology in the Aged Transgenic Mice With Alzheimer Presenilin 1 Mutation. *J. Mol. Neurosci.* **2008,** *34,* 165-171.

(260) Thal, L. J.; Grundman, M.; Berg, J.; Ernstrom, K.; Margolin, R.; Pfeiffer, E.; Weiner, M. F.; Zamrini, E.; Thomas, R. G. Idebenone Treatment Fails to Slow Cognitive Decline in Alzheimer's Disease. *Neurology* **2003,** *61,* 1498-1502.

(261) Scheper, W.; Hoozemans, J. J.; Hoogenraad, C. C.; Rozemuller, A. J.; Eikelenboom, P.; Baas, F. Rab6 Is Increased in Alzheimer's Disease Brain and Correlates With Endoplasmic Reticulum Stress. *Neuropathol. Appl. Neurobiol.* **2007,** *33,* 523-532.

(262) Cole, S. L.; Grudzien, A.; Manhart, I. O.; Kelly, B. L.; Oakley, H.; Vassar, R. Statins Cause Intracellular Accumulation of Amyloid Precursor Protein, Beta-Secretase-Cleaved Fragments, and Amyloid Beta-Peptide Via an Isoprenoid-Dependent Mechanism. *J. Biol. Chem.* **2005,** *280,* 18755-18770.

(263) Holstein, S. A.; Tong, H.; Hohl, R. J. Differential Activities of Thalidomide and Isoprenoid Biosynthetic Pathway Inhibitors in Multiple Myeloma Cells. *Leuk. Res.* **2009**.

(264) Hooff, G. P.; Peters, I.; Wood, W. G.; Muller, W. E.; Eckert, G. P. Modulation of Cholesterol, Farnesylpyrophosphate, and Geranylgeranylpyrophosphate in Neuroblastoma SH-SY5Y-APP695 Cells: Impact on Amyloid Beta-Protein Production. *Mol. Neurobiol.* **2010,** *41,* 341-350.

(265) Hooff, G. P.; Volmer, D. A.; Wood, W. G.; Muller, W. E.; Eckert, G. P. Isoprenoid Quantitation in Human Brain Tissue: a Validated HPLC-Fluorescence Detection Method for Endogenous Farnesyl- (FPP) and Geranylgeranylpyrophosphate (GGPP). *Anal. Bioanal. Chem.* **2008,** *392,* 673-680.

(266) Eckert, G. P.; Hooff, G. P.; Strandjord, D. M.; Igbavboa, U.; Volmer, D. A.; Muller, W. E.; Wood, W. G. Regulation of the Brain Isoprenoids Farnesyl- and Geranylgeranylpyrophosphate Is Altered in Male Alzheimer Patients. *Neurobiol. Dis.* **2009,** *35,* 251-257.

(267) Fassbender, K.; Simons, M.; Bergmann, C.; Stroick, M.; Lutjohann, D.; Keller, P.; Runz, H.; Kuhl, S.; Bertsch, T.; Von Bergmann, K.; Hennerici, M.; Beyreuther, K.; Hartmann, T. Simvastatin Strongly Reduces Levels of Alzheimer's Disease Beta -Amyloid Peptides

Abeta 42 and Abeta 40 in Vitro and in Vivo. *Proc. Natl. Acad. Sci. U. S. A* **2001,** *98*, 5856-5861.

(268) Frears, E. R.; Stephens, D. J.; Walters, C. E.; Davies, H.; Austen, B. M. The Role of Cholesterol in the Biosynthesis of Beta-Amyloid. *Neuroreport* **1999,** *10*, 1699-1705.

(269) Kojro, E.; Gimpl, G.; Lammich, S.; Marz, W.; Fahrenholz, F. Low Cholesterol Stimulates the Nonamyloidogenic Pathway by Its Effect on the Alpha -Secretase ADAM 10. *Proc. Natl. Acad. Sci. U. S. A* **2001,** *98*, 5815-5820.

(270) Peters, I.; Igbavboa, U.; Schutt, T.; Haidari, S.; Hartig, U.; Rosello, X.; Bottner, S.; Copanaki, E.; Deller, T.; Kogel, D.; Wood, W. G.; Muller, W. E.; Eckert, G. P. The Interaction of Beta-Amyloid Protein With Cellular Membranes Stimulates Its Own Production. *Biochim. Biophys. Acta* **2009,** *1788*, 964-972.

(271) Eckert, G. P.; Wood, W. G.; Muller, W. E. Statins: Drugs for Alzheimer's Disease? *J. Neural Transm.* **2005,** *112*, 1057-1071.

(272) Wood, W. G.; Igbavboa, U. Cholesterol Trafficking and Amyloid Beta Peptides. *Pharmacopsychiatry* **2003,** *36 Suppl 2*, S144-S148.

(273) Zhou, Y.; Suram, A.; Venugopal, C.; Prakasam, A.; Lin, S.; Su, Y.; Li, B.; Paul, S. M.; Sambamurti, K. Geranylgeranyl Pyrophosphate Stimulates Gamma-Secretase to Increase the Generation of Abeta and APP-CTFgamma. *FASEB J.* **2008,** *22*, 47-54.

(274) Pedrini, S.; Carter, T. L.; Prendergast, G.; Petanceska, S.; Ehrlich, M. E.; Gandy, S. Modulation of Statin-Activated Shedding of Alzheimer APP Ectodomain by ROCK. *PLoS. Med.* **2005,** *2*, e18.

(275) Zhou, Y.; Su, Y.; Li, B.; Liu, F.; Ryder, J. W.; Wu, X.; Gonzalez-DeWhitt, P. A.; Gelfanova, V.; Hale, J. E.; May, P. C.; Paul, S. M.; Ni, B. Nonsteroidal Anti-Inflammatory Drugs Can Lower Amyloidogenic Abeta42 by Inhibiting Rho. *Science* **2003,** *302*, 1215-1217.

(276) Leuchtenberger, S.; Kummer, M. P.; Kukar, T.; Czirr, E.; Teusch, N.; Sagi, S. A.; Berdeaux, R.; Pietrzik, C. U.; Ladd, T. B.; Golde, T. E.; Koo, E. H.; Weggen, S. Inhibitors of Rho-Kinase Modulate Amyloid-Beta (Abeta) Secretion but Lack Selectivity for Abeta42. *J. Neurochem.* **2006,** *96*, 355-365.

(277) Salminen, A.; Suuronen, T.; Kaarniranta, K. ROCK, PAK, and Toll of Synapses in Alzheimer's Disease. *Biochem. Biophys. Res. Commun.* **2008,** *371*, 587-590.

(278) Scheper, W.; Zwart, R.; Baas, F. Rab6 Membrane Association Is Dependent of Presenilin 1 and Cellular Phosphorylation Events. *Brain Res. Mol. Brain Res.* **2004,** *122*, 17-23.

(279) Dumanchin, C.; Czech, C.; Campion, D.; Cuif, M. H.; Poyot, T.; Martin, C.; Charbonnier, F.; Goud, B.; Pradier, L.; Frebourg, T. Presenilins Interact With Rab11, a Small GTPase Involved in the Regulation of Vesicular Transport. *Hum. Mol. Genet.* **1999,** *8*, 1263-1269.

(280) Lee, M.; You, H. J.; Cho, S. H.; Woo, C. H.; Yoo, M. H.; Joe, E. H.; Kim, J. H. Implication of the Small GTPase Rac1 in the Generation of Reactive Oxygen Species in Response to Beta-Amyloid in C6 Astroglioma Cells. *Biochem. J.* **2002,** *366,* 937-943.

(281) Wang, P. L.; Niidome, T.; Akaike, A.; Kihara, T.; Sugimoto, H. Rac1 Inhibition Negatively Regulates Transcriptional Activity of the Amyloid Precursor Protein Gene. *J. Neurosci. Res.* **2009,** *87,* 2105-2114.

(282) Pilpel, Y.; Segal, M. Activation of PKC Induces Rapid Morphological Plasticity in Dendrites of Hippocampal Neurons Via Rac and Rho-Dependent Mechanisms. *Eur. J. Neurosci.* **2004,** *19,* 3151-3164.

(283) Reddy, P. H.; Mani, G.; Park, B. S.; Jacques, J.; Murdoch, G.; Whetsell, W., Jr.; Kaye, J.; Manczak, M. Differential Loss of Synaptic Proteins in Alzheimer's Disease: Implications for Synaptic Dysfunction. *J. Alzheimers. Dis.* **2005,** *7,* 103-117.

(284) Shimohama, S.; Kamiya, S.; Taniguchi, T.; Sumida, Y.; Fujimoto, S. Differential Involvement of Small G Proteins in Alzheimer's Disease. *Int. J. Mol. Med.* **1999,** *3,* 597-600.

(285) Pak, D. T.; Sheng, M. Targeted Protein Degradation and Synapse Remodeling by an Inducible Protein Kinase. *Science* **2003,** *302,* 1368-1373.

(286) Dekosky, S. T.; Scheff, S. W.; Styren, S. D. Structural Correlates of Cognition in Dementia: Quantification and Assessment of Synapse Change. *Neurodegeneration.* **1996,** *5,* 417-421.

(287) Selkoe, D. J. Alzheimer's Disease Is a Synaptic Failure. *Science* **2002,** *298,* 789-791.

(288) Terry, R. D.; Masliah, E.; Salmon, D. P.; Butters, N.; DeTeresa, R.; Hill, R.; Hansen, L. A.; Katzman, R. Physical Basis of Cognitive Alterations in Alzheimer's Disease: Synapse Loss Is the Major Correlate of Cognitive Impairment. *Ann. Neurol.* **1991,** *30,* 572-580.

(289) Arendt, T. Neurodegeneration and Plasticity. *Int. J. Dev. Neurosci.* **2004,** *22,* 507-514.

(290) Arendt, T. Synaptic Degeneration in Alzheimer's Disease. *Acta Neuropathol.* **2009,** *118,* 167-179.

(291) Carlisle, H. J.; Kennedy, M. B. Spine Architecture and Synaptic Plasticity. *Trends Neurosci.* **2005,** *28,* 182-187.

(292) Schiller, M. R. Coupling Receptor Tyrosine Kinases to Rho GTPases--GEFs What's the Link. *Cell Signal.* **2006,** *18,* 1834-1843.

(293) Tejada-Simon, M. V.; Villasana, L. E.; Serrano, F.; Klann, E. NMDA Receptor Activation Induces Translocation and Activation of Rac in Mouse Hippocampal Area CA1. *Biochem. Biophys. Res. Commun.* **2006,** *343,* 504-512.

(294) Gruart, A.; Munoz, M. D.; Delgado-Garcia, J. M. Involvement of the CA3-CA1 Synapse in the Acquisition of Associative Learning in Behaving Mice. *J. Neurosci.* **2006,** *26,* 1077-1087.

(295) Martinez, L. A.; Klann, E.; Tejada-Simon, M. V. Translocation and Activation of Rac in the Hippocampus During Associative Contextual Fear Learning. *Neurobiol. Learn. Mem.* **2007,** *88,* 104-113.

(296) Tejada-Simon, M. V.; Serrano, F.; Villasana, L. E.; Kanterewicz, B. I.; Wu, G. Y.; Quinn, M. T.; Klann, E. Synaptic Localization of a Functional NADPH Oxidase in the Mouse Hippocampus. *Mol. Cell Neurosci.* **2005,** *29,* 97-106.

(297) Shuai, Y.; Lu, B.; Hu, Y.; Wang, L.; Sun, K.; Zhong, Y. Forgetting Is Regulated Through Rac Activity in Drosophila. *Cell* **2010,** *140,* 579-589.

(298) K.M.Um, F. N. K. R. L. K. R. T. Role of the Rac-GAP Bcr in dendritic and synapse development. [Neuroscience Meeting Planner, Society for Neuroscience.]. 2009. Chicago, IL, 2009.
Ref Type: Conference Proceeding

(299) Miyamoto, Y.; Yamauchi, J.; Tanoue, A.; Wu, C.; Mobley, W. C. TrkB Binds and Tyrosine-Phosphorylates Tiam1, Leading to Activation of Rac1 and Induction of Changes in Cellular Morphology. *Proc. Natl. Acad. Sci. U. S. A* **2006,** *103,* 10444-10449.

(300) Martin, M. G.; Perga, S.; Trovo, L.; Rasola, A.; Holm, P.; Rantamaki, T.; Harkany, T.; Castren, E.; Chiara, F.; Dotti, C. G. Cholesterol Loss Enhances TrkB Signaling in Hippocampal Neurons Aging in Vitro. *Mol. Biol. Cell* **2008,** *19,* 2101-2112.

(301) Ma, Q. L.; Yang, F.; Calon, F.; Ubeda, O. J.; Hansen, J. E.; Weisbart, R. H.; Beech, W.; Frautschy, S. A.; Cole, G. M. P21-Activated Kinase-Aberrant Activation and Translocation in Alzheimer Disease Pathogenesis. *J. Biol. Chem.* **2008,** *283,* 14132-14143.

(302) Kwon, T.; Kwon, D. Y.; Chun, J.; Kim, J. H.; Kang, S. S. Akt Protein Kinase Inhibits Rac1-GTP Binding Through Phosphorylation at Serine 71 of Rac1. *J. Biol. Chem.* **2000,** *275,* 423-428.

(303) Fumagalli, F.; Racagni, G.; Riva, M. A. The Expanding Role of BDNF: a Therapeutic Target for Alzheimer's Disease? *Pharmacogenomics. J.* **2006,** *6,* 8-15.

(304) Phillips, H. S.; Hains, J. M.; Armanini, M.; Laramee, G. R.; Johnson, S. A.; Winslow, J. W. BDNF MRNA Is Decreased in the Hippocampus of Individuals With Alzheimer's Disease. *Neuron* **1991,** *7,* 695-702.

(305) Siegel, G. J.; Chauhan, N. B. Neurotrophic Factors in Alzheimer's and Parkinson's Disease Brain. *Brain Res. Brain Res. Rev.* **2000,** *33,* 199-227.

(306) Petratos, S.; Li, Q. X.; George, A. J.; Hou, X.; Kerr, M. L.; Unabia, S. E.; Hatzinisiriou, I.; Maksel, D.; Aguilar, M. I.; Small, D. H. The Beta-Amyloid Protein of Alzheimer's

Disease Increases Neuronal CRMP-2 Phosphorylation by a Rho-GTP Mechanism. *Brain* **2008,** *131,* 90-108.

(307) Markesbery, W. R.; Carney, J. M. Oxidative Alterations in Alzheimer's Disease. *Brain Pathol.* **1999,** *9,* 133-146.

(308) McGrath, L. T.; McGleenon, B. M.; Brennan, S.; McColl, D.; McILroy, S.; Passmore, A. P. Increased Oxidative Stress in Alzheimer's Disease As Assessed With 4-Hydroxynonenal but Not Malondialdehyde. *QJM.* **2001,** *94,* 485-490.

(309) Sultana, R.; Butterfield, D. A. Role of Oxidative Stress in the Progression of Alzheimer's Disease. *J. Alzheimers. Dis.* **2010,** *19,* 341-353.

(310) Cheret, C.; Gervais, A.; Lelli, A.; Colin, C.; Amar, L.; Ravassard, P.; Mallet, J.; Cumano, A.; Krause, K. H.; Mallat, M. Neurotoxic Activation of Microglia Is Promoted by a Nox1-Dependent NADPH Oxidase. *J. Neurosci.* **2008,** *28,* 12039-12051.

(311) Bruce-Keller, A. J.; Gupta, S.; Parrino, T. E.; Knight, A. E.; Ebenezer, P. J.; Weidner, A. M.; Levine, H.; Keller, J.; Markesbery, W. R. NOX Activity Is Increased in Mild Cognitive Impairment. *Antioxid. Redox. Signal.* **2009**.

(312) Hirooka, Y. Role of Reactive Oxygen Species in Brainstem in Neural Mechanisms of Hypertension. *Auton. Neurosci.* **2008,** *142,* 20-24.

(313) Kahles, T.; Luedike, P.; Endres, M.; Galla, H. J.; Steinmetz, H.; Busse, R.; Neumann-Haefelin, T.; Brandes, R. P. NADPH Oxidase Plays a Central Role in Blood-Brain Barrier Damage in Experimental Stroke. *Stroke* **2007,** *38,* 3000-3006.

(314) Nozoe, M.; Hirooka, Y.; Koga, Y.; Sagara, Y.; Kishi, T.; Engelhardt, J. F.; Sunagawa, K. Inhibition of Rac1-Derived Reactive Oxygen Species in Nucleus Tractus Solitarius Decreases Blood Pressure and Heart Rate in Stroke-Prone Spontaneously Hypertensive Rats. *Hypertension* **2007,** *50,* 62-68.

(315) Patel, M.; Li, Q. Y.; Chang, L. Y.; Crapo, J.; Liang, L. P. Activation of NADPH Oxidase and Extracellular Superoxide Production in Seizure-Induced Hippocampal Damage. *J. Neurochem.* **2005,** *92,* 123-131.

(316) Naassner, M.; Mergler, M.; Wolf, K.; Schuphan, I. Determination of the Xenoestrogens 4-Nonylphenol and Bisphenol A by High-Performance Liquid Chromatography and Fluorescence Detection After Derivatisation With Dansyl Chloride. *J. Chromatogr. A* **2002,** *945,* 133-138.

(317) U.S.Department of Health and Human Services Food and Drug Administration. Guidance for Industry - Bioanalytical Method Validation. U.S.Department of Health and Human Services Food and Drug Administration Center for Drug Evaluation and Research (CDER) Center for Veterinary Medicine (CVM). 1-22. 2001.
Ref Type: Report

(318) Eckert, G. P.; Cairns, N. J.; Maras, A.; Gattaz, W. F.; Muller, W. E. Cholesterol Modulates the Membrane-Disordering Effects of Beta-Amyloid Peptides in the Hippocampus: Specific Changes in Alzheimer's Disease. *Dement. Geriatr. Cogn Disord.* **2000,** *11,* 181-186.

(319) Edwards, P. A.; Lemongello, D.; Fogelman, A. M. Improved Methods for the Solubilization and Assay of Hepatic 3-Hydroxy-3-Methylglutaryl Coenzyme A Reductase. *J. Lipid Res.* **1979,** *20,* 40-46.

(320) Louis, D. N.; Ohgaki, H.; Wiestler, O. D.; Cavenee, W. K.; Burger, P. C.; Jouvet, A.; Scheithauer, B. W.; Kleihues, P. The 2007 WHO Classification of Tumours of the Central Nervous System. *Acta Neuropathol.* **2007,** *114,* 97-109.

(321) Rossetti, H. C.; Munro, C. C.; Hynan, L. S.; Lacritz, L. H. The CERAD Neuropsychologic Battery Total Score and the Progression of Alzheimer Disease. *Alzheimer Dis. Assoc. Disord.* **2010,** *24,* 138-142.

(322) Louhimies, S. Directive 86/609/EEC on the Protection of Animals Used for Experimental and Other Scientific Purposes. *Altern. Lab Anim* **2002,** *30 Suppl 2,* 217-219.

(323) Blanchard, V.; Moussaoui, S.; Czech, C.; Touchet, N.; Bonici, B.; Planche, M.; Canton, T.; Jedidi, I.; Gohin, M.; Wirths, O.; Bayer, T. A.; Langui, D.; Duyckaerts, C.; Tremp, G.; Pradier, L. Time Sequence of Maturation of Dystrophic Neurites Associated With Abeta Deposits in APP/PS1 Transgenic Mice. *Exp. Neurol.* **2003,** *184,* 247-263.

(324) Reising, K.; Meins, J.; Bastian, B.; Eckert, G.; Mueller, W. E.; Schubert-Zsilavecz, M.; Abdel-Tawab, M. Determination of Boswellic Acids in Brain and Plasma by High-Performance Liquid Chromatography/Tandem Mass Spectrometry. *Anal. Chem.* **2005,** *77,* 6640-6645.

(325) Brown, K. R.; Allan, B. M.; Do, P.; Hegg, E. L. Identification of Novel Hemes Generated by Heme A Synthase: Evidence for Two Successive Monooxygenase Reactions. *Biochemistry* **2002,** *41,* 10906-10913.

(326) Dursina, B.; Reents, R.; Delon, C.; Wu, Y.; Kulharia, M.; Thutewohl, M.; Veligodsky, A.; Kalinin, A.; Evstifeev, V.; Ciobanu, D.; Szedlacsek, S. E.; Waldmann, H.; Goody, R. S.; Alexandrov, K. Identification and Specificity Profiling of Protein Prenyltransferase Inhibitors Using New Fluorescent Phosphoisoprenoids. *J. Am. Chem. Soc.* **2006,** *128,* 2822-2835.

(327) Dietschy, J. M. Central Nervous System: Cholesterol Turnover, Brain Development and Neurodegeneration. *Biol. Chem.* **2009,** *390,* 287-293.

(328) Mulder, M. Sterols in the Central Nervous System. *Curr. Opin. Clin. Nutr. Metab Care* **2009,** *12,* 152-158.

(329) Fedorow, H.; Pickford, R.; Hook, J. M.; Double, K. L.; Halliday, G. M.; Gerlach, M.; Riederer, P.; Garner, B. Dolichol Is the Major Lipid Component of Human Substantia Nigra Neuromelanin. *J. Neurochem.* **2005,** *92,* 990-995.

(330) Quinzii, C. M.; DiMauro, S.; Hirano, M. Human Coenzyme Q10 Deficiency. *Neurochem. Res.* **2007,** *32,* 723-727.

(331) Agrawal, A. G.; Somani, R. R. Farnesyltransferase Inhibitor As Anticancer Agent. *Mini. Rev. Med. Chem.* **2009,** *9,* 638-652.

(332) Saxena, N.; Lahiri, S. S.; Hambarde, S.; Tripathi, R. P. RAS: Target for Cancer Therapy. *Cancer Invest* **2008,** *26,* 948-955.

(333) Cunliffe, J. M.; Maloney, T. D. Fused-Core Particle Technology As an Alternative to Sub-2-Microm Particles to Achieve High Separation Efficiency With Low Backpressure. *J. Sep. Sci.* **2007,** *30,* 3104-3109.

(334) Destefano, J. J.; Langlois, T. J.; Kirkland, J. J. Characteristics of Superficially-Porous Silica Particles for Fast HPLC: Some Performance Comparisons With Sub-2-Microm Particles. *J. Chromatogr. Sci.* **2008,** *46,* 254-260.

(335) Novakova, L.; Vlckova, H. A Review of Current Trends and Advances in Modern Bio-Analytical Methods: Chromatography and Sample Preparation. *Anal. Chim. Acta* **2009,** *656,* 8-35.

(336) Kuo, K.; Still, R.; Cale, S.; McDowell, I. Standardization (External and Internal) of HPLC Assay for Plasma Homocysteine. *Clin. Chem.* **1997,** *43,* 1653-1655.

(337) Tomaiuolo, M.; Vecchione, G.; Margaglione, M.; Pisanelli, D.; Grandone, E. Stable-Isotope Dilution LC-ESI-MS/MS Techniques for the Quantification of Total Homocysteine in Human Plasma. *J. Chromatogr. B Analyt. Technol. Biomed. Life Sci.* **2009,** *877,* 3292-3299.

(338) Franke, C.; Noldner, M.; Abdel-Kader, R.; Johnson-Anuna, L. N.; Gibson, W. W.; Muller, W. E.; Eckert, G. P. Bcl-2 Upregulation and Neuroprotection in Guinea Pig Brain Following Chronic Simvastatin Treatment. *Neurobiol. Dis.* **2007,** *25,* 438-445.

(339) Hooff, G. P.; Patel, N.; Wood, W. G.; Muller, W. E.; Eckert, G. P.; Volmer, D. A. A Rapid and Sensitive Assay for Determining Human Brain Levels of Farnesyl-(FPP) and Geranylgeranylpyrophosphate (GGPP) and Transferase Activities Using UHPLC-MS/MS. *Anal. Bioanal. Chem.* **2010,** *398,* 1801-1808.

(340) Olaisen, B. Postmortem Decrease in Brain Temperature. *Z. Rechtsmed.* **1979,** *83,* 253-257.

(341) Crecelius, A.; Gotz, A.; Arzberger, T.; Frohlich, T.; Arnold, G. J.; Ferrer, I.; Kretzschmar, H. A. Assessing Quantitative Post-Mortem Changes in the Gray Matter of the Human Frontal Cortex Proteome by 2-D DIGE. *Proteomics.* **2008,** *8,* 1276-1291.

(342) Robinson, A. A.; Westbrook, J. A.; English, J. A.; Boren, M.; Dunn, M. J. Assessing the Use of Thermal Treatment to Preserve the Intact Proteomes of Post-Mortem Heart and Brain Tissue. *Proteomics.* **2009,** *9,* 4433-4444.

(343) Bruen, P. D.; McGeown, W. J.; Shanks, M. F.; Venneri, A. Neuroanatomical Correlates of Neuropsychiatric Symptoms in Alzheimer's Disease. *Brain* **2008,** *131,* 2455-2463.

(344) Chetelat, G.; Desgranges, B.; Landeau, B.; Mezenge, F.; Poline, J. B.; de, l. S., V; Viader, F.; Eustache, F.; Baron, J. C. Direct Voxel-Based Comparison Between Grey Matter Hypometabolism and Atrophy in Alzheimer's Disease. *Brain* **2008,** *131,* 60-71.

(345) Wolf, H. K.; Buslei, R.; Schmidt-Kastner, R.; Schmidt-Kastner, P. K.; Pietsch, T.; Wiestler, O. D.; Blumcke, I. NeuN: a Useful Neuronal Marker for Diagnostic Histopathology. *J. Histochem. Cytochem.* **1996,** *44,* 1167-1171.

(346) Fonseca, A. C.; Proenca, T.; Resende, R.; Oliveira, C. R.; Pereira, C. M. Neuroprotective Effects of Statins in an in Vitro Model of Alzheimer's Disease. *J. Alzheimers. Dis.* **2009,** *17,* 503-517.

(347) Omkumar, R. V.; Gaikwad, A. S.; Ramasarma, T. Feedback-Type Inhibition of Activity of 3-Hydroxy-3-Methylglutaryl Coenzyme a Reductase by Ubiquinone. *Biochem. Biophys. Res. Commun.* **1992,** *184,* 1280-1287.

(348) Hampton, R. Y. Proteolysis and Sterol Regulation. *Annu. Rev. Cell Dev. Biol.* **2002,** *18,* 345-378.

(349) Gartner, U.; Holzer, M.; Arendt, T. Elevated Expression of P21ras Is an Early Event in Alzheimer's Disease and Precedes Neurofibrillary Degeneration. *Neuroscience* **1999,** *91,* 1-5.

(350) Fritz, G. Targeting the Mevalonate Pathway for Improved Anticancer Therapy. *Curr. Cancer Drug Targets.* **2009,** *9,* 626-638.

(351) Roskoski, R., Jr. Protein Prenylation: a Pivotal Posttranslational Process. *Biochem. Biophys. Res. Commun.* **2003,** *303,* 1-7.

(352) Ho, L.; Fukuchi, K.; Younkin, S. G. The Alternatively Spliced Kunitz Protease Inhibitor Domain Alters Amyloid Beta Protein Precursor Processing and Amyloid Beta Protein Production in Cultured Cells. *J. Biol. Chem.* **1996,** *271,* 30929-30934.

(353) Kokjohn, T. A.; Roher, A. E. Amyloid Precursor Protein Transgenic Mouse Models and Alzheimer's Disease: Understanding the Paradigms, Limitations, and Contributions. *Alzheimers. Dement.* **2009,** *5,* 340-347.

(354) Jorm, A. F.; Jolley, D. The Incidence of Dementia: a Meta-Analysis. *Neurology* **1998,** *51,* 728-733.

(355) Caino, M. C.; Meshki, J.; Kazanietz, M. G. Hallmarks for Senescence in Carcinogenesis: Novel Signaling Players. *Apoptosis.* **2009,** *14,* 392-408.

(356) Tobet, S.; Knoll, J. G.; Hartshorn, C.; Aurand, E.; Stratton, M.; Kumar, P.; Searcy, B.; McClellan, K. Brain Sex Differences and Hormone Influences: a Moving Experience? *J. Neuroendocrinol.* **2009,** *21,* 387-392.

(357) Muller, T.; Jung, K.; Ullrich, A.; Schrotter, A.; Meyer, H. E.; Stephan, C.; Egensperger, R.; Marcus, K. Disease State, Age, Sex, and Post-Mortem Time-Dependent Expression of Proteins in AD Vs. Control Frontal Cortex Brain Samples. *Curr. Alzheimer Res.* **2008,** *5,* 562-571.

(358) Simonen, M.; Ibig-Rehm, Y.; Hofmann, G.; Zimmermann, J.; Albrecht, G.; Magnier, M.; Heidinger, V.; Gabriel, D. High-Content Assay to Study Protein Prenylation. *J. Biomol. Screen.* **2008,** *13,* 456-467.

(359) Perez-Sala, D. Protein Isoprenylation in Biology and Disease: General Overview and Perspectives From Studies With Genetically Engineered Animals. *Front Biosci.* **2007,** *12,* 4456-4472.

(360) Corsini, A.; Maggi, F. M.; Catapano, A. L. Pharmacology of Competitive Inhibitors of HMG-CoA Reductase. *Pharmacol. Res.* **1995,** *31,* 9-27.

(361) Dansette, P. M.; Jaoen, M.; Pons, C. HMG-CoA Reductase Activity in Human Liver Microsomes: Comparative Inhibition by Statins. *Exp. Toxicol. Pathol.* **2000,** *52,* 145-148.

(362) Eckert, G. P.; Kirsch, C.; Leutz, S.; Wood, W. G.; Muller, W. E. Cholesterol Modulates Amyloid Beta-Peptide's Membrane Interactions. *Pharmacopsychiatry* **2003,** *36 Suppl 2,* S136-S143.